ASSESSMENT OF SURFACE WATER AVAILABILITY IN RIVER BASINS OF KONKAN REGION

THESIS

Submitted in partial fulfilment of the requirements

for the Degree of

MASTER OF TECHNOLOGY

IN

AGRICULTURAL ENGINEERING

(IRRIGATION AND DRAINAGE ENGINEERING)

By

Miss. Salvi Akanksha Dipak

(ENDPM/2022/221)

DEPARTMENT OF IRRIGATION AND DRAINAGE ENGINEERING

COLLEGE OF AGRICULTURAL ENGINEERING AND TECHNOLOGY, DAPOLI

DR. BALASAHEB SAWANT KONKAN KRISHI VIDYAPEETH, DAPOLI, RATNAGIRI (MS) 415 712

DECEMBER 2024

ASSESSMENT OF SURFACE WATER AVAILABILITY IN RIVER BASINS OF KONKAN REGION

THESIS

Submitted in partial fulfilment of the requirements

for the Degree of

MASTER OF TECHNOLOGY

IN

AGRICULTURAL ENGINEERING

(IRRIGATION AND DRAINAGE ENGINEERING)

By

Miss. Salvi Akanksha Dipak

Under the Guidance of

Dr. R.T. Thokal

Chief Scientist, AICRP, IWM and Associate Dean, ATE

DEPARTMENT OF IRRIGATION AND DRAINAGE ENGINEERING

COLLEGE OF AGRICULTURAL ENGINEERING AND TECHNOLOGY, DAPOLI

DR. BALASAHEB SAWANT KONKAN KRISHI VIDYAPEETH, DAPOLI, RATNAGIRI (MS) 415 712

DECEMBER 2024

DECLARATION OF STUDENT

I hereby declare that the experimental work and its interpretation of the thesis entitled **"ASSESSMENT OF SURFACE WATER AVILABILITY IN RIVER BASINS OF KONKAN REGION"** or part thereof has neither been submitted for any other degree or diploma of any University, nor the data have been derived from any thesis/publication of any University or scientific organization. The source of materials used and all assistance received during the course of investigation have been duly acknowledged and that no part of the thesis has been submitted for award of any other degree or diploma.

Salvi

Place: Dapoli

(Salvi Akanksha Dipak)

Date: 30 /12/ 2024

ENDPM/2022/221

DEPARTMENT OF IRRIGATION AND DRAINAGE ENGINEERING

Dr. Balasaheb Sawant Konkan Krishi Vidyapeeth

College of Agricultural Engineering and Technology, Dapoli
Dist. Ratnagiri, Maharashtra, 415 712
Phone: 02358 282414/ Fax: 02358 282414
E-mail: caetide@gmail.com

Dr. R T Thokal

Chief Scientist, AICRP, IWM
and Associate Dean, ATE
DBSKKV, Dapoli

Date: 30 / 12 / 2024

CERTIFICATE

This is to certify that the thesis entitled, **"ASSESSMENT OF THE SURFACE WATER AVILABILITY IN RIVER BASINS OF KONKAN REGION"** submitted for the degree of M. Tech. (Irrigation and Drainage Engineering), of the College of Agricultural Engineering and Technology, Dr. Balasaheb Sawant Konkan Krishi Vidyapeeth, Dapoli, is a bonafide research work carried out by Miss. Salvi Akanksha Dipak (ENDPM/2022/221) under my supervision and that no part of this thesis has been submitted for award of any other degree. The student had completed all the Course and Research requirement as per the norms in regular mode and has published one research paper from her M. Tech. work.

The assistance and help received during the course of investigation have been fully acknowledged.

Chairman
Student Advisory Committee

Place: Dapoli
Date: 30 DEC 2024

Countersigned

Head
Department of Irrigation and Drainage Engineering

THESIS APPROVAL BY THE STUDENT'S ADVISORY COMMITTEE
INCLUDING EXTERNAL EXAMINER

This is to certify that the thesis/project report entitled, **"ASSESSMENT OF SURFACE WATER AVAILABILITY IN RIVER BASINS OF KONKAN REGION"** submitted by Miss. Salvi Akanksha Dipak (ENDPM/2022/221) to the College of Agricultural Engineering and Technology, Dr. Balasaheb Sawant Konkan Krishi Vidyapeeth, Dapoli, in partial fulfilment of the requirements for the M.Tech. (Irrigation and Drainage Engineering), in the subject having Watershed Management and Modelling as minor subject of Department of Soil and Water Conservation Engineering has been approved by Student's Advisory Committee, Board of Studies of the Department and Evaluated by One/Two External Examiner after an open Viva Voice examination in the presence of External Examiner on the same held on dated 17/12/24.

1.	Chairman, SAC	**Dr. R. T. Thokal** Chief Scientist, AICRP, IWM and Associate Dean, ATE, DBSKKV, Dapoli	.....
2.	Member	**Dr. P. M. Ingle** Professor and Head Department of IDE, CAET, Dapoli.	.....
3.	Member	**Dr. S. T. Patil** Associate Professor Department of IDE, CAET, Dapoli	.....
4.	Member	**Dr. S. S. More** Jr. Soil Scientist, Regional Fruit Research Station, Vengurla.	.....
5.	External Member/ Examiner	**Dr. B. L. Ayare** Professor and Head Department of SWCE, CAET, Dapoli	.....

Countersigned

Head
Department of Irrigation and Drainage Engineering

Associate Dean
College of Agricultural Engineering and Technology
Dr. Balasaheb Sawant Konkan Krishi Vidyapeeth, Dapoli

Acknowledgements

First and foremost, praises and thanks to the Almighty God for enduring grace, guidance and protection that He has bestowed upon me throughout my research work to complete the research successfully.

I deem it a great privilege to express my profound and sincere gratitude to my research supervisor, ***Dr. R. T. Thokal****, Chief Scientist, AICRP, IWM and Associate Dean, ATE, Dr. Balasaheb Sawant Konkan Krishi Vidyapeeth, Dapoli for his continuous support, patience and guidance throughout my research period. I would also like to thank him for his empathy, great sense of humor and for imparting immense knowledge during the discussions I had with him on research work and thesis preparation. It has been an extreme privilege and one of the most rewarding experiences of life to have been associated with a person of his caliber. I could not have imagined having a better supervisor and mentor for my M. Tech study.*

It is my utmost privilege to express my deep and sincere thanks to the member of my Advisory Committee, ***Dr. P. M. Ingle****, Professor and Head, Department of Irrigation and Drainage Engineering, College of Agricultural Engineering and Technology, Dr. Balasaheb Sawant Konkan Krishi Vidyapeeth, Dapoli for his dynamism, guidance, brilliant suggestions and motivations which inspired me throughout my research work.*

I wish to express my gratitude to the member of the Advisory Committee, ***Dr. S. T. Patil****, Associate Professor (CAS), Department of Irrigation and Drainage Engineering, College of Agricultural Engineering and Technology, Dr. Balasaheb Sawant Konkan Krishi Vidyapeeth, Dapoli for his valuable suggestions from very inception of the research work.*

I wish to express my gratitude to the member of the Advisory Committee, ***Dr. S. S. More****, Jr. Soil Scientist, Regional Fruit Research Station, Vengurla for his valuable suggestions from very inception of the research work.*

I mention my sincere gratitude to ***Dr. P.U. Shahare****, Associate Dean, College of Agricultural Engineering and Technology, Dr. Balasaheb Sawant Konkan Krishi Vidyapeeth, Dapoli and* ***Dr. Y. P. Khandetod****, Ex Associate Dean Ex Director of Research who gave me an opportunity for undergoing this research work and providing necessary facilities whenever necessary.*

I would like to show my gratitude to the supporting staff ***Er. G. G. Kadam and Mr. Vishwajeet Jadhav****, Department of Irrigation and Drainage Engineering, College of Agricultural Engineering and Technology, Dapoli for their unwavering support and kind cooperation during the entire course.*

I am thankful to ***HDUG, Nashik and Groundwater Survey and Development Agencies (GSDA)*** *for their valuable Support and cooperation during research work.*

I extend to sincere thanks to my friends come sisters and profound sense of gratitude to ***Dhanshree Korade, Nikita Patil, Vaishnavi Anarase and Shamali Salunkhe*** *for constant assistance throughout the period of my research work.*

Special thanks to my dearest friends, ***Aniket Kale, Sagar Gavit, Omkar Landage, Manjit Khatal, Abhijeet Kutwal, Akash Kumar, Samip Dalvi and Srishti Negi*** *for their comforting presence and listening ears which have been instrumental in helping me cope with the stress that comes with academic pursuits.*

No mortal words would suffice to express my love and appreciation to my dear grandparents, whose wisdom, unconditional love and prayers have been a guiding light throughout my academic journey. I am truly blessed to have their love and encouragement as a source of strength and inspiration as I worked on this thesis.

It is like a drop in the ocean of words that can never reach its mark to acknowledge infinite love, blessings, sacrifices and constant encouragement of my parents ***Mr. Dipak L. Salvi*** *and* ***Mrs. Dipali D. Salvi*** *who have been the sole source of inspiration for me to proceed ahead in my life. All that I am or hope to be I owe to my parents. Without their patience and sacrifice, I could not have completed this thesis. I extend my heartily thanks to my dear loving brother and sisters* ***Yukta and Ayush,*** *my beloved* ***Aaji*** *and all-family members for their blessings, selfless love, constant encouragement, sacrifices and mental support that have been the most vital source of inspiration and motivation in my life.*

Place: Dapoli
Date: 30 / 12 / 2024

Salvi

(Salvi Akanksha Dipak)

Table of Contents

List of Tables

List of Figures

Abbreviations

%	Percentage
<	Less than
>	Greater than
°C	Degree Celsius
AA	Accuracy Assessment
Agril.Engg.	Agricultural Engineering
AHP	Analytical Hierarchy Process
Mm^3	million cubic meters
CAET	College of Agricultural Engineering and Technology
CGWB	Central Groundwater Board
CI	Consistency Index
CR	Consistency Ratio
cumec	Cubic meter per second
CW	Criteria Weight
D. D	Drainage density
DBSKKV	Dr. Balasaheb Sawant Konkan Krishi Vidyapeeth
DEM	Digital Elevation Model
Def.	Deficit
Dept.	Department
et al.	And Authors
etc.	Etcetera
Eq.	Equation
Fig.	Figure
GCS	Geographic Coordinate System
Geo	Geology
G.M	Geomorphology
GHz	Giga Heartz
GIS	Geographical Information System
GSDA	Groundwater Survey Development Agency
GWD	Groundwater Depth
GWPZ	Groundwater Potential Zones
ha.	Hectare

HDD	Hard Disk Drive
HDUG	Hydrological Data User Group
i.e.	that is
IDW	Inverse Distance weightage
km	kilometer
km^2	Square kilometer
KML	Keyhole Markup Language
LULC	Land use Land Cover
LD	Lineament Density
M.Tech.	Master of Technology
MCM	Million cubic meters
mm	Millimeter
PCS	Projected Coordinate System
Rain	Rainfall
RCI	Random Consistency Index
RS	Remote Sensing
SOI	Survey of India
SRTM	Shuttle Radar Topographic Mission
SWAT	Soil and water assessment tool
slp	Slope
Sur	Surplus
Tal	Taluka
USGS	United Sates Geological Survey
UTM	Universal Transverse Mercator
viz.	Namely
WGS	World Geodetic System
WS	Weighted Sum

CHAPTER I: INTRODUCTION

Water is at the core of sustainable development and is critical for socioeconomic development and the necessity for life, agriculture, healthy ecosystems, and human survival. Water is one of the important natural resources essential for every civilization's survival and livelihood, including food production, access to clean drinking water, sanitation, and hygiene. Adequate water in both quantity and quality underpins health and basic quality of life. It influences the course of a wide variety of ecosystem services. History reveals that most of the civilization started very close to rivers banks due to proximity of water satisfying their demands for various purposes. Water availability is the critical link for major development challenges including food security, rapid urbanization, sustainable rural development, disaster risk management, and adaptation to climate change. The planning, development, operation, and maintenance of all the water resources for the security of the population, in response to the growing need for drinking water, industrial production, agricultural products, and electricity, a general improvement of living conditions is of utmost importance. Surface water is open to the atmosphere and conducted through streams, rivers, lakes, wetlands, and other freshwater bodies. Surface water is a vital natural resource for India, as it is the primary source of water for various uses like irrigation, drinking, and industrial activities. The estimation of spatial-temporal availability of water in a region is an essential part of water resource planning.

Global water demand has surged by 600% in the last century, currently increasing at about 1% annually. By 2050, demand is projected to rise by 20-30%, reaching 5,500-6,000 km^3 per year. Population growth, especially in Africa and Asia, and urbanization drive this trend. Agricultural water use, presently 70% of the total, will increase by 60% by 2025 due to heightened food demand. With manufacturing demand quadrupling, industrial water use, now 20% of the total, will significantly increase, especially in Asia. Energy sector water use will rise by 85% by 2050. Domestic water use, currently 10% of total demand, will grow notably, particularly in Asia. (Boretti et. al. 2019)

India has a total geographical area of 329 M-ha which is about 2% of the world's area but 16% of its population. India is a vast country with a greater degree of climatic variability. The rainfall varies from less than 200 mm to more than 4000 mm. When rain occurs over the land a part of it is intercepted by the vegetation and the remaining amount reaches the ground surface which will either enters it (groundwater) or flows over the surface (surface water). India has very copious water resources as it is endowed with 14 major and 44 medium river basins The total volume of precipitation over a surface is 3838 – 4000 km^3 out of which 48.8 – 50.1 percent goes back to the ocean as stream flow. With 4000 BCM of annual rainfall, the

average runoff generated is only 1869 BCM. Due to various constraints about 1122 BCM of water can be put to beneficial use of which 690 BCM is through surface water.

The geographical area of Maharashtra state is 308 lakh ha, and its cultivable area is 225 lakh ha. Out of this, 40% of the area is drought prone and about 7% of the area is flood prone. It has diverse geomorphology, soils, vegetation and climatic conditions. The highly variable rainfall in Maharashtra ranges from 400 to 6000mm and occurs in a four-months period between June - Sept with the number of rainy days varying between 40 and 100. The estimated average-annual availability of water resources consists of 164 km^3 of surface water and 20.5 km^3 of subsurface water.

Maharashtra is traversed by five river basins systems and only 55% of the dependable yield is available in the four river basins (Krishna, Godavari, Tapi, and Narmada) east of the Western Ghats and fifth river basin system is west flowing rivers. These five river basins comprise 92% of the cultivable land and more than 60% of the population in rural areas. Approximately 49% of the area of these four river basins consisting of 43% of the population is already considered as deficit or highly deficit regarding water availability. The size of these deficit areas is likely to increase steadily with increasing population and economic growth in the years to come.

The Konkan region of Maharashtra is a strip of land between the west coast of India and the Sahyadri mountain range that runs parallel to the coast situated between 15° 37‟ N and 20°20‟ N latitudes and between 72°39‟E and 74°13‟E longitudes. Konkan coastline is 720 km. (450 miles) long beach. This region falls in the border area of four states namely Maharashtra, Goa, Gujarat, and Karnataka. Konkan depends on west-flowing rivers for its water demand which fall in river valley 20 to 25 comprising total of 14 rivers, water resources in the region is surplus but have highly uneven spatio-temporal distribution.

Konkan region has 42 per cent potential water resources of the state only on 10 percent of geographical area of which 8 percent is cultivable and supports 25 percent population of state (Anonymous, 2017) This huge available potential water resource in the region of which only 6.02 per cent is stored in different projects, 0.4 percent is evaporated and remaining 93.4 per cent water flows as surface runoff and meet Arbian sea (Anonymous, 2013a). Despite the region's abundant water resources, only monocropping with rice during the kharif season is practiced. Poor management leads to drought-like conditions in the summer, even resulting in drinking water shortages. This indicates that the untapped runoff water during the monsoon could be harnessed for sustainable agriculture through proper harvesting and the construction of various water harvesting or recharge structures. Therefore, assessing the surface water

potential and enhancing water availability in water-deficit areas is essential for achieving sustainability.

There are different tools and methods are available such as direct measurement method, velocity-area method, formed construction method, non-contact measurement etc among these methods remote sensing and geographic information system have proven better for evaluation and estimation of water resources on regional basis.

The geographic information system is the computer-based systems which can be utilized to retrieve, analyse, synthesis, store and represent graphical data for decision making support. With the interface of RS and GIS many hydrological models such as VIC, MIKE SHE, HEC-HMS, WEAP, MODFLOW etc. are available for basin scale water budgeting. Soil and water Assessment tool (SWAT), a hydrological model developed by USDA Agricultural Research service and Texas agriculture University which works with GIS interface is more reliable and better utilized for basin scale study (Gassman et al., 2014). This tool is widely adapted for different works such as ground water planning, water quality analysis, crop planning, water budgeting and many more applications (Arnold 2007).

The assessment, planning and management of water resources for proper utilization on the regional scale can be done by using the different hydrologic models through the RS and GIS platform. Thus, present study entitled “Assessment of surface water availability in the river basins of Konkan region” is intend to undertaken with the following objectives:

1. To study different methods for assessing surface water availability.
2. To study the impact of parameters like soil, land use, and slope on temporal and spatial variability of water in river basins of the Konkan region.
3. To assess the total surface water availability in river basins of the Konkan region.

CHAPTER II: REVIEW OF LITERATURE

To accomplish the objectives of undertaken study, the literatures pertaining to following topics was reviewed to formulate methodology and extract the relevant inferences to support the result of the study. This chapter contains reviews of study carried out by various researchers are presented under the following main heads.

1. Methods employed for assessing surface water availability
2. Impact of soil, land use, and slope on temporal and spatial variability of water availability
3. Assessment of surface water availability.

2.1. Methods employed for assessing surface water availability

Determining surface water resources is crucial for reliable water management. Water resource assessment is a national responsibility that requires specialized arrangements and capabilities to ensure accurate evaluation. Developing effective methods to reliably quantify sustainable long-term water resources and estimate them on a regional-scale has become increasingly important for water resource studies and environmental impact assessment. In this context, numerous researchers have contributed to the field. A brief review and findings is presented below to identify suitable methods for the current study.

John (1978) examined a wide range of conventional and unconventional discharge measurement techniques applicable to lower-order streams, considering factors such as stream characteristics, required accuracy and available resources, including funding and manpower. He also discussed the criteria that influence the selection of appropriate methods. He concluded that choosing the most suitable technique should account for the flow range, required accuracy, and the specific characteristics of the channel and flow conditions.

Arnold et al. (1990) developed the SWAT model as an extension of the earlier continuous-time model, Simulator for Water Resources in Rural Basins (SWRRB). SWRRB was designed to simulate the effect of management practices on water and sediment movement in ungauged rural basins.

Kaczmarek (1993) developed WatBal, a lumped conceptual model with two main components. The first component calculates potential evapotranspiration using Priestley-Taylor method, while second component computes the water balance of the basin.

Arnold et al. (1998) reported that SWAT is well-suited model to agricultural watersheds. It is a river basin-scale, continuous-time, spatially distributed, physically based model to predict the impacts of land management practices on water, sediment, and agricultural chemical yields in complex catchments with diverse soils, land use and management conditions over period.

Arnold et al. (2000) used SWAT model to predict base flow and aquifer recharge over a large area (roughly 5,00,000 km2) of the Upper Mississippi basin. They found that SWAT's estimates of groundwater recharge and discharge (base flow) for specific 8-digit watersheds compared well with filtered estimates for the basin. This was validated against an interpreted hydrograph (to determine the fraction of base flow) and a calculated water balance (to determine recharge amount). The study demonstrated that SWAT model could reasonably predict base flow and recharge on a monthly basis over a 22-month period.

Oyebande (2001) highlighted that the primary challenge in successfully applying rainfall-runoff model is the lack of monitoring data, particularly the spatial distribution of rainfall over the catchment area, as rainfall is the key input for any hydrological model. Another significant issue is the absence of reliable flow data, which can result in inaccurate calibration and validation of catchment parameters.

Kalbus et al.(2006) reviewed different measurements methods of groundwater and surface water interactions. They reviewed direct measurements of water flux, heat tracer methods, methods based on darcy's law and mass balance approach. They also reviewed methods to determine contaminant concentration. They gave considerations for choosing appropriate methods including spatial and temporal scale, uncertainty and limitations and concluded that multi-scale approach combining multiple measurement methods may consider constrain to estimates flux between groundwater and surface water.

Vijay et al. (2006) concluded that watershed models simulate natural processes such as the flow of water, sediment, chemicals, nutrients, and microbial organisms within watersheds, while also quantifying the impact of human activities on these processes. Simulation of these processes is essential for addressing a wide range of water resources, environmental, and social issues. The current generation of watershed models is highly diverse, differing significantly in terms of sophistication, data requirements and computational demands.

Gassman et al. (2007) reviewed SWAT model, which represents nearly 30 years of modelling efforts. They reported that SWAT has gained international recognition as a robust and flexible interdisciplinary watershed modelling tool, as evidenced by international SWAT conference and over 250 scientific articles published in peer-reviewed journals. The authors described SWAT as a basin-scale, continuous-time, physically based model that is computationally efficient and capable of simulating long-term processes on daily, monthly, and yearly time steps. Major components of the model include weather, hydrology, soil temperature and properties, land management, nutrient, plant growth, pesticides. They further highlighted SWAT's ability to study water resource availability, assess the impact of climate change, impact on hydrology, evaluate pollutant load, calibrate streamflow and analyze related hydrologic processes, as well as assess the

effect of management practices on water, sediment, and agricultural chemical yields in ungauged watersheds.

Kumar et al. (2007) studied the availability and demand of water resources in India as well as described various issues and strategies for developing a holistic approach for sustainable development and management of water resources of country. It also highlighted integration of blue and green flows and concept of virtual water transfer for sustainable management of water resources for meeting the demands of present. They also highlighted problems of flood and draught syndrome, overexploitation of groundwater, reduction in river flow, salt water intrusion in aquifers, waterlogging and salinity in some of the command areas.

Boman and Shukla (2009) examined various methods and instruments used for measuring water in agricultural irrigation and drainage systems. They concluded that the trajectory method is applicable only to streams where flow can be diverted into a pipe.

Neitsch et al. (2009) described SWAT as a spatially distributed, continuous river watershed-scale model that operates on a daily time step. It predicts the impact of land management practices on water, sediment and agricultural chemical yields, accounting for varying soils, land use and management conditions over long time periods.

Easton et al. (2010) used SWAT to predict runoff and sediment losses from the Ethiopian Blue Nile basin (1, 74, 000 km^2). They found that runoff losses, particularly during the monsoon season, increased significantly from shallow soils. Their study indicated that focusing on small areas of the landscape where runoff is generated can be the most effective strategy for controlling erosion and protecting water resources.

Jain et al. (2010) highlighted that remotely sensed data offers valuable and real-time spatial information on natural resources and physical parameter. Geographic Information Systems (GIS) are effective tools in watershed modelling because they allow for the integration of remote sensing data with conventional database to estimate runoff, aiding in the planning of suitable soil and water conservation measures. The current trend in hydrology involves using mathematical models for evaluating watersheds, coupled with the extraction of watershed parameters through remote sensing and GIS.

Kousari et al. (2010) reported that Soil Conservation Service Curve Number (SCS-CN) method remains a widely used and enduring technique for estimating the direct surface runoff volumes in ungauged catchments. This method is based on empirical study of runoff in small catchments.

Abushandi (2011) concluded that assessing water resources availability requires a detailed understanding of hydrological processes. Given the complexity of these hydrological processes, on

sustainable basin management should focus on understanding rainfall characteristics and basin properties. Various hydrologic models are used for water resource assessment, and rainfall-runoff models have been crucial in the optimal planning and management of catchment water resources.

Hilgersom and Luxemburg (2012) integrated the rising bubble technique with modern image processing methods to obtain discharge measurements. They applied this technique in both laboratory and field settings, determining the bubble rising velocity for specific nozzles. By capturing digital photographs of the bubble envelope at the water surface, each picture provided a single discharge measurement. This digital approach resulted in accurate discharge measurements, even in turbulent conditions, and averaging multiple images produced reliable results. The study suggests that the rising bubble technique can be a preferred method for discharge gauging in certain situations.

Najafi et al (2012) compared two methods for streamflow prediction: Climate Signal Weighting Methods and Climate Forecast System Reanalysis. They concluded that the timed volume method is only suitable for streams with low flow rates and small falls.

Arun (2013) estimated runoff for Darewadi watershed of Ahmednagar district, Maharashtra, using remote sensing (RS) & GIS. By applying the SCS curve number method with daily rainfall data over 20 years using the OVERLAY technique. He found that the average curve number for the watershed changed from 85 before treatment to after treatment. Additionally, the maximum recharge capacity of watershed increased from 44.82 mm to 80.72 mm after five days of antecedent rainfall. He concluded that RS & GIS based SCS-CN model is effective for estimating surface runoff depth when hydrological information is limited.

Patel and Srivastava (2013) noted that watershed models provide insight into the availability, requirement, distribution and utilization of water in watersheds. For agricultural watersheds, need-based water allocation is essential for achieving targeted food production, which can be facilitated through the spatial and temporal simulation of water resource availability.

Srivastava et al. (2013) highlighted that distributed hydrological watershed models are highly effective tools for water resources management, particularly for assessing the impacts of land use/land cover (LULC) and climate change on water resources.

Shope et al. (2013) compared six discharge measurement methods at 13 locations with varying slope (1% to 80 %) and discharge levels spanning four orders of magnitude. They identified the weir, acoustic Doppler current profiler (ADPC), and the in-stream velocity area method as most accurate, but noted that each method has limitations under specific conditions.

Bansode et al. (2014) utilized the SCS Curve Number Method and ArcGIS in the Khuldabad basin, Aurangabad district of Maharashtra. The study incorporated factors such as

watershed area, slope, and vegetation cover, using ten years of rainfall data (2003-2012) and IRS LISS-III data to create a land use/cover map at a 1:50,000 scale.

Bhange et al. (2014) applied remote sensing and GIS to estimate the runoff from the Ashti watershed in Beed district, Maharashtra state, using IRS P-6 LISS-III satellite data and ArcGIS software to overlay thematic maps like slope, rainfall and LULC maps. The Soil Conservation Curve Number method was used to determine runoff volume distribution.

Chauhan et al. (2014) compared discharge data from the Ganga River basin using ADCP and conventional current meter, concluding that ADCP yields smaller relative errors compared to the traditional method.

Munyaneza et al. (2014) developed a hydrological model for water resource planning and decision making for better management of Migina catchment (257.4 km^2). They utilized HEC-HMS model, incorporating rainfall from 12 stations and stream flow data from 5 stations. While the model was calibrated, validation could not be performed due to lack of data. However, the results from tracer-based hydrograph separation study were compared with the runoff results of model. The model demonstrated reasonable accuracy in simulating total flow volume, peak flow and timing and distribution of direct runoff and baseflow. The study also revealed significant variations groundwater storage and runoff components across the catchment, offering valuable insights into distinct hydrological processes at the sub-catchment scale.

Devi et al. (2015) evaluated various hydrological models like VIC, TOPMODEL, HBV, MIKE SHE and SWAT across different regions. suitability of various model in different regions. They found that VIC model performs well in moist areas, MIKE SHE is limited to smaller catchments due to its data requirements, SWAT model provides good hydrologic predictions with minimal calibration, HBV gives satisfactory results, and TOPMODEL is suited for catchments with shallow soil and moderate topography.

Mondal et al. (2016) reviewed advances in hydrological science and highlighted the need for incorporating dynamic LULC changes into distributed hydrological models to reduce uncertainty from static assumptions. They emphasized the potential for significant research contributions in Indian hydrology due to its spatial and temporal heterogeneity.

Dobriyal et al. (2017) reviewed streamflow monitoring methods, recommending the timed volume method foe small streams in hilly terrain due to its accuracy and ease of use, and the weir and flume methods for long-term studies despite their higher cost.

Juniati et al. (2018) reviewed the literatures on water availability estimation methods and recommended the water balance method as a more fundamental and appropriate tool for this purpose. They emphasized that improving water availability estimation method can enhance the

formulation of Regional Spatial Plans (RSP) and support evaluation of land use capacity in ensuring sustainable water resources.

Siddi et al. (2018) applied SCS-CN Method with RS and GIS Techniques to estimate rainfall-runoff in the Mandavi Basin, YSR Kadapa District, Andhra Pradesh, revealing a relationship between rainfall and runoff from 1995 to 2014.

Adeniyi and Abdulrasaq (2019) compared various streamflow measurement methods, concluding that while weirs are suitable for small rivers, flumes offer advantages in agricultural systems due to their self-cleaning nature, lower maintenance cost and higher accuracy.

Rankova (2019) examined various methods for creating an operational tool to assess the annual water resource in Vir River of Sofia, Bulgaria. She concluded that the water balance method is generally preferable for water resource assessment because it eliminates the influence of anthropogenic factors on the river flow. The calculations indicated that the surface water resource estimates from this method closely matched those obtained using the hydrological method. However, the water balance method requires substantial information, resources and time, making it more suitable for research purposes. For operational use, applying the water balance method would require readily available data on current water consumption, which is often limited to a small number of cases.

Singh et al. (2020) reviewed hydrological modelling advances in India, highlighting developments in surface and ground water modelling, satellite-based sensing, and uncertainty quantification across various scales and regions.

Gabale and Deshpande (2020) used geospatial technique and SCS-CN method to estimate runoff in Sudha River basin of Indrayani River, demonstrating the utility of GIS and remote sensing for managing watershed hydrological features.

Mbajiorgu (2020) explored the hydrology of surface water resources, focusing on catchment rainfall-runoff processes and modelling. The study reviewed the fundamentals of lumped conceptual and physically-based distributed modelling approaches, emphasizing their integration with water quality models for integrated water resources management (IWRS). Key issues such as calibration, data assimilation and uncertainty were discussed, highlighting both manual/heuristic and automatic calibration methods, including optimization and ensemble inference techniques. The challenge of equifinality in the automatic calibration of hydrological models was also addressed. The SWAT model was presented as a prominent example of a physically-based distributed catchment tool for surface water hydrology and assessment. The stages and procedures of water resources assessment were outlined for different categories of surface water, including rivers, ponds, reservoirs and natural wetlands. The study also covered

monitoring, data collection and analysis, along with the various water quality parameters and indices used to assess the environmental aspects of surface water resources.

Mohammed et al. (2020) studied water availability assessment in the Fincha and Didessa sub-basin of Ethiopia using HEC-HMS. The performance of model was assessed via calibration at gauging station and shows good performance. The parameter optimized at little anger and Neshi gauging station was used for flow simulation to assess water resource availability on monthly and annual basis. The flow component was also separated at small catchment considered for all sub-basin. The result shows that high percentage of flow occupied by Direct runoff for both Didessa and Fincha subbasin.

Samboko et al. (2020) proposed a framework for monitoring volatile, dangerous and difficult to access rivers using only affordable and easy to maintain new technologies. The framework consists of four main components: i) establishment of geometry using airborne photogrammetry and bathymetry; ii) physically based rating curve development through hydraulic modelling of surveyed river sections; iii) determination of non-intrusive observations with for instance simple cameras or satellite observations; and iv) evaluating the institutional and societal impacts of using new technology. They addressed research questions such as the factors impacting on accuracy of geometrical information of the floodplain terrain and bathymetry , the accuracy of a physically based rating curve compared to a traditional rating curve needs to be established, for rapidly changing river segments, it should be investigated if the collection of occasional snapshots of multiple proxies for flow can be used to assess the uncertainty of river flows. The study finally explored the social and institutional impact of using new technologies for remote river monitoring.

Abed (2021) examined the integration of float method and defined the parameters affecting the acceleration of floating sphere in flowing water using experimental measurements. In this different size of solid plastic spheres with different weights were used as a float to measure velocities and then discharge computation. The results indicate that the integrating float technique is feasible and accurate for measuring flow of low velocity in open channels. It was desirable to use small floats with specific gravity closer to unity to get more accurate results. After comparing with discharge obtaining with other method good agreement was observed with an error of less than 2.5%

Toussef et al. (2021) integrated two models – the Soil Water Assessment Too (SWAT) for future climate prediction and the Water Evaluation and Planning (WEAP) model for the simulating water quantity in the Hongshui River Basin (HRB), China, to assess the impacts of climate change. The SWAT model was used to generate streamflows, which were calibrated and validated using observed data from 1991 to 2001. Six scenarios were established to evaluate the basin's response under socio-economic conditions. The simulated results indicated that precipitation and streamflow are likely undergo a slight increase, and available water resources would be sufficient

to meet the existing demands until 2050. However, under the high climate change emission scenario (RCP-8.5), the basin could face water shortages. The study emphasized the need for improved long-term water management policies to ensure the sustainability of water resources and meet future downstream water needs.

Jethe et al. (2022) applied remote sensing and GIS to estimate surface runoff using the NRCS SCS curve number method in the Maharashtra watershed of Tavarja Lake, suggesting high runoff potential in the region.

Kale et al. (2022b) estimated runoff in the Kudavale watershed in Dapoli Tehsil using SCS-CN method and GIS, finding that agricultural land, forest land, barren land and residential area covered 15.42 %, 59.90 %, 21.22 % and 3.4 %, respectively, with average runoff of 1532.27 mm.

Brock et al. (2023) studied methods for measuring streamflow in rivers, emphasizing that the choice of method depends on stream size and discharge. They discussed various sensors and methods for measuring stream stage and discharge in both wadeable and non-wadeable channels.

Wang et al. (2023) proposed three methods for estimating monthly water storage changes across Canada, one based on land surface runoff and two using water budget, concluding that water budget methods, particularly those considering water area dynamics, showed improved accuracy over surface runoff methods, especially in wet climate regions. Their findings are useful for calibrating hydrological models and assessing climate change and human disturbance impacts on water resources, and filling the water storage change data gaps in GRACE-based total water storage decompositions studies.

Among the literatures reviewed, hydrological models were identified as suitable for this study because they account for spatial and temporal variation in land cover/use, climate change and the soils. Among these hydrological models, Soil Water Assessment Tool (SWAT) model was found to be particularly appropriate. SWAT uses the GIS interface and is widely used across different geological and climatic zones due to of its robustness in assessing the impact of land management practices on surface water availability, sediment and agricultural chemical outputs under varying soils, land use and management conditions over long time periods.

2.2 Impact of soil, land use, and slope on temporal and spatial variability of water availability

Wenming et al. (2011) used SWAT to assess the impact of land use and land cover (LULC) changes on hydrology in the Upper San Pedro watershed (7400 km^2) in Mexico. They combined hydrological modelling and multiple regression analysis to quantify the contributions of different LULC classes to changes in hydrological components for four time periods (1973, 1986, 1992 and 1997). The study found that urbanization and mesquite invasion increased runoff, reduced

percolation, and increased evapotranspiration (ET), negatively affecting water resources in the basin. Compared to the LULC baseline in 1973, average annual water yield increased by 0.07 mm in 1986, 0.13 in 1992, and 0.25 mm in 1997, corresponding to increases of 1.9%, 3.5% and 6.8%, respectively.

Nguyen and Nguyen (2012) applied GIS technique and the SWAT model to quantify the impact of topography, land use, soil and climatic conditions on water discharge of Be River basin, Vietnam. GIS was used to input elevation, soil properties, land use and weather data into SWAT, which then simulated various physical processes and displayed discharge data. Their study showed that monitoring flow discharge could provide valuable information for flood forecasting, predicting sediment loads, and assessing the impact of climate change to water resources. The model performance was validated with R^2 and Nash-Sutcliffe Index (NSI) values above 0.7 for the period of 1979 to 1994.

Vara Prasad (2012) evaluated the effect of different land uses on the water yield in Kothakunta sub watershed in India (550 ha). Using SWAT, the study quantified water yield under varying soils, land use and management conditions over a long period. The model simulated water yield by reducing the area under paddy cultivation by 25% and reallocating it for irrigated dry crops, which helped assess aquifer recharge and led to the finalization of an alternate cropping system for sustainable groundwater resources.

Wagner et al. (2013) assessed the impact of land use changes on the hydrology of Mula and Mutha river catchments upstream of Pune, India. By analyzing land use classification for 1989/1990, 2000/2001, and 2009/2010, they found that urbanization increased from 5.1% to 10% and cropland from 9.7% to 13.5% over 20 years. This urbanization led to a 7.6% increase in water yield.

Yan et al. (2013) used SWAT to assess the impact of LULC changes on streamflow and sediment yield in the Upper Du watershed (8973 km^2) in China. Hydrological modelling and partial least squares regression (PLSR) were employed to quantify the contribution of different land use types. The study found that changes in grassland had minimal impact on streamflow and sediment yield.

Ziadat and Taimeh (2013) investigated the effect of rainfall intensity, slope, land use and antecedent soil moisture on soil erosion and runoff. Twelve sites from Al-Muwaqqar watershed, Jordan, were selected representing six slope angles: 1, 2, 3, 5, 7 and 9%. Each slope included two sites - one cultivated with barley and other used as rangeland. Soil erosion was measured under three rainfall intensities (3, 5 and 10 mm h^{-1}) and three different antecedent soil moisture contents (dry, wet and very wet) using a rotating disk rainfall simulator. The results revealed that rainfall intensity was the most important factor influencing soil erosion, with erosion occurring even at

relatively low intensities on wet soils due to successive rainfall events. On cultivated land, soil erosion was mainly driven by moisture content, whereas, on uncultivated land, slope steepness was the dominant factor. Regression equations showed that rainfall intensity, slope and antecedent moisture explained 84–89% of the variation in runoff and 59–66% of the variation in soil loss.

Zhang et al. (2015) conducted a study to develop an effective land use plan on suitable slope gradient to control soil erosion in a red soil hilly watershed of southern China by using the GeoWEPP (Geo-spatial Interface for the Water Erosion Prediction Project) model. The model simulated four typical land uses (forest, farm, orchard and fallow land) to evaluate their impacts on soil erosion. The results showed that the runoff decreased by 44.7% and 61.1% in forest and orchard areas, respectively, compared to the current land use, while sediment yield decreased by 43. 7% and 68.6%. In contrast, runoff and sediment yield increased by 52.2% and 42.6% for farmland and 48.8% and 29.6% for fallow land. Soil erosion also increased with slope gradient, following a quadratic regression equation for all land uses. Although a critical slope gradient of 15^{o} was suggested for converting farmland to forest or other uses, this threshold may not be accurate for the red soil region.

Das et al. (2018) evaluated the impacts of LULC change on the runoff, baseflow and ET in eastern Indian river basins between 1985 and 2005 using the variable infiltration capacity (VIC) approach. The study found that deforestation, urbanization and cropland expansions led to decreased ET and increased runoff and baseflow.

Lohar et al. (2018) studied site suitability analysis for establishing soil and water conservation structures using geoinformatics in Chinnar watershed in Tamil Nadu. In this they used thematic layers such as runoff, slope, land cover/ land use, lineament, drainage density, soil texture and geomorphology. All these layers were prepared with the help of remote sensing images and toposheets and integrated using weighted overlay techniques in GIS environment to derive suitable sites for soil and water conservation structures. The lower value of one was assigned to the factor that is not favourable for the conservation structures and the higher value of nine was assigned to the factor that is highly suitable for conservation structures. All the factor values were summed up and overall site suitability score was computed. The computed score was classified finally into four suitability classes. The results show that only less than one percent area is highly suitable for implementing soil and water conservation structures. About 34 percent of the study area is moderately suitable and about 65 percent area is less suitable for soil and water conservation structures.

Bande et al. (2019) analysed site suitability for water conservation using AHP and GIS techniques in upper Sina River catchment in Ahmednagar. Multicriteria evaluation is carried out using Geographic Information System (GIS) techniques to defining suitable site for construction of water conservation structures. Different layers which were considered for multi-criteria evaluation:

slope, land use land cover, soil texture, lithology, soil depth, soil erosion, wells, lineaments and drainage network. Analytical Hierarchy Processes (AHP) is used for weighted sum to find suitable sites for implementation of water conservation activity using selected criterions. The site suitability map was classified into four classes: highly suitable, moderately suitable, less suitable and not suitable with area of 19.19%, 26%, 49.03% and 5.78, respectively.

Munoth & Goyal (2019) used SWAT to assess the impact of LULC changes on runoff and sediment yield of the Upper Tapi River Sub-basin in India. Analyzing four land use maps from 1975, 1990, 2000, and 2016, they found that LULC changes resulted in increased surface runoff, water yield, and sediment yield.

Zhu et al. (2019) synthesized data from 325 sites across 152 studies to analyze the factors influencing the soil erodibility factor (k), including land use type, climate, topography, soil, and vegetation restoration age. The results indicated that areas with slopes greater than 25° had a higher k factor (k = 0.1047) compared to those with slope less than 6º (k = 0.0637) or between 6º and 25º (k = 0.0832). The k value initially increased with vegetation restoration age but gradually decreased over time. Land use also impacted the k factor, with cropland (k = 0.0697) having higher k value than grassland (k = 0.0663) but lower than that forested areas (k = 0.0967). The study concluded that the soil characteristics most were most important factors affecting the k, followed by topography and climate. Among these, soil nitrogen content and precipitation were identified as the two most critical factors influencing the k value.

Guo et al. (2020) used classical statistical methods and Canonical Correspondence Analysis to study the spatial heterogeneity of soil moisture at depths of 0–20, 20–40, and 40–60 cm on slopes, aiming to identify the main controlling factors and their relative contributions. The results showed that average soil moisture content decreased in the following order: grassland > shrubland > soybean land > maize land > adzuki bean (*Vigna angularis*) land > forestland. The soil moisture content (SMC) profiles could be categorized into four distinct patterns, influenced by vegetation types, root system characteristics, and topographic attributes. The spatial variability of soil moisture was strongly influenced by slope gradient, followed by land use types, elevation and slope position, with slope aspect having the least impact. Additionally, land use type had a greater influence on soil moisture in deeper layers, whereas topographic attributes had a stronger influence on surface layers than on deeper ones. The study highlights how land use types and topographical elements interact to affect soil moisture variability and vertical distribution at differing depths.

Mengistu et al. (2021) analysed the spatio-temporal variability of soil water dynamics in dry regions of South Africa using SWAT model to estimate soil water balance dynamics. The model was calibrated and validated through regionalization based on physical similarity. Unlike the revap water (water drawn upwards from shallow groundwater tables), soil water content, percolation and lateral flow increased with precipitation. The Mann-Kendall trend test indicated no significant trend

of annual and monthly soil water content and percolation. However, there was a decreasing trend of 1.091 mm per annum in the revap water. The contribution of revap water to evapotranspiration varied from 9% during summer to 32% during spring.

Samal and Gedam (2021) examined land use changes in the Upper Bhima basin and their impact on water resources. They used SWAT model to simulate hydrological processes, finding significant correlations between urbanization and surface runoff (R = 0.96), water yield (R = 0.57), and negative correlation with baseflow (R = 0.95) and percolation (R = 0.99).

Ward et al. (2021) used AHP for spatial analysis to determine water surface storage suitability in Cambodia. In this pairwise comparisons between essential engineering criteria: soil drainage, geologic porosity, precipitation, land cover, and slope is done. Then, model weights were calculated based on the comparisons. Using the model weights, a water harvesting suitability model showed that 19% of Cambodian land has high suitability, and about 13% of the land has the best suitability.

Gangarde et al.(2023) study undertaken was Kadivali watershed of Dapoli tehsil in Ratnagiri district for selection of water harvesting structures using remote sensing and GIS technology. The CARTO-DEM (30m) was used to prepare thematic layers viz slope map, drainage map, drainage density map. LISS III image was used to prepare the Land use/ land cover map of study area. Lithology map and Geomorphology map were downloaded from Bhukosh –geological survey of India portal. Soil texture map of Kadivali watershed was prepared using soil texture data obtained from NBSS-LUP, Nagpur. The weightages are assigned to the layers as per their contribution to suitability and ranking is allotted to each thematic layer. Integration of all thematic layers with assigned ranking gave suitability map of study area. Study found forty-five suitable structures for water harvesting.

Ranjan and Singh (2023) assessed the hydrological response to LULC change on the Punpun River basin using high-resolution gridded rainfall and temperature data from 1995 to 2020 with SWAT. The study revealed increases in evapotranspiration (7.01%), built-up area, surface runoff, and water yield, while groundwater contributions decreased over the period studied.

Sahita et.al (2023) studied the Upper Shetrunji River basin using a hydrological model linked with GIS. They used LULC, meteorological, and soil data for watershed modelling, calibrated and validated with SWAT-CUP SUFI-2 algorithm. The LULC change detection indicated significant increases in agricultural, urban, and water body areas between 2000–2010 and 2010–2020. The study concluded that LULC significantly influenced runoff in the upper Shetrunji River basin.

Wang et al. (2023) quantified the spatial variations of soil functions and their influencing factors by analysing eight typical land use types and five slope positions in an agricultural small watershed in the Chinese black soil region. Five soil functions, e.g., primary productivity (PP), water purification and regulation (WPR), climate regulation and carbon sequestration (CRCS), provision of habitat for biodiversity (PHB), and nutrient cycling and provision (NCP) were assessed based on 22 measured soil properties. The results showed variations in all soil properties with respect to land use type and slope position ($p < 0.05$). Soil functions also varied significantly between different land use types and slope positions ($p < 0.05$). Lower soil functions were observed in roads and cropland, particularly at the middle slope position of cropland. Redundancy analysis identified soil cation exchange capacity, available nitrogen, urease, structure stability index, invertase activity, total nitrogen, soil organic matter and alkaline phosphatase were the dominant factors attributed to the spatial variation of soil functions. The corresponding contributions were 13.9 %, 11.4 %, 8.9 %, 7.6 %, 7.0 %, 6.1 %, 5.7 % and 5.50 %. Structural equation modelling further revealed that soil erosion was the dominant process reducing soil functions by altering soil properties. To enhance soil functions in degraded cropland, measures to promote nutrient accumulation and control soil erosion should be implemented.

2.3 Assessment of surface water availability

Somura et al. (2007) applied the SWAT model to the Hii river basin (900 km^2) in Japan to simulate discharge from 1986 to 2005. They observed changes in discharge at each sub basin in response to a 20% change in annual total precipitation.

Britta et al. (2008) used the SWAT to assess the influence of various parameters on streamflow in lowland catchments in northern Germany, specifically in the Stor, Treene, and Kielstau basins (50 to 517 km^2). They found that groundwater parameters were highly sensitive and the most influential factors for improving simulated water discharge.

Groundwater Technical Workgroup (2010) proposed a three-pronged approach – monitoring, mapping and management – to achieve sustainable groundwater management amidst rising water demand in all sectors. The report emphasized that implementing its recommendations would be enhance understanding of groundwater systems, their interaction with land use practices, surface water systems, and their impacts on ecological and public health. It also highlighted the strengths and weaknesses of various tools and reviewed the necessary data for making these approaches effective for a long-term management strategies. The recommendations reflect a broad consensus among water resource professionals on best practices for sustainable water resource management.

Daniel et al. (2011) emphasized the importance of assessing water resource availability for effective planning, development, and management, typically at the basin level. This involves

estimating the flow available at the outlet of a river catchment, achieved by quantifying runoff within the watershed.

Arnold et al. (2012) developed several SWAT calibration techniques, including manual and automated methods, and introduced SWAT-CUP, which incorporates a semi-automated approach (SUFI-2) for calibration and uncertainty analysis. They noted that SWAT-CUP allows for iterative manual adjustments between auto-calibration runs, helping users gain a better understanding of hydrologic processes and parameter sensitivity.

Malunjkar et al. (2015) used SWAT to determine surface runoff for the Maheshgad watershed in Rahuri, Maharashtra, manually calibrating and validating the model. They reported annual simulated runoff values of 42 mm and 81.24 mm for calibration and validation periods, respectively. They concluded that SWAT effectively simulates surface runoff from small watersheds.

Gharde (2015) conducted hydrological modelling of runoff and sediment yield in the Konkan region of Maharashtra using ArcGIS interface for SWAT. The model performed well in predicting daily runoff and sediment yield for Savitri basin and Kal rivers, though it over-predicted surface runoff. Sediment yield was found 1.04 tones/ha/year for Savitri basin and 1.47 tones/ha/hr for Kal river.

Mehendale (2016) modeled streamflow in the Morna catchment using SWAT and compared the SUFI2 and GLUE techniques within SWAT-CUP for calibration and validation. Based on statistical parameters like the coefficient of determination and Nash-Sutcliffe efficiency, she concluded that the SUFI-2 technique was superior for runoff calibration and validation.

Baykond et al. (2017) estimated water availability in Badra River basin of Balehonnuru catchment area using SWAT model. The model was calibrated and validated for the periods 1999-2010 and 2011-2015, respectively, with R2 and NSE values of 0.878 and 0.78 for calibration and 0.869 and 0.76 for validation. Future water availability was estimated using RCP 4.5 and RCP 8.5 scenarios.

Gavit et al. (2017) applied the SWAT model to estimate runoff in Upper Godavari sub-basin, using DEM for delineation and slope mapping. Land Use Land Cover (LULC) map was prepared using IRS-P6 LISS-III images. The model was calibrated and validated using hydro-meteorological data from 1994 to 2014 with coefficient of determination (R^2) values of 0.81 and 0.84 for calibration and validation, respectively. The results showed that SWAT is effective for simulating runoff and testing management scenarios in watersheds.

Gavit (2017) studied rainfall-runoff modelling for Upper and Middle Godavari sub-basins using RS & GIS, finding that the SWAT model performed satisfactorily in simulating runoff during calibration and validation periods for both sub-basins.

Jedhe et al. (2018) assessed the water resources and planning in context of climatic variability for Konkan region. They studied annual and seasonal water surplus/deficit in Konkan region and impact of climatic variability using ArcSWAT model which is calibrated and validated using SWAT-CUP SUFI2 algorithm to assess the monthly water resource availability in Amba River basin. He concluded that average monthly river flow in Amba River basin was highest in the month of August followed by July, September, June, October thereafter flow decreased continuously.

Mistry and Joshi (2018) developed a rainfall-runoff model for Shakkar River using SWAT model, delineating the catchment area into 23 sub-basins. Using 21 years of rainfall and temperature data, they simulated runoff, finding a correlation coefficient of 0.8019 between rainfall and runoff.

Gupta et al. (2019) used the SWAT model to simulate the hydrological processes in the Indrayani and Bhima River basins in Pune district, using GIS data for model setup and streamflow data for calibration. The model effectively simulated the streamflow and can be used for future water resource management.

Parikh and Parekhe (2019) analysed runoff response in the Deo River, Panch Mahal, Gujarat using SWAT, calibrating and validating the model with SWAT-CUP SUFI-2 algorithm. The model performed well, R^2 and NSE values of 0.89 and 0.87 during calibration, and 0.88 and 0.81 during validation, making it useful for runoff prediction and flood forecasting.

Sudhakar *et al.* (2019) applied SWAT to Godavari River basin to derive parameters for hydrological modelling. The model demonstrated effectively in quantifying basin-scale water resources and studying runoff with limited meteorological data.

Herndon et al. (2020) evaluated two global dynamic surface water datasets, 15 spectral indices designed to classify surface water extent, and three decision tree methods specifically developed for identifying surface water in semi-arid environments. The study found that the while global surface water datasets effectively reduce false positives, they significantly underestimate the presence and extent of smaller, more turbid water bodies that are critical to local livelihoods. This limitation makes them less suitable for monitoring water availability in these areas. Among the spectral indices, three demonstrated both high accuracy and threshold stability across different regions and seasons. The performance of the three decision tree methods varied, with only one achieving accuracy comparable to the best-performing spectral indices. The findings suggest that while global surface water datasets area suitable for large-scale analysis, methods calibrated to local conditions may offer better accuracy for localized water monitoring needs.

Ishak et al. (2020) assessed water availability in the Omu watershed using FJ.MOCK, NRECA and SMEC models. The study utilized rainfall, climatological data, catchment area information, and land use data. When comparing the results of water availability analyses with instantaneous discharge values, the FJ.MOCK model proved to be the most accurate, closely

matching the observed discharge values.

Pandey et al. (2020) developed a multi-site calibration approach for large basin, the Karnali-Mohana in western Nepal using SWAT. Their results showed that 34% of annual precipitation in the basin was lost as evapotranspiration, with significant spatio-temporal heterogeneity.

Bera et al. (2021) used They examined the spatio-temporal distribution of surface water in the entire Ganga basin to identify actual caused of water shortage during lean season. Based on DEM, Slope, soil, LULC and weather data, SWAT model was run at catchment scale with good performance under R2 and NSE evaluation methods. The study shows that annual water availability is 1216165.5 cumec. The study also established that actual evapotranspiration of entire basin is much higher than precipitation during the lean season and indicated great deviation between supply and demand.

Talawar and Seelam (2023) estimated discharge values for Mondovi River in Goa state using SWAT, with model simulations calibrated and validated using observed data. The results showed good agreement between simulated and observed values, with R^2 and NSE values of 0.88 and 0.80.

Genjebo et al. (2023) assessed the surface water resources and identified optimum distribution strategies for Ethiopia's upper Bilate watershed. Using historical climatic and streamflow data from 2010–2019, they conducted a rainfall-runoff analysis with Hydrologic Engineering Center Hydrologic Modeling System (HEC-HMS)-Geospatial Hydrologic Modeling Extension. The study found that under current conditions, 99.8% of water supply needs were met, leaving only 0.2% unmet. However, as the average annual water demand was projected to rise from 111.13 MCM to 176.08 MCM in the future, the scenario for 2035 predicted that only 69.8% of the water demand would be met, leaving 30.2% unmet, particularly for irrigation development and population growth. To enhance water availability and optimize distribution, the study recommended constructing a hydraulic structure, such as a dam, upstream of the watershed.

Prajapati et al. (2023) applied the SWAT model to predict hydrological flow in the Sunkoshi River Basin (SRB) of Nepal using 36 years of daily rainfall and temperature data. The study aimed to (i) simulate the long-term hydrologic response, and (ii) generate spatially distributed rainfall–runoff and subbasin-wise water balance components using established performance indicators. Calibration and validation at the outlet of the study area were successful, with the values of R^2/Nash–Sutcliffe efficiency (NSE) calculated as 0.91/0.82 for monthly data and 0.79/0.73 for daily data. In the validation phase, the values of R^2/NSE were 0.91/0.84 for monthly data and 0.82/0.75 for daily data, respectively. This study predicted the average yearly flow and precipitation at the SRB outlet to be 279 m^3/s and 368.25 mm, respectively. Water losses were attributed to evapotranspiration (30%), runoff (18%) and lateral flow (30%).

Khadatare et al. (2024) studied the water balance of the Arjuna River basin of Ratnagiri District of the Maharashtra using ArcSWAT model. They simulated various water balance components, finding minimal groundwater contribution during dry months. The model performed well during calibration and validation, with R^2 values of 0.78 and 0.67, and NSE values of 0.75 and 0.65, respectively.

2.4 Critiques on Reviews

Based on the reviews, it is concluded that remote sensing and GIS-based models have proven to be more reliable for assessing and planning of water resources at basin scale. These models require less data and resources compared to traditional methods, and physically based models, in particular, offer better predictive capabilities for both gauged and ungauged catchments. By estimating surface water availability, it is possible to identify areas of water deficiency and surplus with simple procedures and existing data. This allows for targeted interventions, such as constructing groundwater recharge and conservation structures to store water during surplus period. Additionally, high runoff and flood events can lead to soil erosion and land degradation, resulting in the loss of topsoil and nutrients, reduced agricultural yield, reservoir sedimentation, diminished storage capacity, and shutdowns of hydropower plants. By analyzing parameters such as soil, land use and slope, water resources can be managed more effectively. The information generated from surface water availability assessments supports sustainable water use and facilitates the development and implementation of economic tools for resource management.

CHAPTER III: MATERIALS AND METHODS

Surface Water (SW) and Groundwater (GW) are essential components of the natural hydrological cycle, sustaining life on Earth. Over the past few decades, these water resources have faced significant changes due to both human activities and natural processes (Garci-Ruiz et al., 2011), leading to a reduction in freshwater availability. Advances in scientific knowledge, along with improvements in measurement and modelling techniques, have emphasized the importance of investigating effective conservation and management strategies for these critical resources (Kalbus et al., 2006).

This chapter deals with the methodology adopted and procedures used to study various methods for assessing surface water availability. It also examines the impact of parameters such as soil, land use, and slope on temporal and spatial variability of water availability in river basins of Konkan region. Additionally, it details the assessment of total surface water availability in these river basins to achieve the following objectives.

1. To study different methods for assessing surface water availability.
2. To study the impact of parameters like soil, land use, and slope on temporal and spatial variability of water in river basins of Konkan region.
3. To assess total surface water availability in river basins of Konkan region.

To fulfil objectives of study, detailed procedure and methodology adopted is presented in this chapter under the following sections 3.1 to 3.4

3.1 Study Area

3.1.1 Description of Study Area

Maharashtra, located in is western India, covers a total geographical area of 30.08 Mha and divided into four divisions. One of divisions, Konkan region, is further subdivided into four sub-basins: North Konkan, Mid Konkan, Vashisthi, and South Konkan sub-basins. In north Konkan basin starting with Ullas Basin in Thane, it covers an area of 4513.91 km², representing 19% of the total area. In Palghar, the Vaitarna Basin spans 3837.45 km². In Raigad, the Patalganga-Amba Basin encompasses 2779 km². Ullas, Vaitarna are in valley 21. The Kundalika Basin in Raigad, covering 893.46 km² and the Savitri Basin occupies 2335.46 km² and as outlet of Patalganga and Amba is combined it is also included in valley 22. In Ratnagiri, the Vashisthi Basin spreads across 2562.53 km² and included in valley 23, and the Shastri Basin covers 2570.41 km². Other smaller sub-basins in Ratnagiri include Kajivi (543.12 km²), Kodvali (698.60 km²), Muchkundi (792.81 km²), and Waghton (897.99 km²). In Sindhudurg, the Karli Basin spans 794.51 km² and Gad Basin, at 983.78 km², and the smaller Devgad Basin (704.41 km²) and all this basins from shastri to Devgad are encompasses in valley 24. In Sindhudurg, Terekhol spans 761.51 km² which is

included in valley 25. The study excludes the Daman Ganga and Tillari river basins, as their outlets are in Gujrat and Goa, respectively and also Bharja, Mahsala, Achara and Vengurla as their required data was not available. Konkan region is the narrow strip of land extending from Damanganga basin in the north to the border of Goa in the south. It lies between 16° 10' and 19° 41' N Latitudes and 72° 45' and 73° 44' E Longitudes. Bounded by the Sahyadri ranges to the east and the Arabian Sea to the west, the Konkan strip is about 53 to 60 km wide and 720 km long along, running north to south. The widest section is about 100 km, with the width narrowing as one moves southward. The terrain becomes increasingly hilly, with altitude rising from the coastline towards the east. The region is characterized by medium black soils, with low infiltration rate, in north and lateritic soils, with high infiltration rates and a sloping terrain.

Paddy cultivation is the predominant seasonal crop during the Kharif season in the region, followed by secondary crops such as finger millet (Ragi), sorghum (Jowar), pearl millet (Bajra), maize, and various pulses. Rice is the principal field crop, covering approximately 6.02 lakh hectares of agricultural land. Minor cereals like Nagali and Vari are grown on an estimated 0.70 lakh hectares, while pulses occupy around 0.49 lakh hectares. Additionally, oilseed crops are cultivated on approximately 0.12 lakh hectares. The region is also notable for its horticultural production, particularly of perennial crops such as mango, cultivated over 1.1 lakh hectares, and cashew, which occupies 1.52 lakh hectares. Other horticultural crops, including coconut and various spice crops, also contribute significantly to the region's agricultural profile.

3.1.2 Climate

The Konkan region of Maharashtra experiences a tropical monsoon climate characterized by hot summers, mild winters, and heavy rainfall during the monsoon season. The climate is generally warm and humid and warm, with humidity ranging from 30 to 90% and temperature between 20 to 45^{o}C. The region receives heavy rainfall with an annual average rainfall of 2500-3500 mm, with more than 90% precipitation received during monsoon months of June to September. The Konkan region receives 46% of the state's total precipitation on just 10% of its total geographical area.

3.1.3 Geographical Area

Konkan region is characterized by a 720-km long coastline along the Arabian Sea, stretching from the confluence of the Damanganga River in the north to the Terekhol River in the south. This narrow coastal plain, adjoining to the coast, forms a distinct physiographic entity of the state. This coastal belt, traditionally known as the 'Konkan', is part of a rugged terrain consisting that includes hills, plateaus and plains. To the east, the Konkan region is separated from the upland Maharashtra by a steep west-facing escarpment of the Sahyadri Mountains.

Administratively, the region includes the districts of Palghar, Thane, Raigad, Ratnagiri, Sindhudurg and Mumbai. The river basins flowing in the region, which is the study area, are presented in location map (Fig. 3.1).

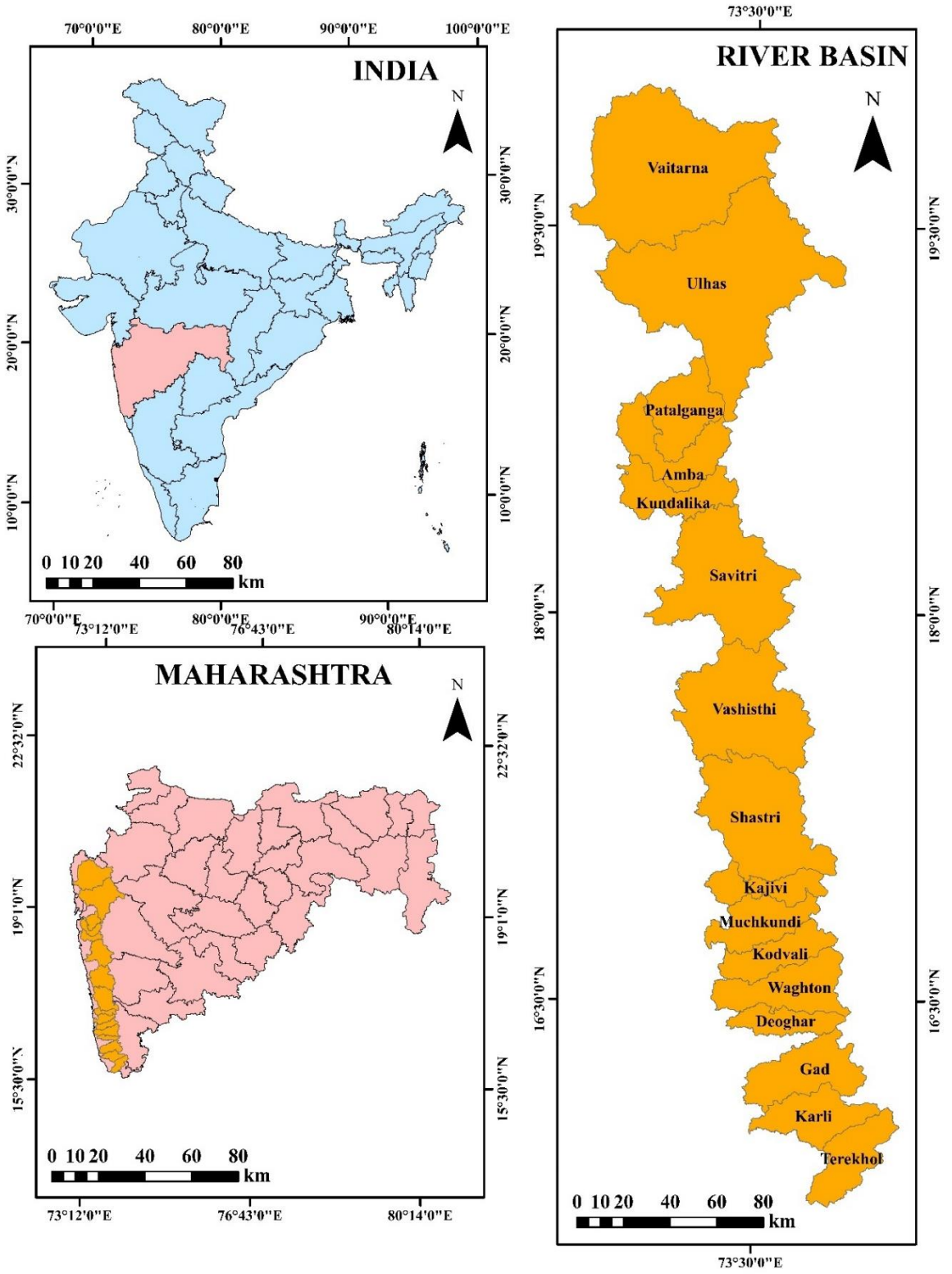

Fig 3.1. Location map of study area indicating the river basins in Konkan region

3.2 Data Collection and Software used

The unique data and information essential for the current research were collected from various sources and then imported into a GIS platform. The data collection process and software specifications are detailed in the following sections.

3.2.1 Data Collection

The data required for the study were collected for various periods, depending on availability, from the different agencies. The details are presented in Table 3.1.

Table 3.1. Data required for study, its period and source

Data	Duration	Retrieving Date	Source
Hydrometeorological Data	1994-2019 (30 Years)	03.09.2023	Hydrology Project, Nashik. Hydrology Data User Group
Soil Data and Soil Map (Scale 1:250,000)	-	10.09.2023	National Bureau of Soil Survey and Land Use Planning and FAO
Digital Elevation Model (DEM) SRTM 30 m Resolution	-	05.04.2024	United States Geological Survey (USGS) https://earthexplorer.usgs.gov/
Land Use/Land Cover Map, Sentinel 2 (10m)	2017, 2019	15.04.2024	ESRI Database Portal https://livingatlas.arcgis.com

3.2.2 Software Used

1. GIS Software and Image Processing Software
2. R Studio
3. Microsoft office

In this study Arc GIS 10.3 software, ArcSWAT version 2012 and Image Processing software has been used for processing the remotely sensed data such as DEM preprocessing, Soil data preprocessing and preparation of LULC Maps and slope map for Assessment of surface water availability. R Studio for arrangement of data in required format.

The Packages of Microsoft office such as Word, Excel and PowerPoint were used for Thesis writing, data analysis and presentation of results.

3.3 Study of different methods to assess surface water availability

Assessing water resource availability is fundamental to effective planning, development, and management of water. This assessment is typically conducted at the basin level, defines as geographic area within a watershed system where streams and rivers converge towards a common

terminus, such as the sea or an inland water body. A critical aspect of water resource assessment is estimating the flow available at the outlet of a river catchment.

Streamflow monitoring methods are tailored to different stream types. Stream channels can be classified based on eight major variables – width, depth, velocity, discharge, slope, roughness of bed and bank materials, sediment load and sediment size. Various methods exist for quantifying and monitoring surface water flow, categorized as follows (based on John, 1978; Martin, 2006; Herschy,2008): (a) direct measurement methods, (b) velocity-area methods, (c) formed constriction or constricted flow methods, (d) Rainfall-Runoff method, and (e) non-contact measurement methods. These methods can be further classified as follows

A) Direct Measurement methods
    1) Timed volume method.
B) Velocity- Area methods
    1) Float Method
    2) Dilution Gauging method
    3) Current meters method
    4) Trajectory method
    5) Electromagnetic Method
    6) Acoustic Doppler current profiler method (ADCP)
    7) Salt-Velocity Method
C) Formed construction or constricted flow methods
    1) Weir Method
    2) Flume Method
D) Rainfall-Runoff method
    1) Rational Method
    2) Cooks Method
    3) Curve Number method
    4) Unit Hydrograph Method
    5) Infiltration Method
    6) Empirical Formulae
E) Non-contact measurement methods
    1) Particle image velocimetry method
    2) Hydrological Modelling.

3.3.1 Direct Measurement Method

In this method, known as time-volumed method, the flow rate is determined by measuring the time it takes to fill a container of known volume. This technique is particularly useful for

streams where the entire flow converges into a single descent. To ensure accuracy and reliability, a large container should be used, and the flow rate should be measured at least five times, with more than three replications across different stream width and depth (Ely 1994; Pfeffer and Wagenet 2007). The flow rate is then calculated as the ratio of the average stream cross-sectional area to the average time taken to fill the container.

This method is accurate, cost effective, time-effective, non-polluting, and requires minimal resources and technical knowledge, making it suitable for small streams (Friederich and Smart, 1982; Weight and Sonderegger, 2001; Najafi et al., 2012; Shope et al., 2013).

3.3.2 Velocity-area Method

Velocity-area methods are based on the principle of fluid flow continuity and are used for instantaneous streamflow measurements and establishing the stage–discharge relationship (Harmel et al., 2009). Discharge and stage measurements are crucial in areas where water management is a priority. This method involves determining the cross-sectional area of the stream flow and the mean velocity, multiplying these values to calculate the stream flow i.e.

$$Q = A \times V \quad \ldots 3.1$$

In which, Q is the discharge, A is the cross-sectional area of the stream flow and V is the mean flow velocity. The cross-sectional area of the stream flow is obtained by measuring the flow at different segments of the stream. Measurement of depth and velocity of flow is conducted simultaneously.

3.3.2.1 Float Method

In float method, a partially filled long-necked bottle or a low-density object is used as a float. A straight channel section about 30 m long with a uniform cross-section is selected. The time it takes for the float to cover this distance is recorded, and the water speed is calculated. The surface velocity of the water is determined by dividing the length of the channel section by the average time the float takes to cross it. The flow rate is then calculated by multiplying the average velocity (surface velocity multiplied by a correction coefficient) by the average cross-sectional area of stream (Michael, 2008).

However, due to vertical turbulence, the float may not accurately represent the actual flow because of velocity differences at various depths of the stream. To address this, the integrated float method was developed (Herschy, 1978, 1995; Hilgersom and Luxem burg, 2012). In this method, a float is released at the bottom of a river or canal, and as it rises with a constant velocity, the depth-integrated horizontal velocity can be determined from the float's displacement as it surfaces (Hilgersom and Luxemburg, 2012).

3.3.2.2 Dilution gauging method

This method is also known as tracer method, chemical method or salt concentration method, measures streamflow by tracking the diffusion rate of a tracer, which can be a chemical substance or a radio isotope (Comina et al., 2014; Dingman, 2015). Common chemical tracers, such as salt (NaCl), are often used with an electrical conductivity (EC) meter or an ion electrode (Flury and Wai, 2003; Otz et al., 2003). Streamflow is calculated by multiplying average cross-sectional area and velocity of the flow.

This method is cost-effective and considered an absolute method since the discharge is determined solely from volume and time (Herschy, 2008). It is particularly useful in turbulent flow conditions where conventional methods are difficult to apply (Gordon et al., 2004). It is especially suitable method for measuring the discharge of small mountain streams with turbulent flows and enables rapid measurement during flood and high flow conditions (Merz and Doppmann, 2006).

However, the method can produce inaccurate results due to the loss or incomplete mixing caused by velocity differences between the upper and lower surfaces of the stream. Special training is required to implement this method in the field. Additionally, in some areas, obtaining permission to inject tracers into streams can be difficult due to potential water pollution concerns (Moore, 2004).

3.3.2.3 Current meter method

The velocity of water in stream or river can be measured directly using a current meter. This method relies on a well-defined channel geometry to calculate flow velocities (Briggs et al., 2012; Hamilton and Moore, 2012). A current meter is a small instrument equipped with a revolving wheel or vane that rotates in response to water movement. For measurements in deep streams, the meter is suspended by a cable, while in shallow streams, it is attached to a rod. Discharge is estimated by multiplying mean velocity of water by the area of cross-section of stream or river. To convert velocity into discharge, the channel geometry must be known. The cross-sectional geometry (channel geometry) is needed to convert the velocity to a discharge. In this method, stream channel cross-section is divided into vertical subsections. The area of each subsection is determined by measuring its average width and depth. Total discharge is the sum of discharge of subsections.

3.3.2.4 Trajectory method

In the trajectory method, all the flow from a stream is diverted into a pipe (Yan, 1996; Hudson, 2004; Salguero et al., 2008). Flow from a horizontal pipe can be estimated using either the California pipe method developed by van Leer (1924), or the trajectory method developed by Greeve (1928). This flow measurement technique is based on measuring brink depth at the end of

the pipe (Berkowitz, 2013). The diverted water is discharged under pressure, and the flow rate is estimated by measuring the characteristics of the jet (Rohwer, 1943; Boman and Shukla, 2009). At least two measurements of the discharging jet are required to calculate the rate of flow of the water (Yan,1996; Liu et al., 2014).

3.3.2.5 Electromagnetic method

The electromagnetic method measures point velocity of a stream by using an electromagnetic meter. To calculate the stream discharge, continuous velocity records at a single point in a cross-section, along with stage readings, are utilized (Egusa et al., 2013). This method is based on Faraday's principle that an electromatic field (emf) is induced in the conductor (water in present case) when it cuts a normal magnetic field. As water flows through the stream, it cuts across the vertical component of the Earth's magnetic field, inducing an electromotive force (EMF) in the water. Electrodes provided at the sides of the channel section measure the small voltage produced due to flow of water in the channel. It is found that the signal output E will be of the order of millivolts and is related to the discharge Q as

$$Q = K_1 \left(\frac{Ed}{I} + K_2\right)^n \quad \ldots 3.2$$

Where, d = depth of flow, I = current in the coil, and n, K_1 and K_2 are system constants.

This method involves sophisticated and instrumentation and has been successfully implemented in numerous installations. One of the advantages is that, once installed, it provides total discharge, making it particularly suitable for field conditions where cross-sectional properties change over time due to sedimentation, weed growth, and other factors. It is also well-suited for tidal channels, where the flow undergoes rapid changes in both magnitude and direction. Commercially available electromagnetic flowmeters can measure discharge with high accuracy, the maximum channel width that can be accommodated being 100 metres.

3.3.2.6 Acoustic doppler current profiler method

Acoustic Doppler current profiler (ADCP) method transmits sound into the water and receives echoes from particles suspended in the stream. The difference in the frequency between the transmitted sound and echoes is used to calculate the velocities of both the particles and the water in which they are suspended (Costa et al., 2000, 2006). Mounted on a ship or a boat, ADCPs provide the quasi-continuous vertical profile of horizontal current (Muste et al., 2004; Chauhan et al., 2014). The ADCP measures the speed and direction of the boat by tracking the river bottom and compensate for the boat's movement in the computation of water velocities (Oberg and Mueller, 2007).

3.3.2.7 Salt-velocity method

Salt- velocity method is based on principle that salt increases the conductivity of water. In this method, two stream cross-sections are selected at a sufficient distance apart and insulated electrode are installed at these locations. The electrode are connected to galvanometer, and the system is energised by electric current. By measuring the distance between the two electrodes, the travel time of the salt solution between them, and the cross-sectional area of stream, the discharge can be computed.

3.3.3 Formed construction or constricted flow methods

These methods are less influenced by the stream roughness and the backwater effects compared to the velocity-area methods. Formed constriction methods are generally suitable for small streams. Common devices used in these methods for measuring water flow include weirs, Parshall flumes, orifices and meter gates.

3.3.3.1 Weir method

In this method, stream discharge is estimated using a constructed check-dam or weir made of plywood, other wooden boards, or reinforced concrete, placed in the cross-section of a stream (Rickard et al., 2003; Gordon et al., 2013). Weirs are used to measure the flow in channels or discharge from canal outlets at the source. They can be built as stationary structures or designed to be portable. The notch of the weir may be rectangular, trapezoidal or triangular, with rectangular weirs and 90° V-notch weirs being the most commonly used. Flow rates can be determined using predefined table (British Columbia, 2006) or calculated using a weir equation that takes into account the flow rate, water head height, and crest width (Ghodsian, 2003; Emiroglu et al., 2011).

3.3.3.2 Flume method

A flume is an artificial open-channel flow section that narrows the stream area and alters its slope, increasing water velocity and changing the flow (Ancey et al., 2008). Unlike weirs, flumes do not create an impoundment, but the water height in the flume is measured using a stilling well (Mutz et al., 2007). By measuring the water height, discharge can be calculated. Different types of flumes are used for specific purposes: HS, H and HL flumes for measuring intermittent runoff, venturi flume for measuring irrigation water and San Dimas flumes for debris-laden flows in mountain streams (USFWS, 2006). Flow calculations are typically made using tables provided by Bos (1976) and Hudson (1993).

Ultrasonic river gauging involves continuously measuring stream velocity at selected depths by recording the time difference of sound pulses sent obliquely across the river in opposite directions. Ultrasonic flowmeters typically operate at frequencies around 500kHz. In a given

installation, calibration is usually performed by the current-meter method. However, accuracy of this method can be affected by the factors such as unstable cross-section, fluctuating weed growth, high loads of suspended solids and salinity and temperature, all of which can influence signal velocity and flow velocity averaging.

3.3.4 Rainfall-Runoff method

The portion of rainfall as well as any other flow, which makes its way towards the river, stream or ocean etc. Since, runoff is through the channel, stream/or river etc., therefore, it is called as channel flow or stream flow.

3.3.4.1 Rational method

This method is usually used to calculate peak runoff rate from small watershed. It involves formula for computing design runoff

$$Q_{Peak} = 1/360 \times (CIA) \quad \text{... 3.3}$$

Where, Q_{Peak} = Peak runoff rate, m^3/s

C = runoff coefficient

I = Rainfall intensity (mm/h) for duration equal to time of concentration and given recurrence interval

A = Watershed area, ha

This method is suitable for small watershed area. It is much easier to represent variation in hydrological responses within that area

3.3.4.2 Cook's method

This method consists of evaluating watershed characteristics such as relief, infiltration rate, vegetation cover and surface storage to determine runoff rate. For these individual characteristics, numerical values are assigned. Numerical values are mainly given based on their features with similar conditions of watershed. Then sum of numerical values assigned for all four characteristics ($\sum W$) and then uncorrelated runoff is computed by using runoff curve against the sum of numerical values. Then runoff value is modified for that geographic location. This done by using formula

$$Q = PRFS \quad \text{… 3.4}$$

Where Q = peak runoff rate for a specified geographic location and desired recurrence interval

P = uncorrelated value of runoff, i.e. obtained from runoff curve

R = Geographic rainfall factor

F = recurrence interval factor

S = shape factor of the watershed

3.3.4.3 Curve number method

This method computes the direct runoff or excess, Strom wise. This method is based on potential retention capacity of watershed, which is determined based on antecedent moisture condition and physical characteristics of watershed. This method assumes that the ratio of direct runoff to rainfall depth minus initial losses (interception, infiltration, depression storage etc) is equal to ratio of actual retention of rainfall to retention capacity. By using following equation Q can be calculated with value of P and S

$$CN = \frac{(P-0.2s)^2}{P+0.8s} \quad \ldots 3.5$$

Retention capacity of watershed can be predicted by using curve number as defined by U.S Soil conservation service (1969)

$$CN = \frac{2540}{25.4+S} \quad \ldots 3.6$$

In which CN is curve number whose range is between 0 to 100. CN Value is depending upon land use condition and hydrologic soil group.

3.3.4.4 Unit hydrograph method

The Unit Hydrograph (UH) is a fundamental concept in hydrology used to describe the temporal distribution of runoff generated by a unit volume of effective rainfall (typically 1 cm) distributed uniformly over a watershed area. It helps in predicting the runoff hydrograph resulting from any given rainfall event. In this method portion of the total rainfall that contributes to runoff after accounting for losses like infiltration and evaporation is calculated. Then a hydrograph that represents runoff from a unit depth of effective rainfall distributed evenly over the watershed for a specific duration is created. Runoff hydrograph is derived from applying unit hydrograph to the actual effective rainfall using convolution. (Suresh, 2021).

3.3.4.5 Empirical formulae method

There have been developed several empirical formulae for computing the runoff for different zones of the country.

3.3.4.5.1 Runoff coefficient method

In this method, the runoff is computed by multiplying the runoff coefficient to rainfall amount given as under

$$R = K \times P \quad \ldots 3.7$$

Where R= Runoff (cm), K= Runoff coefficient, P = rainfall depth, cm

Values of runoff coefficient for urban area are 0.3 for residential buildings and for garden apartment it is 0.5 for commercial and industrial areas it is 0.9 and 0.5 to 0.2 for forest areas.

3.3.4.5.2 Inglis formula

In 1940 Inglis developed two empirical formulae for computing runoff rate for different type of area. These are for ghat area it is R = 0.85P – 30.5 and for non-ghat areas it is

$$R = \frac{P-17.8}{254} \quad \ldots 3.8$$

where, R indicated for runoff depth (cm) and P for rainfall depth(cm). (Inglis, 1940)

3.3.4.5.3 Khosla's formula

This formula was developed by Khosla in 1953 assuming the temperature as a factor in yield of surface runoff. The formula is given by $R = P - \frac{T-32}{374}$ in which R indicated for runoff depth (cm) and P for rainfall depth in cm and T is average temperature (°F) of watershed. (Khosla,1953)

3.3.5 Non-contact measurement methods.

These methods are based on the principle of radar system and may be used to make continuous, near-real-time flow measurements during high and medium flows.

3.3.5.1 Particle image velocimetry

In the particle image velocimetry (PIV) method, the movement of the fluid is tracked by observing the light scattered by liquid or solid particles illuminated by a laser light sheet (Prasad, 2000; Tauro et al., 2016). In most of the studies, tracer particles, which are small and light enough to follow the local flow velocity, are added to the fluid (Brossard et al.,2009). The flow fluid is illuminated twice using two superimposed laser light sheets, creating two separate exposures recorded by a CCD camera sensor (Bosbach et al., 2009). The time interval between the laser pulses, along with camera calibration data, including image magnification and the projection of the local flow velocity vector onto the plane of the sheet, is used to define small interrogation areas within the image. Each interrogation area produces a displacement vector, and the fluid velocity is determined by dividing the particle displacement by the by dividing the particle displacement by the time interval between the two exposures (Harpold et al., 2006; Stamhuis, 2006).

3.3.5.2 Hydrological modelling

Remote sensing and GIS have become increasingly popular as advanced tools for water resources assessment, monitoring and analysis tools. These technologies provide enhanced

capabilities for evaluating land surface resources and offer powerful means of detecting and analyzing temporal changes in our environment. This is essential for a wide range of applications in hydrology, meteorology and agronomy. In the context of river discharge estimation, remote sensing combines ground measurements with satellite data to develop empirical relationships between water surface area and discharge (Bjerklieetal, 2005; Tan et al., 2014). This method utilizes two types of sensors: (a) passive sensors, which detect energy naturally reflected or emitted from the Earth's surface; and (b) active sensors, which emit their own energy and measure the amount that is reflected back from the surface (Xu et al., 2004; Ticehurst et al., 2009). There are three general approaches to estimate stream discharge: (a) direct measurement of water surface level from radar altimeter waveform data; (b) determination of water surface elevations at their point of contact with the land surface using high-resolution satellite imagery and topographic data; and (c) correlation of satellite-derived water surface areas with ground measurements of stage or discharge (Smith, 1997; Papa et al., 2012; Revilla-Romeroetal, 2014). Satellite data offers the potential for unprecedented global coverage of critical hydrologic information that would be logistically and economically challenging to obtain through traditional ground-based observation networks (Koblinsky et al., 1993; Xuetal, 2004; Batra et al., 2006).

Hydrological modelling is a vital tool in hydrology used to estimate the movement, distribution, and quality of water within a watershed. By applying mathematical models and incorporating remote sensing data, hydrologists can replicate the hydrological cycle and predict water flow and storage across various environmental components. A model is simplified representation of real-world system, and the best model is one that closely approximates reality while minimizing the number of parameters and complexity. Models are primarily used for predicting system behaviour and gaining insights into different hydrological processes. The selection of a hydrological model depends on the purpose of study, data availability and the model's capability and suitability for both small and larger catchment hydrologic applications (Aizam, 2010).

Rainfall-runoff models can be classified based on model input, parameters and the degree to which they incorporate physical principles. They are categorized into lumped and distributed models, as well as deterministic and stochastic models. based on the model parameters such as function of space and time and deterministic and stochastic models. In deterministic models, a single set of input values will always produce the same output, whereas stochastic models can generate different outputs from the same set of input values. Lumped models treat the entire river basin as a single unit, ignoring spatial variability and generating output without considering spatial processes. In contrast, distributed models divide the catchment into smaller units, such as square cells or triangulated irregular networks, allowing parameters, inputs and outputs to vary spatially (Moradkhani and Sorooshian, 2008).

3.3.5.2.1 Variable infiltration capacity model (VIC Model)

VIC Model is a semi distributed, macro-scale, grid-based hydrology model that incorporates both energy and water balance equations. The primary inputs for the model include precipitation, daily minimum and maximum temperatures, and wind speed. The model allows for multiple land cover types within each model grid cell. Key hydrological processes such as infiltration, runoff, and base flow are modelled using various empirical relationships. Surface runoff is generated through two mechanisms: infiltration-excess runoff (Hortonian flow) and saturation excess runoff (Dunne flow). The VIC model simulates saturation-excess runoff by accounting for soil heterogeneity and precipitation patterns.

The model consists of three layers: the top layer facilitates quick soil evaporation, the middle layer represents the dynamic response of soil to rainfall events, and lower layer characterises soil moisture behaviour. An improvised version of the VIC model includes both infiltration-excess and saturation-excess runoff, as well as the effects of soil heterogeneity on surface runoff characteristics. It also handles the dynamics of surface and groundwater interactions, including calculations of the ground water table (Gao, 2010), and can be applied in cold climate regions.

3.3.5.2.2 MIKE SHE model (System Hydrologique European)

The model developed in 1990, is physically based and thus requires extensive physical parameters. It simulates various processes of the hydrological cycle, including precipitation, evapotranspiration, interception, river flow, saturated ground water flow, unsaturated ground water flow. The model is capable of simulating surface and groundwater movement, their interactions, and transport of sediment, nutrient and pesticides within the model area. It is also useful for addressing various water quality issues and can be applied to large watersheds. Refsgaard and Storm (1995) provided a detailed description of the model's structure and set up. The model includes pre-processing and post-processing modules and offers various options for displaying results.

3.3.5.2.3 HEC-HMS (HEC- Hydrological Modelling System)

The HEC Hydrological Modelling System (HMS) is a conceptually lumped and straightforward model that requires a few parameters, most of which can be derived from land cover data. It is sensitive to land cover changes and provides a convenient platform for simulating rainfall-runoff processes, as well as impacts assessing the impacts of land use and land cover changes (Furst et al., 2010). The model mainly focusses on runoff, channel routing and water control structures (Garg, 2016). According to the Aizam (2010), HEC-HMS consists of three components: the basin model, the meteorological model and control specifications. These components offer various options for simulating different hydrological processes at lumped scales.

3.3.5.2.4 Water evaluation and planning (WEAP)

The Water Evaluation and Planning (WEAP) system, along with integrated hydrology models, has a long history of development and application in the water planning, effectively addressing the complex dynamics of water system (Yibel et. al., 2015). WEAP can be applied at local scales as well as in more complex river basin systems. It operates on the fundamental principle of water balance accounting. The model's hydrologic processes can utilized as both forecasting tool or a policy analysis tool.

3.3.5.2.5 Soil and water assessment tool (SWAT)

SWAT is complex physically is a complex, physically-based model designed to simulate and forecast water and sediment circulation, as well as agricultural production and chemical transport in ungauged basins. It is highly efficient for performing long-term simulations. The model divides the entire catchment into sub-catchments, which are further broken down into Hydrologic Response Units (HRUs) based on land use, vegetation and soil characteristics. The model utilizes daily inputs of rainfall, maximum and minimum air temperatures, solar radiation, relative humidity and wind speed to describe water and sediment circulation, vegetation growth and nutrients dynamics. Snowfall rates can be determined based on precipitation levels and mean daily air temperatures. For estimating evapotranspiration, SWAT employs methods such as Penman Monteith, Priestly-Taylor and Hargreaves. Accurate forecasting of water, nutrient and sediment circulation requires simulating the hydrologic cycle, which integrates overall water circulation in the catchment area, and SWAT uses the following water balance equation for this purpose.

$$SW_t = SW_0 + \sum_{i=0}^{t}(R_v - Q_s - W_{seepage} - \mathrm{ET} - Q_{gw}) \quad \ldots 3.9$$

Where, SW_t is humidity of soil; SW_0 is base humidity; R_v is rainfall volume in mm water; Qs is surface runoff; $W_{seepage}$ is seepage of water from soil to underlying layers; ET is evapotranspiration; Q_w is groundwater runoff and t is time in days.

3.4 Analysis of the impact of soil, land use, and slope on spatiotemporal variability of water in river basins of the Konkan region

Remote sensing plays an important role in studying the impact of soil, land use and slope on water variability by providing information on various terrain aspects such as soil, slope, geomorphology, land use and land cover. This data aids in determining site suitability (Bhorkar, 2023). The Weighted overlay analysis (WOA) is a pixel-based analysis technique that standardises different layers with varying measurement units such as rainfall in mm, DEM in meter, slope layer in degrees or percentages, and drainage density per kilometre by assigning rankings to bring all layers to a common unit.

3.4.1 Generation of thematic maps

Thematic maps are one of the most effective and easily understandable methods of data analysis, highlighting the spatial variability of specific distributions or themes within a geographic area. Also known as special-purpose, single-topic, or statistical maps, they provide focussed insights into particular aspects of a region. To assess the impacts of various factors on surface water, eight thematic maps were prepared covering soil, slope, rainfall, land use land cover, geomorphology, lineament density, drainage density, and runoff. These maps were produced using a combination of remote sensing and conventional data.

3.4.1.1 Slope map

The slope is a measure of the steepness of a line. A slope map of the study area was created utilizing a Digital Elevation Model (DEM) with 30-meter resolution data from the Shuttle Radar Topography Mission (SRTM), accessed via the USGS Earth Explorer. The lower value of slope shows the flatter terrain and higher value of slope shows the steeper terrain. The slope map was generated using GIS software. Flow chart for preparation of slope map is shown in Fig 3.2.

3.5.1.2 Rainfall Map

Rainfall is essential for providing surface water and replenishing groundwater reserves. In this study, a daily rainfall dataset spanning 30 years (1991 to 2019) was obtained from Hydrologic Data Users' Group (HDUG), Hydrology Project, Nashik and was organized by basins. Flow chart for preparation of Rainfall map is shown in Fig 3.3.

3.4.1.3 Soil Map

The impact of soil on runoff generation primarily depends on its retention capacity or texture. Clay-textured soil, with its smaller pores, leads to more runoff and less infiltration, while sandy soil promotes less runoff and more infiltration. The soil map of the study area was obtained from the National Bureau of Soil Survey and Land Use Planning (NBSS&LUP), Nagpur at 1:250,000 scale.

3.4.1.4 Land Use Land Cover Map

Land use encompasses various human activities, arrangements, and practices, such as settlements, conducted on land. In contrast, land cover pertains to the natural vegetation, water bodies, and minerals that have formed because of land transformation. A land use land cover map is vital for generation of runoff. For this study, a Sentinel-2 land use land cover layer with a 10-meter resolution for the year 2017 and 2019 was downloaded from the ESRI portal. Land use land cover map of year 2017 and year 2019 was used to study how change in LULC impacted on site suitability area.

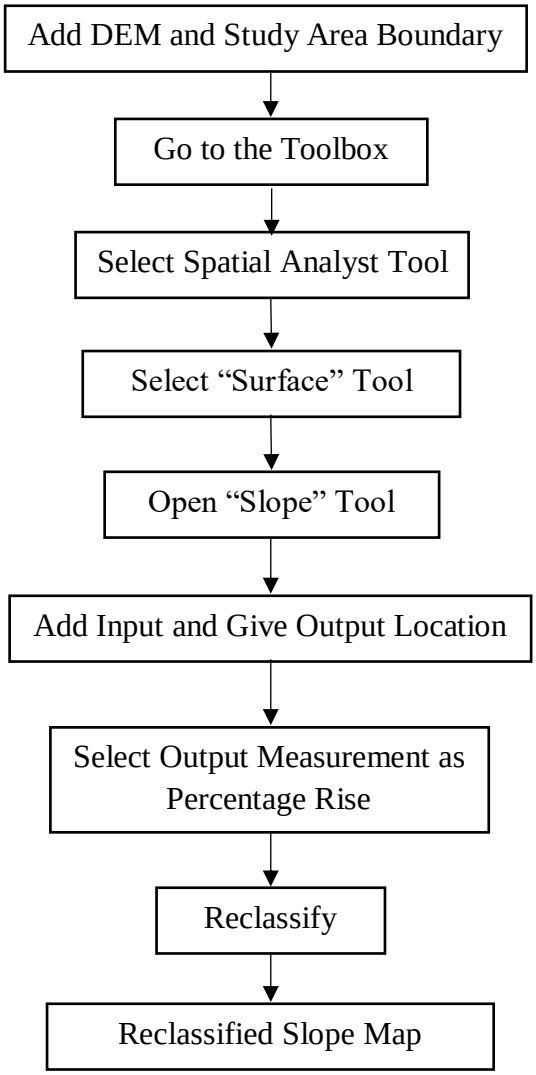

Fig 3.2 Flow chart showing steps Preparation of Slope Map

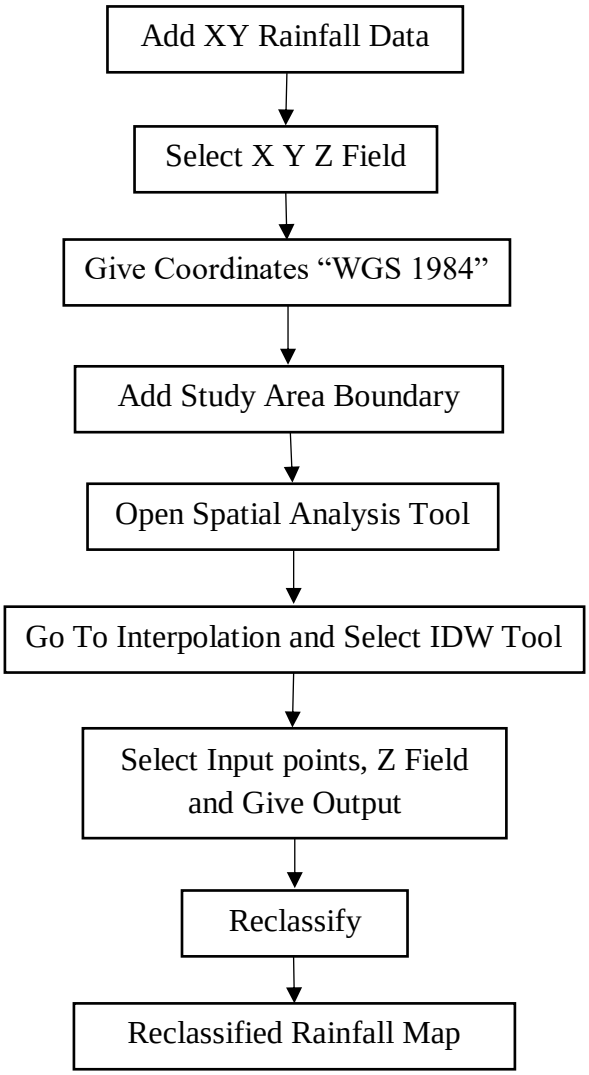

Fig 3.3 Flow chart showing steps Preparation of Rainfall Map

3.4.1.5 Geomorphology map

Geomorphology studies the origin, evolution, form, and distribution of landforms and other Earth features. Geomorphic features significantly influence rock type, soil type, drainage patterns, and the distribution and amount of precipitation that contributes to discharge. (Awasthi et al., 2023) In this study created the geomorphology map using geomorphology data downloaded from the Bhukosh Survey of India portal (http://bhukosh.gsi.gov.in/Bhukosh/Public).

3.4.1.6 Lineament density map

Lineament density is the ratio of the total length of lineaments or drainages to the total area of the drainage basin. Using the "Line Density" in GIS software, a Lineament density map has been prepared for the study area (Awasthi et al., 2023).

Lineament Density (km/km^2) = Total length of lineaments / Total area of drainage basin

3.4.1.7 Drainage density map

Drainage density of watershed gives information related to runoff, relief, infiltration and permeability. Drainage network reflects characteristics of surface and subsurface formations The drainage density map has been prepared in GIS software from drainage/stream network. The flowchart for preparation of drainage density map is shown in Fig 3.4

3.4.1.8 Runoff map

Annual runoff map was created using GIS software, based on data obtained from output file of SWAT as flow out at outlet points of basin. The map was categorized into appropriate classes. The flow chart for the preparation of runoff map is shown in the Fig 3.5.

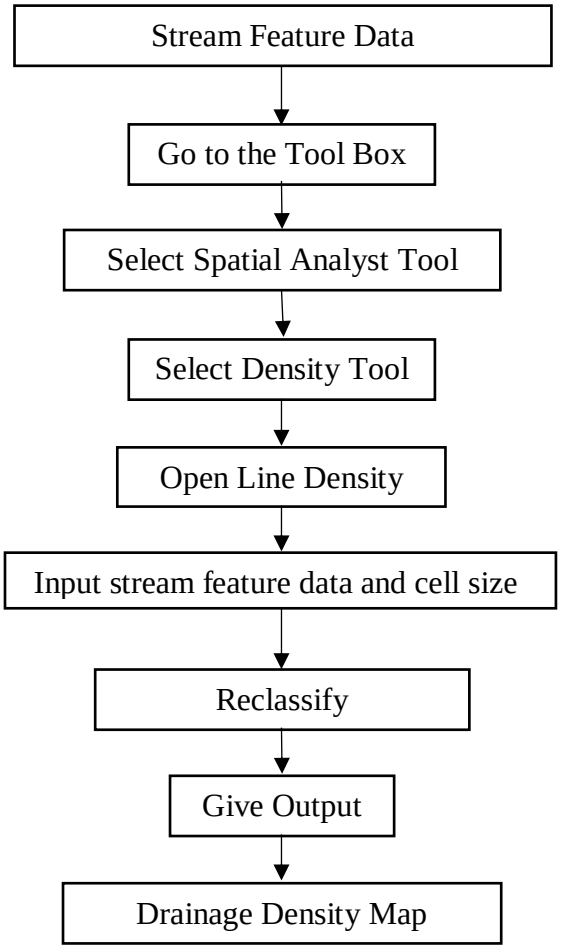

Fig 3.4. Flow chart showing steps Preparation of Drainage Density Map

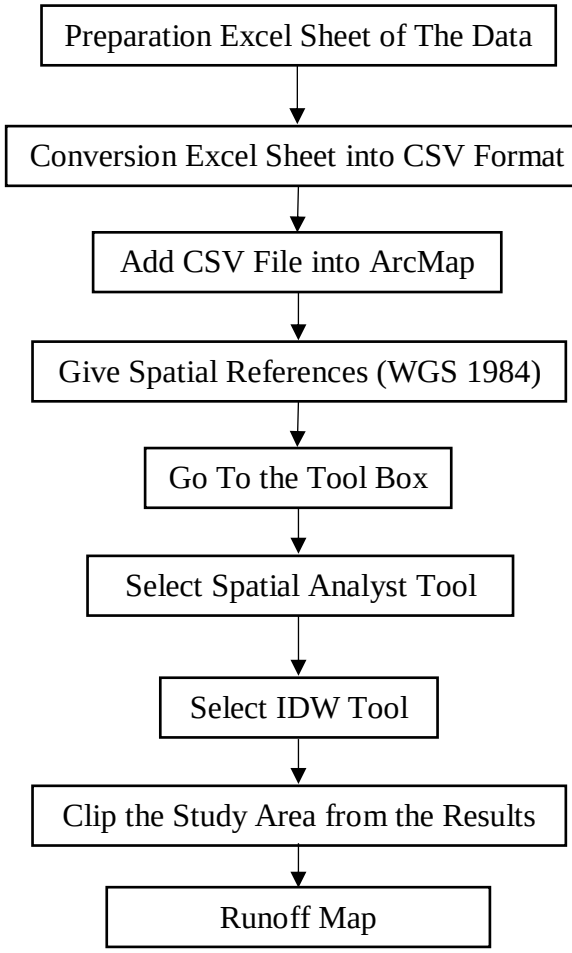

Fig 3.5. Flow chart showing steps Preparation of Runoff Map

3.4.2 Analytical Hierarchy Process (AHP) Method

The analytical hierarchy process (AHP) is a highly flexible and well-structured method capable of addressing complex decision-making problems involving multiple factors (Saaty, 1980; Dou et al., 2017). In this study, the AHP model was employed to determine the weights and ranks of various parameters for assessing site suitability. The AHP is a measurement theory based on pairwise comparisons and relies on expert judgments to establish priority scales. Comparisons are made using a numerical scale from 1 to 9, indicating the relative importance of one layer over

another (Saaty, 2008). A matrix is created by comparing both criteria and assigning ranks based on their relative importance. The diagonal matrix elements are assigned a value of 1, indicating equal importance. Table 3.2 presents the Saaty scale of relative importance. A matrix table for pairwise comparisons of all parameters used in this research is then developed. Next, a normalized pairwise comparison matrix is constructed to determine the criteria weights for the different parameters, followed by the construction of the weighted sum matrix. Then λ_{max} is calculated with help of weighted sum matrix.

Table 3.2. Relative importance given by Saaty's scale

Scale	Numerical Rating (More Important)	Reciprocal Rating (Less Important)
Equal importance	1	
Equal to moderate importance	2	1/2
Moderate importance	3	1/3
Moderate to strong importance	4	1/4
Strong importance	5	1/5
Strong to very strong importance	6	1/6
Very strong importance	7	1/7
Very strong to the extreme importance	8	1/8
Extreme importance	9	1/9

The obtained matrix was checked for consistency and if consistency ratio < 0.1, and then the criteria weights therefore derived were employed for analysis.

Consistency Index (CI):

$$I = \frac{\lambda \max - n}{n-1} \quad \ldots 3.10$$

Where, λ_{max} = average of ratio of weighted sum/criteria weight

n = matrix size

Table 3.3. Saaty's random index

Maximize	1	2	3	4	5	6	7	8	9	10
RI	0	0	0.58	0.90	1.12	1.24	1.32	1.41	1.45	1.49

The importance or weight of each criterion is different, so it is required to determine the priority of each criterion through pairwise comparisons using numerical scale developed by Saaty (2012), as illustrated in Table 3.3. The consistency ratio is calculated as the ratio of consistency index (CI) to the random index (RI). The value of random index (RI) depends on the number of

themes used in the identifying site suitability. In this study, an RI value of 1.41 was chosen for the eight selected themes. By definition, the consistency ratio (CR) is given as

Consistency Ratio (CR):

$$CR = CI/RI \quad \ldots 3.11$$

In this study, the consistency ratio (CR) is considered if it does not exceed 0.1, as this threshold is deemed reasonable for mapping site suitability. If the CR value is exceeds 0.1, it must be readjusted by revising the values in the pairwise matrix, following the guidelines provided by Saaty (2008).

3.4.3 Weighted overlay analysis

Weighted overlay is a technique used to apply a common measurement scale of diverse and dissimilar inputs, enabling an integrated analysis. This technique was used to determine site suitability by considering factors such as slope, rainfall, soil, runoff and land use/land cover conditions. Analytical hierarchy process (AHP) was employed to assign weights to the different layers. All the thematic layers were generated in GIS environment in the vector format. During the weighted overlay analysis, the rasterization of each physiographic unit was performed using conversion tools in the Arc Toolbox. Subsequently, all raster files were reclassified using scale values for each unit, and were ranked based on their influence.

For the suitability analysis, weighted overlay analysis was employed. Weightings were assigned to factors from rank 1 to 4, with lower values (1 and 2) indicating highly suitable and moderately suitable site, respectively, while higher values (3 and 4) represented less suitable and unsuitable sites across the study area. The weighted overlay function was executed using the Spatial Analyst Tool to identify suitability zones, with weights assigned as percentages that sum to 100%. Flow chart of weighted overlay analysis is shown in Fig. 3.6

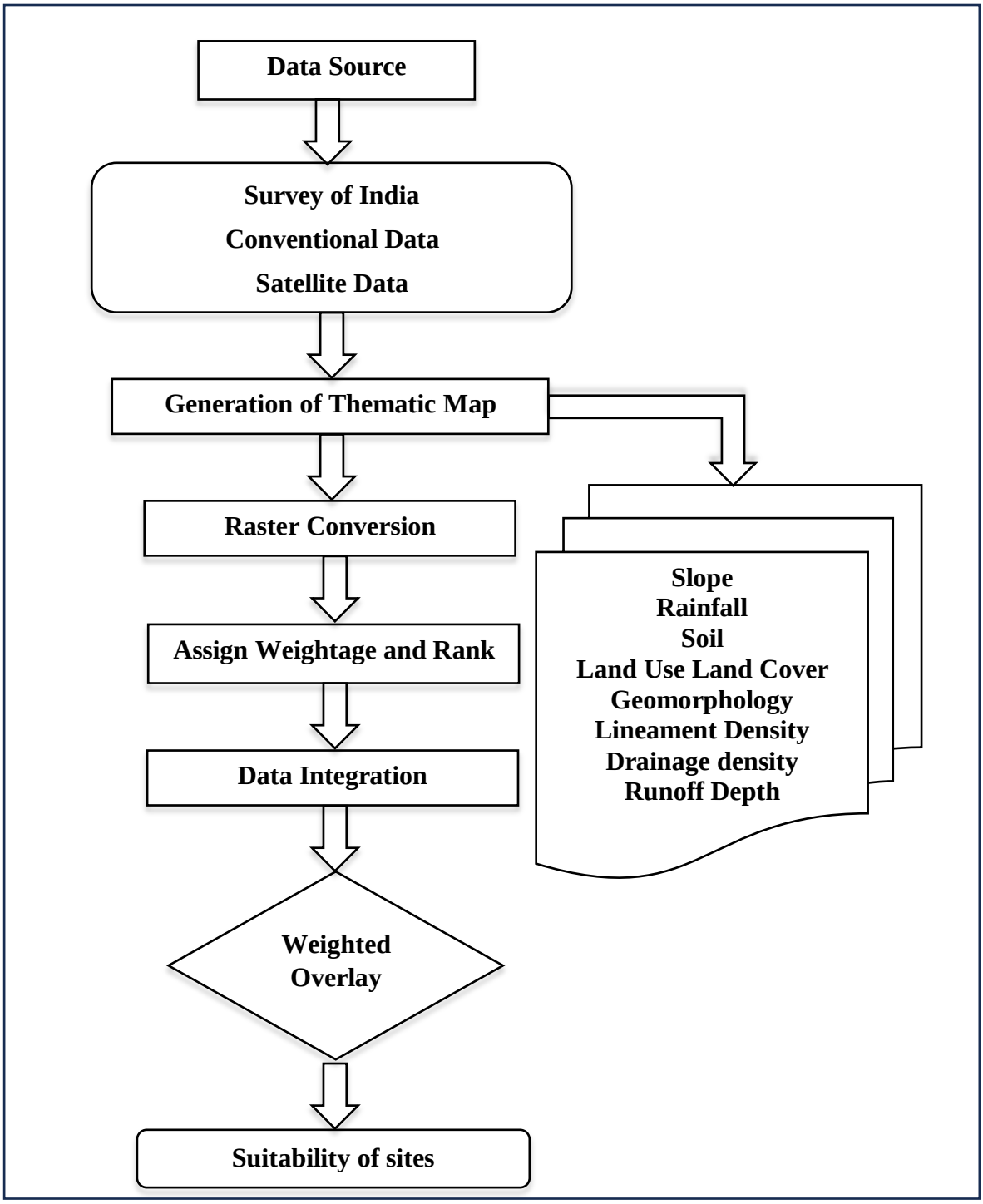

Fig 3.6. Flow chart showing steps of site suitability

3.5 Assessment of Surface Water Availability

Water resource assessment is typically conducted at the basin level, which encompasses geographic area within a watershed where streams and rivers converge toward a common terminus, such as the sea or an inland water body. A key aspect of this assessment is estimating the available flow at the outlet of a river catchment. Water availability at the watershed level is determined by quantifying the runoff generated within the watershed.

Hydrological modelling is the most common method for estimating surface water availability. Various models, such as HEC-HMS, VIC, WEAP, MIKE-SHE, are used to simulate hydrological processes. Among these, the ArcSWAT model is a physically based hydrological

model that accounts for numerous variables, including terrain, land use, soil characteristics and the soil moisture conditions, in simulating basin hydrology. Therefore, the ArcSWAT model was selected for hydrologic modelling of river basins in the Konkan region for this study.

3.5.1 Data Collection

The ArcSWAT model workflow consists of two major steps: ArcSWAT input data (physical and thematic data) and ArcSWAT Operation. A detailed workflow is illustrated in Fig. 3.4, with each step described in the subsequent sections.

The ArcSWAT input data step involves acquiring, preparing and importing the necessary data into the ArcSWAT Model. This includes various spatial datasets such as DEMs, land use/ land cover data, soil data, weather data and other relevant information required for watershed modelling. Following the input data step, the workflow progresses to ArcSWAT operations, which involve setting up and running simulations within the ArcSWAT model. This includes defining watershed boundaries, delineating subbasins, specifying HRUs, configuring simulation parameters, executing simulations and analyzing model output.

3.5.1.1 Thematic data

Thematic data required for ArcSWAT includes Digital Elevation Model (DEM), land use/ land cover data and soil data.

A. Digital Elevation Model (DEM)

DEM data is essential for calculating the flow accumulation, identifying stream networks and delineating watersheds using ArcSWAT Watershed Delineator tool. For this study, a 30m resolution SRTM DEM was downloaded from Spectral Radar Topographic Mission (SRTM) website (http://srtm.csi.cgiar.org). Before importing DEM into the ArcSWAT project, it was reprojected to the WGS-1984 UTM Zone 43N coordinate system using the raster projection in ArcMap. The DEM of the study area is given in Fig. 3.7.

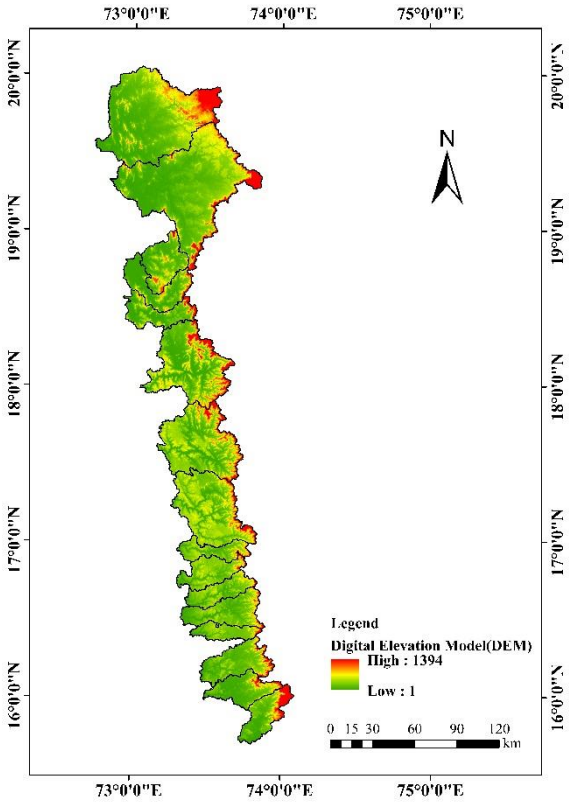

Fig. 3.7. Digital Elevation Model (DEM) of study area

B. Land Use/Land Cover (LULC)

The Land use and land cover data (2019) for the study area was downloaded from (https://livingatlas.arcgis.com/landcover/) of satellite Sentinal-2 with 10m resolution on date 15/04/2024. The map was reprojected to WGS-1984 UTM Zone 43N using raster projection.

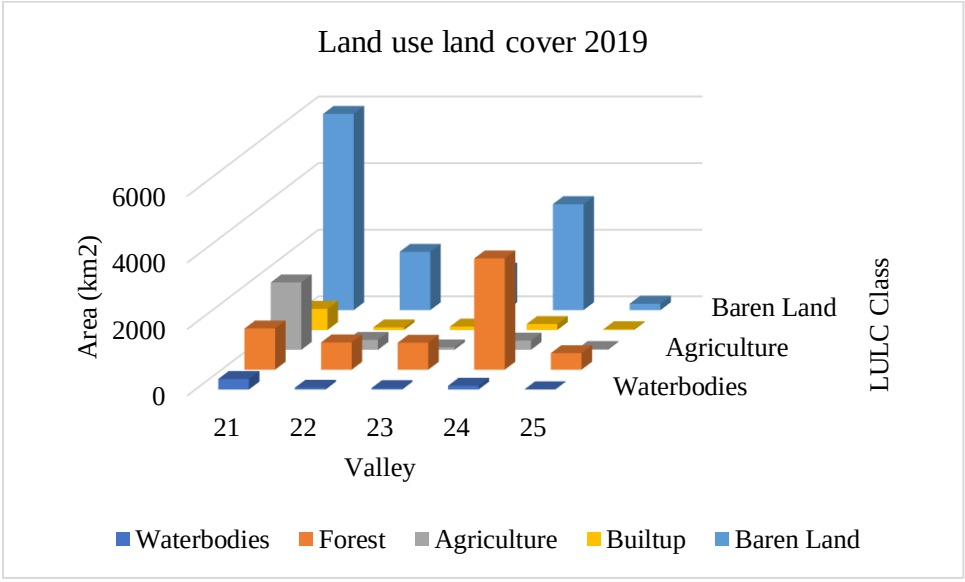

Fig. 3.8. Area Distribution of Land Use Land Cover

C. Soil Map

The soil data for the study area was downloaded in shapefile format at a scale of 1:50,000 and from FAO Soil Data. Then it is projected into WGS1984 UTM Zone 43N using raster projection. The dBase file is also downloaded from the FAO Soil database only.

3.5.1.2. Physical Data

This includes climatological parameters such as rainfall, temperature (Maximum and Minimum), Relative Humidity, and wind velocity. Data on climatological parameters were obtained from the Water Resources Department, Hydrology Project, Nasik, Government of Maharashtra for 29 years (1991 to 2019). Data is then sorted in MS Excel using Pivot Table and input files are prepared using RStudio in .txt format.

3.5.2 Arc SWAT Model

The Arc SWAT is one of the most recent hydrologic models developed jointly by the United States Department of Agriculture-Agricultural Research Services (USDAARS) and Agricultural Experiment Station, Texas. It is physically based, continuous time, long time, simulation, lumped parameter, originated from agricultural models and gives results on daily, monthly as well as yearly basis. ArcSWAT has six main menus,

1. Project setup
2. Watershed delineator
3. HRU analysis
4. Write input tables
5. Edit SWAT inputs
6. SWAT simulation

The ArcSWAT model utilizes detailed physical data such as topography, soil characteristics, vegetation, land management practices, and weather conditions within a watershed. It operates on the principle that water balance drives all processes in the watershed. ArcSWAT directly models physical processes like water flow, sediment transport, crop growth, and nutrient cycling. Using the ArcGIS interface, required and optional thematic maps are inputted into an ArcSWAT project. These maps, which include elevation, soil properties, land use, and hydrological features such as streams and water bodies, are layered to provide comprehensive information on every location within the area of interest.

3.5.3 Arc SWAT Operation

Arc SWAT completes all watershed simulation and modeling work under six main menus SWAT project setup, Watershed delineator, HRU analysis, write input tables, Edit SWAT input, SWAT simulation.

3.5.3.1 SWAT Project Setup

This ArcSWAT menu facilitates the creation of a project structure to organize essential folders and databases generated during simulations. It includes a project directory containing an ArcMap document, two geodatabases, and a subdirectory layout designed to store temporary GIS and SWAT input files.

3.5.3.2 Watershed Delineator

After setting up the project, the next step is watershed delineation, which involves dividing the watershed into hydrologically connected sub-watersheds using a digital elevation model (DEM). This menu also allows setting parameters to control the size and number of sub-watersheds created. The watershed delineation process is divided into five sections: DEM setup, defining streams, specifying outlets and inlets, selecting, and defining the watershed outlet, and calculating sub-basin parameters. The DEM for the study area was imported into the project using the DEM setup submenu, where the vertical units (Z axis) were set to meters.

In the stream definition process, two options are available: using DEM-based flow accumulation and direction or using a pre-defined stream network. In this study, the approach involved utilizing DEM-based flow accumulation and direction first. Subsequently, a stream network was generated by setting a threshold area value, adjusted through trial and error to closely match the details observed in the actual digitized stream network. During this process, natural outlets identified in the initial delineation were removed, and manual outlets were placed on the stream network at appropriate locations to delineate the upper, middle, and lower reaches of the region. The results of the watershed delineation, including attribute tables and a delineation report, store the outcomes of this process.

3.5.3.3 HRU Analysis

The hydrologic response of a watershed is influenced by factors such as land use, soil type, and slope characteristics, which individually or in combination affect the watershed's hydrology. The SWAT model requires detailed information on land use/land cover, soil types, and slope categories. This menu includes two main operations: defining land use/soil/slope categories and defining Hydrologic Response Units (HRUs).

In the first operation, land use/land cover and soil data are imported into the project, and slope categories are defined. The input data for land use/land cover and soil are reclassified using

a lookup table. In this study, the land use/land cover data was reclassified to distinguish different types of land uses. Additionally, five slope classes were defined: 0-10%, 10-20%, 20-30%, 30-40%, and more than 40%. After reclassification, these datasets are overlaid to create composite information.

The second operation involves HRU definition, where specific threshold values for land use/land cover, soil, and slope categories are set to exclude minor categories below these thresholds. In this study, threshold values of 10% for land use/land cover and 15% for soil and slope categories were assigned to define HRUs within each subbasin. After defining HRUs, the model generates multiple HRUs based on combinations of land use/land cover, soil, and slope within each subbasin. A final HRU report is then generated, detailing the area covered by each land use/land cover type, soil type, slope category, and HRU within the region.

3.5.3.4 Write Input Tables

This menu allows to build database files containing the information needed to generate default input for SWAT run. It has three sub menus one for weather data import and second for write SWAT input tables such as soil data, land use, configuration files, sub-basin and HRU files, management files and watershed data and drainage files etc. and third database update which updated all input files to run the model. Weather data imported ones HRUs are created in the project. In this study weather data of all stations in the Konkan region comprising precipitation, temperature, relative humidity, solar radiation, and wind speed in the text file format was loaded into SWAT project. After weather data input the next command write SWAT input tables is activated in which all input parameters files are selected, they are by final error free input tables of selected parameters. These final created tables are updated using third submenu database update.

3.5.3.5 Edit SWAT Input Table

The SWAT model provides tools to modify inputs in its databases and watershed files before and after running simulations. The "Edit SWAT input tables" menu consists of eight sub-menus: databases, point source discharges, inlet discharges, reservoirs, subbasin data, watershed data, rewriting SWAT input files, and integrating the APEX model.

To estimate total surface water availability, adjustments were made to the subbasin data to create scenarios. Monthly weather parameters were adjusted using a manual calibration helper for this purpose.

3.5.3.6 SWAT Simulation

The SWAT simulation menu is used to set up inputs for the SWAT model, this menu has four submenus, Run SWAT, Read SWAT Output, Set default Simulation and Manual Calibration. The first submenu of this section run SWAT was used to specify simulation starting date

(01/01/1991) and ending date (31/12/2019), run was set to monthly simulation, with 3 years warm up period to get hydrologic cycle fully operational. After SWAT run outputs of interested parameters such as were imported to database which was examined for output error by SWAT error checker. The examined output results were saved in the project database.

The output of the SWAT model must be calibrated to check precision of the simulation, which enables the model to closely match the behavior of the real system it represents. Flow chart of SWAT operation is mentioned in Fig.3.9

3.5.4 Calibration and Validation of SWAT Model

Model calibration is the process to compare performance of model against a reference standard, whereas validation is the process to provide degree of assurance that a simulation of model to meet pre-determined acceptance criteria. It is an effort to better parameterize a model to given set of local conditions, thereby reducing the prediction uncertainty. Model calibration is performed by selecting values for model input parameters, these parameters are classified into two groups: physical and process parameters. A physical parameter represents physically measurable properties of the watershed, while process parameters represent properties of the watershed, which are not directly measurable, e.g., average, or effective depth of surface soil moisture storage, the effective lateral inflow rate, the coefficient of non-linearity controlling the rate of percolation to groundwater. Thus, calibrations against available stream flow observations are often conducted to tune the model.

Calibration and validation are typically performed by splitting the available observed data into two datasets: one for calibration, and another for validation. The first step in the calibration and validation process of Arc SWAT is the determination of the most sensitive parameters for a given watershed (Moriasi et al., 2007). This can be achieved by a sensitivity analysis. Sensitivity analysis is aimed at determining the rate of change of model outputs caused by a change of model input parameters. It is a necessary process to identify key parameters and parameter precision required for calibration. Parameters identified from the sensitivity analysis are varied in sequence of their relative sensitivity within their ranges until the volume is adjusted to the required quantity (Zeray, 2007). This process is continued till the volume simulated is within plus minus 15% of the gauged volume (Mengistu and Sorteberg, 2012). For the estimation of the Surface water availability SWAT model was calibrated and validated from the period of 1995 to 2000 and 2001-2005 respectively by using SWAT-CUP Sufi tool. After calibration and validation SWAT is run and required data (Flow_Out) is read from .rch file with help of MS Office tool.

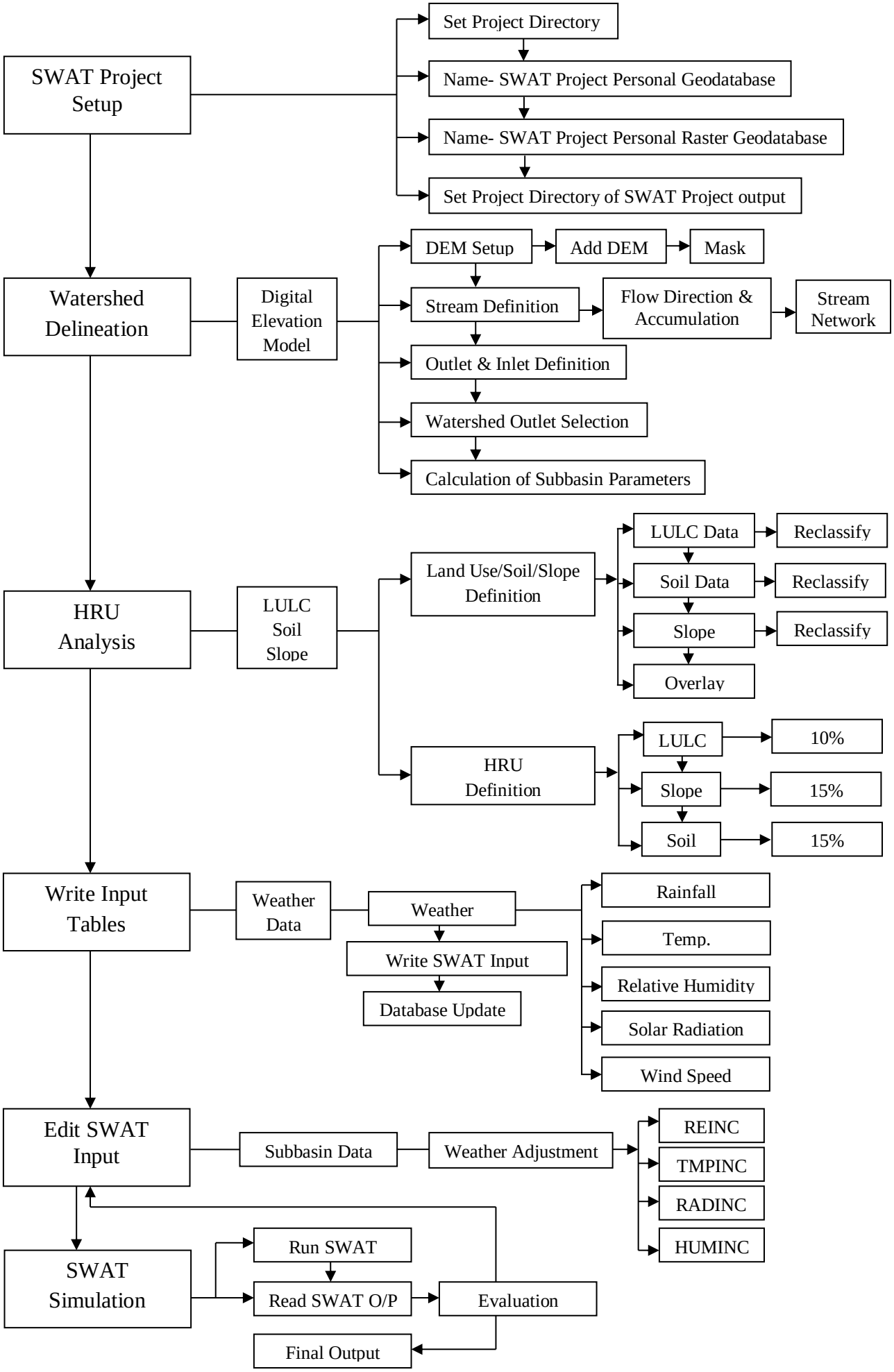

Fig.3.9 Flow Chart of SWAT Operation

3.5.4.1 Assortment of calibration parameters

In this study out of several calibration parameters fourteen parameter were preferred considering that these will provide close concurrence between observed and simulated data for surface runoff. These parameters were preferred for the calibration and validation in SWAT-CUP model along with their respective qualifiers (r_ or v_) as revealed in Table 3.4

Table 3.4 Description of model flow parameters

Sr. No	Parameters	Qualifier	Description of parameters	Subbasin data
1	CN2	r_	SCS runoff curve number	.mgt
2	ALPHA_BF	v_	Baseflow alpha factor (Days)	.gw
3	GW_DELAY	v_	Groundwater Delay (Days)	.gw
4	GWQMN	v_	Threshold depth of water in shallow aquifer required for return flow to occur (mm)	.gw

3.5.5 SWAT-model performance evaluation

To check the accuracy and working precision of the model it felt necessary to check the performance of the model used for the present study; 'Arc SWAT' based on simulated and observed values of different statistical parameters under consideration. The performance of Arc SWAT model was evaluated to determine that how model simulated values fitted with observed values. Mainly those who worked on hydrological study of different watershed and basin by using Arc SWAT have commonly considered two statistical parameters for more reliable evaluation of model viz. coefficient of determination, Nash-Sutcliffe efficiency to check the performance of SWAT (Manfrend and Netsanet, 2013; Jeark and Ariel, 2013; Mengiustu and sortberg,2012). Considering experience, reviews and the accuracy here under this study above two statistical parameters were used to evaluate performance of Arc SWAT model which are being widely used.

3.5.5.1 Coefficient of determination (R^2)

Coefficient of determination describes the degree of co-linearity between simulated and measured/observed data. R^2 describes the proportion of variance in measured data explained by the model. R^2 ranges from 0 to 1, with higher values indicating less error variance and typically values greater than 0.5 are considered acceptable. (Santhi et al., 2001; Van Liew et.al., 2003). The Coefficient of determination is calculated and shown in equation (3.12)

$$R^2 = \left\{ \frac{\sum_{i=1}^{n}(Oi - Si)(Si - S)}{[\sum_{i=1}^{n}(Oi - O)^2]^{0.5}} \right\} \quad \ldots(3.12)$$

Where, R^2= Coefficient of determination

Oi = Observed Data.

O = Average of Observed Data.

Si = Simulated model Output.

S = Average of Simulated Output

n = Number of Observation

3.5.5.2 Nash-Sutcliffe efficiency (NSE)

Nash-Sutcliffe efficiency (NSE) is a normalized statistics that determines the relative magnitude of the residual variance compared to the measured data variance (Nash and Sutcliffe, 1970). NSE indicated how well the plot of observed versus simulated data fits the 1:1 line, NSE ranges between -∞ and 1.0 (1 inclusive), with NSE=1 being the optimal value. Values between 0.0 and 1.0 are generally viewed as acceptable levels of performance, whereas values < 0.0 indicated that the mean observed value is better predicator than the simulated value, which indicated unacceptable performance.

$$NSE = 1 - \left[\frac{\sum_{i=1}^{n}(Oi - Si)^2}{\sum_{i=1}^{n}(Oi - O)^2}\right] \quad \ldots(3.13)$$

Where, NSE= Nash-Sutcliffe efficiency.

Oi= Observed Data

O = Average of observed data

Si = Simulated Model Output

n = Number of observations

3.5.5.3 RSR

RSR is a simple statistical parameter, which calculates the standard deviation of model prediction error. The recommended value is 0.0 − 0.7; zero is very good and 0.7 just satisfactory.

$$RSR = \left(\frac{\sqrt{\sum_{i=1}^{n}(Oi-Si)^2}}{\sqrt{\sum_{i=1}^{n}(Oi-O)^2}}\right) \quad \ldots(3.14)$$

Where, RSR= Standard deviation ratio

Oi= Observed Data

O = Average of observed data

Si = Simulated Model Output

n = Number of observations

3.5.5.4 PBIAS

PBIAS shows the propensity of the calculated discharge to be higher or lower than the observed discharge. While the recommend value varies from -25 − 25 as the value of PBIAS gets closer to 0.0 the accuracy of the model increases, positive value implies underestimation and negative value overestimation (Moriasi et al., 2007; Rouholahnejad et al., 2012).

$$PBIAS = \left[\frac{\sum_{i=1}^{n}(Oi - Si) \times 100}{\sum_{i=1}^{n}(Oi)}\right] \quad \ldots(3.15)$$

Where, Oi= Observed Data

Si = Simulated Model Output

Table No. 3.5 SWAT performance evaluation parameters

Parameter	Value	Rating
Coefficient of Determination (R^2)	> 0.50	Satisfactory
Nash-Sutcliffe efficiency (NSE)	> 0.65	Very Good
	0.54 to 0.65	Adequate
	>0.50	Satisfactory
RSR	0.0 to 0.7	Good
	0.7	Satisfactory
Percent relative bias (PBIAS)	0.0	Accurate
	+ Value	Underestimation
	- Value	Overestimation

To assess how well the model performed Green et al. (2006) and Green and van Griensev (2008) used standards of NSE >0.4 and R^2 >0.5. Moriasi et al. (2007) suggested that model simulation can be considered satisfactory if NSE > 0.5 and RSR ≤ 0.7, and if PBIAS ± 25% for streamflow for the monthly step as shown in Table 3.5.

3.6 Estimation of total surface water availability.

In this study, ArcSWAT was utilized to simulate and analyse various components of water balance within each basin. This component includes surface runoff, total precipitation and potential evapotranspiration. Output from SWAT model is read with help of MS Office tool and required data is extracted discharge (flow_out), potential evapotranspiration (PET_mm) and runoff (SURG_mm) from output file for analysis.

3.7 Estimation of water surplus/deficit in river basin.

Seasonal variation in rainfall and climatic variables influence temporal water availability, which is important for water resource management. An uneven distribution and erratic nature of seasonal rainfall in Konkan region (Mandale, 2016) revealed a need to assess annual and intra-annual water resources availability in region. In present study monthly water surplus/deficit in Konkan region is estimated based on climatic water supply (rainfall) and climatic water demand (potential crop evapotranspiration). This water surplus/deficit is an indicator for spatial and temporal water conditions of region. A climatic water balance approach is used, which is difference between rainfall (P) and potential crop evapotranspiration (PET) gives water surplus or deficit (Choudhury et al., 2012; Bhagat and Patil, 2014). A positive value of difference indicates that climatic water supply (rainfall) is greater than the climatic water demand (potential crop evapotranspiration) i.e. water surplus and negative value indicated climatic water demand is more than the climatic supply i.e. water deficit. In present study monthly climatic water balance study was worked out for Konkan region by using following equation (15) and water surplus/deficit are estimated as:

$$SUR/DEF = \pm (P - ET_{0)} \quad \ldots (3.16)$$

Were,

SUR = Amount of water surplus (mm)

DEF = Amount of water deficit (mm)

P = Precipitation (mm)

ET_0 = Reference evapotranspiration (mm)

CHAPTER IV: RESULTS AND DISCUSSION

This chapter presents the findings of the present study conducted on "Assessment of surface water availability in river basins of Konkan region". It systematically describes, discusses and interprets the results obtained from various used to assess surface water availability. Additionally, the impact of parameters such as soil, land use, and slope on spatiotemporal variability of water is analyzed. Finally, in line with the study's objectives, an estimation of surface water availability in different river basins and districts is provided.

The objective-wise results obtained in this study are presented, described and discussed in the following sections of the chapter.

1) Different methods for assessing surface water availability.
2) Impact of soil, land use, and slope on spatiotemporal variability of water availability
3) Assessment of surface water availability in river basins.

4.1 Methods to assess surface water availability

The study examined various methods for assessing surface water availability in the river basins, as outlined in Section 3.2 of Chapter 3. The principles of operation, applicability, suitability, advantages and limitations of each method are discussed in the subsequent sections of this chapter. Based on this analysis, the most suitable method for estimating surface water availability in the river basin was selected to use in this study.

4.1.1 Direct method

The direct method is particularly useful for streams where the entire flow converges into a single descent. It operates on the time-volume principle and known for being accurate, cost and time-efficient, and environmentally friendly. Additionally, it requires minimal resources and technical expertise (Friederich and Smart 1982; Najafi et al., 2012). However, this method is best suited for small, narrow streams with uniform cross-sectional area (Weight and Sonderegger, 2001; Shope et al., 2013).

4.1.2 Velocity-Area method

This method includes float method, dilution gauging (or tracer) method, current meter method, trajectory method, electromagnetic method, Acoustic Doppler Current Profiler (ADCP) method and salt-velocity method.

Float method is simple, non-polluting and does not require extensive resources and advanced skills (Grant and Brian, 1997; Hauer and Lamberti, 2007). However, it is often inaccurate because vertical turbulent can cause differences in velocity between various streams surfaces, and the float may not represent the actual flow (Hilgersom and Luxemburg, 2012), and is best suited for small, straight streams or canals with low, uniform flow (Hudson, 1993) and is unreliable for larger streams.

The dilution gauging (or tracer) method is used in turbulent flow conditions where conventional methods are challenging to apply (Gordon et al., 2004). However, errors can occur due to tracer loss or incomplete mixing, often caused by velocity differences between stream's upper and lower surfaces. Specialized training is required, and obtaining permission to inject tracers can be difficult due to the potential for water pollution (Moore, 2004).

The current meter method is accurate, time-efficient and well suited for hilly terrains (United States Geological Survey, 2007), making it commercially viable (United States Department of Agriculture, 2001). However, current meters are expensive and typically only used for short periods.

Trajectory method provides reasonably accurate discharge measurements under specific size and flow conditions and can be used when the flow is diverted through a pipe (Hudson, 1993; Boman and Shukla, 2009). This method can also be adapted for small open channels where flow can be directed to a pipe (Liu et al., 2014), but it requires trained personnel and involves complex calculations (Boman and Shukla, 2009).

The electromagnetic method is suitable for streams up to 70 m wide and can accommodate varying flow stages. It produces accurate results but requires specialized training to operate the probes (Ryckborst and Christie, 1977; Van Gent et al., 2008).

ADCP method provides faster and more accurate discharge measurements as it covers a larger portion of the water column (Mueller and Wagner, 2009). While non-invasive, it is expensive and requires skilled operators. Improper techniques can lead to inaccurate results, and it is primarily suited for larger streams and rivers in flat terrains (Visbeck, 2001; Flener et al., 2015). However, with tethered boats, small powered launches, or catamarans, this method can also be used on small rivers with two operators (Herschy, 2008; Flener et al., 2015).

The salt-velocity method is suitable for small streams with uniform cross-sections, but it may negatively impact water quality and aquatic ecosystems.

4.1.3 Formed construction or constricted flow methods

This method utilizes various devices to measure streamflow or water flow, including weirs, Parshall flumes, orifices and meter gates. The weir method requires skilled operators (Peterson and Cromwell, 1993) and significant drop between the upstream and downstream water surfaces, which is often not available in flat-grade ditches. It is frequently necessary to construct a pool or stilling basin upstream of the weir to reduce water velocity. This process can be time-consuming, costly and the installation of weirs may disrupt local habitats (Rickard et al., 2003). Additionally, accurate measurements require strict adherence to proper conditions, and weirs cannot easily be combined with turnout structures. Siltation can also affect the reliability of the results (Hudson, 2004). A pre-measured flow rate is necessary before constructing a weir (Martin, 2006), and the weir must be sized appropriately to handle the expected flow range. In many cases, the natural

flow range may be too broad for a single weir, though compound weirs can help expand the measurable range.

Flumes when properly manufactured and installed, provide accurate results and do not require calibration. However, their accuracy is influenced by the approach velocity of the water and siltation (Hudson, 2004). This method is unsuitable for streams with significant debris, sediment or solids, and the construction and installation of flumes can be challenging (Shieh et al., 1996; Baffaut et al., 2015). Flumes are generally more limited than weirs in terms of the flow range they can measure and are only suitable for smaller streams. Furthermore, flume construction is more difficult than that of weirs.

The ultrasonic method is particularly effective for rivers up to about 300 m wide, especially in situations where there is no stable stage–discharge relationship, and where a physical measuring structure is impractical or too costly. This method is ideal in conditions where backwater effects from dams, tides, or other factors are present, or where the installation of a traditional measuring structure is either financially prohibitive or lacks the necessary head or afflux.

4.1.4 Rainfall-Runoff method

This category includes methods such as Rational Method, Cook's Method, Curve Number Method, Unit Hydrograph, and various empirical formulae, including Runoff Coefficient Method, Inglis Method, Khosla's method.

Rational method is suitable for small watershed area, where it is easier to account for variations in hydrological responses. However, it has limitations, as it assumes constant rainfall intensity over the entire watershed during the storm, which is uncommon. It also neglects losses due to declining storage and infiltration. Additionally, the runoff coefficient used in this method does not account for seasonal variations or changes in rainfall characteristics. One of the primary drawbacks of the Rational Method is that it typically provides only a single point on the runoff hydrograph (Burra et al., 2021).

Cook's Method is relatively simple and accessible to practitioners with limited hydrological expertise. It relies on numerical values derived from watersheds with similar conditions. As an empirical method, it is based on observations rather than theoretical principles, which can limit its accuracy if local conditions differ significantly from those used to develop the method.

The Curve Number method is widely accepted due to its simplicity and minimal input requirements. It has been successfully applied in various hydrological studies and engineering projects. Based on extensive empirical data and field observations, this method is reliable for a range of agricultural conditions, soil types, land uses and moisture levels. It also integrates with Geographic Information System (GIS) for spatial analysis and large-scale hydrological modelling (Mishra et al., 2003; Hawkins et al., 2009; Ponce et al., 1996; Kim et al., 2008). However, the

method is sensitive to the choice of curve number, leading to potential variability in runoff estimates. Additionally, it assumes uniform rainfall distribution across the catchment, which is often unrealistic. The method may not be suitable for large or highly urbanized watersheds where hydrological processes are more complex (Van Mullem and Hawkins, 1990; Ponce, and Hawkins, 1996; Mishra and Singh, 2003).

The Unit Hydrograph method is suitable for small to medium-sized watersheds (more than 25 km^2) and assumes uniform rainfall distribution and homogenous watershed characteristics. It is particularly useful in areas where rapid runoff response is important for flood forecasting and management. However, the assumption of uniform distribution makes it less applicable for large or heterogenous watersheds. This method is not recommended for large, urbanized watersheds with significant spatial variability in rainfall and land use, or where detailed physical modelling is required (Nigussie et al., 2016; Candela et al., 2014).

4.1.5 Noncontact measurement methods

Most of the methods mentioned above are suitable in accessible terrains. For streams that are difficult to access or complex in nature, non-contact methods can be employed. Particle Image Velocimetry (PIV) is a non-contact method that provides high-resolution flow velocity information over a flat surface at a single point in time (Stamhuis, 2006). However, it requires specialized training and expensive equipment and is applicable primarily in flat terrains (Adrian and Westerweel, 2011). While PIV generally yields more accurate results compared to other methods, it does not involve direct measurement, making validation of the results necessary (Hauet et al., 2008).

Traditional method for assessing natural resources is often cumbersome, time-consuming and not cost-effective. Geographic Information System have emerged as a proven technology for site-specific assessment and planning of water and land resources. GIS is now integrated with various hydrological models to assess and simulate land and water resources in areas of interest. Hydrological models vary in terms of input parameters and the extent of physical principles they incorporate. They can be classified as lumped and distributed models based on the whether parameters are a function of space and time, and into deterministic and stochastic models depending on how uncertainty is handled.

Another classification distinguishes between event-based and continuous models. A key distinction in hydrological modelling is empirical, conceptual, and physical models, with specific details provided in Table 4.1.

Table 4.1. Distinguishing characteristics of different models

Parameters	Empirical Model	Conceptual Model	Physically based model
Type	Data based or metric or black box model	Parametric or grey box model	Mechanistic or white box model
Based On	Mathematical equations, derived values from available time series	Model of reservoirs and include semi-empirical equations with physical basis	Spatial distribution, evaluation of parameters describing physical characteristics
Consideration	Little consideration of features and process system	Parameter derived from field data and calibration	Require data about initial state of model and morphology of catchment
Features	High predictive power, low explanatory depth	Simple and can be easily implemented in computer code	Complex model, requires human expertise and computation capability
Limitations	Cannot be generated to other catchments	Require large hydrological and meteorological data	Suffer from scale related problems
Examples	ANN, Unit hydrograph	TOPMODEL, HBV model	SHE or MIKE SHE models, SWAT
Other	Valid within the boundary of given domain	Calibration is involved, curve fitting makes difficult physical interpretation	Valid for wide range of situations

(Source: Devi et al., 2015)

Various hydrological models are available that integrate GIS interface, including HEC-HMS, VIC, MIKE SHE, WEAP and SWAT. Specifications of these models are given in Table 4.2.

Table 4.2. Hydrologic models with their specifications

Model	**HEC-HMS**	**SWAT**	**MIKE**	**VIC**
Advantage	Focus on runoff, channel routing and water control structures	Focus on water quantity, quality and representation of groundwater	Simulates complete land phase of hydrologic cycle	Sub grid variability, Macroscale model, large scale effect
Limitations	Suitable only for events and not for long-term hydrological simulations	Snow process representation requires improvement	Simplified representation of forest cover, High purchase Cost	Large grid size, does not consider urban class in LULC
Runoff	Empirical	Empirical	Physical	Physical

Baseflow/ Groundwater	Empirical	Empirical	Physical	Physical
Watershed Scale	Small to Large	Small to Large	Small to Large	Medium to Large
Climate Regime	Rain or snow	Rain or snow	Rain or snow	Rain or snow/Mixed
Output	FH, AY, PF, LF, SW, ET, WB, SM, IF, OF, SF, GF, RO	FH, AY, PF, LF, SW, ET, WB, SM, IF, OF, SF, GF, RO, SE, NF, WQ	FH, AY, PF, LF, SW, ET, WB, SM, IF, OF, SF, GF, RO, WQ	FH, AY, PF, LF, SW, ET, WB, SM, IF, OF, SF, GF, RO

(Source: Beckers et al., 2009)

(FH = Full hydrograph, AY = Annual Yield, PF = Peak Flow, LF = Low flow, SW = Snow water equivalent, ET = Evapotranspiration, WB = Water balance, SM = Soil moisture, IF = Infiltration, WT = Water Table, OF = Overland flow, SF= Shallow subsurface flow, GF = Groundwater flow, RO = Basin total runoff, SE = Sediment soil erosion, NF = Nutrient Fluxes, WQ = Water quality)

Soil Water Assessment Tool (SWAT) model, developed by the USDA Agricultural Research Service in collaboration with Texas Agricultural University, is widely regarded as a reliable tool for basin-scale studies (Gassman et al., 2014). This GIS-based interface is universally adopted for various works such as water and land resource planning, water quality analysis, crop planning, and water budgeting, provided proper calibration and validation are conducted (Aloui et al., 2012; Arnold et al., 2012). The Arc SWAT model has been applied across diverse regions, watershed scales, climatic zones, environmental conditions and management systems globally, showcasing its capacity for quantitative evaluating hydrological regimes and water resources (Valentina & Mike, 2015).

SWAT offers comprehensive capabilities for assessing and modelling surface water, groundwater dynamics, soil water, snow processes, irrigation systems, impoundment and water management strategies. It also evaluates water quality by analysing nonpoint-source pollution, sediment transport and losses. Furthermore, SWAT is effective in assessing the impact of best management practices (BMPs) in agriculture, urban settings and land use changes. It can evaluate the effects of global and regional climate change and human activities such as land-use expansion, deforestation, and unsustainable water use on hydrological balance components (Bell, 2015).

The model estimates daily overland flow for each Hydrologic Response Unit (HRU) by resolving water budget components, including precipitation, runoff, evapotranspiration, percolation, and groundwater flow. SWAT conceptualizes landscapes as large fields (HRUs) with uniform soil and vegetation sloping towards streams, though real-world flow paths are often more complex. HRUs, which represent unique combination of land use, soil type and slope, dictate hydrologic responses. SWAT partitions daily rainfall into infiltration and runoff using a modified

curve-number method and calculates evapotranspiration based on soil moisture and climate. It also accounts for runoff interception by ponds and wetlands within subbasins (James et al., 2010). Reservoirs, both natural and human-made, influence peak flows and trap significant amounts of sediments and nutrients.

Compared to other land surface models, the following are the distinguishing hydrologic features of SWAT model:

1) SWAT divides watersheds into sub-basins, which are further subdivided into hydrologic response units (HRUs) based on land use, soil type, and slope. This approach allows for a detailed spatial representation of the watershed characteristics (Arnold, 1998).
2) SWAT can integrate various climate change scenarios and LULC changes to evaluate their impacts on hydrology and water resources, making it a valuable tool for assessing the effect of both climate change and LULC changes in related studies (Gosain et al., 2006).
3) SWAT integrates surface water and groundwater interactions, enabling a comprehensive assessment of water movement, storage and dynamics within the watershed.
4) SWAT has capability to model urban hydrology, accounting for the effects of impervious surfaces, stormwater runoff, and the implementation of urban best management practices (Bosch et al., 2010).
5) It provides a user-friendly interface and extensive documentation, making it accessible to a broad range of users, including researchers to practitioners (Neitsch et al., 2005)

4.2 Impact of soil, land use, and slope on spatiotemporal variability of water availability

This section examines the impact of parameters such as soil, land use and slope on temporal and spatial variability of water availability. Additionally, suitable areas for the implementation of water conservation structures are identified. A detailed discussion of the study's results is provided below.

4.2.1 Thematic maps to identify influence on variability of water availability

The eight thematic layers - slope, soil texture, geomorphology, lineament density, rainfall, drainage density, land use land cover and runoff depth, were generated for the river basins of Konkan region to identify the variability in water availability.

4.2.1.1 Slope

Slope plays a crucial role in assessing the variability of surface water. Water tends to accumulate in lower topographical regions rather than higher areas. In regions with steep slopes, water accumulates less, leading to increased runoff, whereas areas with moderate slopes experience reduced runoff. In this study, a slope map was generated from SRTM DEM using ArcGIS software. The study area was divided into three categories: very low to gentle (0-5%), moderate (5-10%), and moderately steep (10-15%) and steep to very steep (> 15%), following the

classification by Kadam et al. (2017). These categories were used to reclassify the zones into storage, recharge and runoff areas. Table 4.3 provides the area covered by each class in the study area (Konkan region), and the distribution of slopes and their corresponding zones are shown in Fig. 4.1.

Table 4.3. Slope classes/zones and area under each class in study area

Slope (%)	Slope Category	Zone	Area (km^2)	Area (%)
0-5	Nearly level to gentle	Storage Zone	16248.72	63.3
5-10	Moderate	Recharge Zone	5980.966	23.3
10-15	Moderately steep	Runoff Zone	2207.567	8.6
>15	Steep to very steep	Runoff Zone	1257.8	4.9

The majority of the Konkan region is covered by the 0-5% slope class (63.3%), representing the nearly flat to gentle slope or storage zone, which is predominately found in northern and southern parts of area (Table 4.3 and Fig.4.1). This is followed by the 5-10% slope class, representing the moderate slope or recharge zone, which is primarily scattered across the central part of the region. The runoff zone, consisting of slopes in the 10-15% and >15% classes, is mainly concentered in the eastern part of the Konkan region, covering 13.5% of the area.

4.2.1.2 Soil texture

Soil is formation results from weathering of parent rocks due to temperature variations and hydration effect. Among the factors influencing runoff generation, soil texture is the most significant. The coarse-textured soils in areas with low slopes tend to have higher infiltration rates, making them more likely to support groundwater potential. In contrast, soils with clay or loam texture, high slope range and shallow depths are prone to runoff and soil erosion, with lower potential of groundwater recharge.

The soil map of the Konkan region was obtained from National Bureau of Soil Survey & Land Use Planning (NBSS & LUP), Nagpur. The region contains four major textural classes: sandy clay loam, loam, clay loam, and sandy loam. The numerical distribution of these soil textural classes is iterated in Table 4.4 and their spatial distribution is mapped in Fig. 4.2.

Table 4.4. Soil Textural classes and their distribution in Konkan region

Sr. No	Soil Texture	Area (km^2)	Area (%)
1	Sandy clay loam	5133.88	20.0
2	Loam	11782.25	45.9
3	Clay loam	8727.59	34.0
4	Sandy loam	25.67	0.1

The results in Table 4.4 revealed that the loam soil texture is distributed in 45.9% area, followed by the clay loam soil texture (34%). The sandy clay loam and sandy loam soils are scantily available in 20.1% area of the study area. The distribution of clay loam is mainly concentrated in the northern part of the Konkan region, while loam soil is mainly distributed in central to southern part of the region. The sandy clay loam soils are distributed in northern and southern parts of the study area (Fig. 4.2).

4.2.1.3 Land use land cover (LULC) change

Land use refers to human activities and various purposes for which land utilized, while land cover represents the natural features such as vegetation, water bodies, rock/soil, artificial covers that result from land transformation (Balachander et al., 2010). River basins are dynamic and complex systems involving several natural or natural or anthropogenic physical processes at various spatial and temporal scales (Deshmukh et al., 2013). Natural or anthropogenic activities can often affect hydrology adversely. Agricultural expansion and intensification, urban growth, and changes in economic levels force land use/land cover changes in river basins to meet increasing population demands (Lee, 2005; Smith et al., 2016; Aneseyee et al., 2020). Remote sensing data captured information about the land surface, from which land use must be inferred. In the study area, satellite imagery identified land use and land cover (LULC) features, including water bodies, agricultural land, forest, barren land, built-up areas and flooded vegetation. For this study, Sentinel 2 (10m) land use land cover data for 2017 and 2019 was procured from ESRI. The LULC data of both years was analyzed to assess changes between 2017 to 2019 and their impact on surface water availability, while the 2019 LULC data was used in the SWAT model to estimate surface water availability in the river basins under the recent conditions. The distribution of LULC in the study area is presented in Table 4.5.

Table 4.5. Distribution of Land Use Land Cover in Konkan region

		2017		2019	
Sr. No	LULC Class	Area (km^2)	Area %	Area (km^2)	Area (%)
1	Water bodies	646.87	2.52	592.96	2.31
2	Forest	10383.26	40.45	8968.88	34.94
3	Agriculture	2908.34	11.33	2993.05	11.66
4	Built-up	831.69	3.24	1129.45	4.40
5	Barren land	10899.22	42.46	11985.03	46.69

The land use land cover (LULC) results in Table 4.5 show that the majority of the area is classified as under barren land, which increased from 10899.22 km^2 (42.46%) in 2017 to 11985.03 km^2 (46.69%) in 2019. The rate of increase is observed very fast, might be due to the lack of interest for agriculture. Conversely, the area covered by forested land decreased from 10383.26 km^2 (40.45%) in 2017 to 8968.88 km^2 (34.94%) in 2019. The proportion of land occupied by water

bodies also shrinked from 646.87 km^2 (2.52%) in 2017 to 592.96 km^2 (2.31%) in 2019. This could be due to transformation of wetlands and swampy areas into bare land and decrease in river water in the study area. The built-up area expanded, rising from 831.69 km^2 (3.24%) in 2017 to 1129.45 km^2 (4.4%) in 2019. Agricultural land saw only minor increase, from 11.33% in 2017 to 11.66% in 2019. The change in LULC in the river basin has many implications for river's streamflow and surface water availability. LULC type, soil parameters and yearly precipitation directly relate to average annual stream flow. The reduced water storage capacity of the expanded barren land and the shrinkage in forest and agricultural land might result in increased water runoff and lateral flow in the river basin. The spatial distribution of LULC in Konkan region is presented in Fig.4.3(a) for year 2017 and in Fig 4.3(b) for year 2019.

The results of spatial distribution of LULC in Fig. 4.3 (a and b) indicate that the barren land in northern part of the study area tremendously increased during 2019 as compared to that in 2017. This change was seen in other parts of the area, but with less intensity. The built-up area in Thane district is seen tremendously increased as compared to other parts.

According to Thapa et al. (2017), LULC replenishes groundwater. It gives essential information on soil moisture, infiltration, groundwater, and surface water while also giving insight into the water requirements of the groundwater (Chen et al., 2022; Yeh et al., 2016; Hussain et al., 2022). The waterbodies had the highest potential for groundwater recharge, with a highest weight value compared to other LULC types. On the other hand, built-up areas had the lowest potential for groundwater recharge with the lowest weight.

4.2.1.4 Geomorphology

Hydrology and geomorphology are closely interrelated through the process of erosion and deposition, which create a dynamic equilibrium in healthy watersheds. The hydrologic behavior and geomorphic evolution of watersheds are tightly connected - runoff generation and water storage are influenced by the topography and properties of the surface and subsurface. Litwin et al. (2022) noted that watersheds store and release water in response to precipitation in complex ways, strongly impacted by the topography and subsurface characteristics. Overlong, timescales, water flow significantly shapes these attributes through erosion and subsurface weathering. Therefore, many landscapes are expected to show strong connections between topographic features and hydrological properties. Their study showed that hillslope length increases with greater transmissivity relative to the recharge rate, three topographic metrics – steepness index, Laplacian curvature and topographic index – can be used to interpret landscapes that the coevolved with runoff driven by shallow subsurface flow.

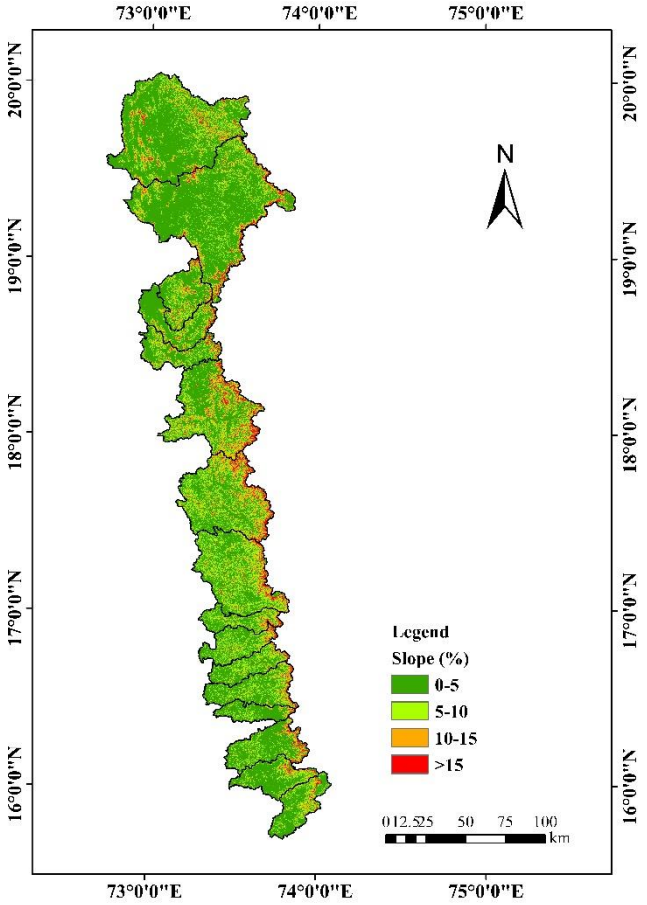

Fig. 4.1. Spatial distribution map of Slope categories in Konkan region

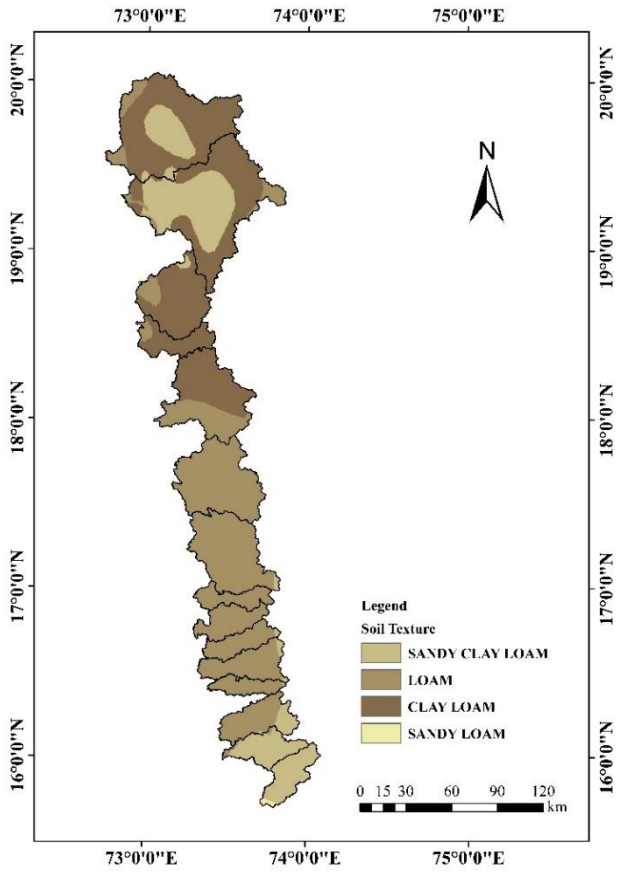

Fig 4.2. Spatial distribution map of Soil texture in Konkan region

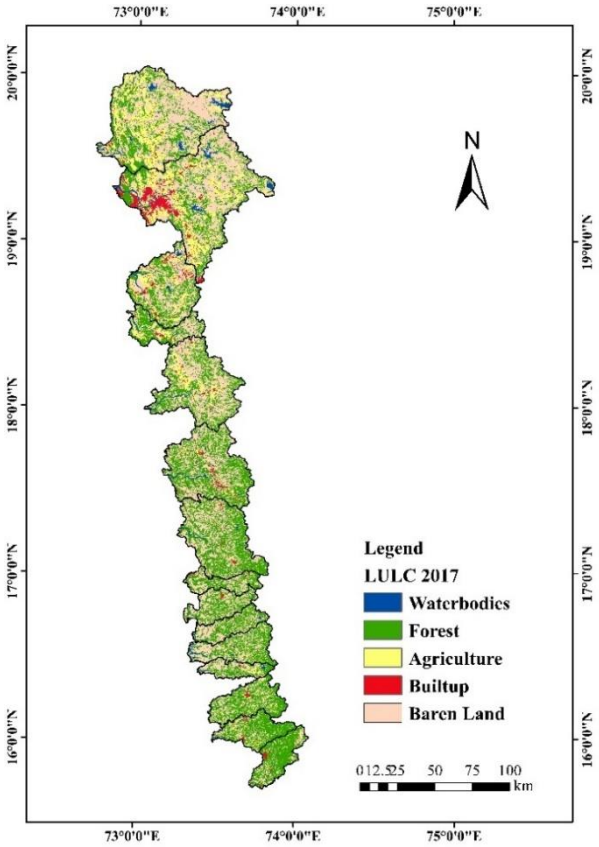

Fig. 4.3 (a). Land use land cover (LULC) distribution in Konkan region during 2017

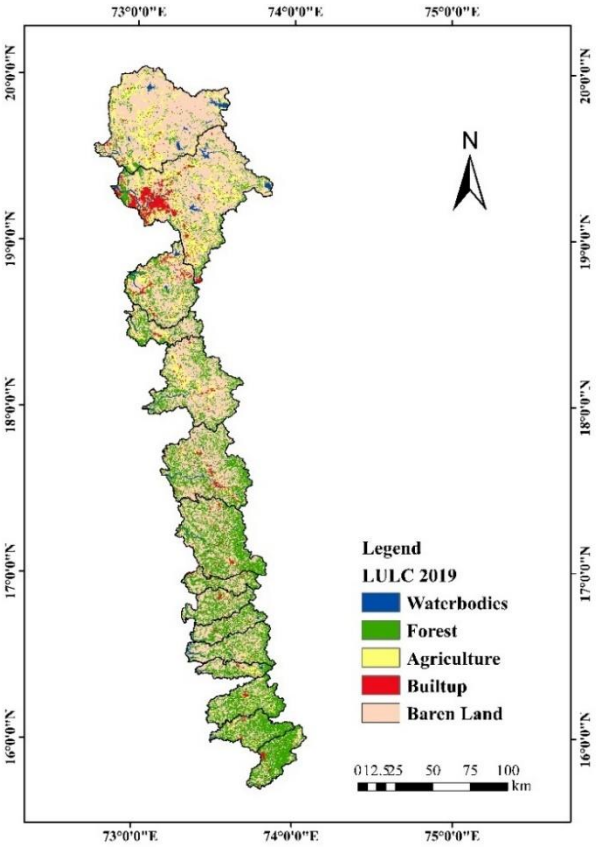

Fig. 4.3 (b). Land use land cover (LULC) distribution in Konkan region during 2019

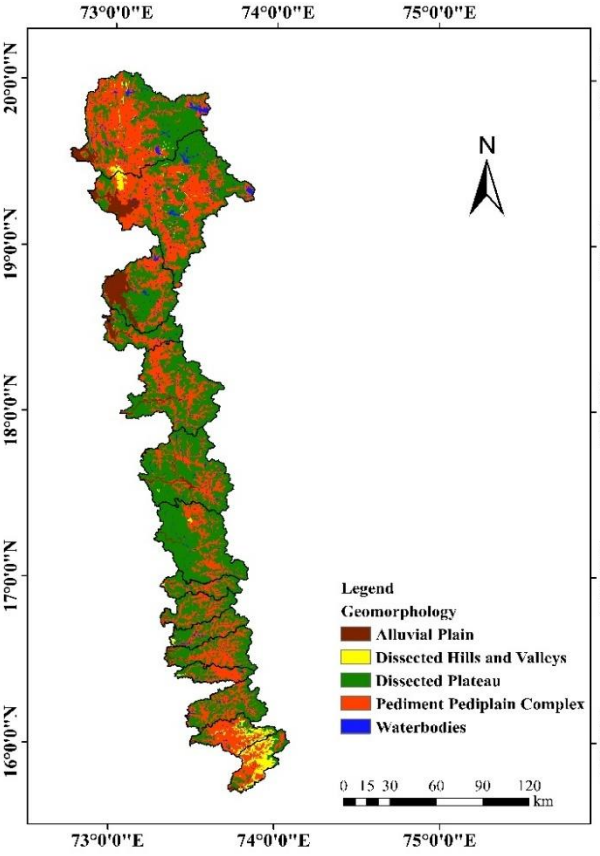

Fig 4.4. Spatial distribution map of geomorphology of Konkan region

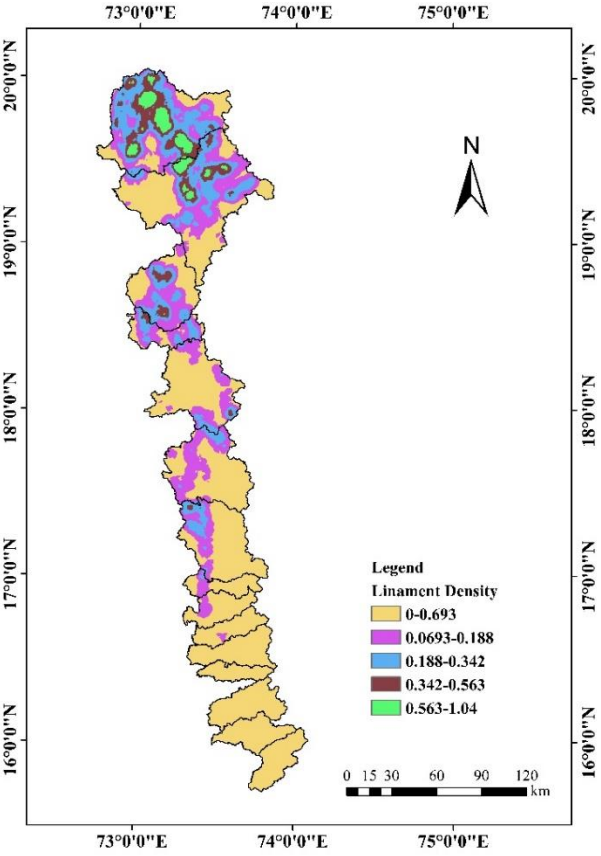

Fig 4.5. Lineament density contour map of Konkan region

Geomorphology is the study of Earth's structures and landforms, was applied in this study to map the Konkan region using a digitized vector shapefile in GIS software. Sixteen geomorphic units were identified, including Dissected Hills and Valleys – 1) Highly Dissected Hills and Valleys, 2) Moderately Dissected Hills and valleys, 3) Low Dissected Hills and Valleys, Dissected Plateau – 1) Low disserted plateau, 2) Moderately disserted plateau, 3) Highly dissected plateau, Waterbodies – 1) river, 2) salt pan, 3) dams and reservoirs, 4) Flood plains, 5) Offshore Island, 6) other, Pediment Pediplain Complex – 1) Flood Plain, 2) Coastal Plain, 3) Quarry and Mine Dump, 5) Anthropogenic terrain, and Alluvial Plain. For simplicity, these were grouped into five categories as: Dissected Hills and Valleys, Dissected plateau, Pediment Pediplain Complex and Alluvial Plain and the units are detailed in Table 4.6.

Table 4.6. Geomorphology in Konkan region

Sr. No	Geomorphological Units	Area (km^2)	Area (%)
1	Dissected Hills and Valleys	646.87	2.52
2	Dissected Plateau	13553.43	52.8
3	Waterbodies	467.18	1.82
4	Pediment Pediplain Complex	8840.53	34.44
5	Alluvial Plain	2161.36	8.42

The dissected plateau occupied the maximum area in Konkan region with 13553.43 km^2 area, which is 52.80% of the total geographical area followed by the Pediment pediplain complex occupying area of 8840.53 km^2 (34.44%), while the alluvial plain occupied 2161.36 km^2 (8.42%), dissected hills and valleys occupied 646.87 km^2 (2.52%) and water bodies occupied only 467.18 km^2 (1.82%) area (Table 4.6).

To assess the surface water flow in the different surface topography and geological formations in the Konkan region, the spatial distribution map of geomorphology is illustrated in Fig. 4.4. The dissected plateau units, identified as having poor to moderate groundwater potential (Gurav and Babar, 2019), are widespread across the Konkan region, particularly on the eastern hilly and western plains. In western plains, plateau units with slopes of 5-10% may serve as effective groundwater recharge zones, while those with slopes exceeding 10% tend to generate more runoff (Table 4.3 and Fig. 4.1). The pediments, characterized by erosional surfaces extending from hills to neighboring basins and exhibiting moderate slope (5-10%) with sparse vegetation, can also function as recharge zones but have limited groundwater recharge potential.

Dissected hills and valleys, formed by tectonic processes and extensively dissected by drainage lines, can be classified based on dissection into highly, moderately and low dissection areas, depending on the density of joints and drainage (Nandhagopal et al., 2015). These features

are predominantly found in southern part of the region, with a small portion in northern Konkan, mainly composed of granite gneiss, leuco granite and have very low water retention properties.

Pediplain units, offering good to moderate groundwater potential, are dominantly found in the northern part of Konkan region but are scattered throughout the area. The alluvial plain units, primarily concentrated in the western coastal plains of Palghar, Thane and Raigad districts, fall within 0-5% slope range and are considered as storage zone (Table 4.3 and Fig. 4.1). These plains receive new alluvium, consisting of coarse-grained sediments deposited in and close to stream. Due to high porosity, alluvial plains are considered favorable for water retention (Anonymous, 1997; Anonymous, 2003).

Geomorphological features are ranked based on their suitability of surface water retention. Waterbodies, with highest retention potential, receive highest ranking, while dissected hills and valleys - due to poor retention – are assigned lower rankings.

4.2.1.5 Lineament Density

Lineaments are linear or curvilinear features that are structurally controlled. The term ‘lineament’ has been defined in various ways in the literature, with different attributes sometimes describing it assumed origin or the data source from which it has been derived. Some researchers also use alternative terms such as ‘fracture trace’ or ‘photo linear’. Lineaments are extended, mappable linear or curvilinear features on the surface, whose parts align in straight or nearly straight patterns, often representing subsurface structures like folds, fractures or faults. These features, mappable at various scales, are important in groundwater exploration. Several studies have shown a strong correlation between lineaments and groundwater flow and yield (Mabee et al., 1994; Magowe and Carr, 1999; Fernandes and Rudolph, 2001). Typically, lineaments are associated with zones of weathering and increased permeability and porosity.

Some researchers investigated the relationship between groundwater productivity and number of lineaments within specifically designed areas or lineament density - referring to number of lineaments in a specific area - rather than focusing solely on the lineaments themselves (Hardcastle, 1995). Therefore, mapping of lineaments, which are closely linked to groundwater occurrence and yield, is essential to groundwater surveys, development and management.

Remote sensing and GIS have been widely used to create various thematic maps and integrate them for different applications. In this study, the lineament density map of the area was generated using the “Line Density” in a GIS environment. Based on lineament density values, the area was categorized into five classes, with coverage details presented in Table 4.7.

Table 4.7. Lineament density distribution and their coverage areas in Konkan region

Sr. No	Lineament Density (km/km^2)	Area (km^2)	Area (%)
1	0-0.0693	10013.63	39.01
2	0.0693-0.188	5701.17	22.21
3	0.188-0.342	4214.91	16.42
4	0.342-0.563	3888.91	15.15
5	0.563-1.04	1850.76	7.21

The results in Table 4.7 show that the lineament density in the study area ranges from 0 to 1.04 km/km^2. Most of the area is covered by lineament densities between 0 – 0.0693 km/km^2, followed by densities in the range of 0.0693 – 0.188 km/km^2.

The purpose of the fracture density analysis is to calculate frequency of fractures per unit area. In this study, the lineament density was analyzed to identify the distribution trends across the area. As a result, a map was generated to highlight the concentrations of lineaments within the study area (Fig. 4.5).

The lineament/ fracture analysis revealed that the study area contains numerous long and short fractures, with structural trends predominantly oriented in an east-west direction. In the northeastern parts of the study area, specifically in Palghar and Thane districts, the density of cross-cutting lineaments is relatively high, while it is lower in the other areas. The least cross-cutting lineaments is found in Sindhudurg district, located in the southern part of study area.

The zones with high density of lineament intersection suggest reduced runoff and are considered feasible zones for groundwater prospecting within the river basin. In contrast, areas with very low lineament density are observed, indicating a low degree of hydraulic connectivity between the above lithologic units, as surface water is unable to circulate these discontinuities. This observation confirms the lithologies in these regions have been influenced by tectonic activity.

Lineament density is crucial in identifying the groundwater resources, as higher densities are associated with increased productivity for groundwater (Hatefi and Ekhtesasi, 2016). It is characterized by curved and straight linear alignments in structural drainage patterns, lithological, and topographical anomalies (Tamesgen et al., 2023). The occurrence and movement of groundwater show a positive correlated with lineament density (Varade et al., 2018). Areas with lineament densities ranging from 0.563 to 1.04 km/km^2 are assigned the highest rank, while the areas with lower lineament densities receive the lowest rankings.

4.2.1.6 Drainage density

Water bearing formations on the crust of the Earth act as a a medium for transmission as well as reservoirs to store the water. High relief along with steep slopes provides higher runoff, whereas topographical depressions improve the infiltration. Drainage density has an inverse relationship with infiltration capacity, permeability and vegetative cover (Horton, 1945). It is the ratio of total stream length to the total area of the basin. This metric helps to understand the extent of surface water flow and is used to assess the potential for runoff, and water availability. An area with high drainage density also boosts surface runoff as compared to the area with low drainage density. Drainage density, surface-water discharge and groundwater movement are shown to be parts of a single physical system in a river basin. Water bodies on the surface, like wells, rivers, ponds and so on, can become recharge zones (Murugesan et al., 2012).

Drainage density map of study area was prepared using channel network with the help of 'Line density tool' of GIS atmosphere. The lower drainage density means permeable subsoil or highly resistant, dense vegetative cover, low relief and runoff, whereas the higher drainage density has a more stream number that results in rapid stream response (Nag, 1998). According to Tucker et al. (2001), drainage density reflects the intensity to which a given landscape is dissected. Berger and Entekhabi (2001) concluded that high drainage density is strong associating with highly dissected terrain and torrential runoff resulting into intense floods and intense soil erosion. Therefore, it is noteworthy that drainage density is a good indicator and measure of physical and hydrological characteristics of a river basin.

In the study area, the density of drainage ranges from 0.095 to 4.8 km/km^2. For the analysis purpose, the drainage density range is categorised into five classes (i) very low (0.095 – 1.0), (ii) low (1.0 – 2.0), (iii) medium (2.0 – 3.0), (iv) high (3.0 – 4.0) and (v) very high (4.0 – 4.48) drainage density (km/km2). These classes and area occupied under each class are given in Table 4.8.

Table 4.8. Drainage density classes and area occupied under different classes in Konkan region

Sr. No	Drainage Density (km/km^2)	Area (km^2)	Area (%)
1	0.095-1	387.61	1.51
2	1 - 2	3031.55	11.81
3	2 -3	12018.40	46.82
4	3-4	9387.29	36.57
5	4-4.8	844.52	3.29

The regions with high drainage density show high surface runoff and low infiltration, hence low probability of groundwater potential. Similarly, areas with low drainage density may have high infiltration, low runoff creation, thus, higher probability of groundwater potential. In the present study, the area occupied under drainage density of medium to very high (2.0 – 4.8 km/km^2)

is 22250.21 km^2 (86.68%) having higher probability of runoff creation. On the contrary, only 3419.16 km^2 (13.32%) area has higher infiltration characteristics and can create low runoff. These features suggest that the region is highly suitable for groundwater recharge. These results can be verified with geomorphology and land use land cover result of the area. These results are in line with the results of Neelam Kumari et al. (2023) for Kal River and Gharde and Kothari (2016) for Savitri River of Konkan region.

Drainage density is a key factor in assessing groundwater recharge and groundwater availability, as it provides valuable insights into the hydrological landscape, including infiltration rates and underlying lithology (Pande et al., 2020; Melkamu et al., 2022). Areas with high drainage density experience greater runoff and reduced infiltration, leading to lower groundwater recharge (Waikar and Nilawar, 2014; Viswanathan et al., 2021). In the study area, the drainage density ranges from 0.095 to 4.8 km/km^2 and is classified into five categories as presented in Table 4.8. Aquifer permeability is inversely related to drainage density, affecting both runoff distribution and infiltration levels (Andualem and Demeke, 2019). Regions with high drainage densities (4 to 4.8 km/km^2) are considered poorly suitable for water retention, while regions with low drainage densities (0.095 to 1.0 km/km^2) are deemed highly suitable (Table 4.8). The spatial distribution of drainage density classes across the study area is presented in Fig. 4.6.

The spatial distribution of the drainage density indicates that the high drainage density is widely distributed all over the region, making the land surfaces suitable for surface runoff and unsuitable for groundwater potential. Mostly the drainage lines are seen east to west facing in direction.

4.2.1.7 Rainfall

Rainfall plays a crucial role in the hydrological cycle, in assessing surface water resources and significantly impacts groundwater potential and recharge (Saravanan et al., 2020). It is considered the primary source of groundwater storage and determines the fluctuation (Magesh et al., 2012; Agarwal et al., 2013; Sai et al., 2024). The intensity of rainfall directly affects groundwater recharge, with higher intensity leading to increased recharge and vice versa. Daily rainfall data was collected from 92 hydrometeorological stations spread across 14 river basins, sourced from the Hydrological Data Users' Group (HDUG), Nashik. This data aggregated into annual totals and used to prepare a spatial distribution map by employing the Inverse Distance Weighing (IDW) interpolation method. The region consistently receives rainfall during monsoon season, occurring more than 90% of the total spanning through June to September. The interpolated rainfall distribution and the area corresponding to each rainfall range are summarized in Table 4.9.

Table 4.9. Distribution of precipitation in Konkan region

Sr. No	Rainfall (mm)	Area (km^2)	Area (%)
1	500-1000	10.27	0.04
2	1000-2000	41.07	0.16
3	2000-3000	10049.56	39.15
4	3000-4000	13068.28	50.91
5	4000-5000	2500.20	9.74

The wide variation in precipitation is seen in Konkan region ranging from 500 to 5000 mm. Highest area occupied under the rainfall range of 3000-4000 mm rainfall is highest amounting to 13068.28 km^2 (50.91%) followed by the range from 2000-3000 mm rainfall on 10049.56 km^2 (39.15%). The area under 4000 to 5600 mm rainfall range is 2500.20 km^2 (9.74% of the total study area).

Areas with the lowest rainfall were assigned the lowest rank and the highest rainfall area was assigned the highest rank. The spatial distribution of rainfall indicates that the Sahyadri ranges receives significantly higher rainfall (> 4000 mm) compared to the surrounding plains (Fig. 4.7). In the northern part of Konkan, rainfall ranges between 2000 and 3000mm, with amounts increasing towards the southern part of the study area. A small area in northwestern part of Raigad district shows rainfall between 500-1000 mm, though this is likely due to interpolation error and can be disregarded.

4.2.1.8 Runoff Depth

Rainfall-generated runoff is crucial in hydrologic studies and a number of water supply planning and management practices, including flood control and its management, irrigation scheduling, design of irrigation and drainage network, etc. The runoff output from ArcSWAT model was retrieved and the values were aggregated to total for annual runoff depths, which was used to create the runoff depth map for all river basins in the study area. The runoff was categorized in appropriate classes, with weightages assigned according to their relative importance from a surface water perspective. The runoff depth ranges and area occupied under each range in the study area are presented in Table 4.10. Table 4.10. Runoff depth ranges and areas occupied under each range in study area.

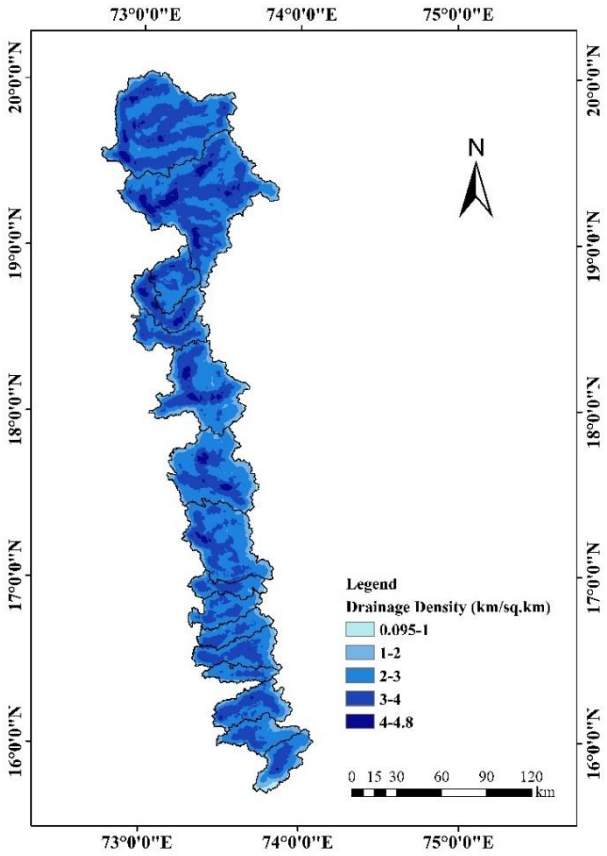

Fig. 4.6. Spatial distribution map of Drainage density in Konkan region

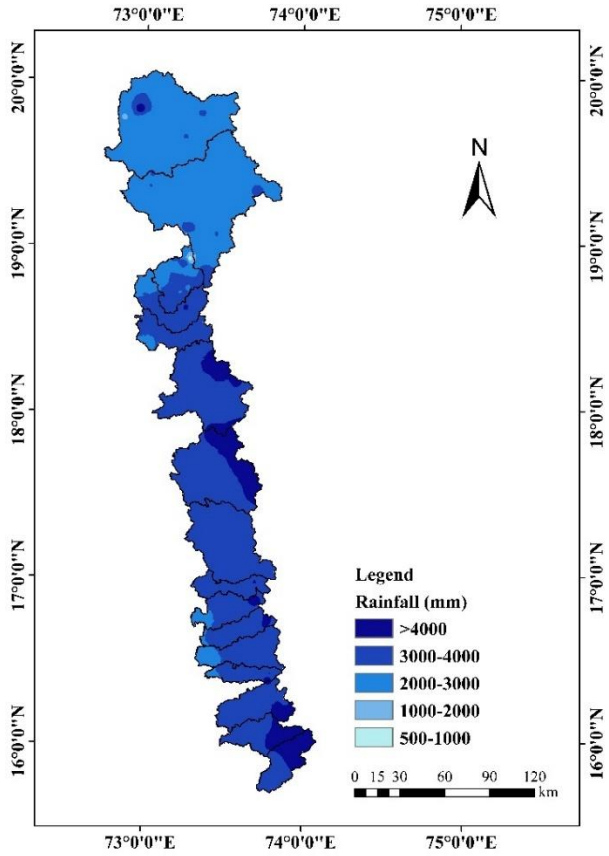

Fig. 4.7 Spatial distribution map of Rainfall in Konkan region

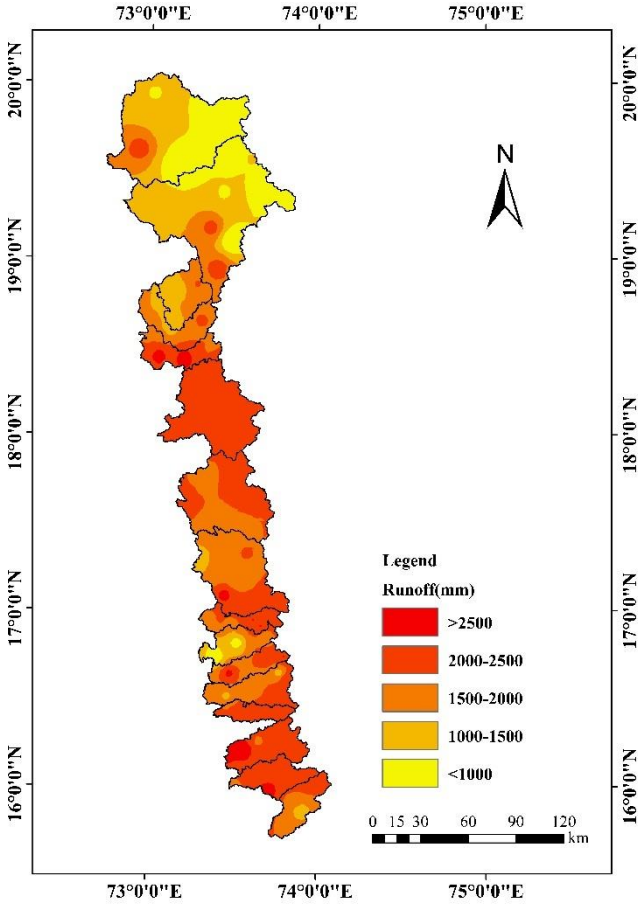

Fig. 4.8. Spatial distribution map of runoff depth in Konkan region

Table 4.10 Distribution of Runoff Depth in Konkan Region

Sr. No	Runoff Depth (mm)	Area (km^2)	Area (%)
1	200-1000	3704.09	14.43
2	1000-1500	5169.81	20.14
3	1500-2000	7187.43	28.00
4	2000-2500	9148.57	35.64
5	2500-2900	460.05	1.80

Table 4.10 shows that an area of 9148.57 km^2 (35.64% of total area) falls within the runoff range of 2000-2500 mm, followed by areas of 7187.43 km^2 and 5169.81 km^2 within the runoff ranges of 1500-2000 mm and 1000-1500 mm, respectively. This indicates that 83.78% area experiences significant runoff exceeding 1000 mm, primarily due to the combined effect of heavy and intense rainfall, topographic conditions, and coarse soil. The spatial distribution of runoff created in the study area is shown in Fig. 4.8.

The runoff generated in the northern part of the region is mostly below 1500 mm, with some areas exceeding 2000 mm. The northern region is characterized by soils with higher clay content, and topography ranging from flat to moderately sloped. In contrast, most areas in the southern part of the study region experience runoff exceeding 2000 mm, which is likely due to steeper slopes and prevalence of laterite soils.

4.2.2 Assessment of impact of slope, soil, LULC on variability of water

Suitability area map for water retention was prepared using weighted sum model in GIS software by integrating thematic layers such as slope, soil texture, geomorphology, lineament density, rainfall, drainage density, land use land cover and runoff depth. Fig. 3.6 illustrates the workflow for assessing the suitability of the area in ArcGIS software. Analytical Hierarchical Process (AHP) method was employed to generate suitability map.

Analytical hierarchy process (AHP) is a flexible and well-structured tool for solving complex decision-making problems that involve multiple factors (Saaty, 1980; Dou et al., 2017). In this study, the AHP model was applied to determine the weights and rankings of various parameters for a suitability assessment. The method uses a numerical scale from 1 to 9 to compare the relative the relative importance of each layer (Saaty, 2008). A comparison matrix was constructed to rank the criteria, where the diagonal elements assigned a value of 1, indicating equal importance. Table 3.2 presents the Saaty scale of relative importance. A pairwise comparison matrix was developed for all parameters, followed by a normalized matrix to calculate the criteria weights.

Next, a weighted sum matrix was constructed, and λ_{max} was calculated using this matrix. The thematic factors were ranked according to Saatys' scale (2008) as shown in Table 4.11. A

normalized pairwise comparison matrix was developed, and criteria weights (CW) for each thematic factor are shown in Table 4.12. The weighted sum matrix was established by calculating the modified weights for each factor, as displayed in Table 4.13**.**

Table 4.11. Pairwise comparison matrix for all parameters

Sr. No.	Theme	Theme							
		Slope	Rainfall	LULC	Soil	Runoff	GM	DD	LD
1	Slope	1	2	1	2	3	2	1	3
2	Rainfall	0.50	1	3	2	1	3	1	3
3	LULC	1.00	0.33	1	3	2	2	3	2
4	Soil	0.50	0.50	0.3	1	2	2	3	1
5	Runoff	0.33	1.00	0.5	0.5	1	3	1	1
6	GM	0.50	0.33	0.5	0.5	0.33	1	2	1
7	DD	1.00	1.00	0.3	0.3	1.00	0.50	1	1
8	L.D	0.33	0.33	0.5	1.0	1.0	1.0	1	1
	SUM	5.17	6.50	7.2	10.3	11.33	14.50	13.0	13.0

(*Note.* DD – Drainage Density, GM – Geomorphology, LD – Lineament Density)

Table 4.12. Normalized pairwise comparison matrix

Sr. No.	Theme	Theme								CW/Avg.
		Slope	Rainfall	LULC	Soil	Runoff	GM	DD	L.D	
1	Slope	0.19	0.31	0.14	0.19	0.26	0.14	0.08	0.23	0.19
2	Rainfall	0.10	0.15	0.42	0.19	0.09	0.21	0.08	0.23	0.18
3	LULC	0.19	0.05	0.14	0.29	0.18	0.14	0.23	0.15	0.17
4	Soil	0.10	0.08	0.05	0.10	0.18	0.14	0.23	0.08	0.12
5	Runoff	0.06	0.15	0.07	0.05	0.09	0.21	0.08	0.08	0.10
6	GM	0.10	0.05	0.07	0.05	0.03	0.07	0.15	0.08	0.07
7	DD	0.19	0.15	0.05	0.03	0.09	0.03	0.08	0.08	0.10
8	L.D	0.06	0.05	0.07	0.10	0.09	0.07	0.08	0.08	0.07
	SUM	1.0	1.0	1.0	1.0	1.0	1.0	1.0	1.0	1.0

(*Note.* DD – Drainage Density, GM – Geomorphology, LD – Lineament Density)

Table 4.13. Weighted Sum (WS) matrix

Sr. No.	Theme	Theme								WS	WS/ CW
		Slope	Rain	LULC	Soil	Run	GM	DD	L.D		
1	Slope	0.19	0.37	0.17	0.23	0.29	0.15	0.09	0.22	1.72	8.91
2	Rain	0.10	0.18	0.52	0.23	0.10	0.22	0.09	0.22	1.66	9.07
3	LULC	0.19	0.06	0.17	0.35	0.20	0.15	0.26	0.15	1.54	8.94
4	Soil	0.10	0.09	0.06	0.12	0.20	0.15	0.26	0.07	1.05	8.91
5	Runoff	0.06	0.18	0.09	0.06	0.10	0.22	0.09	0.07	0.88	8.92
6	GM	0.10	0.06	0.09	0.06	0.03	0.07	0.18	0.07	0.66	8.86
7	DD	0.19	0.18	0.06	0.04	0.10	0.04	0.09	0.07	0.77	8.77
8	L.D	0.06	0.06	0.09	0.12	0.10	0.07	0.09	0.07	0.66	8.94
										λ_{max}	8.91

(Note: Rain – Rainfall DD – Drainage Density, GM – Geomorphology, LD – Lineament Density)

The ratio of the weighted sum (WS) to criteria weight (CW) was calculated for each thematic factor to estimate λ_{max}, which was determined to be 8.91. The consistency index (CI) was then calculated, yielding a value of 0.13 and the consistency ratio (CR) was found to be 0.093, which is below the acceptable threshold of 0.1, indicating an acceptable level of consistency.

Finally, the rank assignment for the thematic maps was performed based on their relative importance to water retention in the area. Thematic factors were ranked on a scale from 1 to 5, where a higher overall score indicated greater suitability for water retention. The rankings and weightages of different thematic factors - slope, soil texture, geomorphology, lineament density, rainfall, drainage density, land use land cover and runoff depth are detailed in Table 4.14.

To study the impact of change in LULC on variability of area suitability, LULC data of year 2017 and 2019 were analyzed. The assigned ranks were integrated into the raster layers of all thematic maps. The reclassified thematic maps with ranking values were combined using the "weighted sum" tool in ArcGIS software for the year 2017 and 2019 separately. Suitability areas were classified into four categories: highly suitable, moderately suitable, less suitable, and not suitable. The area occupied under each suitability class of water retention for LULC categories in the Konkan region during 2017 and 2019 are presented in Table 4.15, and the spatial extent is illustrated in Fig. 4.9 (a) and Fig. 4.9 (b) for 2017 and 2019, respectively.

Table 4.14. Weightage and ranking for different thematic map by AHP

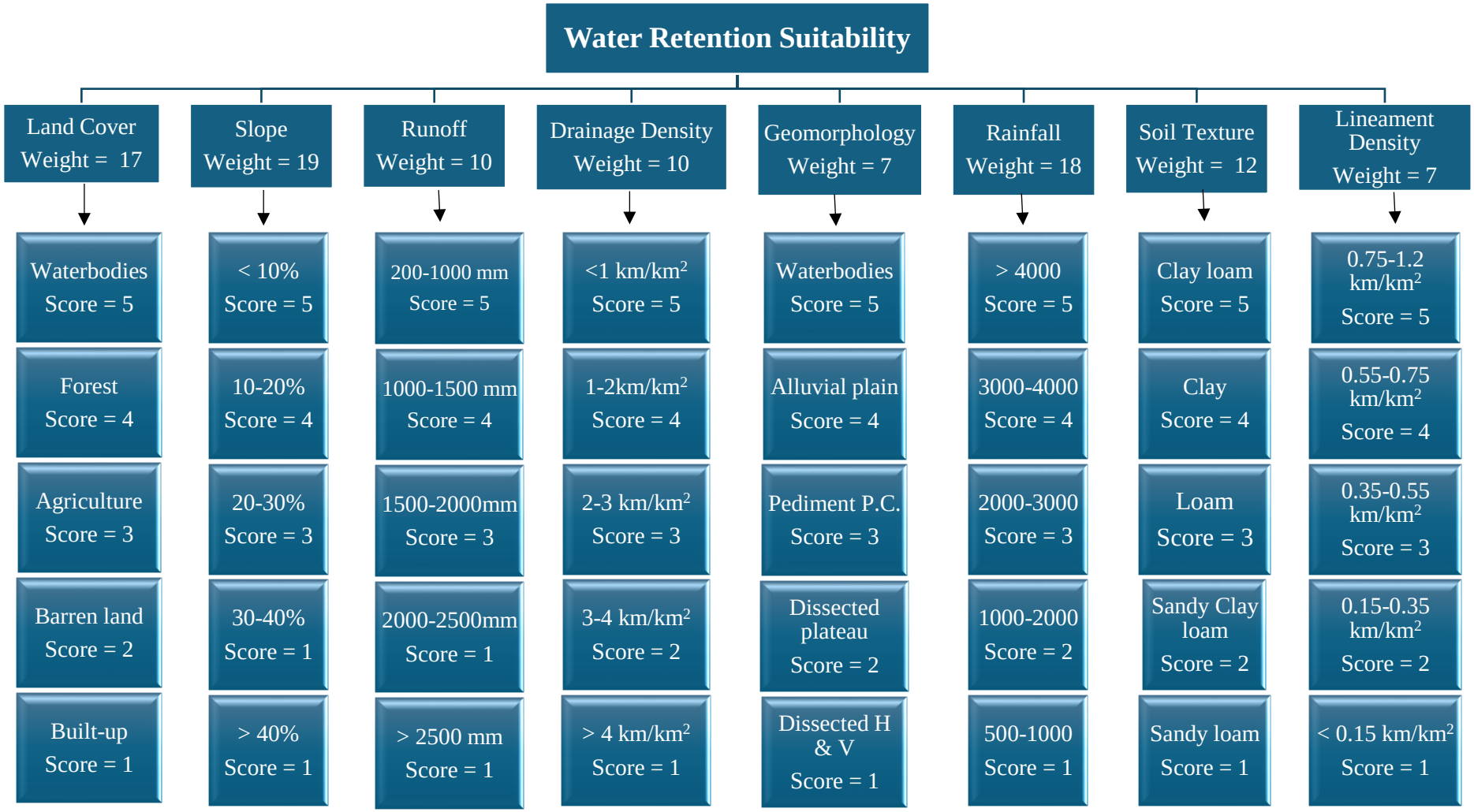

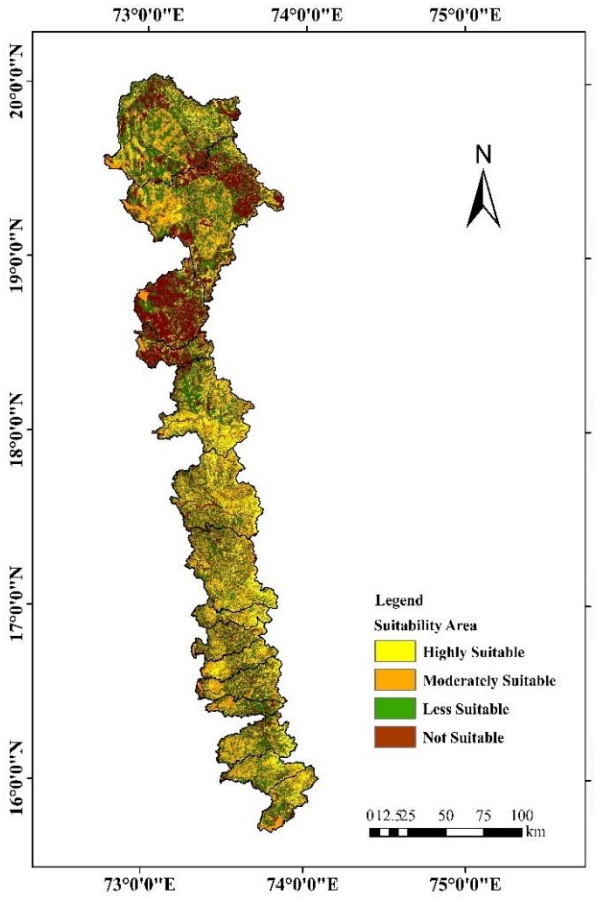

Fig. 4.9 (a). Area distribution of water retention site suitability (2017)

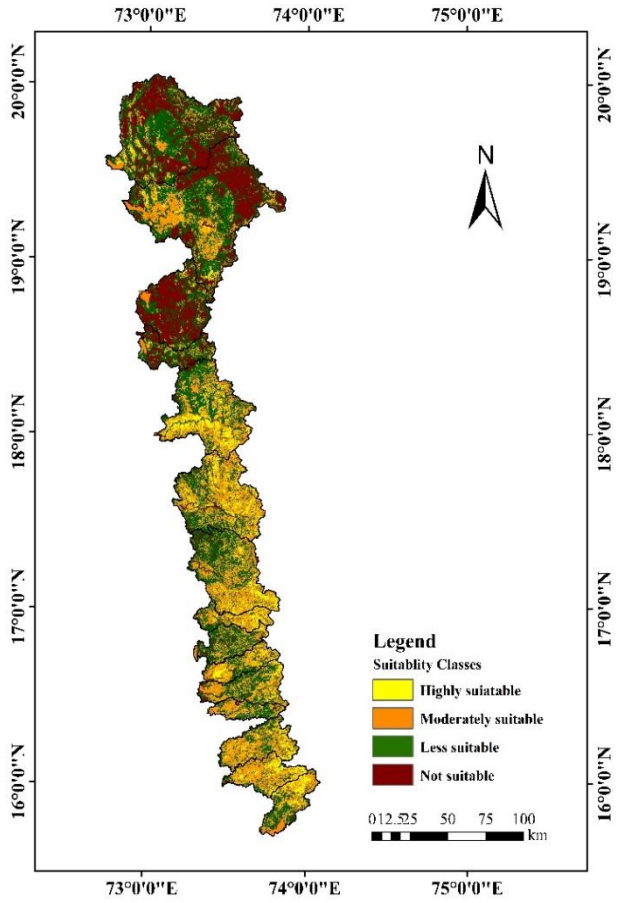

Fig. 4.9 (b). Area distribution of water retention site suitability (2019)

Table 4.15. Area occupied under suitability classes for LULC categories in Konkan region during 2017 and 2019

LULC	Suitability Class	2017		2019	
		Area (km^2) under suitability Class	Percent of geographic area	Area (km^2) under suitability Class	Percent of geographic area
Water	Highly Suitable	2.05	0.01	0.51	0.008
	Moderately Suitable	14.12	0.06	9.75	0.04
	Less Suitable	69.56	0.27	127.06	0.50
	Not Suitable	561.39	2.19	455.37	1.77
Forest	Highly Suitable	1198.50	4.67	734.40	2.86
	Moderately Suitable	2700.68	10.52	3250.26	12.66
	Less Suitable	4184.37	16.30	3621.69	14.11
	Not Suitable	2298.44	8.95	1363.04	5.31
Agriculture	Highly Suitable	20.54	0.08	8.21	0.03
	Moderately Suitable	336.27	1.31	306.49	1.19
	Less Suitable	1591.24	6.20	1443.65	5.62
	Not Suitable	960.29	3.74	1235.98	4.82
Built-up	Highly Suitable	138.10	0.54	68.79	0.27
	Moderately Suitable	460.77	1.80	613.24	2.39

	Less Suitable	200.22	0.78	361.94	1.41
	Not Suitable	33.37	0.13	85.22	0.33
Barren Land	Highly Suitable	1902.61	7.41	1145.11	4.46
	Moderately Suitable	4276.52	16.66	4376.37	17.05
	Less Suitable	3801.89	14.81	4487.78	17.48
	Not Suitable	917.94	3.58	1975.00	7.69

The site suitability map produced using AHP technique and weighted sum method categorized the region into four classes: highly suitable, moderately suitable, less suitable and not suitable. The results in Table 4.15 show that area of water bodies decreased across the highly suitable, moderately suitable and not suitable classes in 2019 compared to 2017, while the area under the less suitable class increased. Specifically, the area of water bodies shrank from 646.87 km^2 (2.52%) in 2017 to 592.96 km^2 (2.31%) in 2019, a reduction of 53.91 km^2 or 8.4% (Table 4.5). This decline, particularly in highly and moderately suitable areas, raises concerns about surface water availability, likely due to increased anthropogenic activities.

Additionally, the area of forest decreased from 10383.26 km^2 in 2017 to 8968.88 km^2 in 2019 (Table 4.5). The forest area in the highly suitable class dropped by 464.10 km^2 (38.7% reduction from 2017), while the area under moderately suitable category increased by 549.58 km^2 (20.3% increase from 2017) (Table 4.15). The shift, with concurrent reductions in the less suitable and not suitable categories, could be viewed positively. However, the reduction in highly suitable forest areas is concerning and suggests that reforestation could help restore highly suitable areas, improve water retention and mitigate potential water scarcity.

Moreover, the area classified as less and not suitable for built-up land doubled, coinciding with a significant reduction in the highly suitable category over the two-year period, which is a cause for further concern. Similar trends were observed in agricultural and barren lands. Czigany et al. (2023) demonstrated that soil moisture in loamy soils is strongly influenced by land use, with soils under pasture having the most stable moisture level, while ploughed land exhibited the highest fluctuations. Given that the northern part of the region is dominated by loamy soils, the rapid decline in highly suitable areas of water retention requires closer scrutiny. Solutions must be explored, particularly in the context of climate change, to prevent water shortages during non-monsoon seasons, despite an observed increase in rainfall over the past decade.

The results in Fig. 4.9 (a and b) indicate a rapid increase in the areas classified as not suitable and less suitable, particularly in the northern part of the region. This increase is likely due to the expansion of built-up and barren land over the two-year study period, highlighting the need to prioritize these areas for improving water retention suitability.

4.3 Assessment of total surface water availability

The use of hydrological models for assessment of surface water availability is crucial for effective water resource management. To assess the surface water availability in Konkan region,

the SWAT model was used and run for each river basin of five total vallies in the region. Total 23 river basins are available across Konkan region, which are divided in six valleys (Valley 20 to 25), out of which Daman Ganga River (Valley 20) in north of region, Tillari river (Valley 25) in south of the region are excluded from the study as their outlets are in Gujrat and Goa, respectively and hydrometeorological data could not be made available. Also, some of the rivers name as Masala, Bharja (Valley No 22), Achara and Vengurla (Valley 24) are also excluded due to lack of availability of adequate data. Some of the rivers are tributaries of the other and their outlet points along the gauge points are combined, making total river basin as 16. The results of surface water availability are systematically analyzed and are discussed as per valley number.

4.3.1 Assessment of surface water availability in Valley 21

The river valley 21 has total geographic area of 12.06 lakh ha and comprises three major rivers viz. Vaitarna, Ullas and Patalganga, however, the river Patalganga has combined outlet with Amba river and discharges in Valley 22. Geographic area of Vaitarna river basin is 3837.45 km^2 (3.83 lakh ha) and lies between East longitude of 72° 45' to 73° 35' and North latitude of 19° 25' to 20° 20' while Ullas river basin occupies 4513.93 km^2 (4.51 lakh ha) area and lies between East longitude of 72° 45' to 73° 48' and North latitude of 18° 44' to 19° 42' as illustrated in Fig. 4.10

4.3.1.1 Land use/ Land cover of Valley 21

The Land use and land cover (LULC) data used for 2019 was downloaded from Sentinal-2 satellite via the Living Atlas (https://livingatlas.arcgis.com/landcover/), with 10m resolution as of 15/04/2024. The map was projected to WGS1984 UTM Zone 43N using raster projection. The predominant land use/ land cover types in the study area's river basins were barren lands, followed by agriculture, forest, Urban Area, and water bodies. Table 4.16 and Fig. 4.11 provide detailed information on LULC of valley.

Table 4.16. Land use Land cover details of Valley 21

River	Classes	Waterbodies	Forest	Agriculture	Built-up	Barren Land
Vaitarna	Area (km^2)	130.47	268.62	798.19	84.42	2555.74
	Area (%)	3.4	7.0	20.8	2.2	66.6
Ullas	Area (km^2)	130.90	568.75	956.95	442.36	2414.94
	Area (%)	2.9	12.6	21.2	9.8	53.5
Total	Area (km^2)	258.89	835.13	1753.79	526.13	4977.41
	Area (%)	3.1	10.0	21.0	6.3	59.6

In Vaitarna basin area under barren land is more than Ullas basin similarly built-up area is also more due urbanization and industrial area. Forest cover is more in Ullas than Vaitarna basin which is responsible for generation of more runoff. According to Table 4.16, the largest area is under Baren Land (59.6%) followed by Agriculture land (21.0%) and least area is occupied by waterbodies (3.1%).

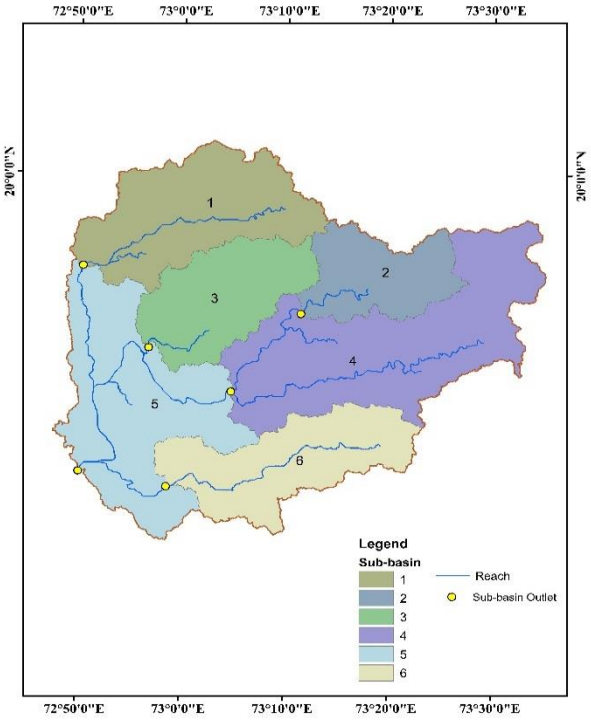

(a) Vaitarna

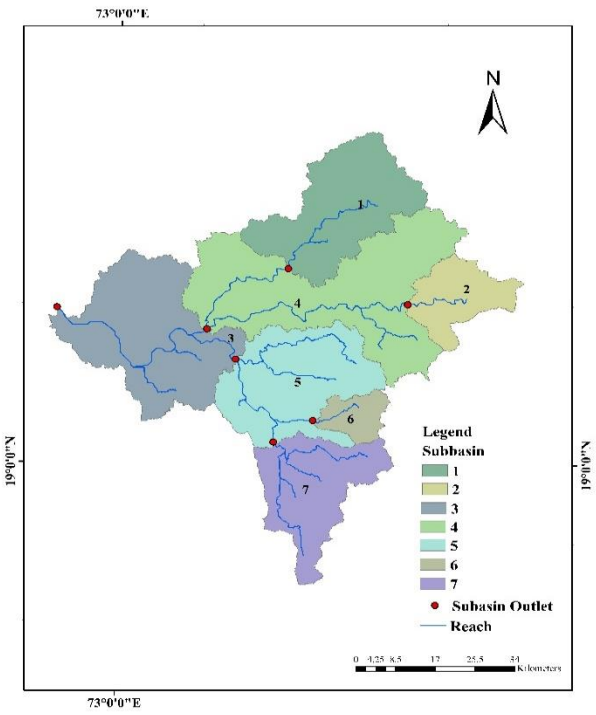

(b) Ullas

Fig.4.10 Subbasin map of river basin in Valley 21

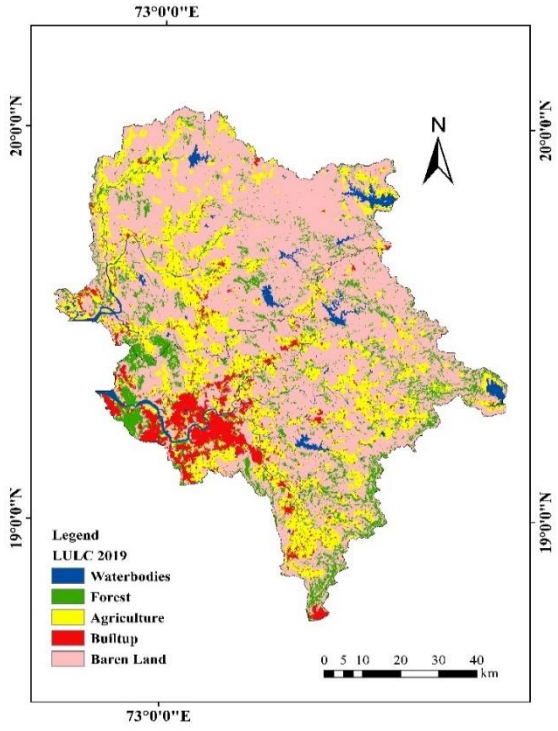

Fig 4.11 Land use land cover (LULC) distribution in Valley 21

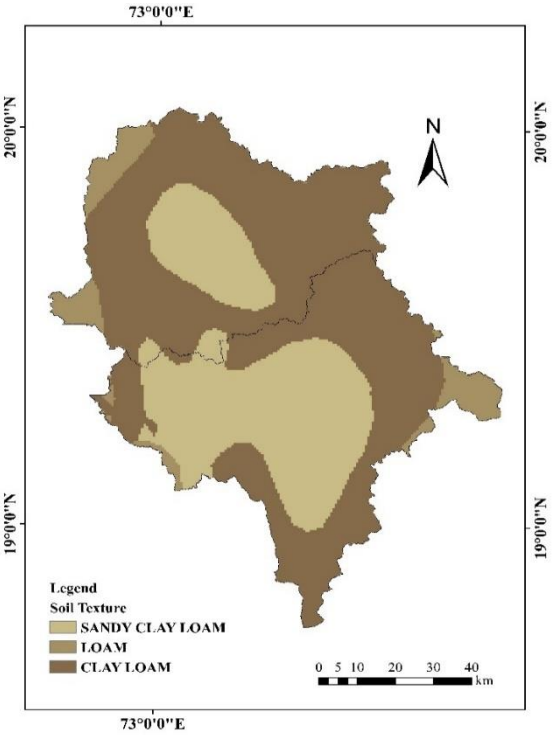

Fig. 4.12 Areal distribution of soil texture in Valley 21

4.3.1.2 Soil type of Valley 21

The soil data for the study area was downloaded in shapefile format at a scale of 1:50,000 and from FAO Soil Data. It is projected into WGS1984 UTM Zone 43N using raster projection. The dBase file was also downloaded from the FAO Soil database. Area under each soil types are given in Table 4.17. and Fig 4.12

Table 4.17 Areal distribution of soil texture in Valley 21

River	Class	Sandy clay loam	Loam	Clay loam
Vaitarna	Area (km^2)	816.99	227.94	2792.51
	Area (%)	21.29	5.94	72.77
Ullas	Area (km^2)	2121.09	165.21	2227.61
	Area (%)	46.99	3.66	49.35
Total	Area (km2)	2925.48	394.18	5031.69
	Area (%)	35.03	4.72	60.25

In Valley 21 three types of soil texture are found sandy clay loam, loam, clay loam from which region is prominently occupied by clay loam followed by sandy clay loam and least occupied by Loam type.

4.3.1.3 Topographic details of Valley 21

Konkan region is characterized by hilly region, thus, the slope ranges in the river basins are also wide along the ridge line and reduced towards mainstreams. Area is categorized in the different zones as per the slope categories: storage zone (0-5%), recharge zone (5-10%), runoff zone (>10%). The basin-wise area under each slope category is presented in Table 4.18 and shown in Fig. 4.13.

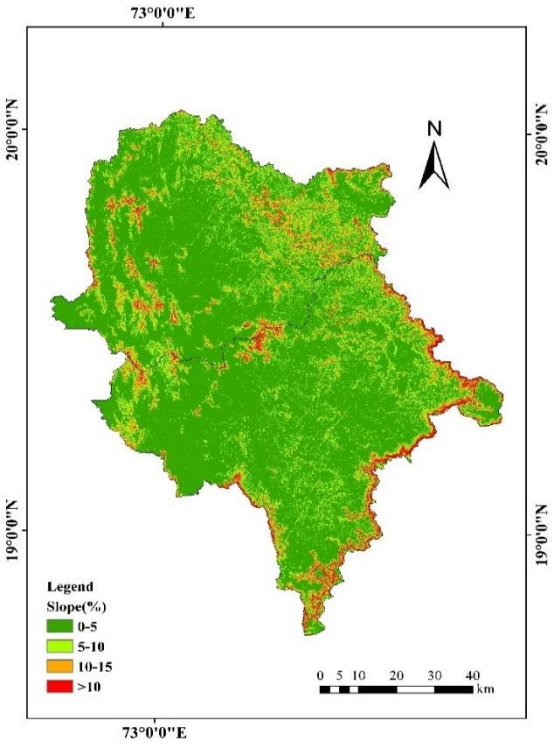

Fig 4.13 Spatial distribution map of Slope categories in Valley 21

Table 4.18 Topographic details of Valley 21

River basins	Area Distribution (km^2)	Storage Zone	Recharge Zone	Runoff Zone
		(0-5%)	(5-10%)	(>10%)
Vaitarna	Area (km2)	878.2	1014.2	1945.0
	Area (%)	22.9	26.4	50.7
Ullas	Area (km2)	996.6	1208.2	2309.1
	Area (%)	22.1	26.8	51.2
Total	Area (km2)	1874.8	2222.5	4254.1
	Area (%)	22.4	26.6	50.9

According to Table 4.18 major area (72.35%) of Valley is under topography >10% in indicates high rate of runoff. Nearly 26% area is under 5-10% slope and remaining 22.4% area is under topography of 0-5% slope which indicates high surface water flow.

4.3.1.4 Climatic condition of Valley 21

Climatic data required for input is collected from HDUG, Nashik of 10 hydrometeorological stations located in Vaitarna basin namely Andhari, Chinchghar, Khodala, Khutal, Paryachapada, Savarkhand, Suskale, Suryamal, Ogade and Savian from year 1991 to 2019 (29 years) and 9 Meteorological station located in Ullas basin are Dhamani, Kalamb, Kondhane, Naldhe, Nandgaon, Tadwadi, Kaman, Khapari, Kocahra detail location are given in Annexure I and used for assessment.

Average annual rainfall of the Vaitarna river is 3055 mm and Ullas is 2557 mm, and it is highest in July followed by August and September. Relative humidity is highest during month of August (90%) and lowest during month of March (41%). Minimum temperature is lowest(16°C) during the winter months of December, January, and February and maximum temperature peak during the pre-monsoon is reaching highest (39°C) in April followed by March and May. Wind speed is high during the months of July (4.3 m/s) followed by June and August and lowest during November (1.8m/s). Monthly climatic details of the valley are given in Annexure II.

4.3.1.5 Estimation surface water resource availability.

4.3.1.5.1 Calibration and validation of SWAT Model

In the present study calibration of SWAT model was done with help of SWAT-CUP SUFI2 program as described in chapter 3 section 3.5.3 SWAT model was calibrated having an outlet of meteorological stations of Water Resource Department, (Surface Water) Government of Maharashtra. Simulation was started from 1991 with 3 years of model warmup period and output of simulation was available for 25 years from 1994 to 2019. Performance evaluation criteria is tabulated in Table 4.19 and shown in Fig. 4.14 and details of calibration parameter are mentioned in Appendix IV

Table 4.19 Performance criteria of simulated data

		Calibration					Validation				
Basin	Sites	Year	NSE	R^2	PBIAS	RSR	Year	NSE	R^2	PBIAS	RSR
Ullas	Kalamb	1995-2000	0.6	0.65	2.97	0.3	2001-2005	0.6	0.61	2.95	0.28
Vaitarna	Saivan	2001-2005	0.65	0.69	-1.77	0.27	2008-2012	0.62	0.69	-1.77	0.33

4.3.1.5.2 Sub-basin wise monthly river flow availability

The Arc-SWAT Model was calibrated, validated and applied to river basin to evaluate surface water availability along with their seasonal variations. Prior to its application in the basin, the model underwent calibration and validation processes. The first analysis obtained after running the SWAT model was the river flow availability of river basins which is extracted from output file as a Flow_out parameter.

Table No 4.20 Monthly River flow in Valley 21 (cumec)

	Ullas	Vaitarna	Total
Jan	4.96	4.76	9.72
Feb	1.04	1.05	2.09
Mar	0.52	0.70	1.23
Apr	0.23	0.27	0.50
May	1.19	2.33	3.52
Jun	78.79	103.95	182.73
Jul	254.86	242.15	497.02
Aug	215.90	189.19	405.09
Sep	162.52	153.61	316.14
Oct	81.29	74.04	155.34
Nov	37.77	36.26	74.02
Dec	17.50	16.89	34.38
Total	856.57	825.21	1681.78

Table 4.21 Available surface water potential in the river fat selected locations

	Co-ordinate Location		
Basin	Long	Lat	Water availability (Mm3)
Vaitarna	72.9282	19.6193	8097.79
Ullas	73.0677	19.2677	9248.49

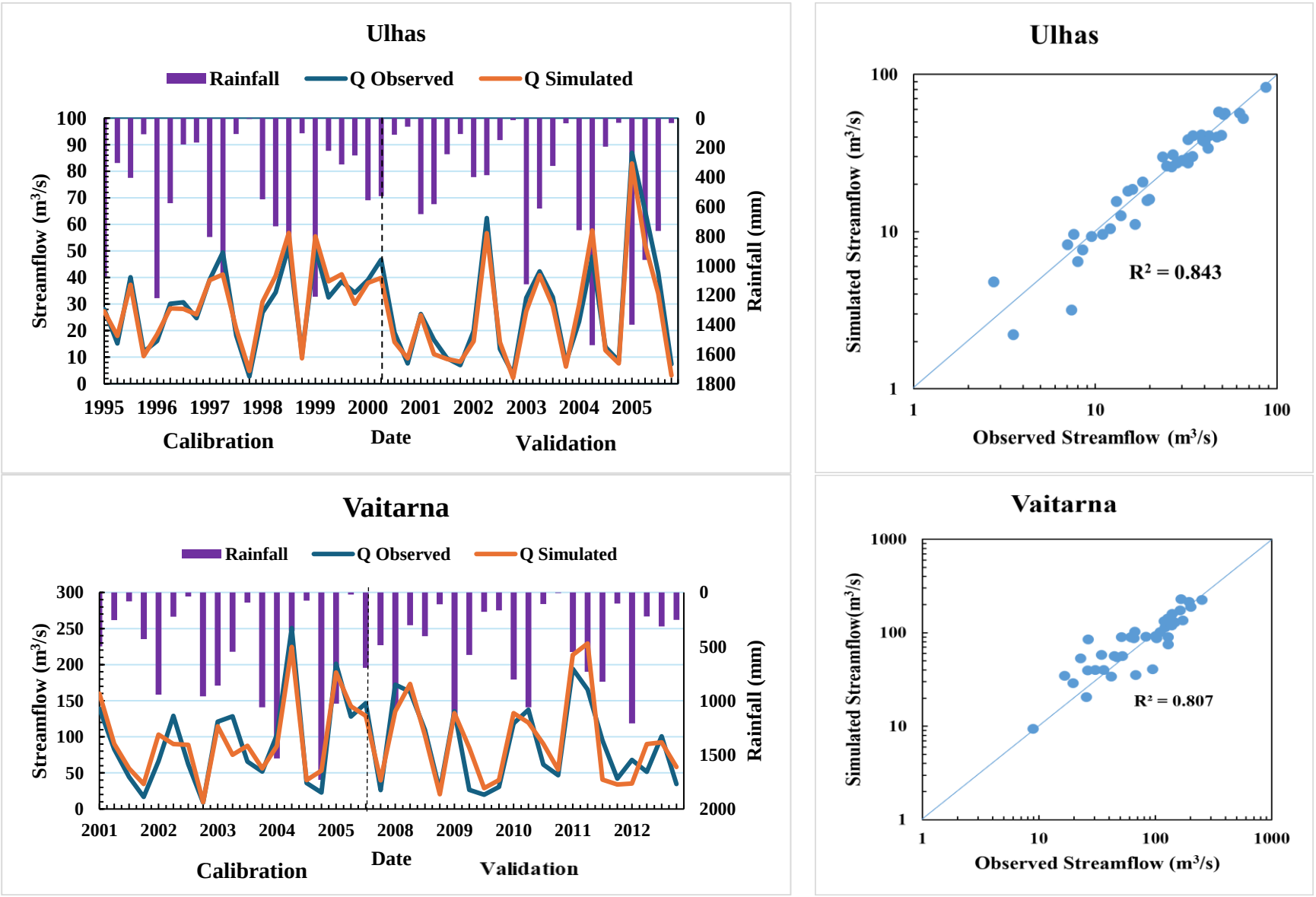

Fig.4.14 Monthly observed and simulated streamflow over a period 1994-2005 (a.Seasonal variation, b. Scatter plot)

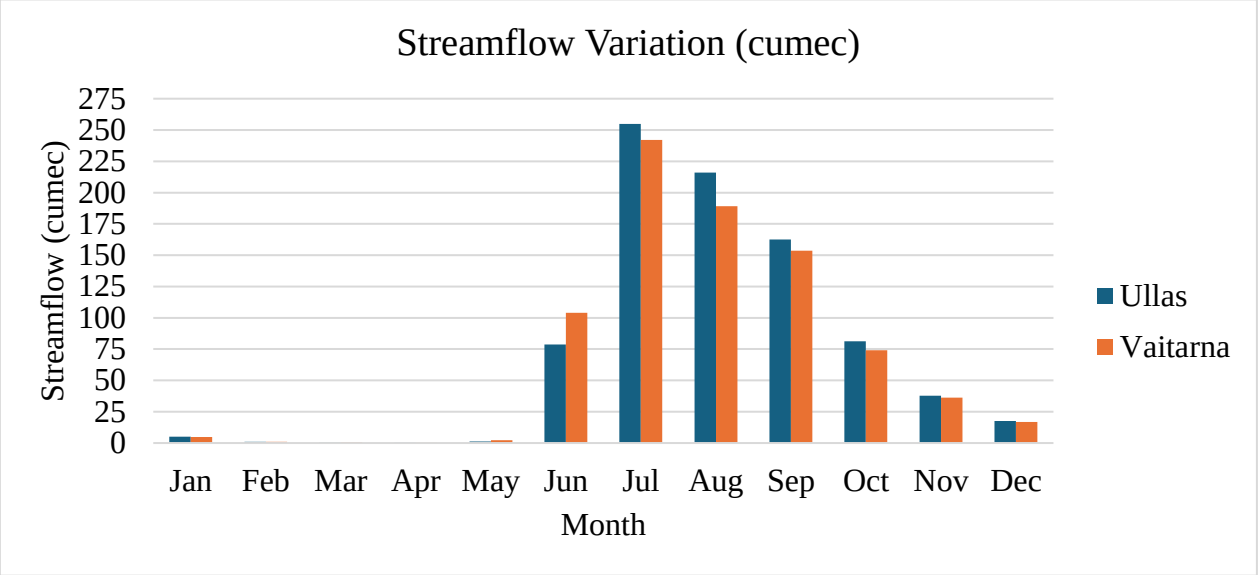

Fig 4.15 Monthly River flow(cumec) in Valley 21

The analysis of basin-wise monthly mean of river flow is tabulated in Table No 4.20 and illustrated in Fig.4.15 It reveals notable variation throughout the year. Heightened river flow is evident during the rainy months of June, July, August, and September, predominantly driven by rainfall. The heavy monsoon accumulated in the form of river flow. From Fig. 4.15 it becomes apparent that July consistently witnesses the highest river flow (497.02 cumec) across all basins because of high rainfall receive during this month and it is lowest in April (0.5cumec) due high evapotranspiration rate. Throughout the analysis period, river flow generally peaks during June and July, gradually decreasing thereafter until April. Total surface water availability in Valley 21 is 1681.78 cumec. Table 4.21 shows available surface water potential in river from selected location and Table 4.22 shows average annual volumes of basin.

Table 4.22 Average annual volume of basin in valley 21

Basin	Water Yield (mm)	Base flow(mm)	Surface Flow (mm)
Vaitarna	1848.3	601.7	1130.3
Ullas	1876.2	614.1	1125.5

4.3.1.6 Estimation of basin-wise monthly surplus and deficit water availability

Annual water availability plays an important role for effective water resource management during lean period. Monthly water surplus/deficit was carried out by using climatic water supply (rainfall) and climatic water demand (evapotranspiration). Monthly water availability variation in the year was evaluated based on methodology discussed in section 3.7 Results of basin wise monthly basis water surplus/deficit in Valley 21 are presented in Table 4.23

Table 4.23 Temporal variation of annual water surplus/deficit in Valley 21

District	Vaitarna			Ullas		
Months	PET (mm)	Rainfall (mm)	Sur/Def (mm)	PET (mm)	Rainfall (mm)	Sur/Def (mm)
Jan	87	13	-74	81	0	-81
Feb	104	7	-97	99	1	-99
Mar	154	4	-150	152	1	-151
Apr	161	4	-157	160	1	-159
May	159	11	-149	154	7	-147
Jun	95	442	346	92	411	319
Jul	63	962	898	61	814.08	754
Aug	67	676	609	64	576.47	512
Sep	84	350	266	81	391	310
Oct	103	75	-27	99	114	15
Nov	89	9	-80	83	10.92	-72
Dec	83	19	-64	75	2	-74

Note: RF = Rainfall (mm) PET = Potential evapotranspiration(mm) Sur = Surplus Def = deficit

From Table 4.23 it is revealed that monthly water demand varied between 63 to 161 mm in Vaitarna basin and in Ullas basin it is from 61 to 160 mm. Monthly water demand is increased from July to May. Due to high temperature and lower humidity water demand is highest during month of April and lowest during month of July due to higher humidity and low temperature.

Monthly water supply is highest during the month of June to October due average annual rainfall in region is concentrated during this season. It is varied between 4 to 962 mm in Vaitarna basin district, from 1 to 814.08 mm in Ullas basin.

According to Table 4.23 positive values shows surplus water and negative value shows deficit water condition, it is concluded that water is surplus during month of June to October it is highly surplus in month of June and July, and it is deficit from November to May and it more deficit in month of April and May. In Vaitarna basin it is water condition is highly surplus in month of July which is 962 mm and deficit in month of March and April (157 mm) while in Ullas basin same trend is observed it is highly surplus in month of July 754 mm and deficit in month of April (159 mm) due high evapotranspiration rate.

The temporal variability of water balance components, including rainfall, evapotranspiration (ET), runoff was analysed throughout the year to evaluate the monthly surplus and deficit water availability in the region. Monthly water balance components of valley 21 is illustrated in Fig. 4.16

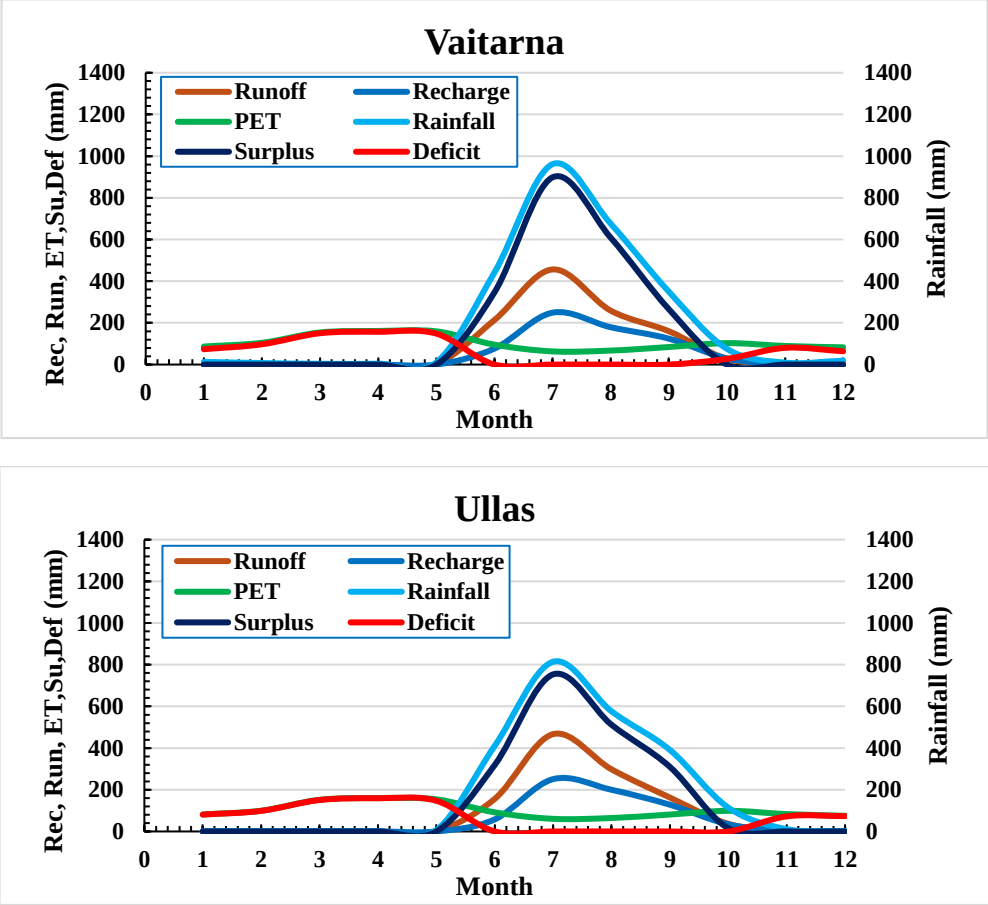

Fig 4.16 Temporal variation of water balance components of river in valley 21

Fig. 4.16 illustrates the variation of all water balance components throughout the year across all districts in Konkan region. Evapotranspiration peaks during April and May and reaches its lowest point in July when the precipitation is at its highest peak. Due to high evapotranspiration during January to May and low precipitation these months are water deficit and form June to October evapotranspiration rate is lowest point and precipitation is highest which results surplus water during these months. This excess water availability during month of June to October have vast scope for water harvesting and construction of water storage structures as well as recharge structure at suitable site in region.

4.3.2 Assessment of surface water availability in Valley 22

Valley 22 comprised of five river basins namely Amba, Savitri, Kundalika, Mhasala, Bharja which are situated in Raigad district. However, Masala and Bharja rivers are excluded from the study due unavailability of adequate data. As Patalganga and Amba has combined outlet therefore it is included in Valley 22. Geographical area of Patalganga and Amba river is 1730.09 km^2 and lies between East longitude of 72° 58' to 73° 20' and North latitude of 18° 50' to 18° 26' while Kundalika occupies 742.06 km^2 of geographic area and lies between North latitudes of 18º 36' to 18º 20' and East longitudes of 72º 52' to 73º 30' and Geographic area of Savitri is 2235.97

km^2 it lies between North latitudes of 18º 26' to 17º 50' and East longitudes of 73º 80' to 73º 40' illustrated in Fig 4.17

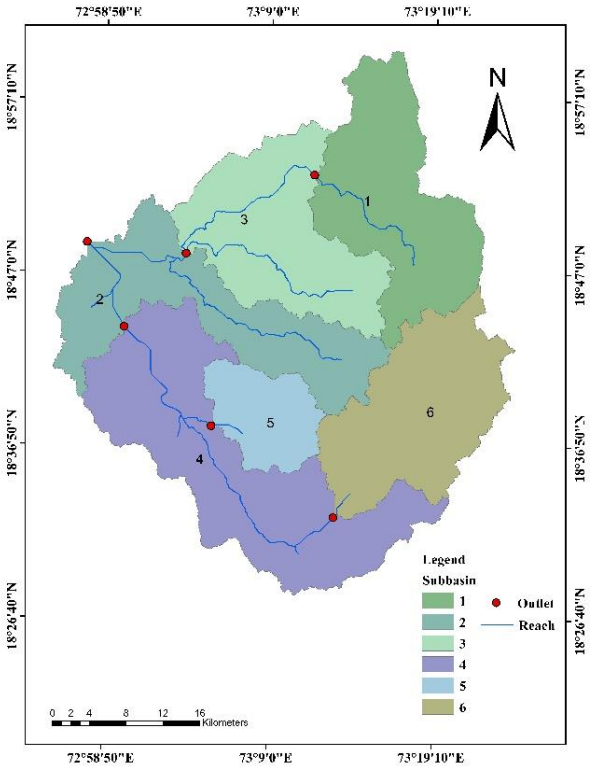

(a) Patalganga-Amba

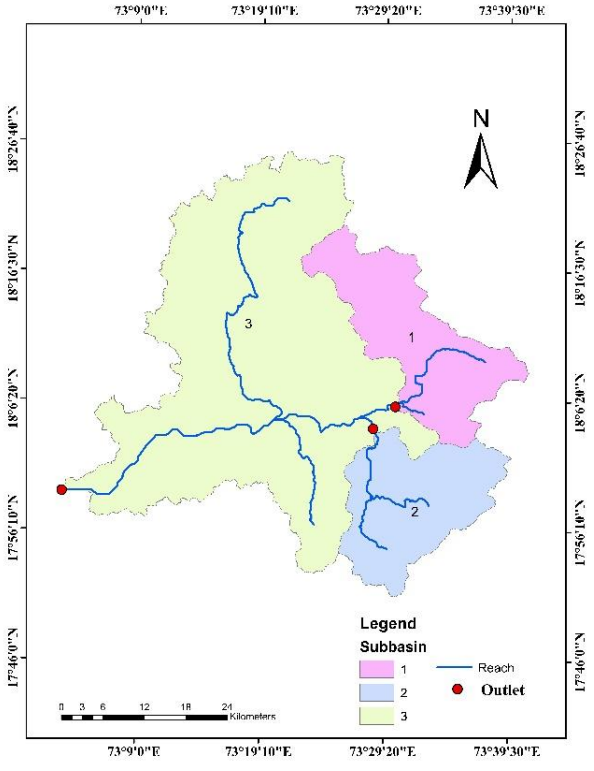

(b) Savitri

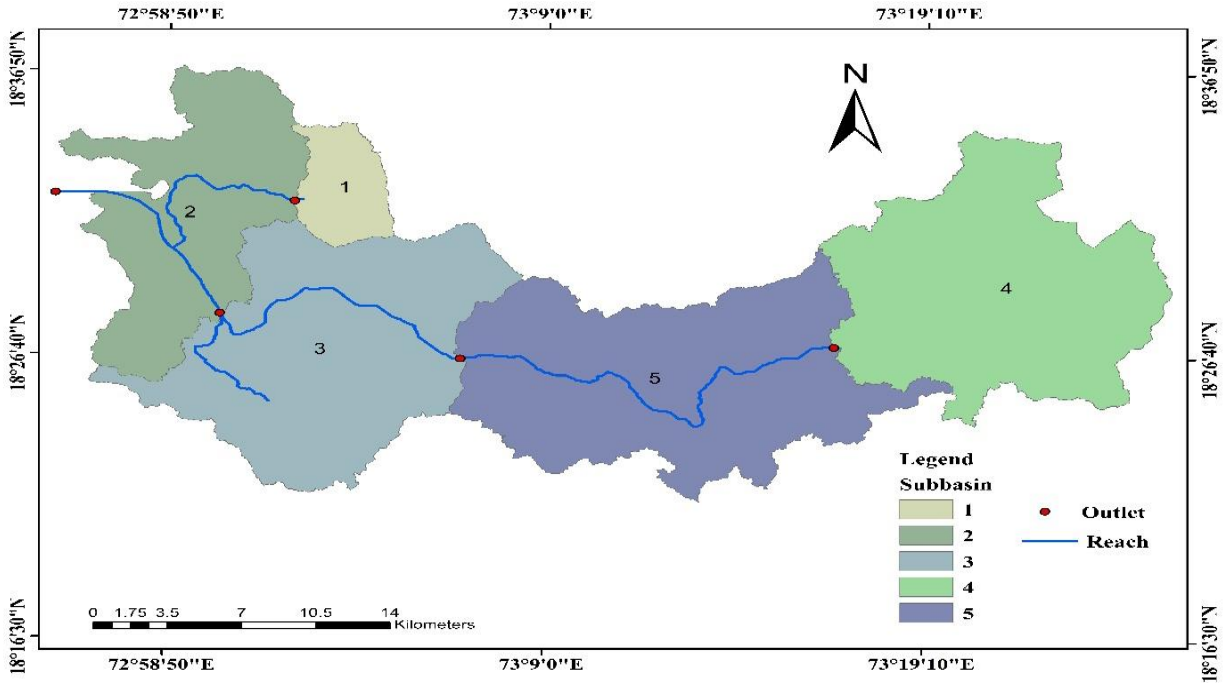

(c) Kundalika

Fig. 4.17 Basin map of river in Valley 22

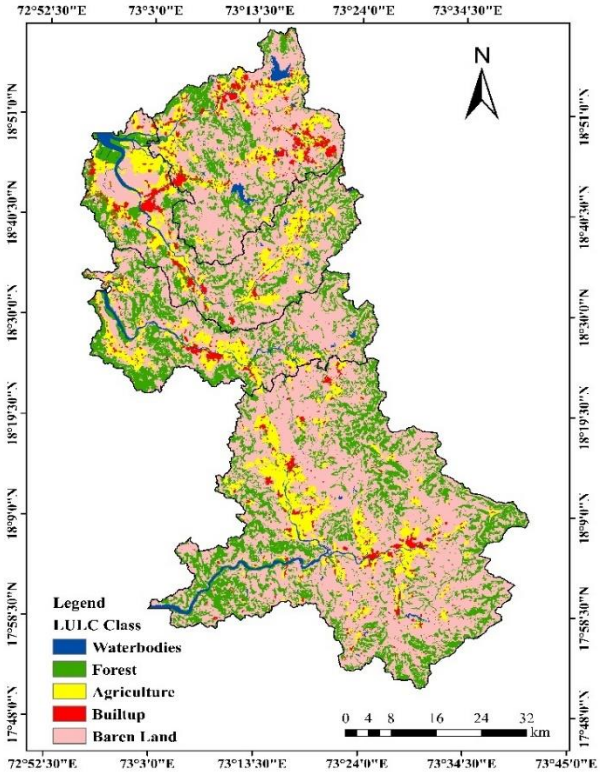

Fig 4.18 Land use land cover (LULC) distribution in Valley 22

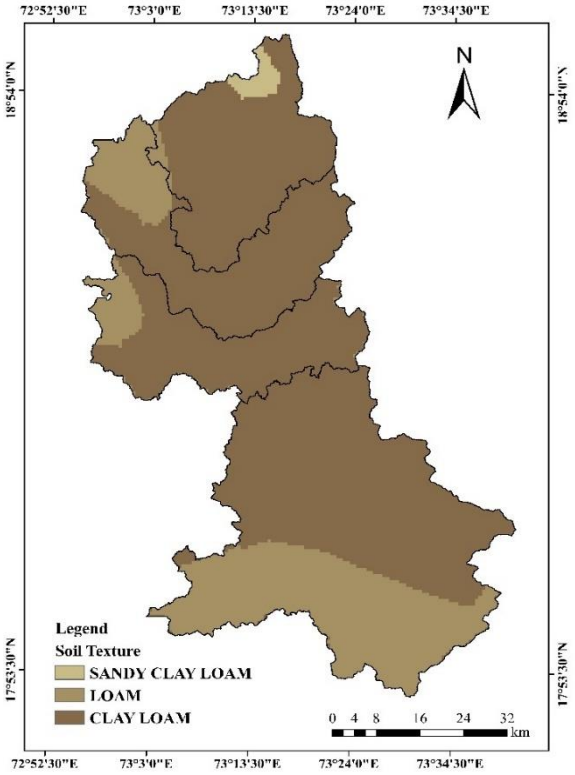

Fig. 4.19 Areal distribution of soil texture in Valley 22

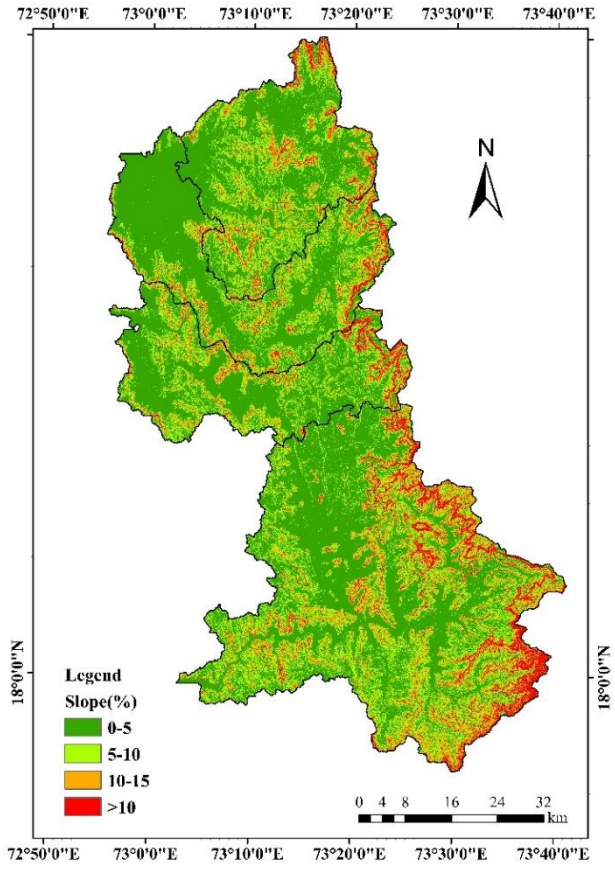

Fig 4.20 Spatial distribution map of Slope categories in Valley 22

4.3.2.1 Land use/ Land cover of Valley 22

The Land use and land cover (LULC) data for 2019 was downloaded from Sentinal-2 satellite via the Living Atlas (https://livingatlas.arcgis.com/landcover/), with 10m resolution as of 15/04/2024. The map was projected to WGS1984 UTM Zone 43N using raster projection. River basins are dynamic and complex systems involving several natural or natural or anthropogenic physical processes at various spatial and temporal scales (Deshmukh et al., 2013). Natural or anthropogenic activities can often affect hydrology adversely. Agricultural expansion and intensification, urban growth, and changes in economic levels force land use/land cover changes in river basins to meet increasing population demands (Lee, 2005; Smith et al., 2016; Aneseyee et al., 2020). The predominant land use/ land cover types in the study area's river basins were barren lands, followed by agriculture, forest, Urban Area, and water bodies. Table 4.24 and Fig. 4.18 provide detailed information on LULC of valley.

Table 4.24 Areal distribution of Land use land cover in Valley 22

River	Classes	Waterbodies	Forest	Agriculture	Built-up	Barren Land
Patalganga-Amba	Area (km^2)	88.40	636.06	426.73	172.36	1456.44
	Area (%)	3.18	22.88	15.35	6.20	52.39
Kundalika	Area (km^2)	21.53	281.80	102.03	26.18	461.92
	Area (%)	2.41	31.54	11.42	2.93	51.70
Savitri	Area (km^2)	37.37	603.25	221.87	59.09	1413.89
	Area (%)	1.60	25.83	9.50	2.53	60.54
Total	Area (km^2)	147.30	1521.11	750.63	257.63	3332.24
	Area (%)	2.45	25.31	12.49	4.29	55.46

According to table 4.24, majorly area is under barren land (55.46%), followed by forest area and least area is under waterbodies. Agriculture area is only 12.49% while built-up area is 4.29%. Built-up area is concentered in Northen part of valley due presences industrial area nearby Patalganga basin. Forest area is scattered towards ghat region and southern western region of Kundalika basin and barren land is scattered all over valley.

4.3.2.2 Soil type of Valley 22

FAO soil data is downloaded in shapefile format at scale of 1:50,000 and projected into WGS1984 UTM Zone 43N using raster projection. The dBase file was also downloaded from the FAO Soil database. Area under each soil types are given in Table 4.25. and Fig 4.19

Table 4.25 Areal distribution of soil texture in Valley 22

River	Soil Texture	Area (km^2)	Area (%)
Patalganga-Amba	Sandy clay loam	77.05	2.77
	Loam	277.44	9.98
	Clay loam	2425.54	87.25
Kundalika	Loam	95.61	10.7
	Clay loam	797.86	89.3
Savitri	Loam	904.29	38.72
	Clay loam	1431.17	61.28

According to Table 4.25 and Fig 4.19 valley 22 consist of three types of soil texture namely, sandy clay loam, loam and clay loam. Sandy clay occupies only 77.05 km^2 (1.28%) in the northern part of Patalganga. Major part of the area is occupied by clay loam which is 77.46% of total area with combination of high slope range and shallow depths it is prone to runoff and soil erosion. Clay loam occupies 21.26% of the area which is concentered at northern-western part of the Amba and Kundalika river and southern part of Savitri River.

4.3.2.3 Topographic details of Valley 22

Konkan region is characterized by hilly region, thus, the slope ranges in the river basins are also wide along the ridge line and reduced towards mainstreams. Area is categorized in the different zones as per the slope categories: storage zone (0-5%), recharge zone (5-10%), runoff zone (>10%). The basin-wise area under each slope category is presented in Table 4.26 and shown in Fig. 4.20.

Table 4.26 Topographic details of Valley 22

River basins	Area Distribution (km^2)	Storage Zone	Recharge Zone	Runoff Zone
		(0-5%)	(5-10%)	(>10%)
Patalganga-Amba	Area (km2)	1760.05	641.74	378.20
	Area (%)	63.31	23.08	13.60
Kundalika	Area (km2)	548.67	216.10	128.70
	Area (%)	61.41	24.19	14.40
Savitri	Area (km2)	1169.31	630.46	535.69
	Area (%)	50.07	27.00	22.94

Major area of valley is under 0-5% slope which is near about 3478.03km^2 (60%) which is concentred near coastline and area under steep slope which >10% is near the ghat section of region.

4.3.2.4 Climatic condition of Valley 22

Climatic data required for input is collected from HDUG, Nashik for 1991-2019 (29) years of 22 hydrometeorological stations out of which 12 station are located in Patalganga-Amba river, 2 in Kundalika basin, 9 are located in Savitri basin. Details of hydrometeorological stations are mentioned in Annexure I and used for the input.

Average annual rainfall of the Patalganga-Amba river is 2873 mm, Kundalika is 2893 mm while in Savitri basin it is around 3500 mm and it is highest in July followed by August and September in all basins. Relative humidity is highest during month of August (90%) and lowest during month of March (47%). Minimum temperature is lowest (16°C) during the winter months of December, January, and February and maximum temperature peak during the pre-monsoon is reaching highest (38°C) in April followed by March and May. Wind speed is high during the months of July (4.5 m/s) followed by June and August and lowest during November (1.9m/s). Monthly climatic details of the valley are given in Annexure II.

4.3.2.5 Estimation surface water resource availability

4.3.2.5.1 Calibration and validation of SWAT Model

SWAT model was calibrated having an outlet of meteorological stations of Water Resource Department, (Surface Water) Government of Maharashtra. Simulation was started from 1991 with 3 years of model warmup period and output of simulation was available for 25 years from 1994 to 2019. Performance evaluation criteria is tabulated in Table 4.27 and shown in Fig. 4.21 and details of calibration parameter are mentioned in Appendix IV

Table 4.27 Performance criteria of simulated data for Valley 22

		Calibration					Validation				
Basin	Sites	Year	NSE	R^2	PBIAS	RSR	Year	NSE	R^2	PBIAS	RSR
PA	Pali	1994-1999	0.74	0.74	-1.92	0.24	2000-2005	0.72	0.72	-1.84	0.26
Kundalika	Mahan	1997-1999	0.68	0.65	-2.91	0.18	2000-2002	0.65	0.65	-1.81	0.21
Savitri	Kangule	1995-2000	0.90	0.90	-3.6	0.29	2001-2005	0.65	0.73	-2.8	0.23

Note: PA - Patalganga-Amba

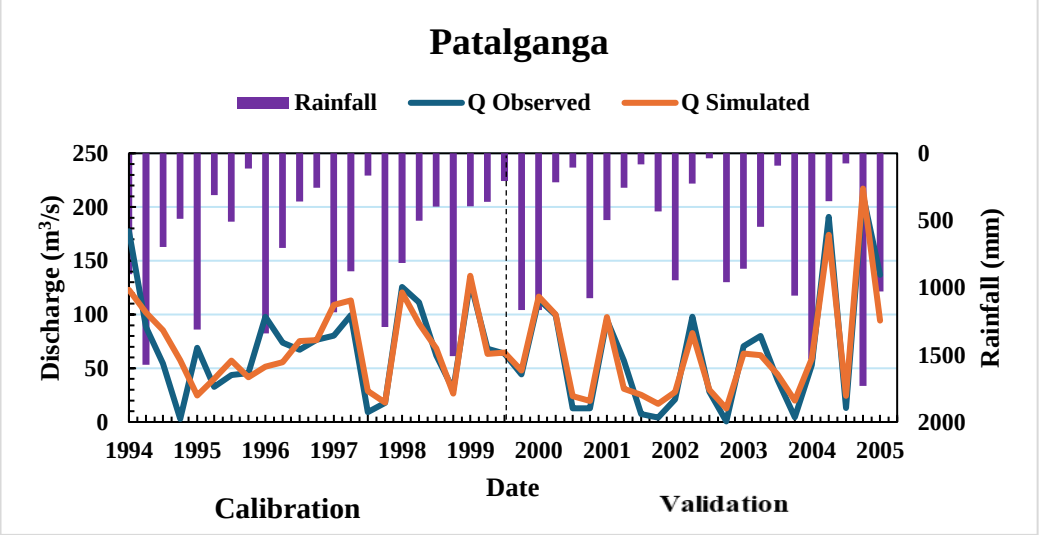

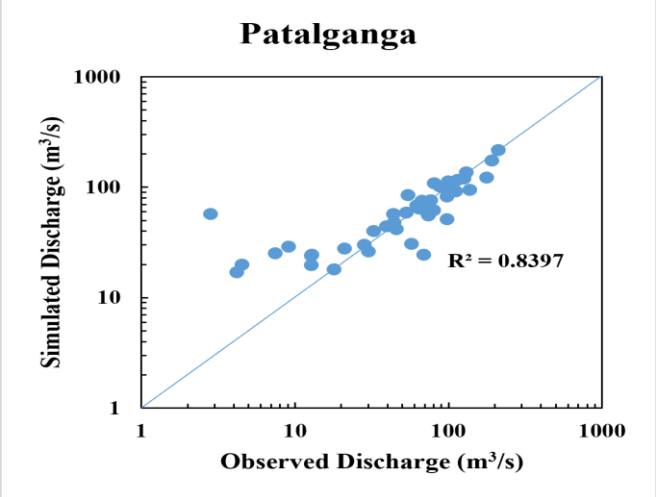

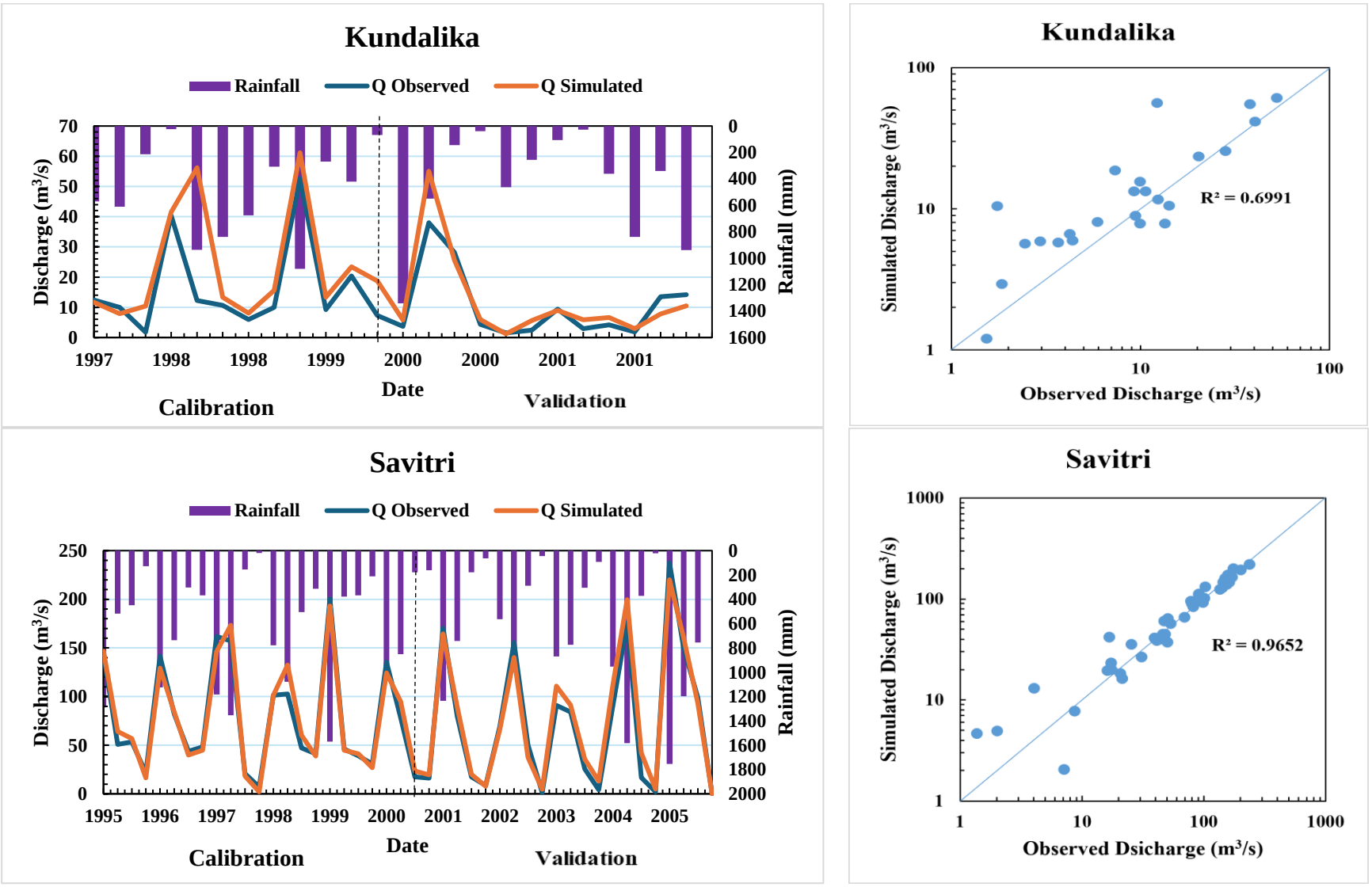

Fig.4.21 Monthly observed and simulated streamflow over a period 1994-2005 (a.Seasonal variation, b. Scatter plot)

4.3.1.5.2 Sub-basin wise monthly river flow availability

The Arc-SWAT Model was calibrated, validated and applied to river basin to evaluate surface water availability along with their seasonal variations. Prior to its application in the basin, the model underwent calibration and validation processes. The first analysis obtained after running the SWAT model was the river flow availability of river basins which is extracted from output file as a Flow_out parameter.

Table No 4.28 Monthly River flow in sub-basins of valley 22 (cumec)

	Patalganga-Amba	Savitri	Kundalika	Total
Jan	35.90	17.82	7.82	61.55
Feb	34.35	3.90	1.88	40.12
Mar	31.10	1.96	1.04	34.10
Apr	28.56	1.21	0.65	30.43
May	26.62	0.75	0.61	27.98
Jun	63.64	520.50	293.12	877.26
Jul	158.73	1223.31	633.84	2015.88
Aug	131.05	1004.63	445.15	1580.84
Sep	91.17	602.15	333.16	1026.48
Oct	64.18	272.69	145.49	482.36
Nov	47.34	112.48	60.92	220.73
Dec	39.67	52.61	27.98	120.25

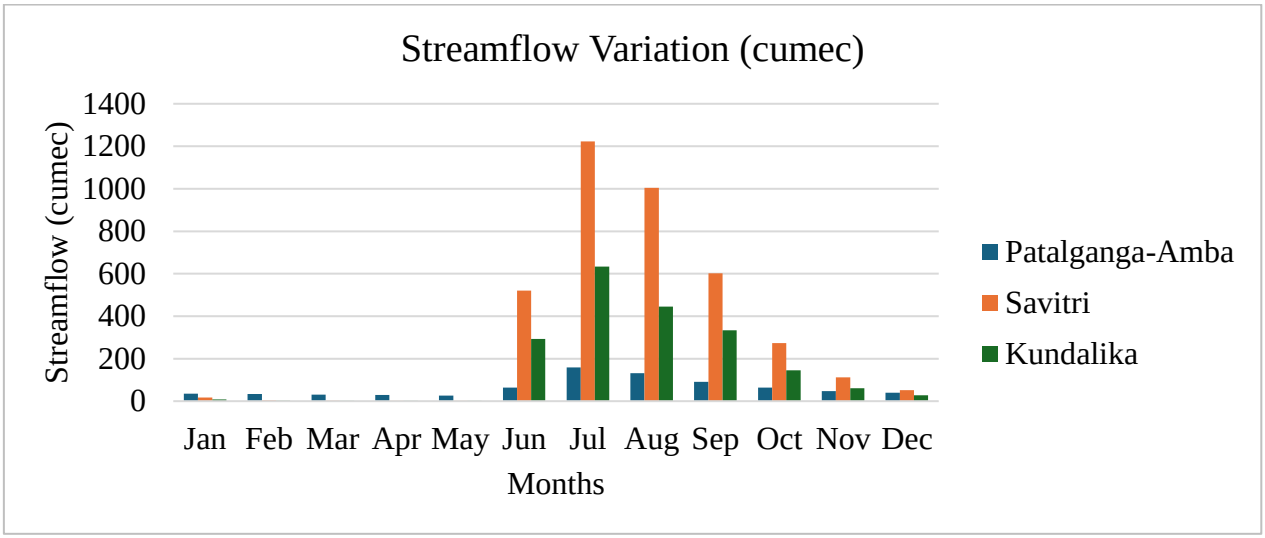

Fig 4.22 Monthly River flow(cumec) variation in Valley 22

Table 4.29 Available surface water potential in the river from selected locations

	Co-ordinate Location		
Basin	Long	Lat	Water availability (Mm^3)
Patalganga-Amba	73.0827	18.7420	5430.92
Kundalika	72.9916	18.5290	1338.76
Savitri	73.3139	18.1531	4707.17

The analysis of basin-wise monthly mean of river flow is tabulated in Table No 4.28 and illustrated in Fig.4.22 It reveals notable variation throughout the year. Heightened river flow is evident during the rainy months of June, July, August, and September, predominantly driven by rainfall. The heavy monsoon accumulated in the form of river flow. From Fig. 4.22 it becomes apparent that July consistently witnesses the highest river flow (2015.88 cumec) across all basins because of high rainfall receive during this month and it is lowest in April (27.98cumec) due high evapotranspiration rate. Throughout the analysis period, river flow generally peaks during June and July, gradually decreasing thereafter until April. Table 4.29 shows available surface water potential in river from selected location and Table 4.30 shows average annual volumes of basin.

Table 4.30 Average annual volumes of basin in valley 22

Basin	Water Yield (mm)	Base flow(mm)	Surface Flow(mm)
Patalganga-Amba	2884.61	1435.97	1173.31
Kundalika	2604.60	763.37	1673.40
Savitri	3435.28	236.37	3103.47

4.3.2.6 Estimation of basin-wise monthly surplus and deficit water availability

Annual water availability plays an important role for effective water resource management during lean period. With use of climatic water supply (rainfall) and climatic water demand (evapotranspiration) monthly water surplus/deficit was carried out. Based on methodology discussed in section 3.7 monthly water availability variation in the year was evaluated. Results of basin wise monthly basis water surplus/deficit in Valley 22 are presented in Table 4.31

Table 4.31 Temporal variation of annual water surplus/deficit in Valley 22

Basin	Patalganga-Amba			Kundalika			Savitri		
Months	Rainfall (mm)	PET (mm)	Sur/Def (mm)	Rainfall (mm)	PET (mm)	Sur/Def (mm)	Rainfall (mm)	PET (mm)	Sur/Def (mm)
Jan	0	86	-86	0	86	-86	0	83	-83
Feb	0	101	-101	0	101	-101	0	98	-98
Mar	0	142	-142	0	140	-140	0	137	-137
Apr	1	155	-154	0	154	-154	0	149	-149
May	4	155	-151	3	154	-151	0	147	-147
Jun	586	90	497	648	89	559	751	84	666
Jul	1231	62	1169	1132	62	1070	1404	59	1345
Aug	877	66	811	698	65	633	1020	62	958
Sep	441	82	359	419	82	337	475	78	396
Oct	134	100	35	94	100	-5	126	96	30
Nov	2	86	-84	0	86	-86	0	83	-83
Dec	0	79	-79	0	79	-79	0	76	-76

Note: RF = Rainfall in mm, PET = Potential evapotranspiration(mm) Sur = Surplus Def = deficit

Monthly water demand varied between 62 to 155 mm in Patalganga-Amba basin and same trend is observed in Kundalika basin while in Savitri basin it is varied between 59 to 149 mm. Monthly water demand is increased from July to May. Due to high temperature and lower humidity water demand is highest during month of April and lowest during month of July due to higher humidity and low temperature.

Average annual rainfall is concentrated in month of June to October due to which monthly water supply is highest during this season. It is varied between lowest to 1 mm in April to highest 1231 mm in July in Patalganga-Amba river. Similarly, in Kundalika basin water supply is highest in July (1132mm) and in Savitri basin it is 1404 mm.

From Table 4.31 positive values shows surplus water and negative value shows deficit water condition, it is concluded that water is surplus during month of June to October it is highly surplus in month of June and July, and it is deficit from November to May and it more deficit in month of April and May. In Patalganga-Amba basin water condition is highly surplus in month of July 1170 mm and deficit in month of March and April (154 mm). In Kundalika basin water is available abundantly in July 1070mm and in Savitri basin it is 1345mm. In month of April high water shortage is observed across all basin which is near about 154 mm.

The temporal variability of water balance components, including rainfall, evapotranspiration (ET), runoff was analysed throughout the year to evaluate the monthly surplus and deficit water availability in the region. Monthly water balance components of valley 22 is illustrated in Fig. 4.23 Water shortage is observed in month from November to April where evapotranspiration rate is highest during these months and excess water is available during month of June to October results in flooding which can be manged by implementing suitable soil and water conservations practices. Similar trend is observed in all basins of Valley 22.

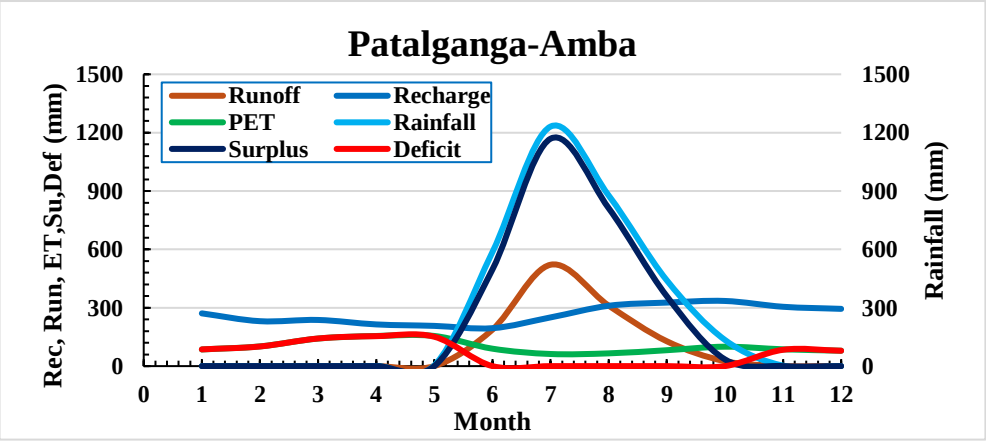

(a)

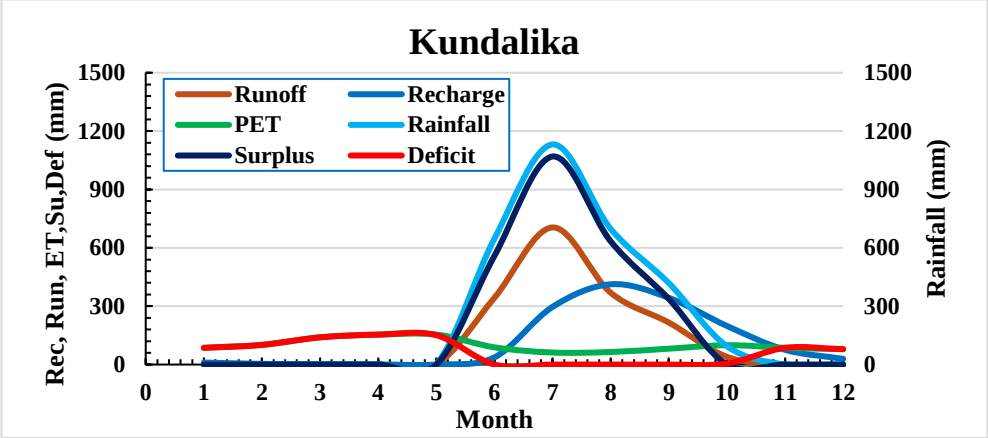

(b)

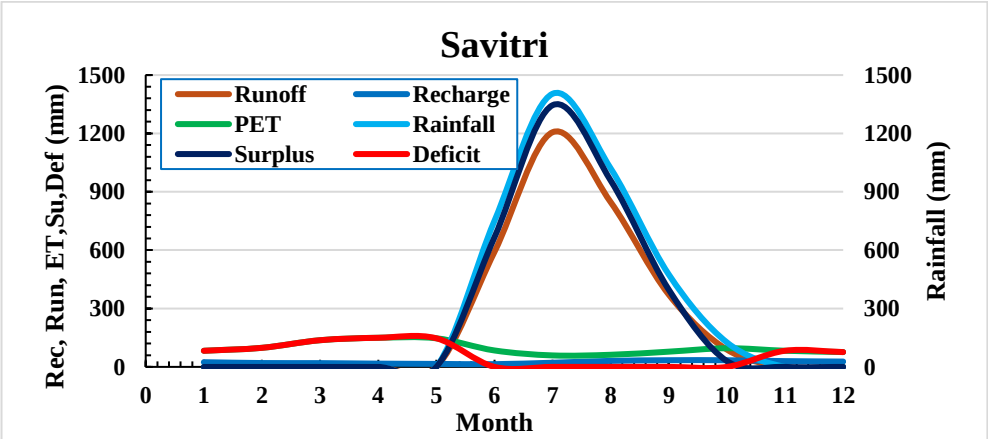

(c)

Fig 4.23 Temporal variation of water balance components of valley 22

4.3.3 Assessment of surface water availability in Valley 23

Valley 23 is located in middle part of the Konkan region and comprised of two river basin namely Vashisthi and Jagbudi out of which Jagbudi is tributary of Vashisthi river therefore outlet of both basins are combined together. Geographic area of Vashisthi river is 2562.54 km^2 and lies between East longitude of 73° 00' to 73° 40' and North latitude of 18° 00' to 17° 20' illustrated in Fig.4.24

4.3.3.1 Land use/ Land cover of Valley 23

Required data for LULC was procured from Sentinal-2 satellite via the Living Atlas (https://livingatlas.arcgis.com/landcover/), with 10m resolution as of 15/04/2024 and projected in WGS1984 UTM Zone 43N using raster projection. Land use land cover data is classified into five class viz. waterbodies, forest, Urban area, agriculture and barren land. Detail areal distribution is provided in Table 4.32 and Fig. 4.25

Table 4.32 Land use Land cover details of Valley 23

River	Classes	Waterbodies	Forest	Agriculture	Built-up	Barren Land
Vashisthi	Area (km^2)	49.46	936.35	84.56	118.65	1373.78
	Area (%)	1.93	36.54	3.30	4.63	53.61

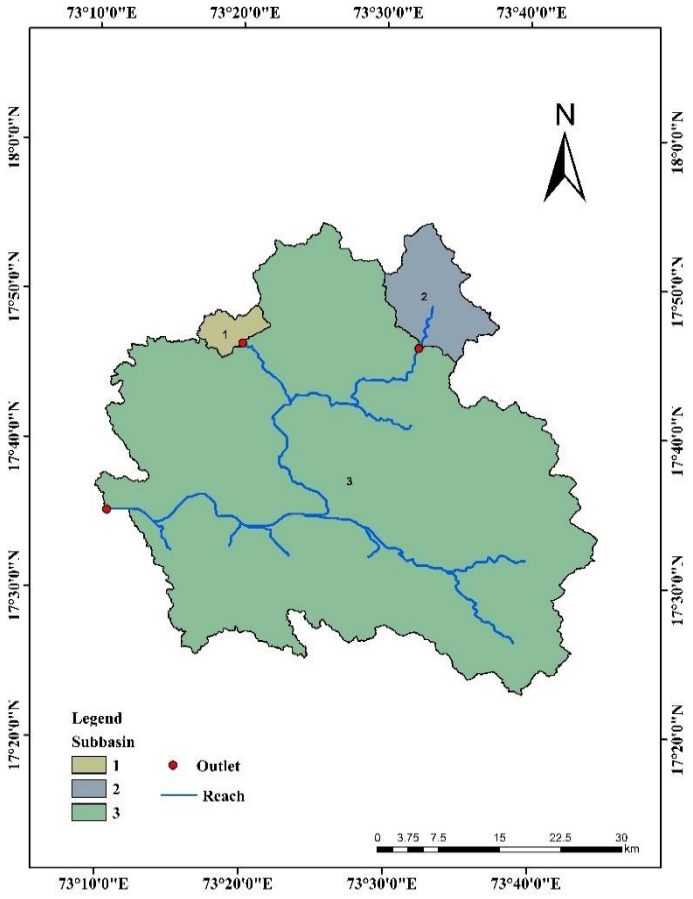

Fig.4.24 Subbasin map of river basin in Valley 23

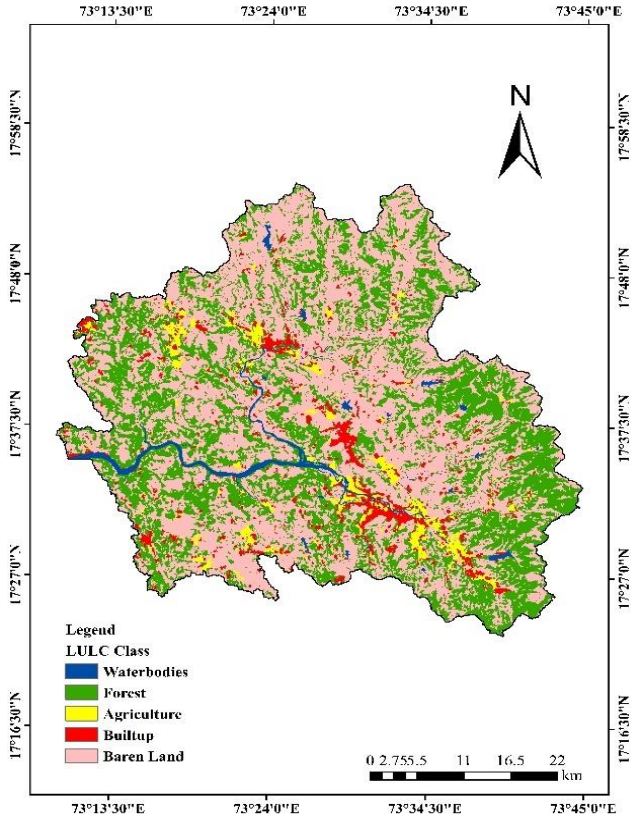

Fig.4.25 Land use land cover (LULC) distribution in Valley 23

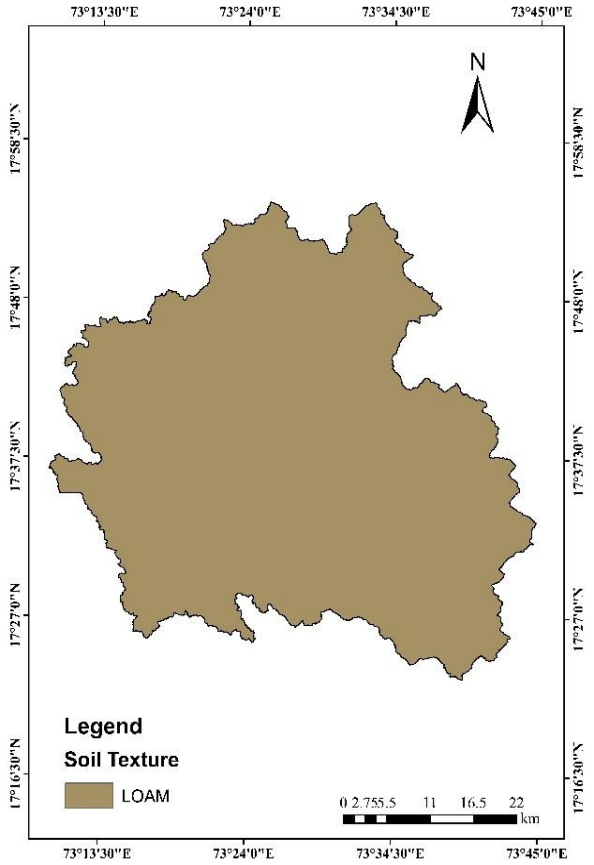

Fig. 4.26 Areal distribution of soil texture in Valley 23

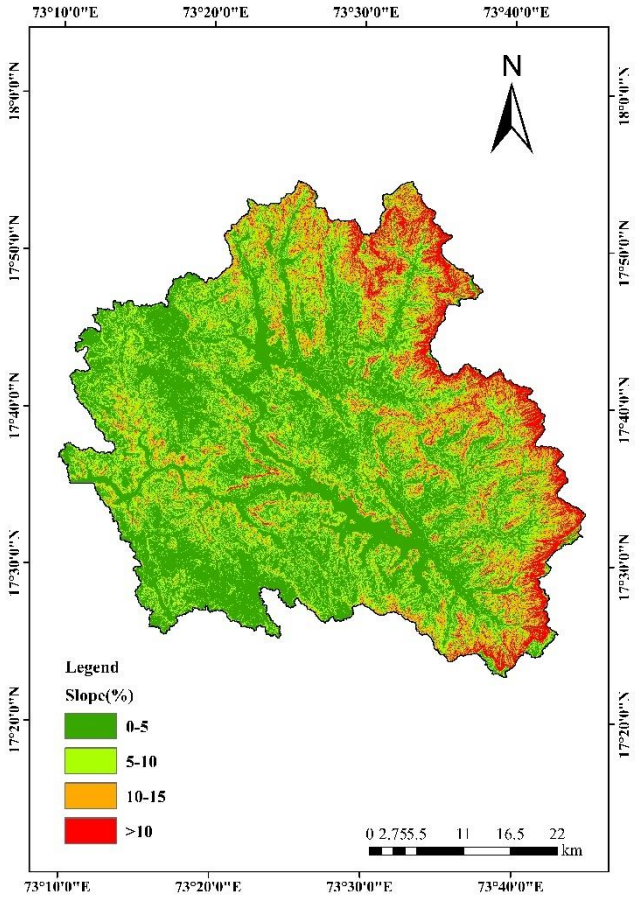

Fig. 4.27 Areal distribution of slope in Valley 23

LULC is classified into five classes area is prominently occupied by Barren land (53.61%) and scattered all over the basin. Built up area is about 4.63% mainly concentred around river. Agriculture area is 3.30%, forest is covered in 36.54% of area and area under waterbodies is least (1.93%) among all.

4.3.3.2 Soil type of Valley 23

The soil data for the study area were acquired in shapefile format at a scale of 1:50,000 from the FAO Soil Database. The data were reprojected into the WGS1984 UTM Zone 43N coordinate system using raster projection techniques. Additionally, the associated dBase file was obtained from the FAO Soil Database for further analysis. In valley 23 only loamy (2562.54km^2) type of soil texture is found as shown if Fig. 4.26

4.3.3.3 Topographic details of valley 23

The Konkan region is characterized by a predominantly hilly terrain, resulting in a wide range of slope gradients within the river basins. The slopes are generally steep along the ridgelines and gradually decrease in steepness toward the main river channels. To understand area under different zones it classified into three class as storage zone (0-5%), recharge zone (5-10%), runoff zone (>10%). Table 4.33 provide details of area under each category.

Table 4.33 Topographic details of Valley 23

River basins	Area Distribution (km^2)	Storage Zone (0-5%)	Recharge Zone (5-10%)	Runoff Zone (>10%)
Vashisthi	Area (km2)	1244.76	773.52	544.26
	Area (%)	48.6	30.2	21.2

Out of total geographic area major area is under 0- 5% followed by 5-10% (30.2%) and remaining area (21.2%) is under steep slope as shown in Fig. 4.27

4.3.3.4 Climatic condition of Valley 23

Climatic parameter includes rainfall, minimum and maximum temperature, relative humidity and wind speed which is required as input data for model is collected from HDUG, Nashik of 29 year from 1991 to 2019 of 8 meteorological stations. Details related to meteorological station and data is mentioned in Annexure I.

Valley 23 experience heavy rainfall mainly concentered during month of June to October. Highest rainfall is observed in July which sometimes lead to flooded condition. Average annual rainfall is 3525 mm. Average temperature is range between 16°C to 38°C. It is highest during summer month up to 38°C and lowest during winter month up to 16°C. Relative humidity is lowest during summer month (49%) and it higher in rainy seasons reaches upto 90%. Wind speed in this region is ranges between 2m/s to 5 m/s. Details are mentioned in Annexure II.

4.3.3.5 Estimation of surface water resource availability

4.3.3.5.1 Calibration and Validation of model

The Arc-SWAT Model was calibrated, validated and applied to river basin to evaluate surface water availability along with their seasonal variations. Simulation was started from 1991 with 3 years of model warmup period and output of simulation was available for 25 years from 1994 to 2019. Streamflow data is calibrated and validated at HDUG meteorological station Chatav for river basin in Valley 23. Performance evaluation criteria is tabulated in Table 4.34 and shown in Fig. 4.28. Details of calibration parameter are mentioned in Appendix IV

Table 4.34 Performance criteria of simulated data of valley 23

		Calibration					Validation				
Basin	Sites	Year	NSE	R^2	PBIAS	RSR	Year	NSE	R^2	PBIAS	RSR
Vashisthi	Chatav	1995-2000	0.96	0.96	-0.68	0.19	2001-2005	0.89	0.89	-0.76	0.14

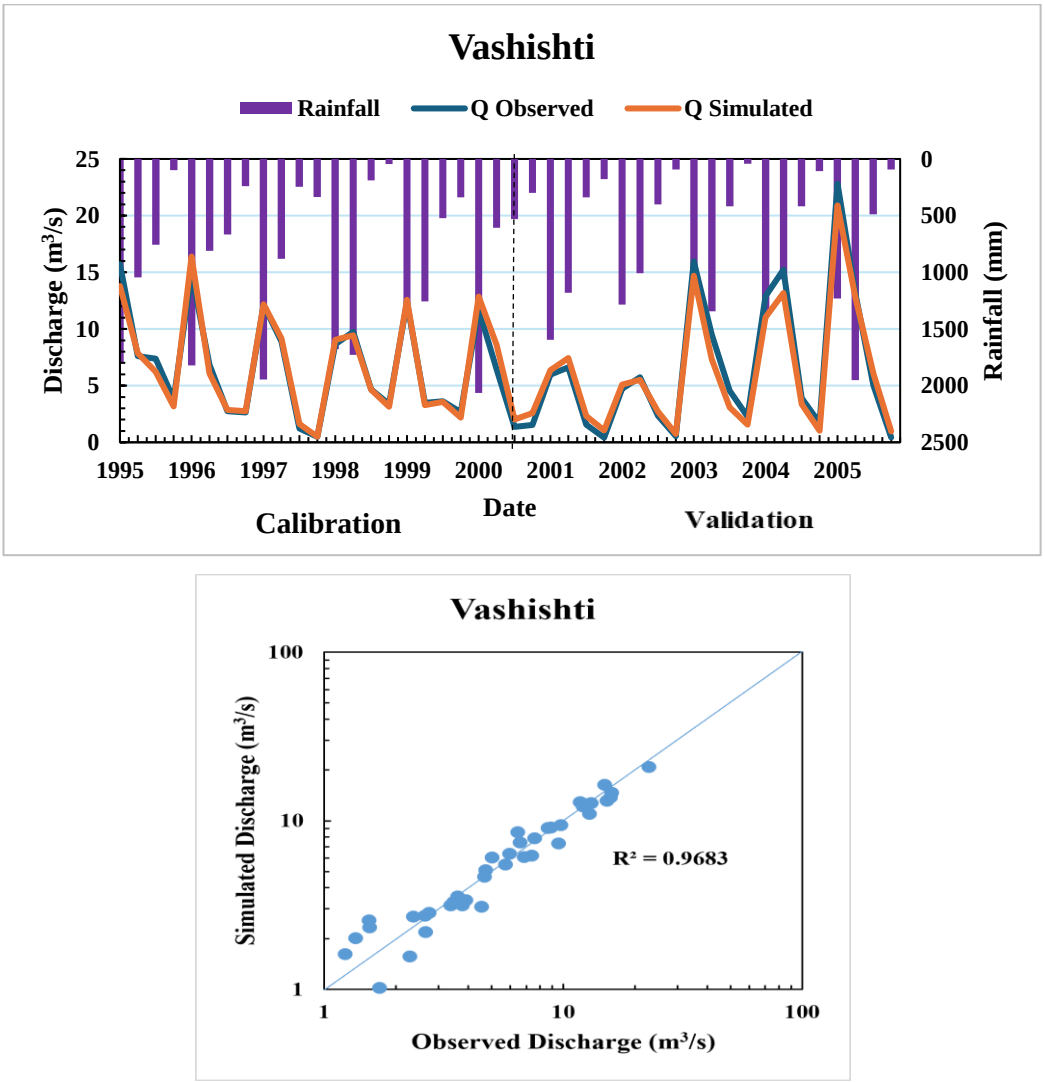

Fig.4.28 Monthly observed and simulated streamflow over a period 1994-2005(a. Seasonal variation, b. Scatter plot of Valley 23

4.3.3.5.2 Sub-basin wise monthly river flow availability

The Arc-SWAT Model was calibrated, validated and applied to river basin to evaluate surface water availability along with their seasonal variations. Prior to its application in the basin, the model underwent calibration and validation processes. The first analysis obtained after running the SWAT model was the river flow availability of river basins which is extracted from output file as a Flow_out parameter.

Table No 4.35 Monthly River flow in Valley 23

Months	Jan	Feb	Mar	Apr	May	Jun	Jul	Aug	Sep	Oct	Nov	Dec
Vashisthi	63	56	47	41	35	457	798	588	326	184	91	71

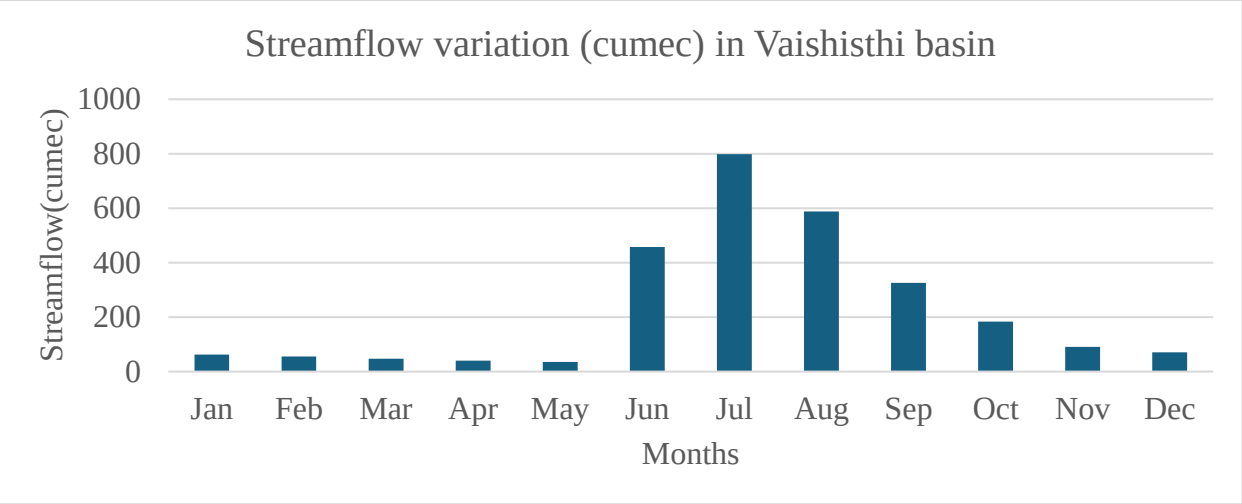

Fig 4.29 Monthly River flow(cumec) variation in Valley 23

Table 4.36 Available surface water potential in the river from selected locations in Valley 23

	Co-ordinate Location		
Basin	Long	Lat	Water availability (Mm^3)
Vashisthi	73.1779	17.5858	4997.5

The analysis of basin-wise monthly mean of river flow is tabulated in Table No 4.35 and illustrated in Fig.4.29 It reveals notable variation throughout the year. Heightened river flow is evident during the rainy months of June, July, August, and September, predominantly driven by rainfall. The heavy monsoon accumulated in the form of river flow. From Fig. 4.29 it becomes apparent that July consistently witnesses the highest river flow (798 cumec) across all basins because of high rainfall receive during this month and it is lowest in April (41 cumec) due high evapotranspiration rate. Throughout the analysis period, river flow generally peaks during June and July, gradually decreasing thereafter until April. Total surface water availability in Valley 23 is 2756.06 cumec. Table 4.36 shows available surface water potential in river from selected location and Table 4.37 shows average annual volumes of basin.

Table 4.37 Average annual volumes of different parameter of basin in valley 23

Basin	Water Yield (mm)	Base flow(mm)	Surface Flow(mm)
Vashisthi	3115.95	838.09	2068.69

4.3.3.6 Estimation of basin-wise monthly surplus and deficit water availability

Annual water availability plays an important role for effective water resource management during lean period. Monthly water surplus/deficit was carried out by using climatic water supply (rainfall) and climatic water demand (evapotranspiration). Monthly water availability variation in the year was evaluated based on methodology discussed in section 3.7 Results of basin wise on monthly basis water surplus/deficit in Valley 23 are presented in Table 4.38

Table 4.38 Temporal variation of annual water surplus/deficit in Valley 23

District	Vashisthi		
Months	PET (mm)	Rainfall (mm)	Sur/Def (mm)
Jan	86	0	-86
Feb	102	0	-102
Mar	140	0	-139
Apr	150	0	-150
May	144	3	-141
Jun	80	779	699
Jul	58	1326	1268
Aug	64	846	782
Sep	79	420	341
Oct	94	148	53
Nov	83	3	-80
Dec	78	0	-78

Note: RF = Rainfall in mm, PET = Potential evapotranspiration(mm) Sur = Surplus Def =Deficit

From Table 4.38 it is revealed that monthly water demand varied between 58 to 150 mm in Vashisthi basin. Monthly water demand is increased from July to May. Due to high temperature and lower humidity water demand is highest during month of April and lowest during month of July due to higher humidity and low temperature. Monthly water supply is highest during the month of June to October due average annual rainfall in region is concentrated during this season. It is varied between 0 to 1326 mm in Vashisthi.

According to Table 4.38 it is concluded that water is surplus during month of June to October it is highly surplus in month of June and July, and it is deficit from November to May and it more deficit in month of April and May. In Vashisthi basin water condition is highly surplus in month of July which is 1268 mm and deficit in month of March and April (150 mm) due high evapotranspiration rate.

The temporal variability of water balance components, including rainfall, evapotranspiration (ET), runoff was analysed throughout the year to evaluate the monthly surplus and deficit water availability in the region. Monthly water balance components of valley 23 is illustrated in Fig. 4.30

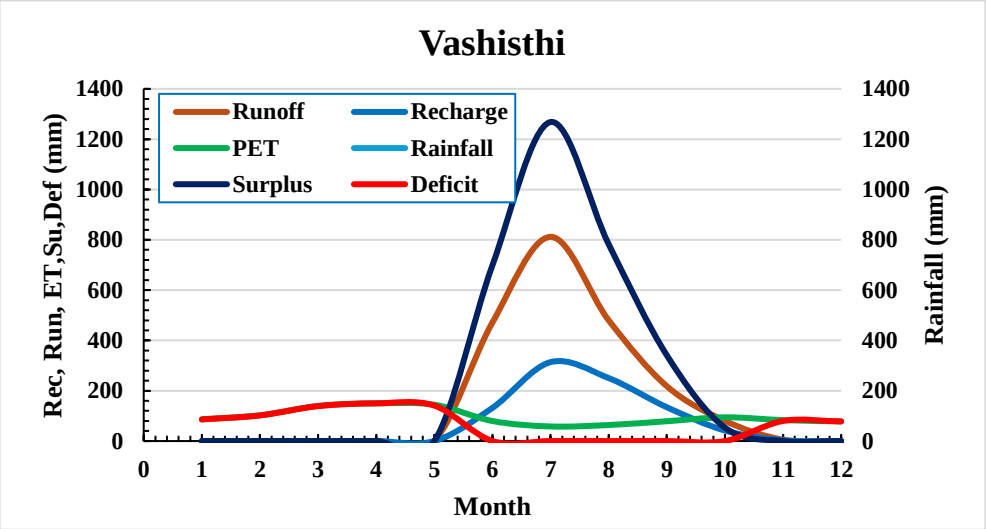

Fig 4.30 Temporal variation of water balance components of valley 23

Fig. 4.30 illustrates the variation of all water balance components throughout the year across all districts in Konkan region. Evapotranspiration peaks during April and May and reaches its lowest point in July when the precipitation is at its highest peak. Due to high evapotranspiration during January to May and low precipitation these months are water deficit and form June to October evapotranspiration rate is lowest point and precipitation is highest which results surplus water during these months.

4.3.4 Assessment of surface water availability in Valley 24

Valley 24 is located at the southern part of the Konkan region in district of Ratnagiri and Sindhudurg. This valley consists of total 10 rivers viz Shastri, Muchkundi, Kajvi, Kodavali, Waghotan, Achara, Gad, Devgad, Karli, Vengurla. Out of all the basin Achara and Vengurla river is excluded from study due lack of adequate data availability. Out of total total geographic area of Valley 24 Shastri occupies 2570.41 km^2, Muchkundi occupies 792.19 km^2, Kajivi occupies 543.18 km^2, Kodavali occupies 698.60 km^2, Waghton comprised of 897.99 km^2, Gad occupies 983.78 km^2, Devgad consist of about 704.41 km^2 and Karli occupies 794.51 km^2. Subbasin wise area is shown in Fig. 4.31

4.3.4.1 Land use/ Land cover of Valley 24

The Land use and land cover (LULC) data for 2019 was downloaded from Sentinal-2 satellite via the Living Atlas (https://livingatlas.arcgis.com/landcover/), with 10m resolution as of 15/04/2024. The map was projected to WGS1984 UTM Zone 43N using raster projection. The

predominant land use/ land cover types in the study area's river basins were barren lands, followed by agriculture, forest, Urban Area, and water bodies. Table 4.39 and Fig. 4.32 provide detailed information on LULC of valley.

Table 4.39. Areal distribution of Land use Land cover details of Valley 24

River	Classes	Waterbodies	Forest	Agriculture	Built-up	Barren Land
Shastri	Area (km^2)	30.33	1208.35	47.55	78.91	1205.27
	Area (%)	1.18	47.01	1.85	3.07	46.89
Muchkundi	Area (km^2)	11.25	326.07	16.16	24.16	414.55
	Area (%)	1.42	41.16	2.04	3.05	52.33
Kajivi	Area (km^2)	4.56	229.28	12.00	20.64	276.64
	Area (%)	0.84	42.21	2.21	3.80	50.93
Kodvali	Area (km^2)	14.32	302.28	13.20	14.25	354.47
	Area (%)	2.05	43.27	1.89	2.04	50.74
Waghton	Area (km^2)	26.40	367.19	34.12	13.38	456.99
	Area (%)	2.94	40.89	3.80	1.49	50.89
Gad	Area (km^2)	9.54	545.41	62.08	17.51	349.24
	Area (%)	0.97	55.44	6.31	1.78	35.50
Devgad	Area (km^2)	16.98	267.11	62.83	18.17	339.24
	Area (%)	2.41	37.92	8.92	2.58	48.16
Karli	Area (km^2)	13.35	492.60	65.55	18.11	204.82
	Area (%)	1.68	62.00	8.25	2.28	25.78
Total	Area (km^2)	126.73	3738.28	313.50	205.15	3601.23
	Area (%)	1.59	46.82	3.93	2.57	45.10

LULC is classified into five classes area is major area occupied by Forest land (46.82%) followed by barren land (45.10%) scattered all over the basin. Built up area is about 2.57%. and area under Agriculture is 3.93% and waterbodies cover only 1.59% of area.

4.3.4.2 Soil type of Valley 24

The soil data for the study area was downloaded in shapefile format at a scale of 1:50,000 and from FAO Soil Data. It is projected into WGS1984 UTM Zone 43N using raster projection. The dBase file was also downloaded from the FAO Soil database. Area under each soil types are given in Table 4.40. and Fig 4.33

In valley 24 only two types of soil texture are found viz. loam and sandy clay loam majorly occupied by loam type of soil texture especially northern part of valley and southern part is occupied by loam type of soil. Area under sandy clay loam is 86.30% and 13.70% area is occupied by clay loam type of soil texture.

Table 4.40 Areal distribution of soil texture in Valley 24

River	Class	Area (km^2)	Area (%)
Shastri	Sandy clay loam	39.0702	1.52
	Loam	2531.34	98.48
Kajivi	Sandy clay loam	0.76045	0.14
	Loam	542.42	99.86
Muchkundi	Loam	792.19	100
Kodvali	Sandy clay loam	15.7884	2.26
	Loam	682.812	97.74
Waghton	Sandy clay loam	54.5978	6.08
	Loam	843.392	93.92
Devghar	Sandy clay loam	8.5938	1.22
	Loam	695.816	98.78
Gad	Sandy clay loam	226.663	23.04
	Loam	757.117	76.96
Karli	Sandy clay loam	748.508	94.21
	Loam	46.0021	5.79
Total	Sandy clay loam	1093.98	13.70
	Loam	6891.09	86.30

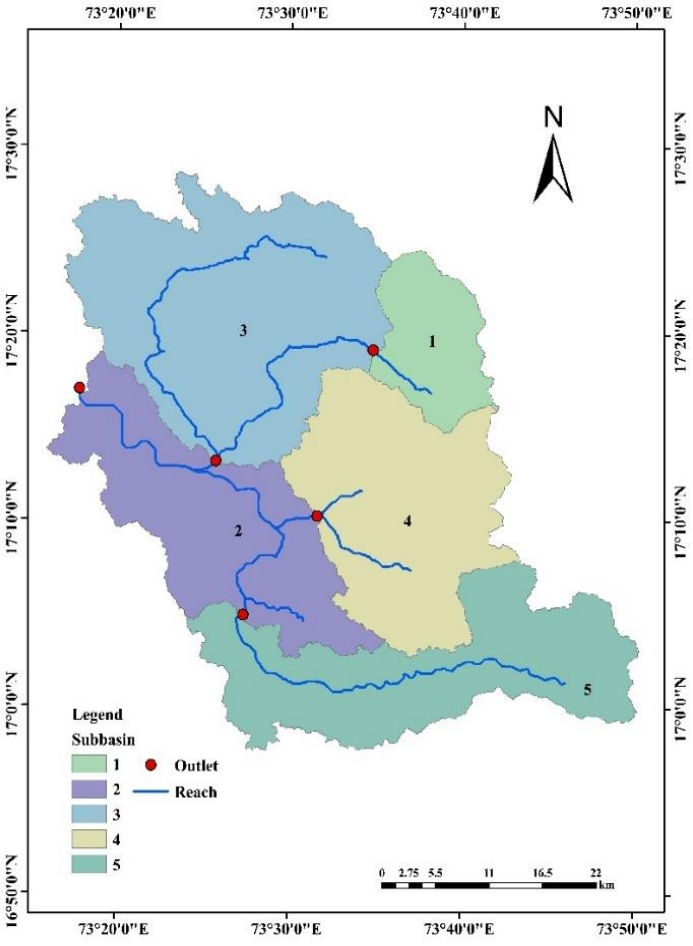

(a) Shastri basin

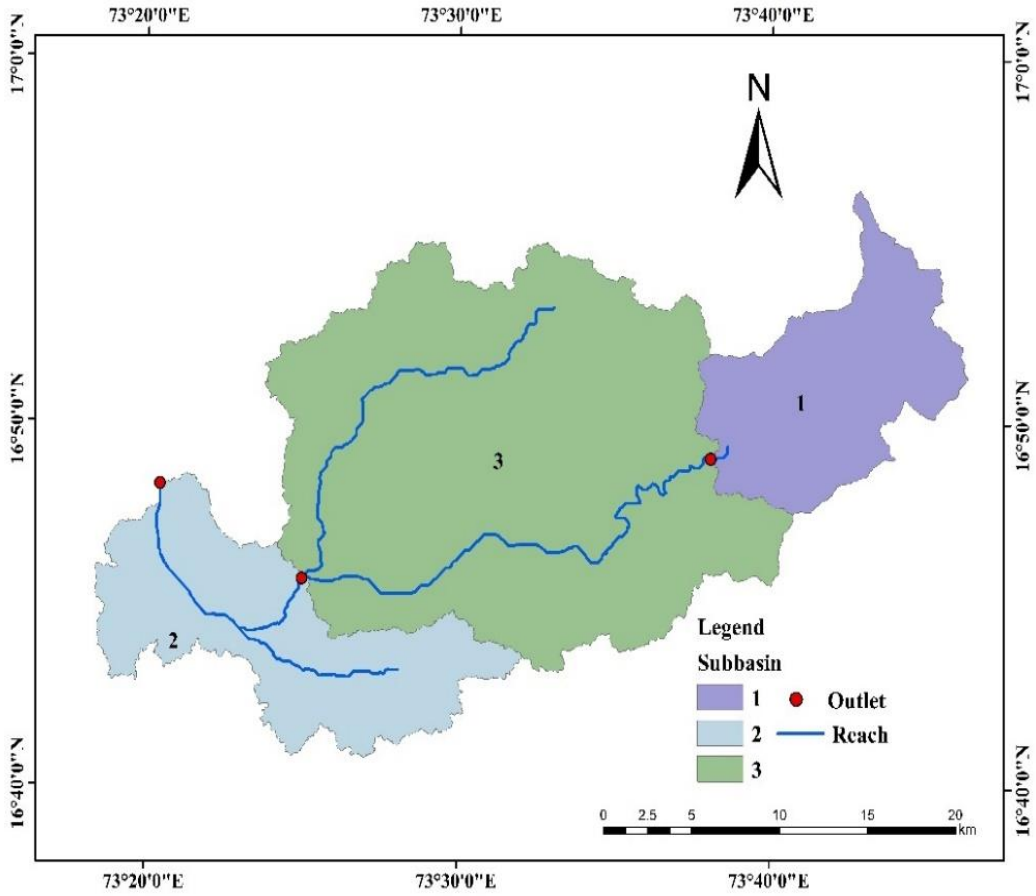

(b)Muchkundi basin

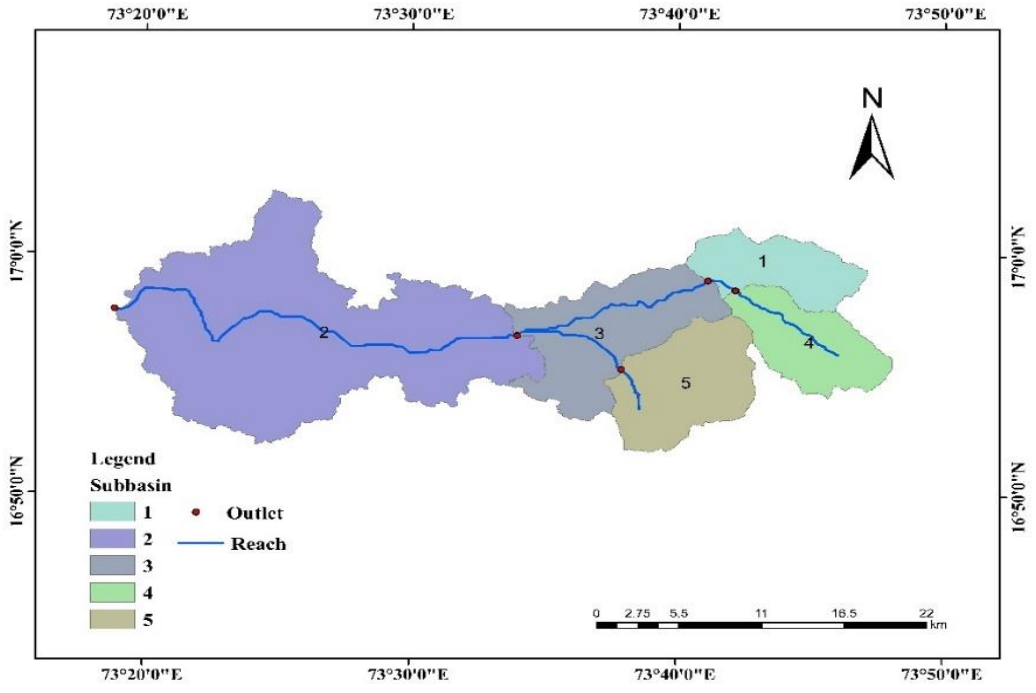

(C) Kajivi basin

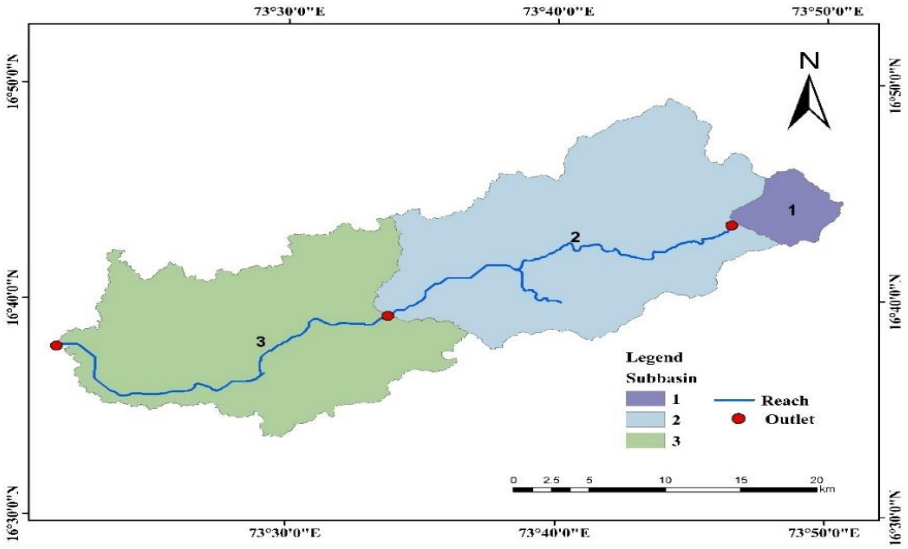

(d) Kodvali basin

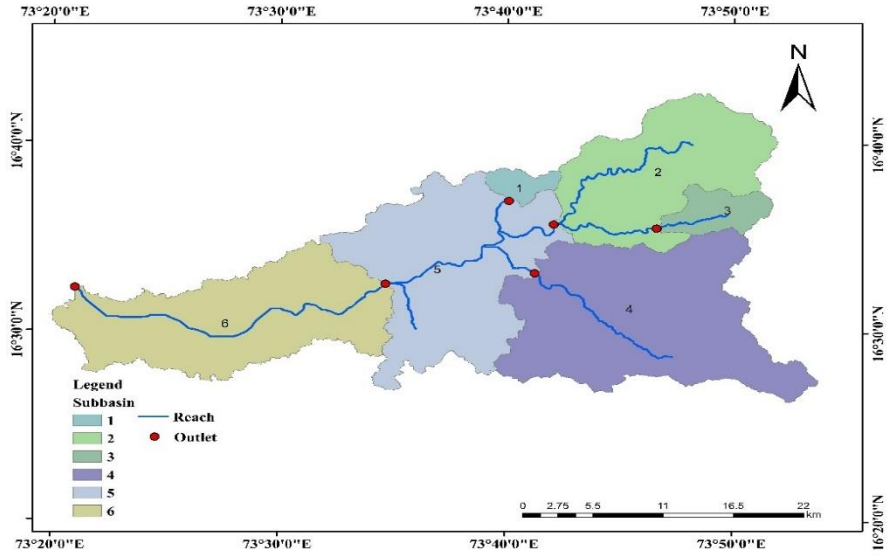

(e) Waghton basin

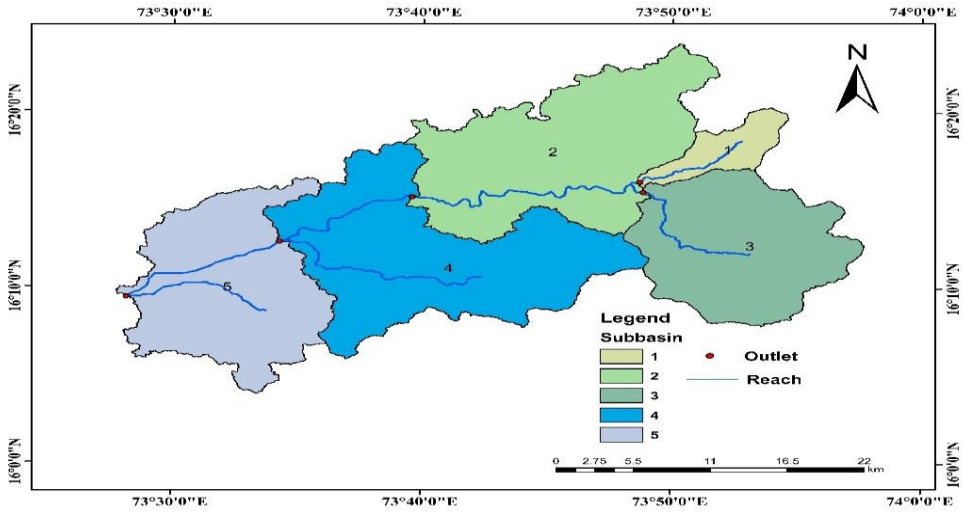

(f) Gad basin

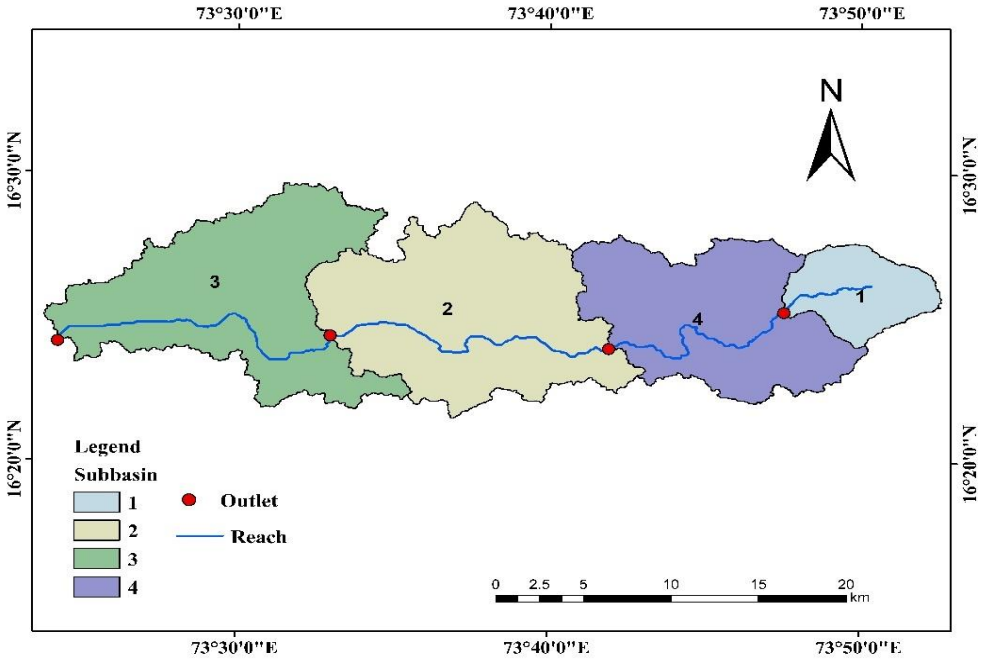

(g) Devgad basin

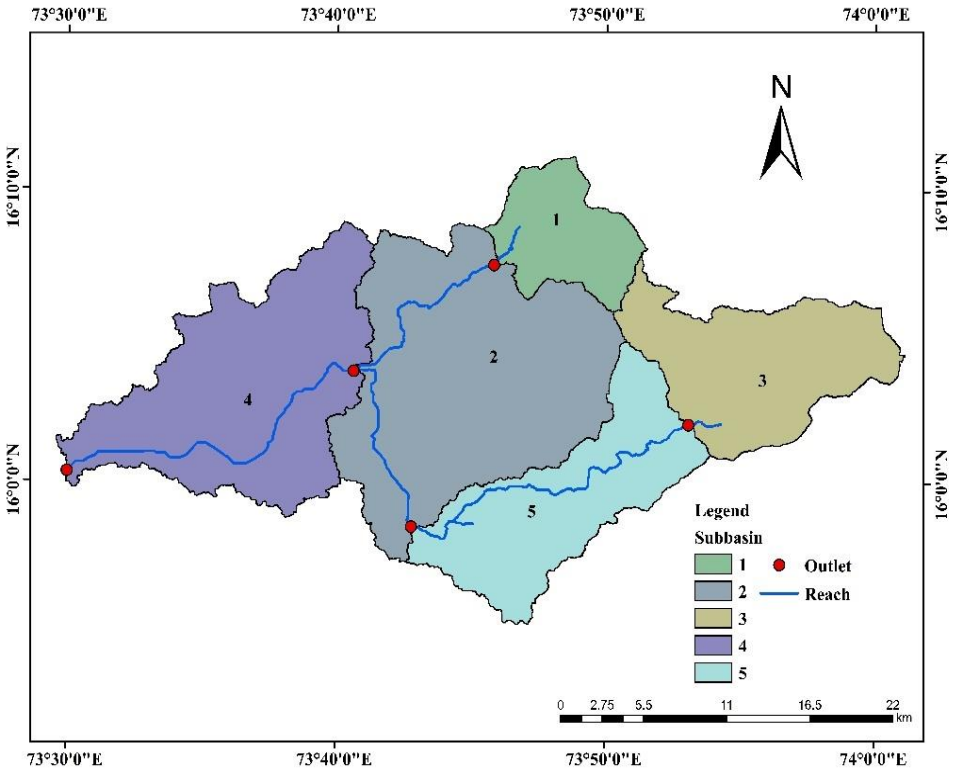

(h) Karli Basin

Fig.4.31 Subbasin map of river basin in Valley 24

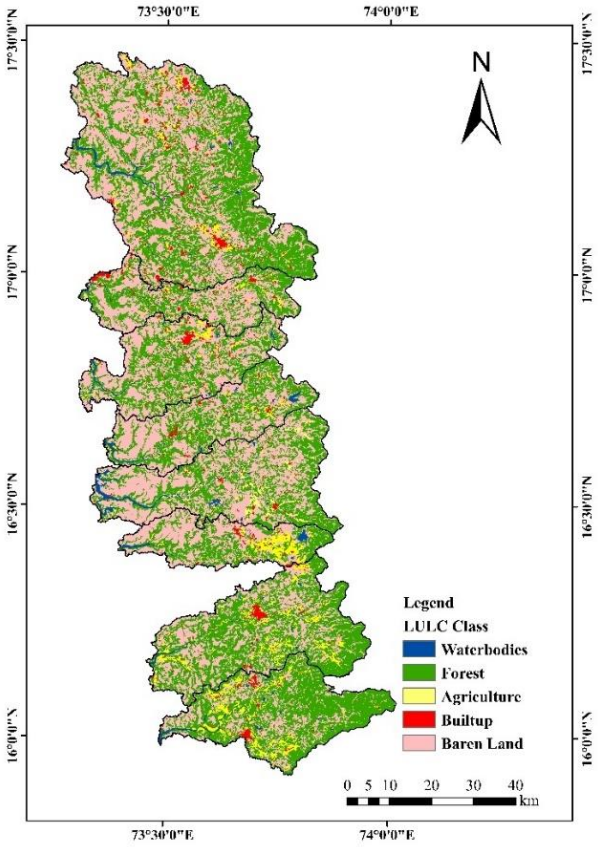

Fig.4.32 Land use land cover (LULC) distribution in Valley 24

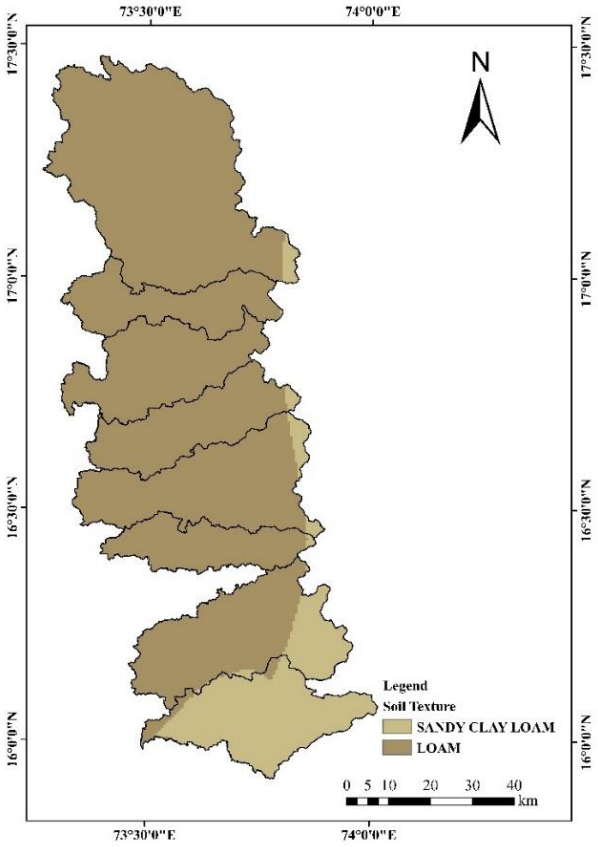

Fig. 4.33 Spatial distribution of soil texture in Valley 24

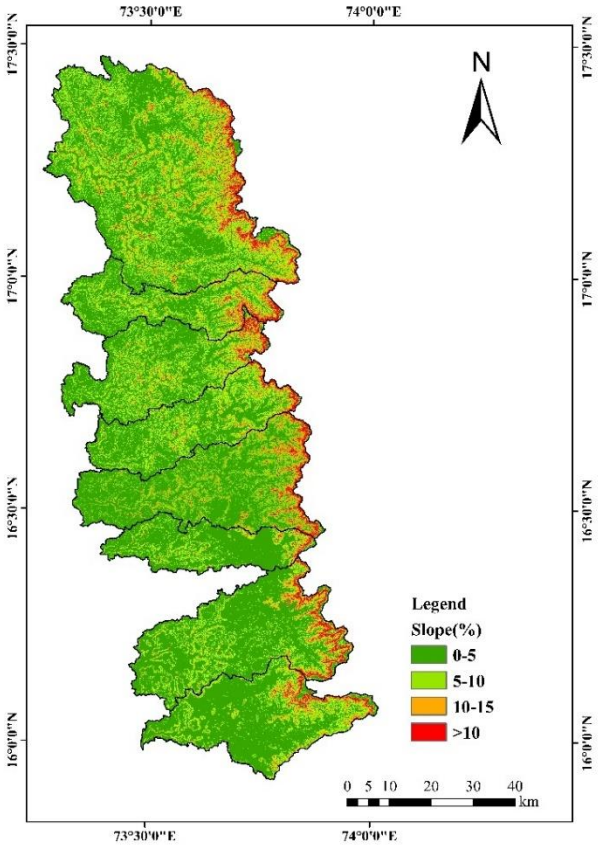

Fig 4.34 Spatial distribution map of Slope categories in Valley 24

4.3.4.3 Topographic details of Valley 24

Konkan region is characterized by hilly region, thus, the slope ranges in the river basins are also wide along the ridge line and reduced towards mainstreams. Area is categorized in the different zones as per the slope categories: storage zone (0-5%), recharge zone (5-10%), runoff zone (>10%). The basin-wise area under each slope category is presented in Table 4.41 and shown in Fig. 4.34

Table 4.41 Topographic details of Valley 24

River basins	Area Distribution (km^2)	Storage Zone	Recharge Zone	Runoff Zone
		(0-5%)	(5-10%)	(>10%)
Shastri	Area (km2)	1364.31	823.58	382.53
	Area (%)	53.08	32.04	14.88
Muchkundi	Area (km2)	488.18	224.73	79.28
	Area (%)	61.62	28.37	10.01
Kajivi	Area (km2)	303.24	161.78	78.16
	Area (%)	55.83	29.78	14.39
Kodvali	Area (km2)	334.41	155.05	53.72
	Area (%)	61.57	28.55	9.89
Waghton	Area (km2)	559.49	225.00	113.50
	Area (%)	62.31	25.06	12.64
Gad	Area (km2)	311.37	426.02	246.35
	Area (%)	31.65	43.31	25.04
Devgad	Area (km2)	539.16	123.95	41.29
	Area (%)	76.54	17.60	5.86
Karli	Area (km2)	551.91	161.80	80.80
	Area (%)	69.47	20.36	10.17
Total	Area (km2)	4452.07	2301.90	1075.63
	Area (%)	56.86	29.40	13.74

The majority of the Konkan region is covered by the 0-5% slope class (56.86%), representing the nearly flat to gentle slope or storage zone, which is predominately found in southern parts of area (Table 4.41 and Fig.4.34). This is followed by the 5-10% slope class, representing the moderate slope or recharge zone, which is primarily scattered across the western part of the region. The runoff zone, consisting of slopes in the 10-15% and >15% classes, is mainly concentered in the eastern part of the Konkan region, covering 13.74% of the area.

4.3.4.4 Climatic condition of Valley 24

Climatic parameter includes rainfall, minimum and maximum temperature, relative humidity and wind speed which is required as input data for model is collected from HDUG, Nashik of 29 year from 1991 to 2019 of 8 meteorological stations. Details related to meteorological station and average monthly data is mentioned in Annexure I.

Valley 24 experience heavy rainfall mainly concentered during month of June to October. Highest rainfall is observed in July. Average annual rainfall is 2380 mm. Average temperature is range between 18°C to 37°C. It is highest during summer month up to 37°C and lowest during winter month up to 18°C. Relative humidity is lowest during summer month (50%) and it higher in rainy seasons reaches up to 91%. Wind speed in this region is ranges between 2.6 m/s to 5.1 m/s. Details are mentioned in Annexure II.

4.3.4.5 Estimation surface water resource availability

4.3.4.5.1 Calibration and validation of SWAT Model

In the present study calibration of SWAT model was done with help of SWAT-CUP SUFI2 program as described in chapter 3 section 3.5.3 SWAT model was calibrated having an outlet of meteorological stations of Water Resource Department, (Surface Water) Government of Maharashtra. Simulation was started from 1991 with 3 years of model warmup period and output of simulation was available for 25 years from 1994 to 2019. Performance evaluation criteria is tabulated in Table 4.42 and shown in Fig. 4.35. Details of monthly streamflow data calibrated and validated at different station is mentioned in annexure I and details of calibration parameter are mentioned in Appendix IV.

Table 4.42 Performance criteria of simulated data of river basin in Valley 24

	Calibration					Validation				
Basin	Year	NSE	R^2	PBIAS	RSR	Year	NSE	R^2	PBIAS	RSR
Shastri	1995-2000	0.77	0.76	-3.27	0.2	2001-2005	0.77	0.76	-2.18	0.4
Kajivi	1995-2000	0.84	0.81	-10.21	0.3	2001-2005	0.84	0.78	-10.21	0.3
Muchkundi	1995-2000	0.75	0.73	-8.5	0.2	2001-2005	0.72	0.73	-7.2	0.3
Kodvali	2007-2009	0.69	0.7	3.46	0.5	2010-2012	0.65	0.62	-1.23	0.2
Waghton	1995-2000	0.69	0.75	4.87	0.5	2001-2005	0.5	0.51	2.34	0.5
Devghar	1995-2000	0.73	0.73	2.97	0.5	2001-2005	0.71	0.7	-1.3	0.5
Gad	1994-2000	0.69	0.8	2.16	0.1	2000-2004	0.63	0.74	2.14	0.3
Karli	1999-2002	0.56	0.61	-2.29	0.4	2006-2009	0.5	0.63	-1.04	0.5

Performance criteria are found to be good and satisfactory as mentioned in Table 3.1 for all river basin. Graphical presentation is presented in Fig. 4.35

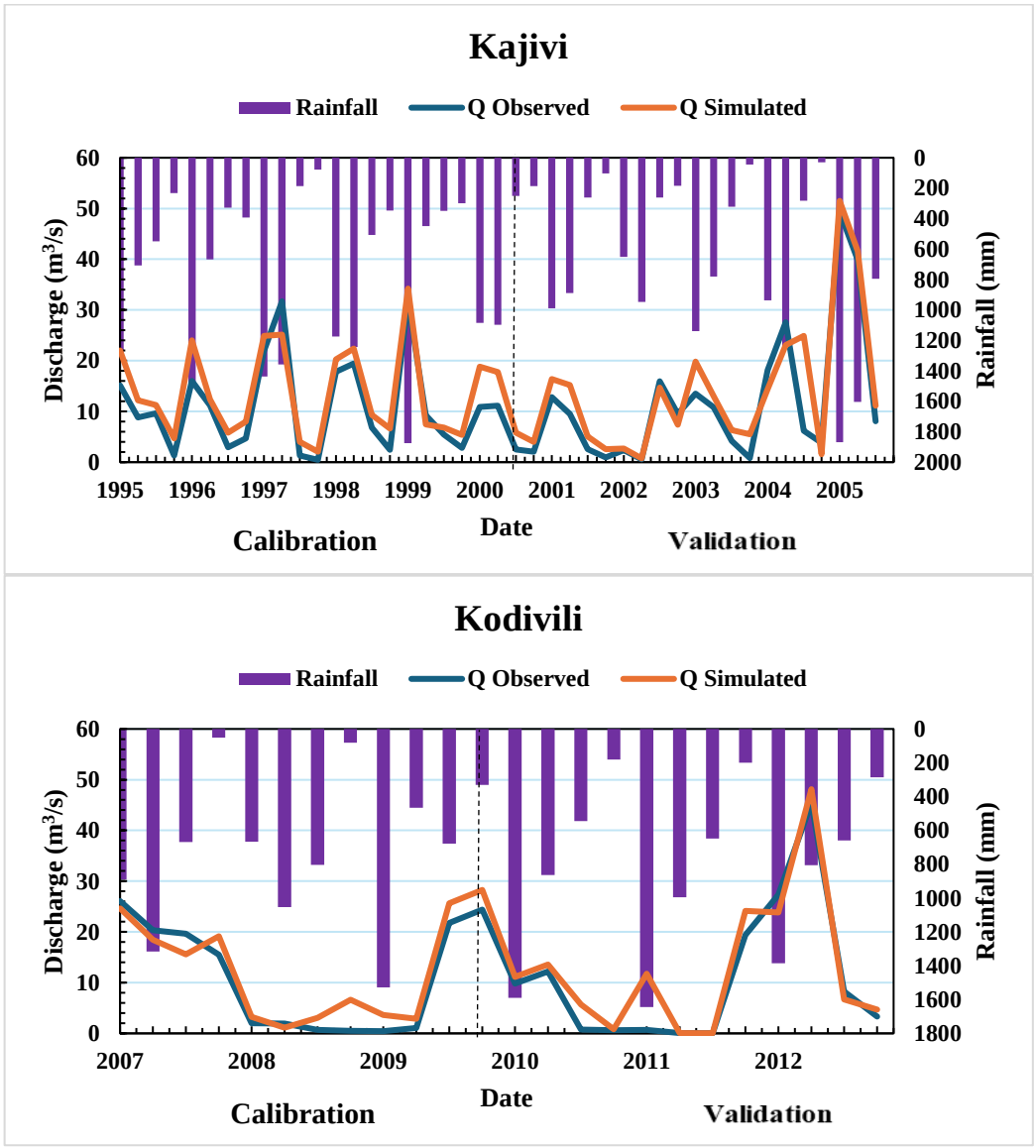
Kajivi
Rainfall
Q Observed
Q Simulated
Discharge (m³/s)
Rainfall (mm)
0
10
20
30
40
50
60
0
200
400
600
800
1000
1200
1400
1600
1800
2000
1995
1996
1997
1998
1999
2000
2001
2002
2003
2004
2005
Calibration
Date
Validation

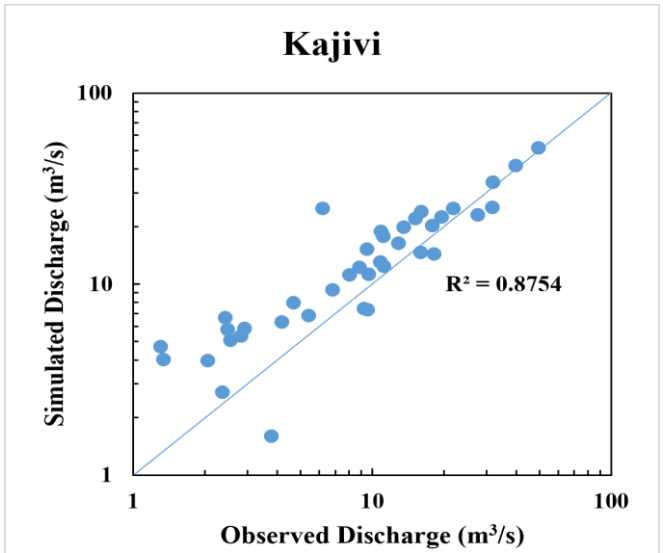
Kajivi
Simulated Discharge (m³/s)
Observed Discharge (m³/s)
R² = 0.8754
1
10
100

Kodivili
Rainfall
Q Observed
Q Simulated
Discharge (m³/s)
Rainfall (mm)
0
10
20
30
40
50
60
0
200
400
600
800
1000
1200
1400
1600
1800
2007
2008
2009
2010
2011
2012
Calibration
Date
Validation

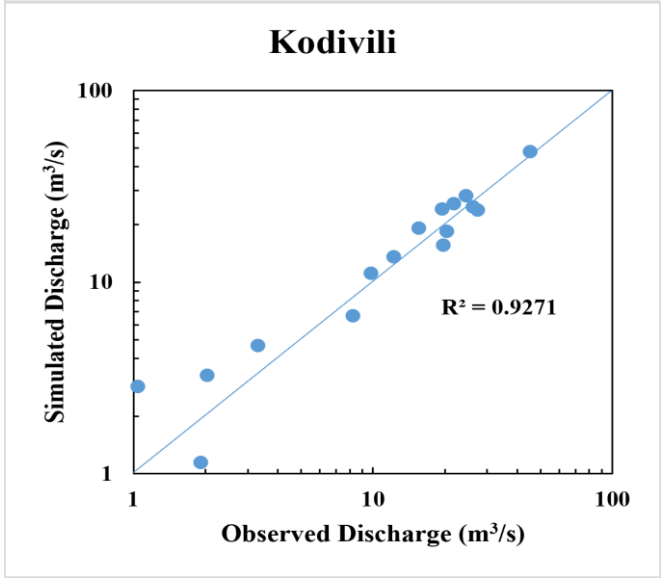
Kodivili
Simulated Discharge (m³/s)
Observed Discharge (m³/s)
R² = 0.9271
1
10
100

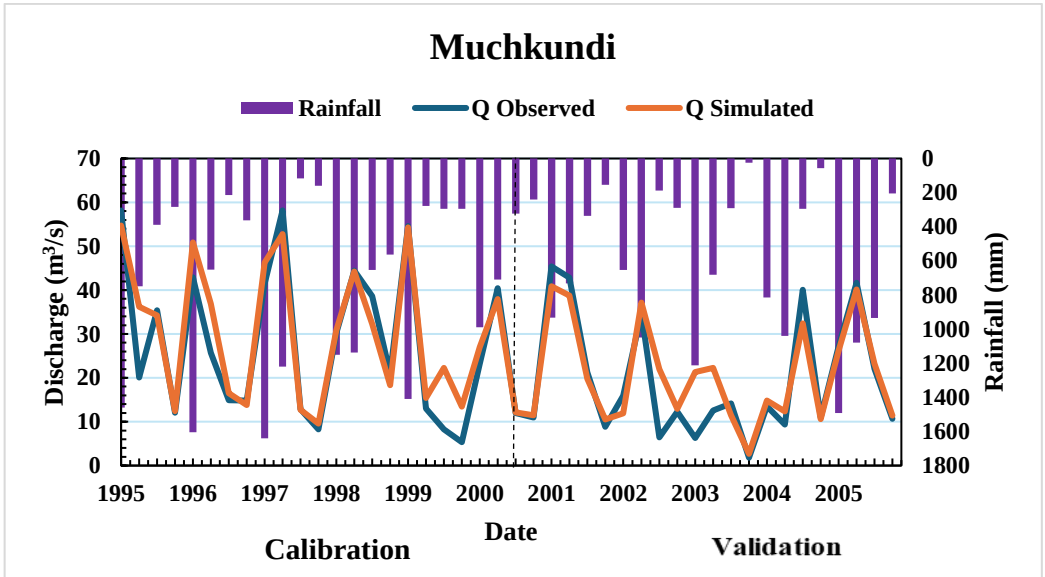
Muchkundi
Rainfall
Q Observed
Q Simulated
Discharge (m³/s)
Rainfall (mm)
0
10
20
30
40
50
60
70
0
200
400
600
800
1000
1200
1400
1600
1800
1995
1996
1997
1998
1999
2000
2001
2002
2003
2004
2005
Calibration
Date
Validation

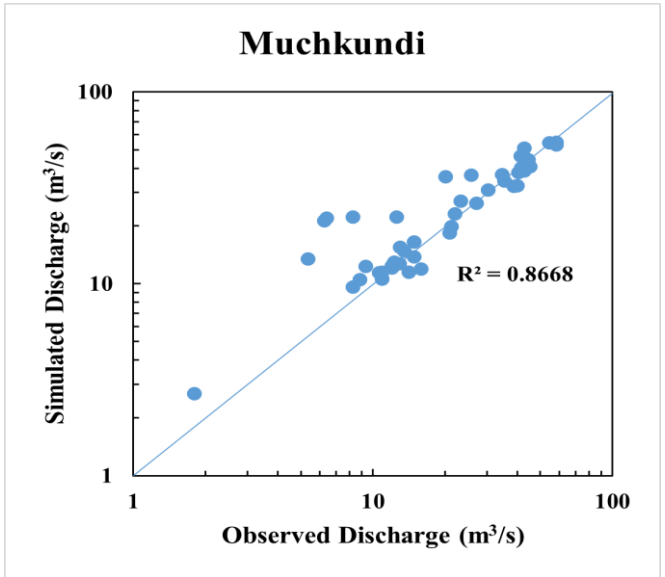
Muchkundi
Simulated Discharge (m³/s)
Observed Discharge (m³/s)
R² = 0.8668
1
10
100

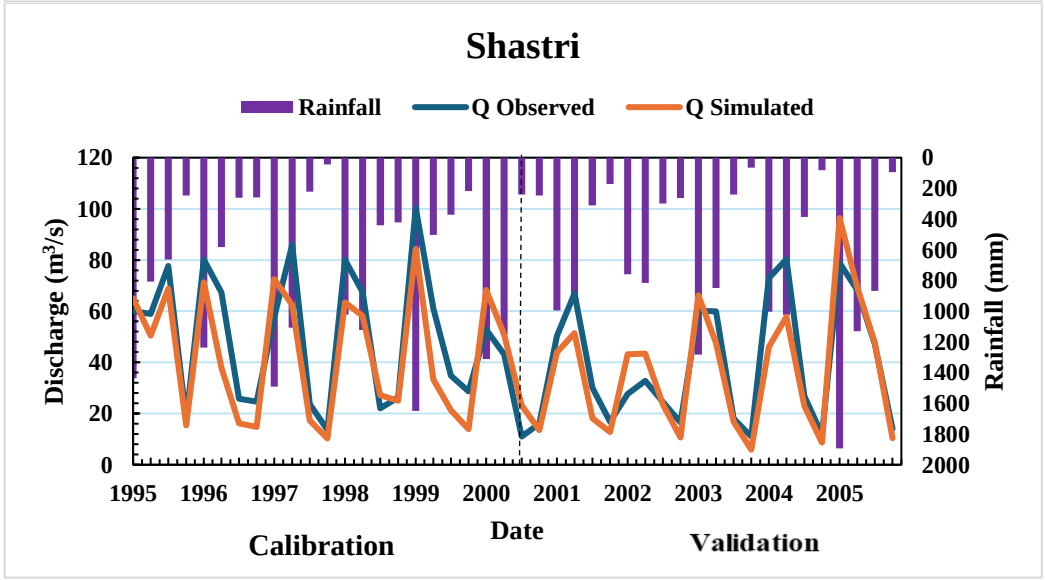
Shastri
Rainfall
Q Observed
Q Simulated
Discharge (m³/s)
Rainfall (mm)
0
20
40
60
80
100
120
0
200
400
600
800
1000
1200
1400
1600
1800
2000
1995
1996
1997
1998
1999
2000
2001
2002
2003
2004
2005
Calibration
Date
Validation

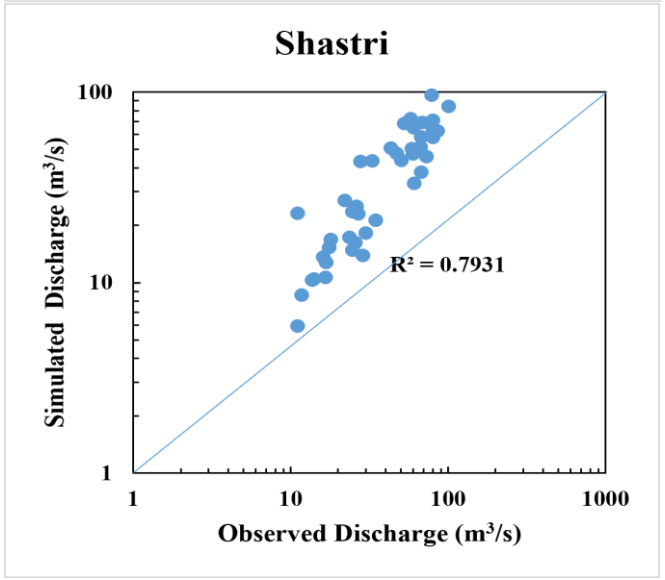
Shastri
Simulated Discharge (m³/s)
Observed Discharge (m³/s)
R² = 0.7931
1
10
100
1000

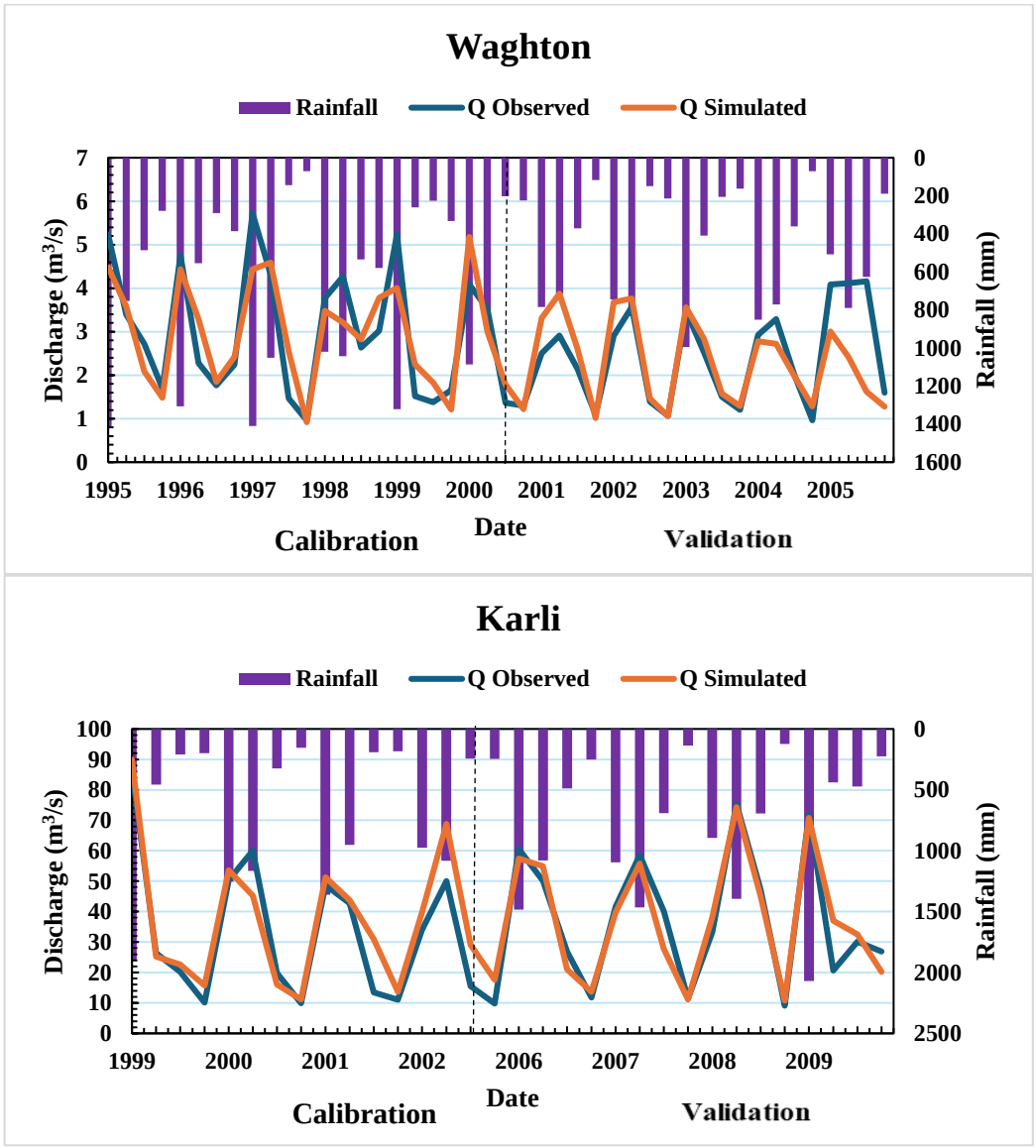
Waghton
Rainfall
Q Observed
Q Simulated
Discharge (m³/s)
Rainfall (mm)
0
1
2
3
4
5
6
7
0
200
400
600
800
1000
1200
1400
1600
1995
1996
1997
1998
1999
2000
2001
2002
2003
2004
2005
Calibration
Date
Validation

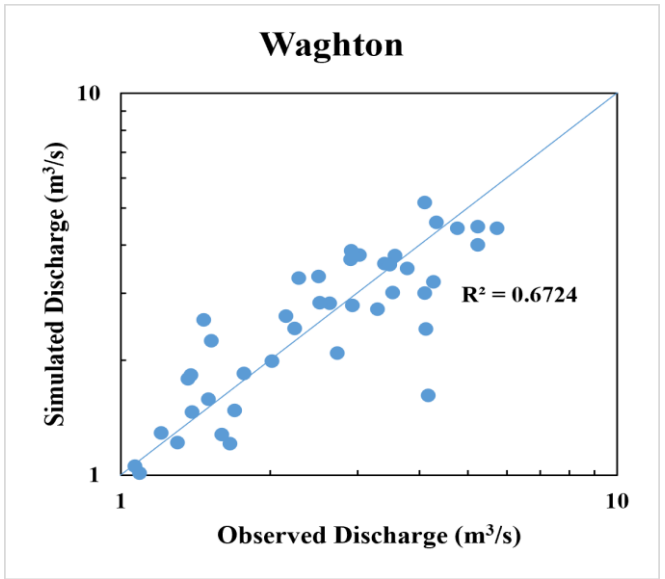
Waghton
Simulated Discharge (m³/s)
Observed Discharge (m³/s)
R² = 0.6724
1
10
1
10

Karli
Rainfall
Q Observed
Q Simulated
Discharge (m³/s)
Rainfall (mm)
0
10
20
30
40
50
60
70
80
90
100
0
500
1000
1500
2000
2500
1999
2000
2001
2002
2006
2007
2008
2009
Calibration
Date
Validation

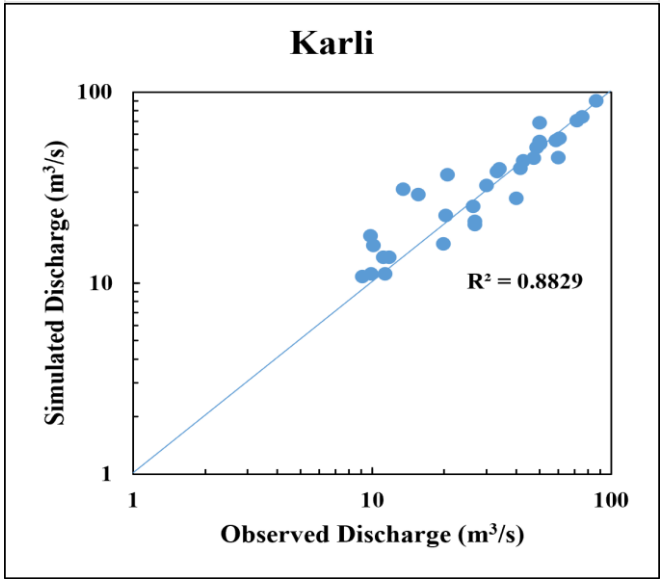
Karli
Simulated Discharge (m³/s)
Observed Discharge (m³/s)
R² = 0.8829
1
10
100
1
10
100

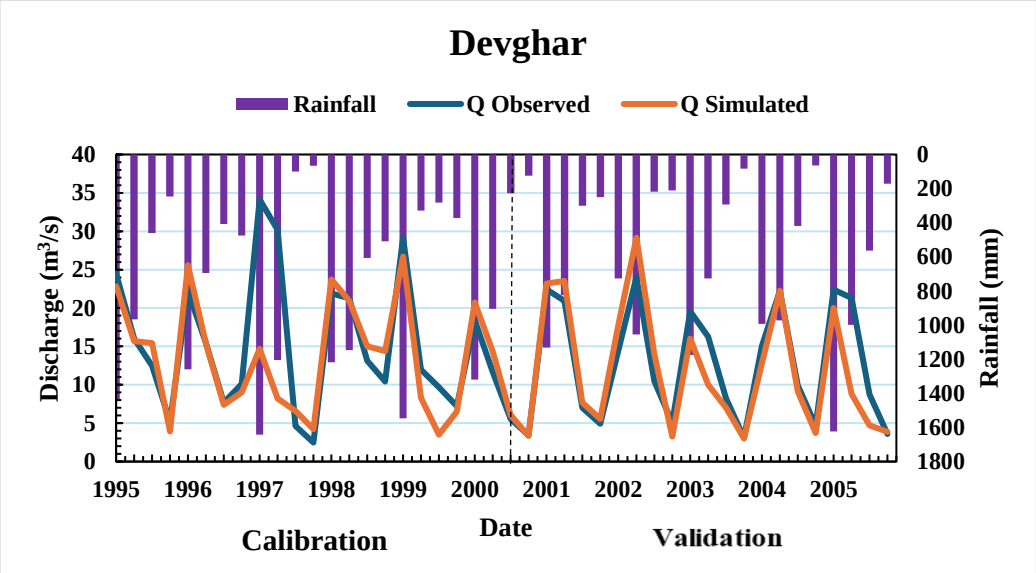

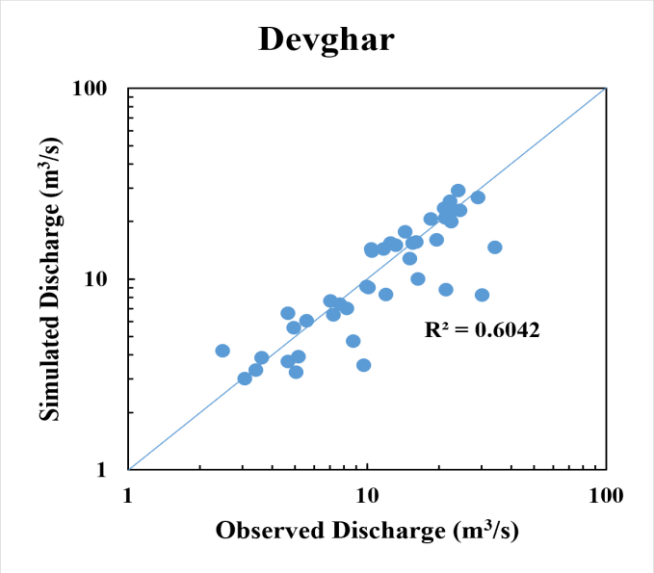

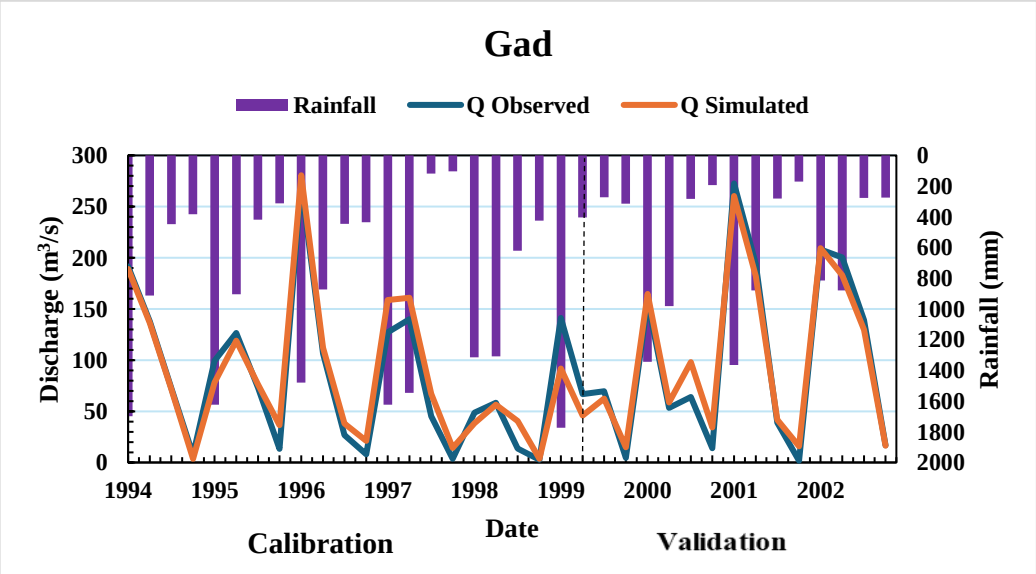

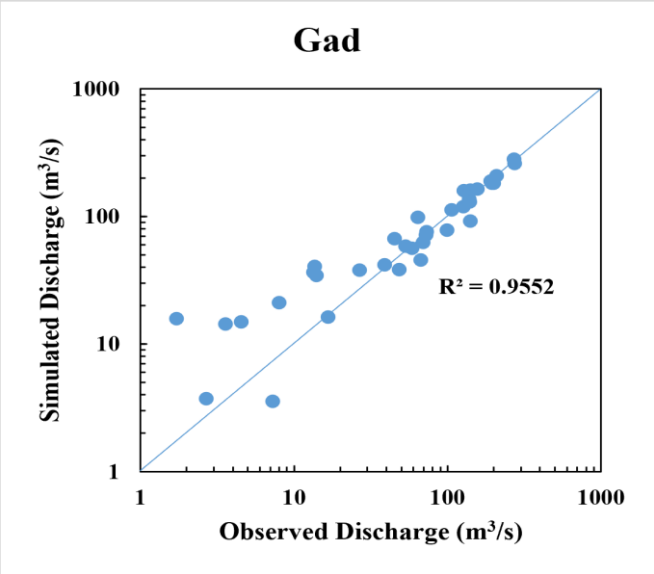

Fig.4.35 Monthly observed and simulated streamflow over a period 1994-2005 (a.Seasonal variation, b. Scatter plot) of Valley 24

4.3.4.5.2 Sub-basin wise monthly river flow availability

To assess surface water availability and seasonal fluctuations, the Arc-SWAT Model was calibrated, validated, and applied to a river basin. The model underwent calibration and validation procedures before being used in the basin. The river flow availability of river basins, which is taken from the output file as a Flow_out parameter, was the first analysis produced after the SWAT model was run.

Table No 4.43 Monthly River flow in river basin of Valley 24

Month	Shastri	Muchkundi	Kajivi	Kodvali	Waghton	Gad	Devgad	Karli
Jan	3.6	76.2	10.8	8.0	13.9	15.0	12.6	16.3
Feb	2.5	72.1	4.6	1.8	3.0	7.0	6.2	3.8
Mar	1.8	63.9	1.2	0.8	1.3	2.2	2.4	1.7
Apr	1.3	57.9	0.7	0.5	0.9	1.1	1.0	1.3
May	0.9	52.7	0.5	0.3	2.5	0.7	6.4	15.7
Jun	291.0	198.0	181.8	193.1	270.3	240.4	190.3	381.2
Jul	839.5	358.4	366.3	351.2	534.6	461.3	357.5	681.4
Aug	715.2	286.9	279.1	277.9	420.5	375.9	281.6	539.7
Sep	438.4	207.6	208.9	200.1	296.4	249.9	207.3	350.3
Oct	188.0	144.0	116.2	112.7	173.7	154.4	131.1	215.5
Nov	48.0	107.9	50.0	45.6	72.0	68.8	58.0	89.2
Dec	8.9	87.2	24.3	21.9	35.3	33.5	30.0	42.6

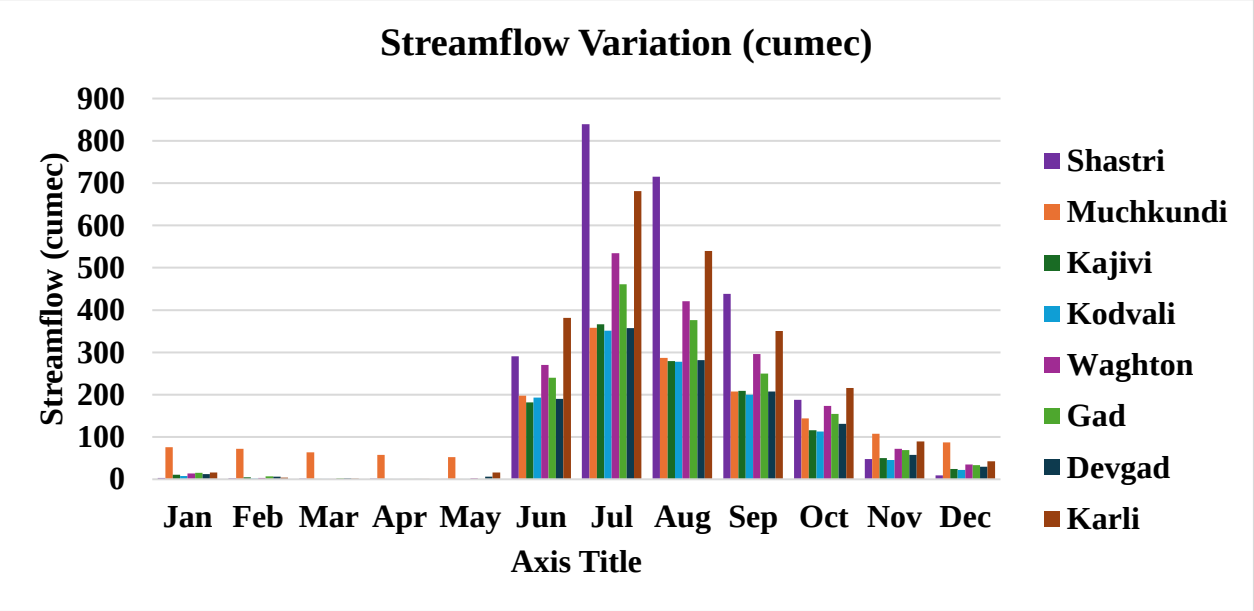

Fig 4.36 Monthly River flow(cumec) in Valley 24

Table 4.44 Available surface water potential in the river from selected locations in Valley 24

	Co-ordinate Location		
Basin	Long	Lat	Water availability (Mm3)
Shastri	73.2964	17.2830	4793.71
Muchkundi	73.3409	16.8044	914.64
Kajivi	73.3144	16.9612	1118.65
Kodvali	73.3577	16.6297	698.08
Waghton	73.3499	16.5378	1732.81
Gad	73.4696	16.1571	1942.05
Devgad	73.4044	16.4020	985.82
Karli	73.5001	16.0054	1371.09

Table No. 4.43 presents the analysis of the monthly mean river flow for each basin, while Fig. 4.36 shows the results. It shows significant variance over the course of the year. Increased water flow in rivers is noticeable in the rainy months of June, July, August, and September, mostly due to precipitation. River flow was the accumulation of the heavy monsoon. According to Fig. 4.36, river flow is maximum in July (3950 cumec) due to high rainfall received in the month, and lowest in April (64.7 cumec) due to high evapotranspiration rate across all basins. River flow typically peaks in June and July and then steadily declines until April throughout the analysis period. Total availability of valley 24 is about 13556.89 Mm^3 and basin wise availability is tabulated in Table 4.44 and Table 4.45 shows average volume parameters of valley

Table 4.45 Average annual volumes of parameter of basin in valley 24

Basin	Water Yield (mm)	Base flow(mm)	Surface Flow(mm)
Shastri	3315.88	1034.12	2098.40
Muchkundi	2745.81	1198.90	1175.94
Kajivi	3212.21	920.96	2205.69
Kodvali	2846.91	874.54	2097.58
Waghton	3064.35	977.57	1946.25
Gad	3452.45	458.56	2688.54
Devgad	3266.11	1132.05	1964.48
Karli	3443.18	974.40	2315.63

4.3.4.6 Estimation of basin-wise monthly surplus and deficit water availability.

The effective management of water resources during a lean period is dependent on annual water availability. The monthly surplus/deficit of water was calculated using rainfall and evapotranspiration, which are climatic water supply and demands. The methodology covered in section 3.7 was used to assess the monthly variation in water availability throughout the year. The results of the basin-wise monthly basis water surplus/deficit in Valley 24 are tabulated in Table 4.46.

Table 4.46 (a) Temporal variation of annual water surplus/deficit in Valley 24

Basin	Shastri			Muchkundi			Kajivi		
Months	PET	Rainfall	Sur/Def	PET	Rainfall	Sur/Def	PET	Rainfall	Sur/Def
Jan	89	0	-89	91	0	-91	80	0	-80
Feb	102	0	-102	102	0	-102	94	0	-94
Mar	135	0	-135	132	1	-131	125	0	-125
Apr	146	0	-146	139	1	-139	153	0	-153
May	142	0	-142	135	7	-127	154	2	-152
Jun	79	805	726	79	817	738	88	645	557
Jul	58	1293	1235	63	1275	1212	59	1178	1119
Aug	64	845	780	71	894	823	60	854	794
Sep	79	445	366	84	495	411	79	418	339
Oct	96	175	79	97	207	110	95	118	22
Nov	86	0	-85	88	3	-85	82	1	-82
Dec	81	0	-81	84	2	-82	78	0	-78

Table 4.46 (b) Temporal variation of annual water surplus/deficit in Valley 24

Basin	Kodvali			Waghton			Gad		
Months	PET	Rainfall	Sur/Def	PET	Rainfall	Sur/Def	PET	Rainfall	Sur/Def
Jan	111	0	-111	95	1	-94	89	0	-89
Feb	123	0	-123	107	0	-107	102	0	-102
Mar	157	0	-157	138	0	-138	136	0	-136
Apr	166	0	-166	147	1	-146	145	0	-145
May	161	0	-161	141	6	-135	140	5	-135
Jun	95	810	715	81	777	697	79	809	730
Jul	77	1231	1154	64	1182	1118	60	1268	1208
Aug	86	845	759	72	783	710	66	888	822
Sep	58	443	384	86	424	338	81	430	349
Oct	85	187	102	98	191	92	96	193	97
Nov	75	0	-75	88	2	-86	86	3	-83
Dec	70	0	-70	85	1	-84	81	0	-81

Table 4.46 (c) Temporal variation of annual water surplus/deficit in Valley 24

Basin	Devgad			Karli			Valley 24		
Months	PET	Rainfall	Sur/Def	PET	Rainfall	Sur/Def	PET	Rainfall	Sur/Def
Jan	84	0	-84	82	0	-82	90	0	-90
Feb	105	2	-103	102	0	-102	105	0	-104
Mar	138	2	-136	136	0	-136	137	0	-137
Apr	149	1	-148	145	3	-142	149	1	-148
May	132	13	-119	140	49	-91	143	10	-133
Jun	72	833	761	79	901	822	81	800	718

Jul	54	1279	1225	60	1329	1269	62	1254	1192
Aug	61	844	783	68	919	851	69	859	790
Sep	81	452	371	82	429	347	79	442	363
Oct	94	218	124	98	218	120	95	188	93
Nov	79	15	-64	82	0	-82	83	3	-80
Dec	75	12	-63	80	0	-80	79	2	-78

Table 4.46 indicates that the monthly water demand in the valley ranges from 60 mm to 149 mm. Water demand increases progressively from July to May, with April exhibiting the highest demand due to elevated temperatures and low humidity, and July showing the lowest demand. The region's annual rainfall is concentrated between June and October, resulting in the highest monthly water supply during this period, fluctuating from 0 mm to 1254 mm.

Based on the analysis in Table 4.46, which presents positive values for water surplus and negative values for water deficit, it is evident that the region experiences surplus water conditions from June to October, with significant surpluses in June and July. In contrast, from November to May, the region faces water deficits, with April and May experiencing the most pronounced shortages. During the peak rainfall months (July to October), there is an excess of approximately 1192 mm, whereas in April, the water shortage reaches up to 133 mm. A similar pattern of water surplus and deficit is observed across all basins within Valley 24.

The temporal variability of water balance components, including rainfall, evapotranspiration (ET), and runoff, was analysed over the course of the year to assess the monthly water surplus and deficit in the region. The monthly water balance components for Valley 24 are illustrated in Fig 4.37.

Evapotranspiration peaks during April and May and reaches its lowest point in July when the precipitation is at its highest peak. Due to high evapotranspiration during January to May and low precipitation these months are water deficit and form June to October evapotranspiration rate is lowest point and precipitation is highest which results surplus water during these months. This excess water availability during month of June to October have vast scope for water harvesting and construction of water storage structures as well as recharge structure at suitable site in region.

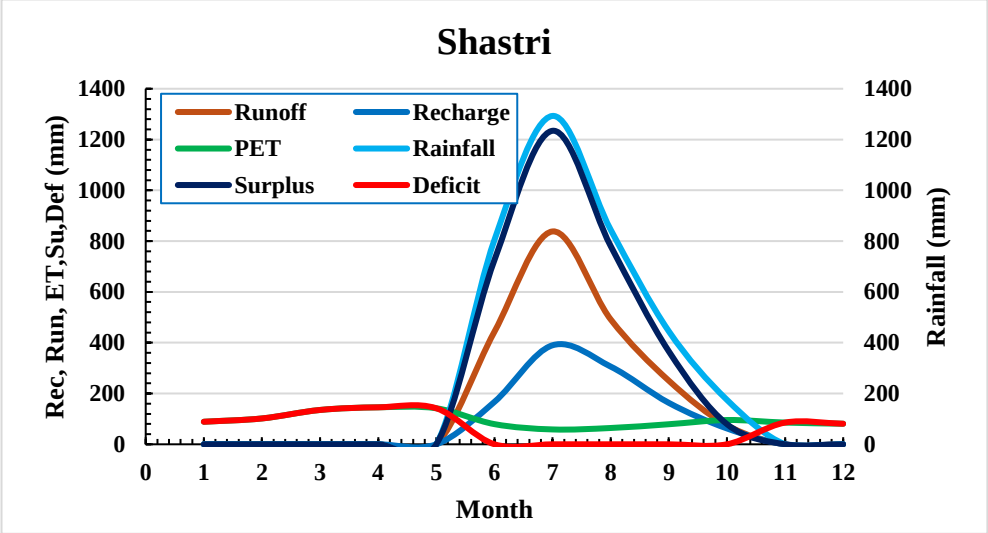
Shastri
Runoff
Recharge
PET
Rainfall
Surplus
Deficit
Rec, Run, ET,Su,Def (mm)
Rainfall (mm)
Month
0
200
400
600
800
1000
1200
1400
0 1 2 3 4 5 6 7 8 9 10 11 12

(a)

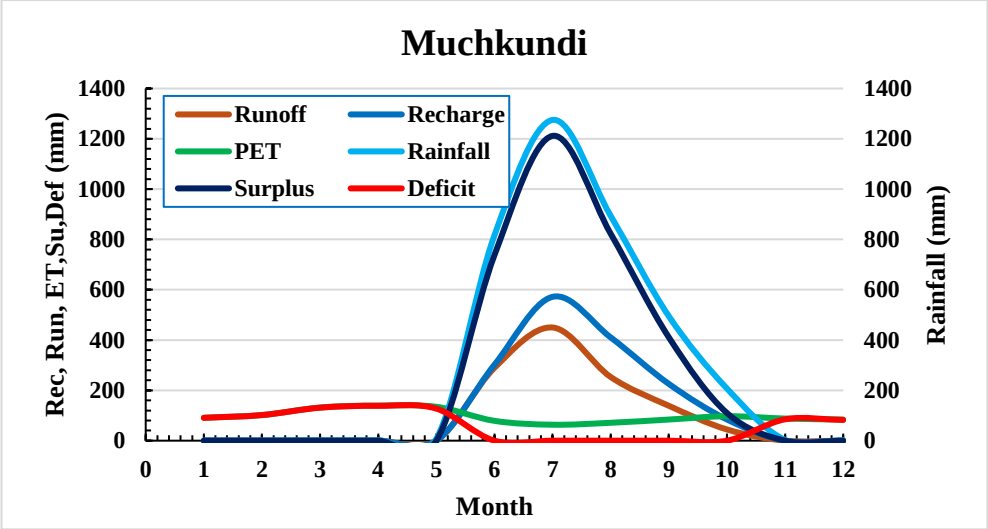
Muchkundi
Runoff
Recharge
PET
Rainfall
Surplus
Deficit
Rec, Run, ET,Su,Def (mm)
Rainfall (mm)
Month
0
200
400
600
800
1000
1200
1400
0 1 2 3 4 5 6 7 8 9 10 11 12

(b)

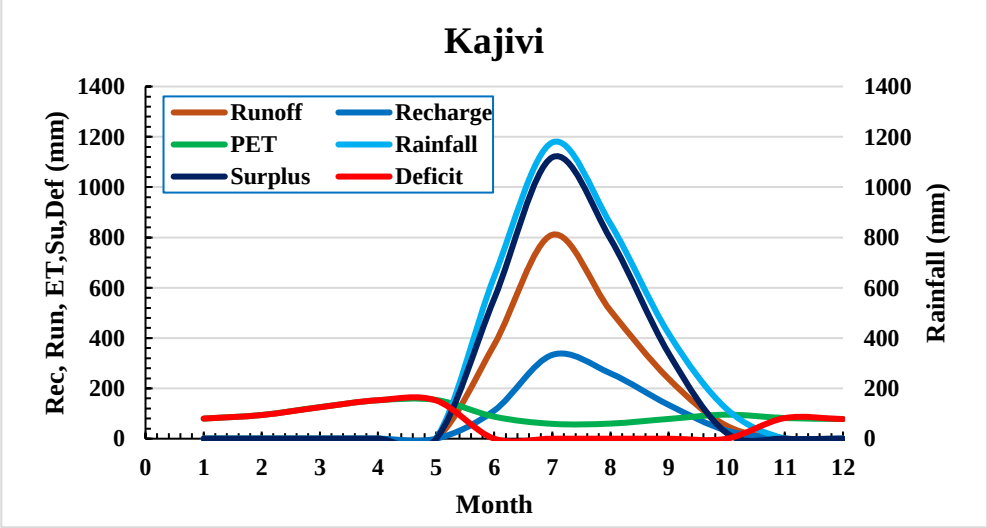
Kajivi
Runoff
Recharge
PET
Rainfall
Surplus
Deficit
Rec, Run, ET,Su,Def (mm)
Rainfall (mm)
Month
0
200
400
600
800
1000
1200
1400
0 1 2 3 4 5 6 7 8 9 10 11 12

(c)

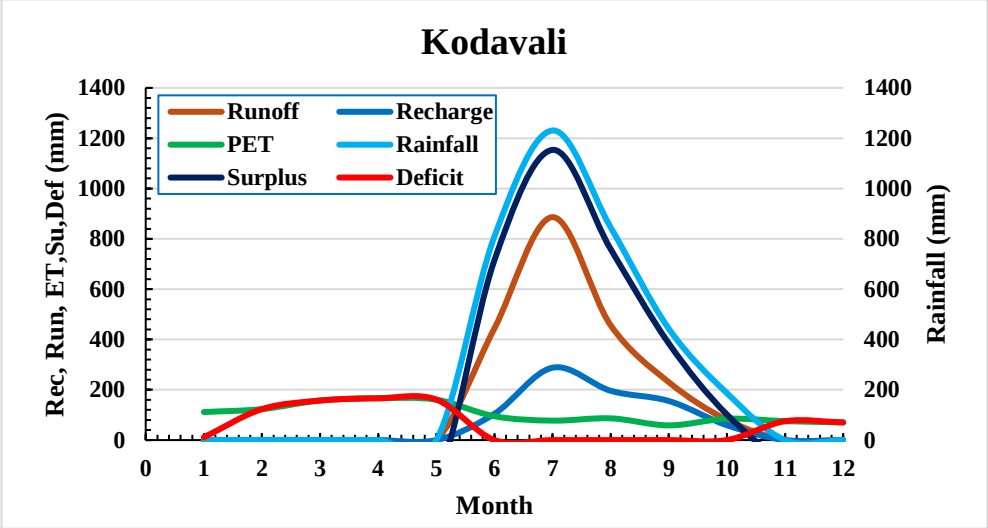
Kodavali
Runoff
Recharge
PET
Rainfall
Surplus
Deficit
Rec, Run, ET,Su,Def (mm)
Rainfall (mm)
Month
0
200
400
600
800
1000
1200
1400
0 1 2 3 4 5 6 7 8 9 10 11 12

(d)

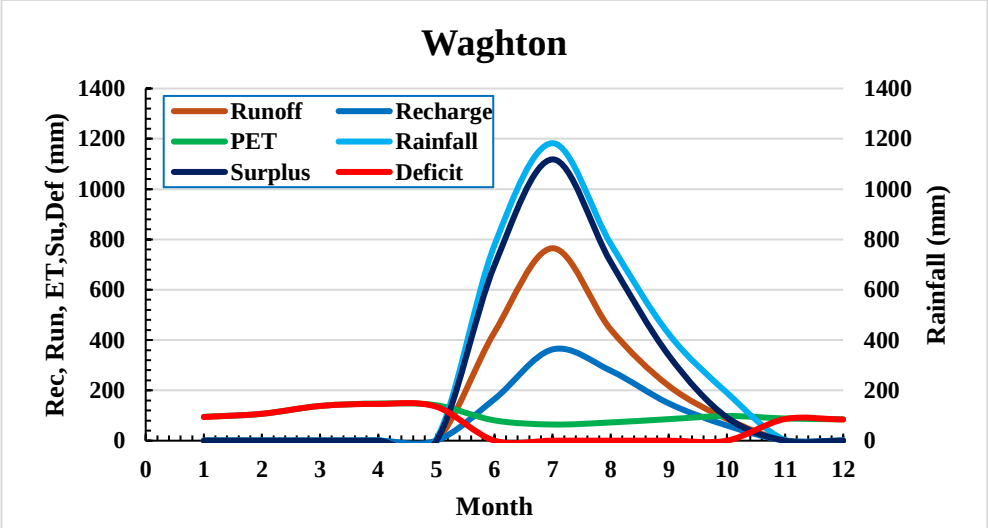
Waghton
Runoff
Recharge
PET
Rainfall
Surplus
Deficit
Rec, Run, ET,Su,Def (mm)
Rainfall (mm)
Month
0
200
400
600
800
1000
1200
1400
0 1 2 3 4 5 6 7 8 9 10 11 12

(e)

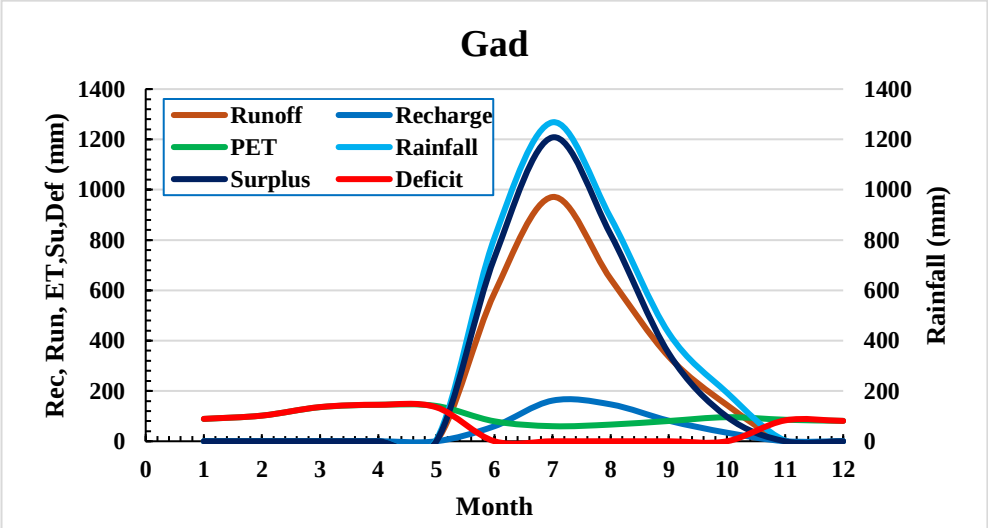
Gad
Runoff
Recharge
PET
Rainfall
Surplus
Deficit
Rec, Run, ET,Su,Def (mm)
Rainfall (mm)
Month
0
200
400
600
800
1000
1200
1400
0 1 2 3 4 5 6 7 8 9 10 11 12

(f)

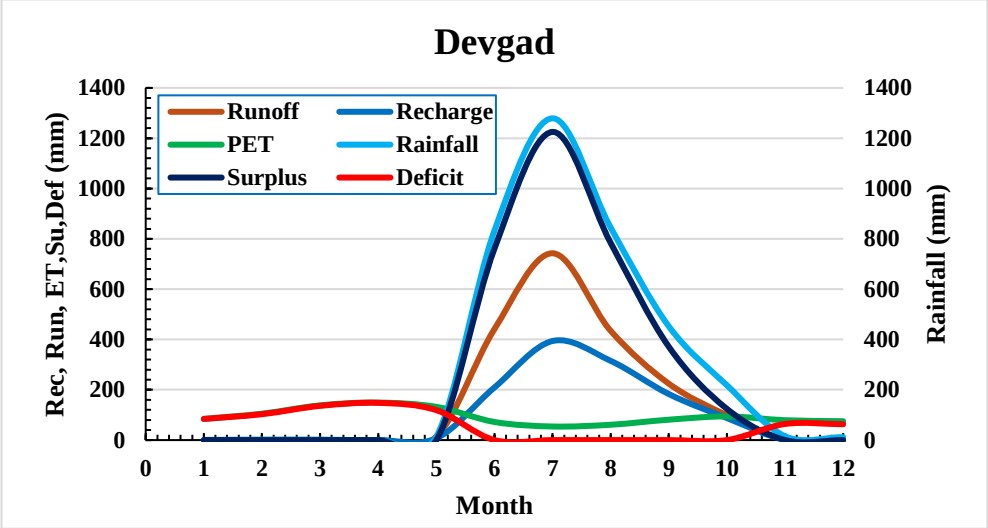

(g)

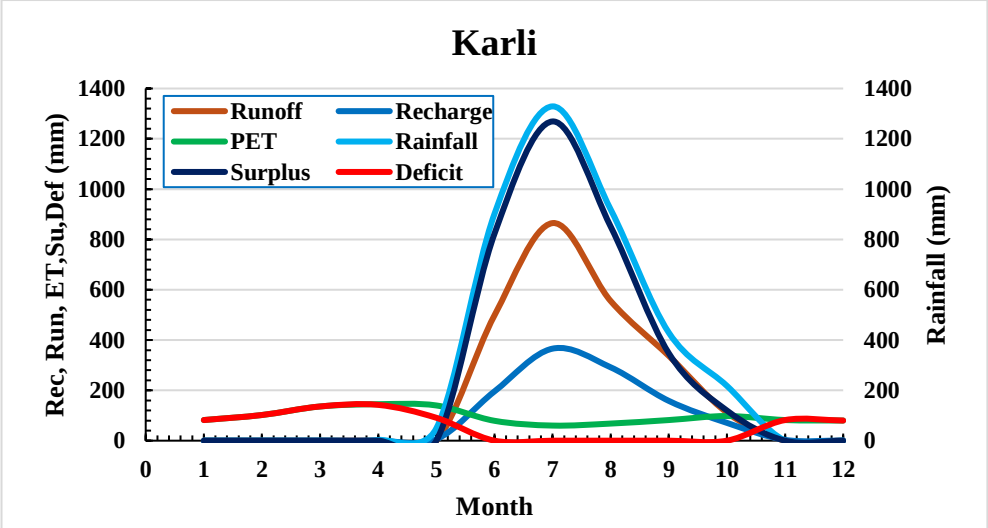

(h)

Fig 4.37 Temporal variation of water balance components of each river of valley 24

4.3.5 Assessment of surface water availability in Valley 25

Valley 25 is located in southern part of the Konkan region and comprised of two river basins namely Terekhol and Tillari. As outlet of Tillari river is in Goa and hydrometeorological data could not be made available therefore river is excluded from study. Total geographic area of valley is 1.47 Lakh ha out of Terekhol river occupies 761.5 km^2 and lies between East longitude of 73° 00’ to 74° 45’ and North latitude of 16° 5’ to 15° 40’. Terekhol river is subdivided into five subbasin having an outlet at subbasin no 5. Fig.4.38 illustrate basin area with subbasin and their outlet.

4.3.5.1 Land use/ Land cover of Valley 25

Land use land cover (LULC) data for the study was obtained from the Sentinel-2 satellite through the Living Atlas platform (https://livingatlas.arcgis.com/landcover/), with a spatial resolution of 10 meters as of April 15, 2024. The dataset was projected using the WGS 1984 UTM

Zone 43N coordinate system to ensure spatial consistency in raster analysis. LULC classification was performed, categorizing the land cover into five distinct classes: waterbodies, forest, urban areas, agricultural land, and barren land. The detailed areal distribution of these land cover classes is presented in Table 4.47, and the spatial representation is illustrated in Figure 4.39.

Table 4.47 Land use Land cover details of Valley 25

River	Classes	Waterbodies	Forest	Agriculture	Built-up	Barren Land
Terekhol	Area (km^2)	7.23	505.95	27.11	23.76	197.46
	Area (%)	0.95	66.44	3.56	3.12	25.93

The land use and land cover (LULC) analysis of the Terekhol River basin reveals a dominance of forested areas, covering 505.95 km² or 66.44% of the total area. This suggests that the basin is primarily characterized by dense vegetation, which plays a crucial role in maintaining the ecosystem's stability and regulating water resources. Waterbodies, though essential for hydrological processes, occupy a relatively small portion, covering only 7.23 km² or 0.95% of the area. Agricultural land accounts for 3.56% (27.11 km²), indicating limited agricultural activities in the basin. Built-up areas, representing urbanization, cover 23.76 km² or 3.12%, suggesting a moderate level of human settlement and infrastructure development. Barren land constitutes 25.93% (197.46 km²) of the basin, which may indicate areas unsuitable for vegetation or agriculture.

4.3.5.2 Soil type of Valley 25

The soil data for the study area were acquired in shapefile format at a scale of 1:50,000 from the FAO Soil Database. The data were reprojected into the WGS1984 UTM Zone 43N coordinate system using raster projection techniques. Additionally, the associated dBase file was obtained from the FAO Soil Database for further analysis.

Table 4.48 Areal distribution of soil texture in Valley 25

River	Soil Texture	Area (km^2)	Area (%)
Terekhol	Sandy clay loam	726.937	95.46
	Sandy Loam	34.5726	4.54

The soil texture analysis of the Terekhol River basin shows that the majority of the area, 95.46% (726.94 km²), consists of sandy clay loam, which supports moderate water retention and agricultural potential. A smaller portion, 4.54% (34.57 km²), comprises sandy loam, characterized by good drainage but lower water retention capacity. Spatial distribution of soil texture of Terekhol river is shown in Fig. 4.40

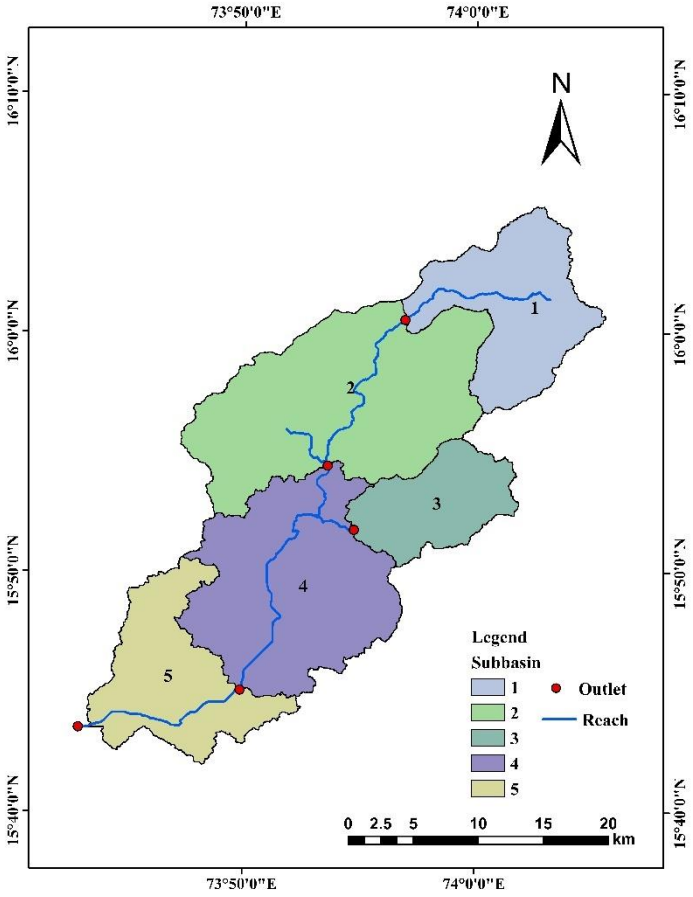

Fig.4.38 Subbasin map of river basin in Valley 25

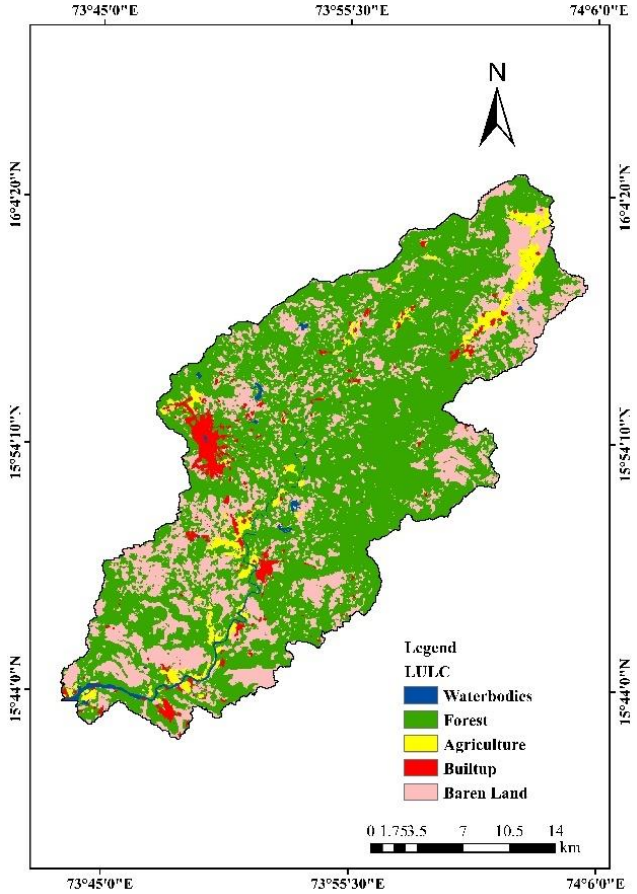

Fig.4.39 Land use land cover (LULC) distribution in Valley 25

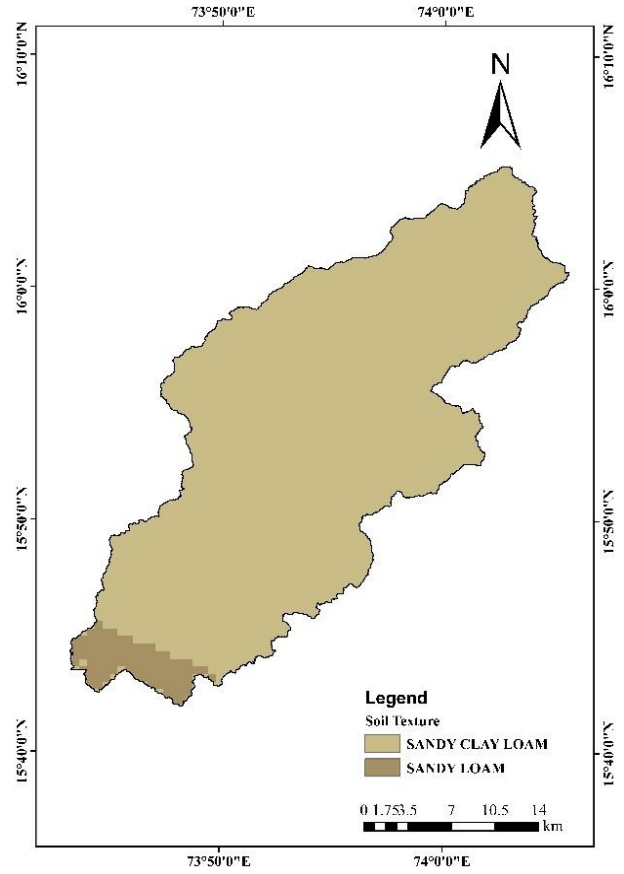

Fig. 4.40 Areal distribution of soil texture in Valley 25

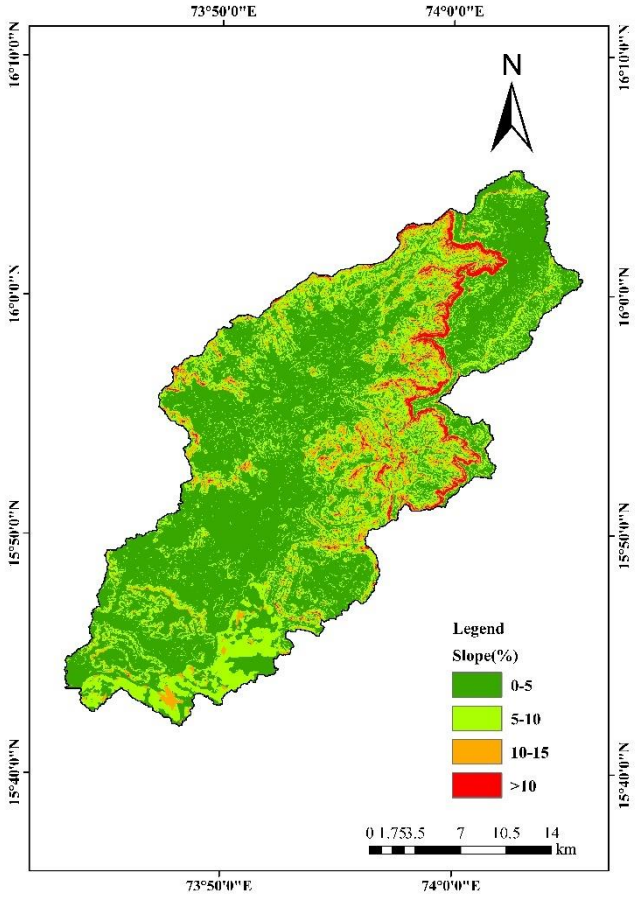

Fig 4.41 Spatial distribution map of Slope categories in Valley 25

4.3.5.3 Topographic details of valley 25

The slopes are generally steep along the ridgelines and gradually decrease in steepness toward the main river channels. To understand area under different zones it classified into three class as storage zone (0-5%), recharge zone (5-10%), runoff zone (>10%). Table 4.49 provide details of area under each category and illustrate in Fig.4.41

Table 4.49 Topographic details of Valley 25

River basins	Area Distribution (km^2)	Storage Zone	Recharge Zone	Runoff Zone
		(0-5%)	(5-10%)	(>10%)
Terekhol	Area (km2)	475.1	190.2	83.4
	Area (%)	63.5	25.4	11.1

Terekhol River basin is predominantly characterized by storage zones (0-5% slope), covering 63.5% (475.1 km²), which suggests significant potential for water retention and groundwater recharge. Recharge zones (5-10% slope) account for 25.4% (190.2 km²), indicating areas where water infiltration is moderate. Runoff zones, with slopes exceeding 10%, cover 11.1% (83.4 km²), contributing to higher surface runoff.

4.3.5.4 Climatic condition of Valley 25

The climatic parameters of Valley 25, including rainfall, minimum and maximum temperatures, relative humidity, and wind speed, were obtained from HDUG, Nashik. The dataset spans 29 years, from 1991 to 2019, and covers five meteorological stations (details provided in Annexure I).

Valley 25 experiences a predominantly monsoonal climate, characterized by heavy rainfall concentrated between June and October, with July recording the highest precipitation levels. The region's average annual rainfall is approximately 4542 mm. Temperature variations throughout the year range from a minimum of 19°C during the winter months to a maximum of 37°C during the summer. The summer months exhibit the highest temperatures, while winter months are considerably cooler. Relative humidity in Valley 25 also varies seasonally, with the lowest values observed during the summer months (around 49%) and the highest values, reaching up to 90%, occurring during the monsoon season. Wind speeds in the region fluctuate between 2 m/s and 5 m/s, with further details available in Annexure II.

4.3.3.5 Estimation of surface water resource availability

4.3.3.5.1 Calibration and Validation of model

The Arc-SWAT Model was calibrated, validated and applied to river basin to evaluate surface water availability along with their seasonal variations. Model is calibrated and validated with help of SWAT-CUP SUFI2 program as described in chapter 3 section 3.5.3. SWAT model was calibrated having an outlet of meteorological stations of Water Resource Department, (Surface

Water) Government of Maharashtra. Simulation was started from 1991 with 3 years of model warmup period and output of simulation was available for 25 years from 1994 to 2019. Streamflow data is calibrated and validated at HDUG meteorological station Sarambala for river basin in Valley 25. Performance evaluation criteria are found satisfactory and tabulated in Table 4.50 and shown in Fig. 4.42. Details of calibration parameter are mentioned in Appendix IV

Table 4.50 Performance criteria of simulated data for Valley 25

	Calibration					Validation				
Basin	Year	NSE	R^2	PBIAS	RSR	Year	NSE	R^2	PBIAS	RSR
Terekhol	1996-1999	0.68	0.68	-2.83	0.33	2000-2003	0.68	0.68	-2.67	0.45

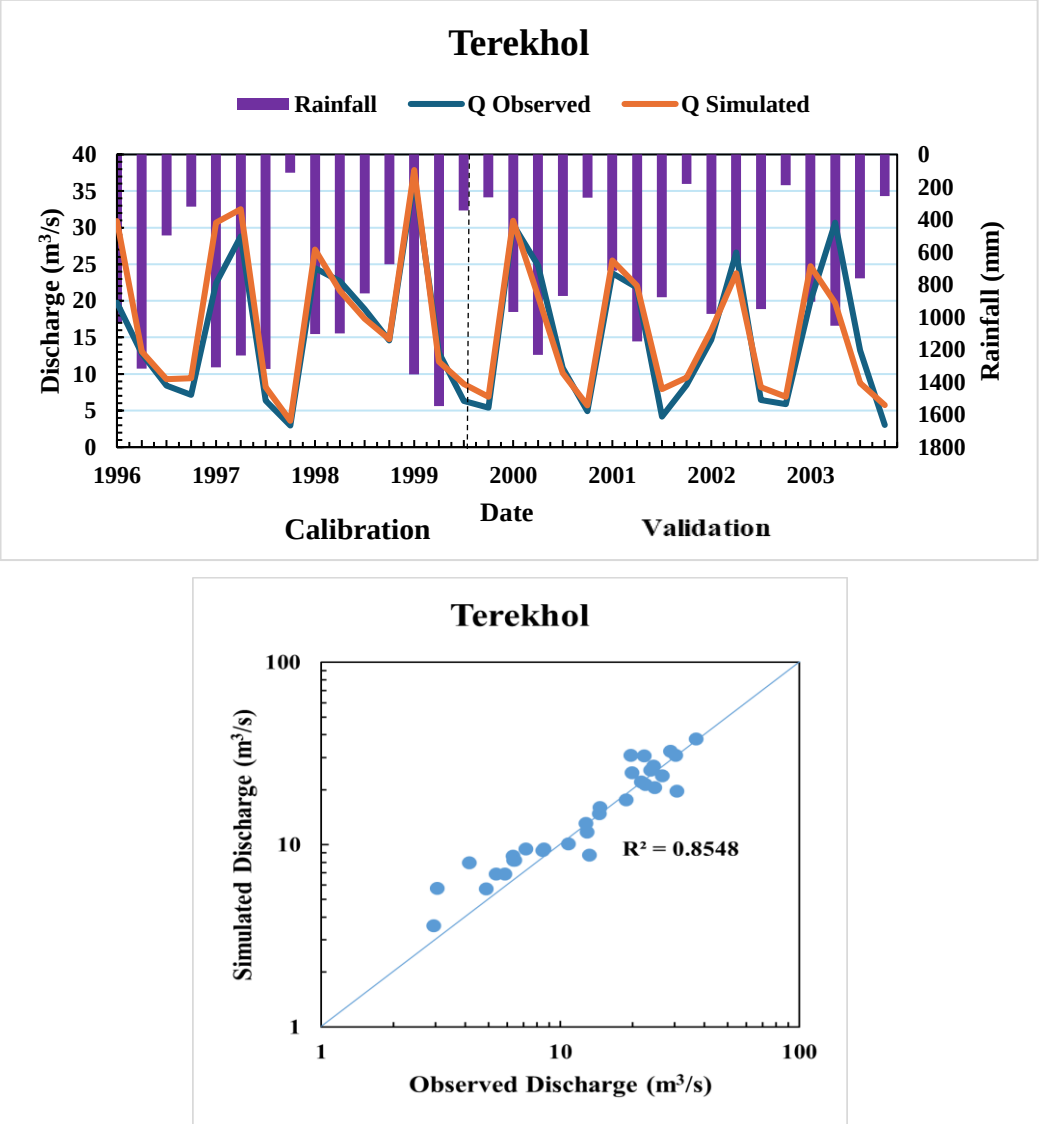

Fig. 4.42 Monthly observed and simulated streamflow over a period 1994-2005 (a. seasonal variation, b. scatter plot)

4.3.3.5.2 Sub-basin wise monthly river flow availability

The Arc-SWAT Model was calibrated, validated and applied to river basin to evaluate surface water availability along with their seasonal variations. Prior to its application in the basin, the model underwent calibration and validation processes. The first analysis obtained after running the SWAT model was the river flow availability of river basins which is extracted from output file as a Flow_out parameter.

Table No 4.51 Monthly River flow variation in Valley 25

Months	Jan	Feb	Mar	Apr	May	Jun	Jul	Aug	Sep	Oct	Nov	Dec
Terekhol	8.6	2.0	0.9	0.6	0.8	235.4	433.5	343.9	213.4	121.2	47.8	23.2

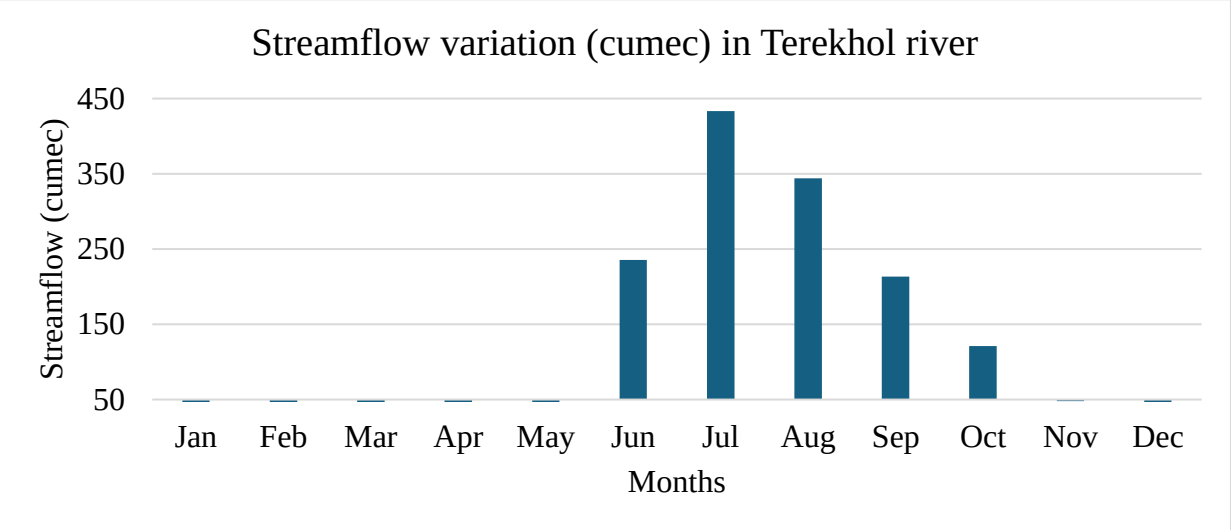

Fig 4.43 Monthly River flow(cumec) in Valley 25

Table 4.52 Available surface water potential in the river from selected locations

	Co-ordinate Location		
Basin	Long	Lat	Water availability (Mm^3)
Terekhol	73.4864	15.7609	2168.48

The monthly river flow data for Terekhol River in Valley 25 shows significant seasonal variation, indicating a clear response to the regional monsoon. During the dry months from January to May, river flows remain extremely low, ranging from 0.6 m^3/s to 8.6 m^3/s, reflecting minimal precipitation and dry conditions. However, starting in June, with the onset of the monsoon, flows increase sharply, peaking in July at 433.5 m^3/s. The flow decreases gradually from August (343.9 m^3/s) to December (23.2 m^3/s). This pattern highlights the region's reliance on monsoon rainfall for surface water availability, with notable discharge during the wet season as shown in Table .4.51. Total water availability of Terekhol river is 2168.48 Mm^3.

Table 4.53 Average annual volumes of parameter basin in valley 25

Basin	Water Yield (mm)	Base flow(mm)	Surface Flow(mm)
Terekhol	4124.96	1313.49	2612.43

4.3.3.6 Estimation of basin-wise monthly surplus and deficit water availability

Annual water availability plays an important role for effective water resource management during lean period. Monthly water surplus/deficit was carried out by using climatic water supply (rainfall) and climatic water demand (evapotranspiration). Monthly water availability variation in the year was evaluated based on methodology discussed in section 3.7 Results of basin wise on monthly basis water surplus/deficit in Valley 25 are presented in Table 4.54

Table 4.54 Temporal variation of annual water surplus/deficit in Valley 25

Basin	Terekhol		
Months	PET (mm)	Rainfall (mm)	Sur/Def (mm)
Jan	85	0	-84
Feb	103	0	-103
Mar	137	0	-137
Apr	146	2	-144
May	137	29	-108
Jun	77	1003	926
Jul	58	1543	1485
Aug	65	1161	1095
Sep	81	533	451
Oct	96	237	141
Nov	82	12	-70
Dec	79	1	-78

Note: RF = Rainfall in mm, PET = Potential evapotranspiration in mm Sur = Surplus

Def = deficit

The temporal variation of annual water surplus/deficit in the Terekhol Basin of Valley 25 reveals a strong correlation between rainfall and water balance. From January to May, the basin experiences a significant water deficit, as Potential Evapotranspiration (PET) exceeds rainfall by large margins. The deficit ranges from -84 mm in January to -144 mm in April, with no or minimal rainfall.

However, with the onset of the monsoon in June, the water balance shifts dramatically. Rainfall far surpasses PET, resulting in a surplus of 926 mm in June and peaking in July with a surplus of 1,485 mm. This surplus continues through August (1,095 mm) and gradually declines in September and October, as rainfall decreases but still remains higher than PET. By November

and December, the basin returns to a deficit state as monsoon rains cease, leaving a minimal or negative water balance. This cycle emphasizes the basin's heavy reliance on monsoonal precipitation for water surplus.

The temporal variability of water balance components, including rainfall, evapotranspiration (ET), runoff was analysed throughout the year to evaluate the monthly surplus and deficit water availability in the region. Monthly water balance components of Valley 25 are illustrated in Fig. 4.44

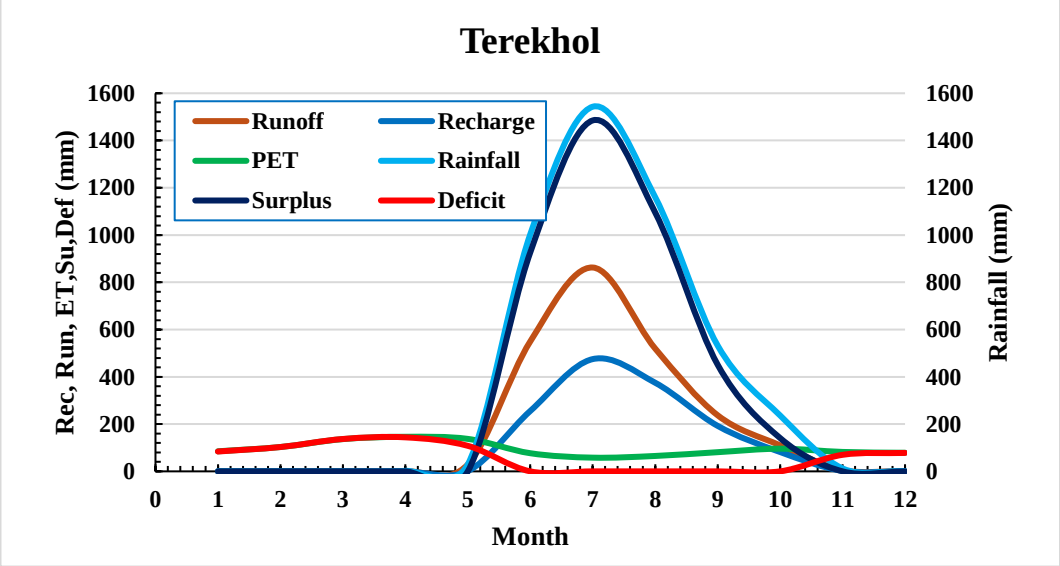

Fig 4.44 Temporal variation of water balance components of valley 25

Fig. 4.44 illustrates the variation of all water balance components throughout the year across all districts in Konkan region. Evapotranspiration peaks during April and May and reaches its lowest point in July when the precipitation is at its highest peak. Due to high evapotranspiration during January to May and low precipitation these months are water deficit and form June to October evapotranspiration rate is lowest point and precipitation is highest which results surplus water during these months.

4.3.7 Estimation of valley- wise annual total surface water availability

The analysis of water availability across the valleys highlights significant spatial variability in resource distribution within the study area. Valley 21 exhibits the highest water availability at 17,346.28 Mm^3, indicating a potentially abundant surface water resource. In contrast, Valley 25 records the lowest availability, at 3,768.48 Mm^3, underscoring localized limitations that may reflect differences in precipitation, catchment characteristics, or land use patterns. Valley 24 and Valley 22 show intermediate levels of water availability, at 13,556.85 Mm^3 and 11,476.85 Mm^3, respectively, suggesting moderately favourable hydrological conditions. Meanwhile, Valley 23, with an availability of 4,997.50 Mm^3, represents another area of relatively limited resources. This distribution underscores the need for tailored water management strategies that account for the

heterogeneous nature of water availability across the valleys, emphasizing efficient allocation and sustainable use, particularly in regions with lower water availability

4.3.7 Estimation of district- wise monthly surplus and deficit water availability

The temporal variability of water balance components, including rainfall, evapotranspiration (ET), runoff and recharge, was analysed throughout the year for each district to evaluate surplus and deficit water condition in the region. The monthly water balance components are illustrated in Fig. 4.45 (a to e).

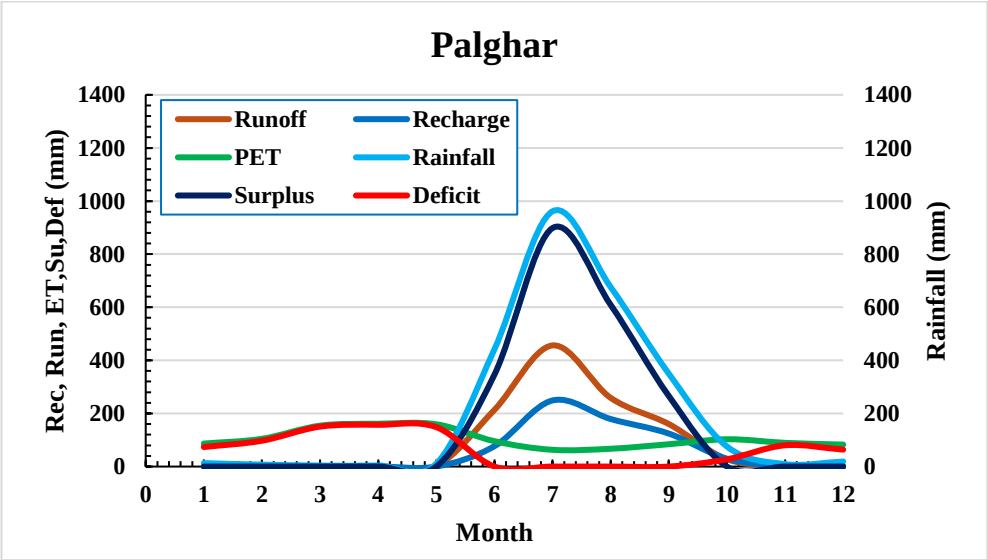

(a)

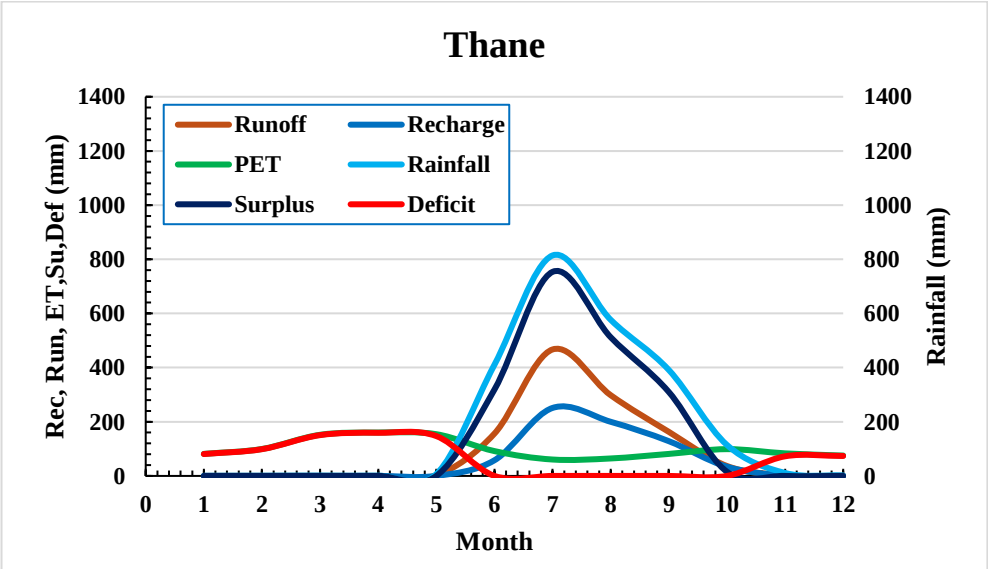

(b)

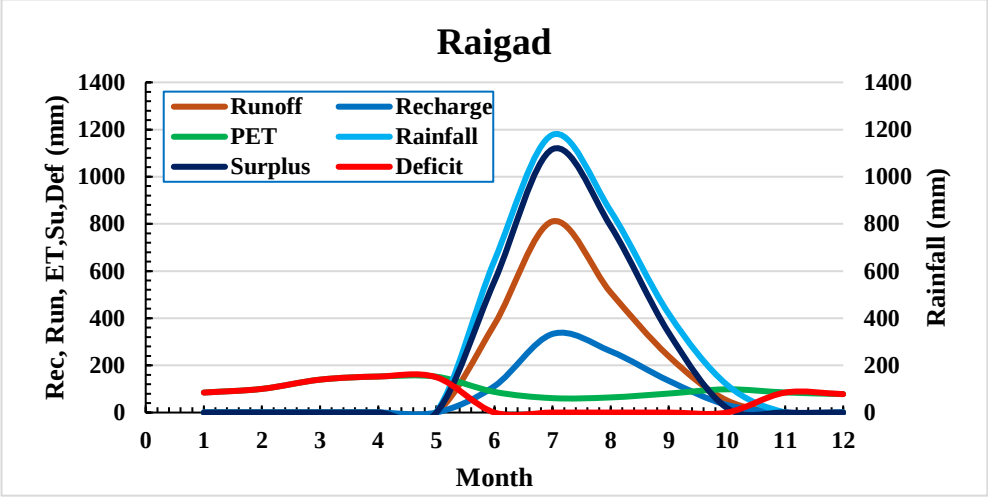

(c)

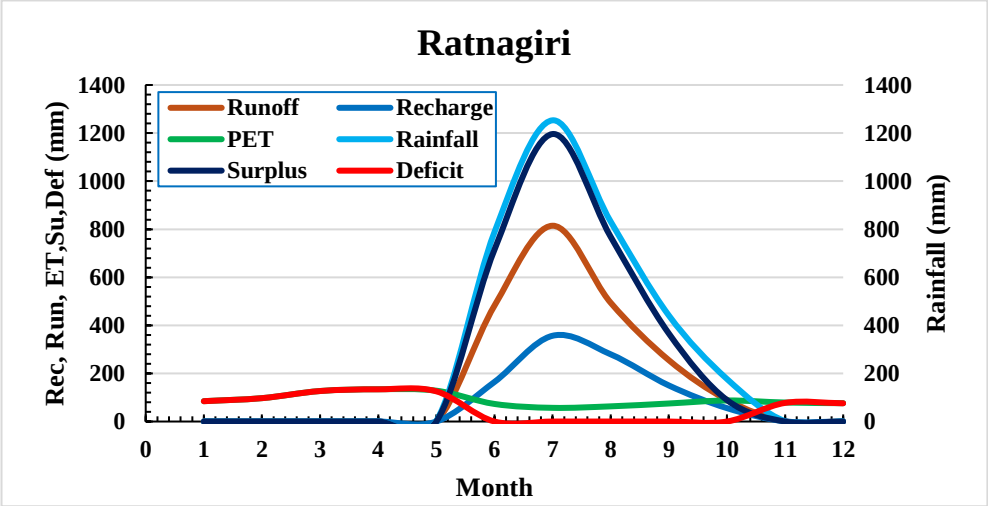

(d)

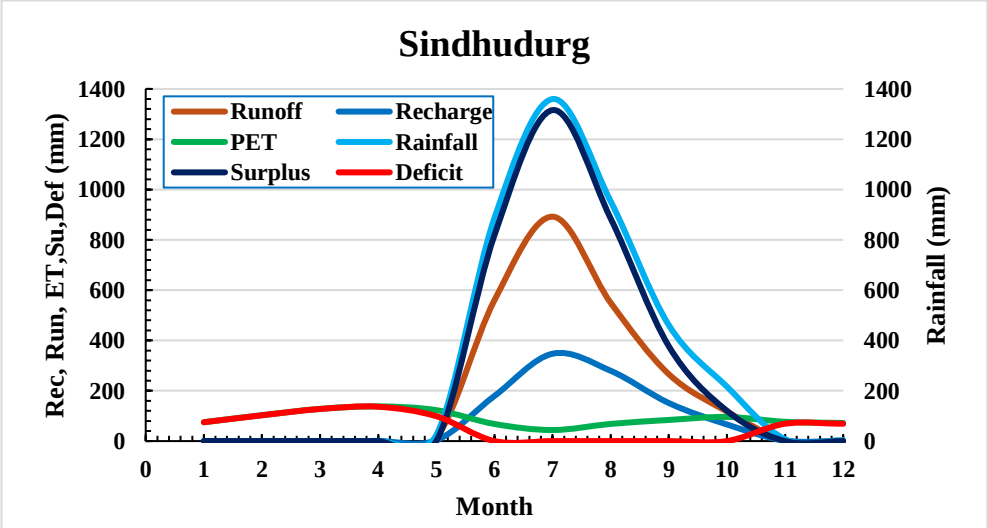

(e)

Fig.4.45 Temporal variation of water balance components across all districts of Konkan region

Fig. 4.45 illustrates the variation of all water balance components throughout the year across all districts in Konkan region. Evapotranspiration peaks during April and May and reaches its lowest point in July when the precipitation is at its highest peak. Groundwater recharge begins in June, peaks in July and then gradually decreases. Runoff follows a similar pattern to rainfall. This trend is consistent across all districts. To quantify the annual surplus and deficit water condition due, the annual water balance components, for all districts in the Konkan region are presented in Table 4.55.

Table 4.55 Annual water balance components and recharge with its share of rainfall across all districts in Konkan

	Annual water balance component				
District	Rainfall(mm)	ET (mm)	Runoff(mm)	Recharge	Surplus/Deficit
Palghar	2571	1250	1130	660	1321
Thane	2329	1202	1126	672	1127
Raigad	3215	1184	1983	872	2031
Ratnagiri	3496	1083	2138	1008	2413
Sindhudurg	3914	1076	2406	1030	2838

The results from Table 4.55 indicate that the Konkan region receives an annual average rainfall ranging from 2571 to 3914 mm, with a decreasing trend from Southern to Northern districts. Between 25 to 50% of this annual rainfall is lost through evapotranspiration, with the highest value observed in Palghar district and the lowest in Sindhudurg district. Surplus and deficit water condition also varies across the region due to multiple influencing factors. In Palghar district, annual surplus water was estimated 1321mm. The highest water surplus condition was observed in Sindhudurg (2838 mm), followed by Ratnagiri district (2413 mm. While these annual surplus water condition values provide an overview at the district level, it is important to identify areas amount of surplus water and how to conserved it to fulfil demands during lean season. This allows for strategic planning and prioritization of water harvesting and conservation effects.

CHAPTER V: SUMMARY AND CONCLUSION

This chapter summarizes the study carried out for assessment of the surface water availability in river basins of the Konkan region, study of different methods used for assessment and impact of parameters like soil, land use, and slope on temporal and spatial variability of water in river basins of the Konkan region.

5.1 Summary

Water is at the core of sustainable development and is critical for socioeconomic development and the necessity for life, agriculture, healthy ecosystems, and human survival. Adequate water in both quantity and quality underpins health and basic quality of life. Effective assessment of surface water resources is critical for sustainable water management, particularly considering increasing global water demand due to population growth, urbanization, and agricultural and industrial expansion. The entire Konkan region relies heavily on monsoon for its water supply. Surface runoff generated by this precipitation serves as the primary source for agricultural activities as well as sustainable development. Numerous researchers have noted significant shifts in precipitation patterns, with recent year witnessing an increase in intensity but a decrease in duration, while overall precipitation remains constant. This phenomenon leads to both flooding and water scarcity during summer even for drinking water. Variation in climatic parameters affects availability of both annual and intra-annual water resources in region. To address the anticipated challenges related to water resource availability, basin-scale assessment is imperative.

The Konkan region, a narrow coastal plain along the Arabian Sea, extends 720 km from the Daman Ganga River in the north to the Terekhol River in the south, spanning 16°30′–19°30′N latitude and 72°00′–75°00′E longitude in western Maharashtra. Covering 3.08 Mha (10% of the state's area), it comprises hills, plateaus, and plains. The Sahyadri Mountains form a distinct eastern boundary with a steep west-facing escarpment. Agro-climatically, Konkan is a high-rainfall zone (2500–3500 mm) with varied soils: medium black soils with low infiltration in the north and lateritic soils with high infiltration in the south. The northern region includes basins like Ulhas, Vaitarna, and Patalganga (Valley 21). Raigad features Kundalika and Savitri basins (Valley 22), while Ratnagiri contains the Vashishti Basin and sub-basins like Shastri and Muchkundi (Valleys 23–24). Southern Sindhudurg encompasses rivers like Karli and Terekhol within Valley 25.

In this study, the primary task was to study the different methods used for assessment of surface water availability, followed by studying impact of parameters like soil, land use, and slope on temporal and spatial variability of water. The third task involved estimating total surface water availability as well as surplus and deficit water spatially and temporarily. Various methodologies

are utilized to measure, model, and analyse surface water availability, each with distinct applications, advantages, and limitations.

Direct measurement methods, such as the timed-volume and dilution gauging techniques, offer accurate, cost-effective solutions for small streams but are limited in scale and duration. Velocity-area methods, including float and current meter techniques, are widely used for streamflow estimation and provide reliable results in turbulent conditions, though they require specialized equipment. Formed constriction methods, such as weirs and flumes, accurately measure discharge in small to medium-sized streams but can disrupt ecosystems and are sensitive to site-specific factors. Rainfall-runoff models, including Cook's Method, the Rational Method, and the Curve Number (CN) Method, are essential for runoff estimation in watersheds. Cook's Method is a simple empirical approach, though it lacks accuracy when applied outside its region of origin. The Rational Method, suitable for small watersheds, is limited by its assumption of constant rainfall intensity.

The CN Method is widely used due to its simplicity and integration with Geographic Information Systems (GIS), though its performance declines in larger watersheds. The Unit Hydrograph (UH) method effectively predicts runoff hydrographs for rainfall events, making it valuable for flood forecasting in small to medium-sized watersheds. Hydrological models, such as SWAT, HEC-HMS, and MIKE SHE, simulate water movement and storage across watersheds, integrating GIS data for enhanced analysis. SWAT is particularly effective for long-term simulation of both surface and groundwater dynamics and is widely used to assess watershed responses to land-use and climate changes, especially in agricultural regions.

Impact of slope, soil and land use on temporal and spatial variability of water availability. Additionally, suitable areas for the implementation of water conservation structures are identified. It was done using different thematic factors such as slope, soil texture, geomorphology, lineament density, rainfall, drainage density, land use land cover and runoff depth. Out of these factors, the majority of data are easily available in different open access platforms concerning government departments. The Analytical Hierarchy Approach (AHP) model was implemented for identifying suitability areas. The integration of thematic maps is crucial in identifying water retention suitability zones and was done using the weighted sum method in the spatial analyst tool. Each parameter within the thematic maps was ranked and assigned weights based on their influence characteristics. This approach helped determine the water retention suitability zones within the study area based on these factors. Land use land cover was given a weight of 17%, slope 19%, lineament density 7%, rainfall 18%, soil texture 12%, runoff depth 10%, drainage density 10% and geomorphology 7%. The water retention suitability map was divided into four categories: 'Highly suitable', 'Moderately suitable', 'less suitable', and 'not suitable'. To study the impact of

change in LULC on variability of water retention suitability area used Land use land cover of year 2017 and 2019. In 2017 Highly suitable area was found to be 11.45%, moderately suitable found to be 30.32%, less suitable found to be 36.65% and not suitable is found to be 21.57%. Due increase in baren land and decrease in forest area highly suitable area is become 12.63%, moderately suitable area become 31.98%, less suitable area decreases to 35.71% and not suitable area increase to 19.68%.

The water and resource analysis were conducted to measure the availability of surface water in river basins of Konkan region. Historical data pertaining to rainfall, maximum/minimum temperature, relative humidity and wind speed were collected from the 93 meteorological stations from the water resource department, Hydrological Project (Surface water), Nashik, Government of Maharashtra. Assessment of surface water availability was conducted using ArcSWAT model. The model underwent calibration and validation process utilizing the SWAT-CUP SUFI2 algorithm to evaluate monthly water resource availability in the basin.

The study of the water balance in each basin, utilizing ArcSWAT simulation output, revealed significant variability in monthly river flow influenced by weather and land use/ land cover characteristics. Basin wise water resource availability was assessed from 1991 to 2019, with results indicating high surface runoff due to monsoon rainfall. Understanding, these dynamics is crucial for water management, as depicted assessment of various water balance components. Potential evapotranspiration showed seasonal variation, inversely related to rainy days. Average monthly river flow in river basin was highted in the month of July followed by August, June, September, October and thereafter river flow showed declined trend up to April month.

The assessment of total water availability in various valleys revealed significant variation, with the highest availability in Valley 21, followed by Valleys 24, 22, 23, and 25. Both monthly and annual patterns of water surplus and deficit were analysed. The climatic water demand was found to range from 58 to 160 mm, while climatic water supply varied from 0 to 1231 mm, with the highest availability during the rainy season. The analysis indicated a water surplus from June to October, peaking in July, and a water deficit from November to April, with the most severe shortage occurring in April.

A district-wise analysis of annual surplus and deficit conditions showed that Palghar district had an annual water surplus of 1321 mm. The highest surplus was observed in Sindhudurg (2838 mm), followed by Ratnagiri (2413 mm). While these figures provide a broad overview at the district level, it is crucial to identify specific areas with surplus water and develop conservation strategies to meet demand during the dry season.

5.2 Conclusion

1. Various methods for surface water assessment are studied, including direct method, Velocity- area method, rainfall-runoff methods, formed construction method, as well as non- contact method. Among this SWAT model was selected for its ability to simulates surface water availability across the Konkan regions river basins as it is identifying critical hydrological pattern across study area.
2. The Analytical Hierarchy Approach (AHP) model was implemented for identifying suitability areas. This approach helped determine the water retention suitability zones within the study area based on factors affecting. The analysis revealed that in 2017, 11.45% of the area was highly suitable for water retention, 30.32% moderately suitable, 36.65% less suitable, and 21.57% not suitable. By 2019, due to increased barren land and decreased forest cover, highly suitable areas rose to 12.63%, moderately suitable to 31.98%, while less suitable areas decreased to 35.71% and not suitable to 19.68%. Urbanization, particularly in Thane, further reduced groundwater recharge.
3. The SWAT model was calibrated and validated with high accuracy for predicting streamflow and surface water availability in the study area. The model outputs suggest its reliability for planning water resource management and future studies on water availability.
4. River flow dynamics, with increases from June to July and decreases till April, highlighting the challenges in managing water resources in seasonally fluctuating environment.
5. Evapotranspiration reaches its peak during April and May, coinciding with low precipitation, resulting in a water deficit from January to May. Conversely, from June to October, evapotranspiration decreases significantly while precipitation peaks, leading to surplus water during these months. This inverse relationship between evapotranspiration and precipitation highlights the critical role of seasonal climatic patterns in influencing water availability in the region.
6. Sindhudurg district recorded the highest annual water surplus (2838 mm), followed by Ratnagiri (2413 mm) and Palghar (1321 mm). Identifying surplus zones is essential for developing strategies to store water for use during lean seasons. The study highlighted the need for water conservation structures in high runoff zones, particularly in districts with lower infiltration capacities. Strategic placement of these structures in flat storage zones can help balance seasonal water availability.

The study underscores the critical role of hydrological modelling and suitability analysis in managing water resources in the Konkan region. The calibrated SWAT model reliably predicted streamflow dynamics, revealing seasonal water surplus and deficit patterns. AHP analysis highlighted land-use changes impacting water retention, emphasizing the need for targeted conservation structures in high-runoff zones.

CHAPTER VI: BIBLIOGRAPHY

Abed, Basim. 2021 Flow Measurements in Open Channels Using Integrating-Floats . Journal of Engineering. 27. 10.31026/j.eng.2021.01.09.

Abushandi E. H., 2011. Rainfall Runoff Modelling in Arid Areas. Ph. D. Thesis, Faculty for Geosciences, Geo-technique and Mining of the Technische University Bergakademie Freiberg, Germany.

Adeogun, Adeniyi & Mohammed, Abdulrasaq. (2019). Review of Methods of Measuring Streamflow Using Hydraulic Structures. 10.5772/intechopen.82342.

Adrian RJ, Westerweel J (2011) Particle image velocimetry (vol 30). Cambridge University Press, Cambridge

Agarwal, E.; Agarwal, R.; Garg, R.D. and Garg, P.K. 2013. Delineation of groundwater potential zone: an AHP/ANP approach. Journal of Earth System Science. 122: 887-898.

Andualem, T.G. and Demeke, G.G. 2019. Groundwater potential assessment using GIS and remote sensing: a case study of Guna tana landscape, upper Blue Nile basin, Ethiopia. Journal of Hydrology: Regional Studies. 24. 100610.

Aneseyee, A.B.; Soromessa, T. and Elias, E. 2020. The effect of land use/land cover changes on ecosystem services valuation of Winike watershed, Omo Gibe basin, Ethiopia. Human and Ecological Risk Assessment: An International Journal. 26 (10): 2608-2627. https://doi.org/10.1080/10807039.2019.1675139

Anonymous, 2003. Design manual - Geo-hydrology (Vol. 4). Hydrology Project. Govt of India and Govt of The Netherlands.

Arnold J. G., Moriasi D. N., Gassman P. W., Abbaspour K. C., White M. J., Srinivasan R., Santhi C., Harmel R. D., Griensven A., Van Liew M. W., Kannan N., Jha M. K. 2012. SWAT: Model use, Calibration and Validation. Transactions of the ASABE, Vol. 55 (4): 1491-1508.

Arnold J. G., Moriasi D. N., Gassman P. W., Abbaspour K. C., White M. J., Srinivasan R., Santhi C., Harmel R. D., Griensven A., Van Liew M. W., Kannan N., Jha M. K. 2012. SWAT: Model use, Calibration and Validation. Transactions of the ASABE, Vol. 55 (4): 1491-1508.

Arnold J. G., Muttiah R. S., Srinivasan R. and Allen P. M. 2000. Regional estimation of base flow and groundwater recharge in the upper Mississippi basin. J. Hydrol. Vol. 227 (1-4): 21-40

Arnold J. G., Srinivasan R., Muttiah R. S., and Williams J. R. 1998. Large-area Hydrologic modelling and assessment: Part I. Model development. J. Am. Water Resour. Assoc. Vol. 34 (1): 73-89.

Arnold J. G., Williams J. R., Griggs R. H., and Sammons, N. B. 1990. SWRRBWQ – A basin scale model for assessing management impacts on water quality. USDA Agric. Res. Service, Washington, D.C.

Arnold J. G., Williams J. R., Nicks A. D., and Sammons N. B., 1990. SWRRB, A basin scale simulation model for soil and water resources management. Texas A&M Univ. Press, College Station, TX.

Arnold, J. G., R. S. M. Srinivasan, and J. R. Wiliams. 1998. Large-area hydrologic modelling and assessment: Par I. Model development. Journal of the American Water Resources Association 34(1):73-89.

Bande Yogesh, Mendhe Ravindra, Shelar Tushar. 2019. Site Suitability Analysis for Water Conservation Using AHP and GIS Techniques: A Case Study of Upper Sina River Catchment, Ahmednagar (India). Hydrospatial Analysis, 3(2), 49-59, 2019.

Bansode A. and Patil K.A. 2014. Estimation of Runoff by Using SCS Curve Number Method and ArcGIS. International Journal of Scientific and Engineering Research, 5 :1283-1287.

Beckers,J., Smerdon, B. and Wilson, M. 2009. Review of hydrologic models for forest management and climate change applications in British Columbia and Alberta. Forum for research and Extension in Natural Resources Society (FORREX) Series 25, Kamloops, British Columbia, Canada

Bera S., and Maiti R. 2021. Assessment of water availability with SWAT model: A study on Ganga River. Journal of the Geological Society of India, 97(7), 781-788.

Berger, K.P. and Entekhabi, D. 2001. Basin hydrologic response in relation to distributed physiographic descriptors and climate. Journal of Hydrology. 247: 169-182.

Bhange H. N., Deshmukh V. V., Rajankar P. B., Ayare B. L., Gharde K. D. and Patil S. T. , 2014. Estimation of Runoff from Watershed using Remote Sensing and GIS International, Journal of Engineering Innovation and Research, 3 :900-903.

Boman B., and Shukla S. 2009. Water measurement for agricultural irrigation and drainage systems. Agricultural and Biological Engineering Department, Florida Cooperative Extension Service, University of Florida.

Boman B., and Shukla S. 2009. Water measurement for agricultural irrigation and drainage systems. Agricultural and Biological Engineering Department, Florida Cooperative Extension Service, University of Florida.

Boretti, A., Rosa, L. Reassessing the projections of the World Water Development Report. *npj Clean Water* **2**, 15 (2019). https://doi.org/10.1038/s41545-019-0039-9

Bos MG (1976) Discharge measurement structures. Publication 20 International Institute for Land Reclamation and Improvement (ILRI), Wageningen

Bosbach J, Ku¨hn M, Wagner C (2009) Large scale particle image velocimetry with helium filled soap bubbles. Exp Fluids 46(3):539–547

Bosch D. D., Arnold, J. G., Martin V. Allen P.M., Simulation of a low-gradient coastal plain watershed using the swat landscape model 2010, American Society of Agricultural and Biological Engineers ISSN 2151-0032 53(5): 1445-1456

British Columbia (2006) Water supply factsheet. Ministry of Agri cultural and Lands Abbotsford, British Columbia

Britta S., Filipa T., and Nicola F. 2008. Modelling hydrological processes in mesoscale lowland river basins with SWAT: Capabilities and challenges. J. Hydrological Sciences.Vol.53 (5): 989-1000.

Brock M, Sahoo D, Sawyer C, Pike J. 2023 Streamflow: what is it, and how do we measure it? Clemson (SC): Clemson University Cooperative Extension Service, Land-Grant Press by Clemson Extension; LGP 1160.

Brossard C, Monnier JC, Barricau P, Vandernoot FX, Le Sant Y, Champagnat F, Le Besnerais G (2009) Principles and applica tions of particle image velocimetry. Aerosp Lab J 1:1–11

Byakod K., Shivapur A., Venkatesh B. 2017. Application of SWAT Model for generating surface runoff and estimation of water availability for Balehonnuru catchment area of Badhra river basin. International research journal of engineering and technology, 4(8), 1143-1148

Chauhan M.S., Kumar V., Dikshit P.S., Dwivedi S.B. 2014. Comparison of discharge data using ADCP and current meter. Int J Adv Earth Sci 3(2):81–86

Chen, Y.; Chen, W.; Pal, S.C.; Saha, A.; Chowdhari, I.; Adeli, B.; Janizadeh, S.; Dineva, A.A.; Wang, X. and Mosavi, A. 2022. Evaluation efficiency of hybrid deep learning algorithms with neural network decision tree and boosting methods for predicting groundwater potential. Geocarto International. 37: 5564-5584. https://doi.org/10.1080/10106049.2021.1920635

Daniel E. B., Camp J. V., Eugene J. L., Jessica R. P., James P. D. and Abkowitz M. D. 2011. Watershed Modeling and its Applications: A State-of-the-Art Review. J. The Open Hydrology, Vol. (5): 26-50.

Das, Pulakesh & Behera, Mukunda & Patidar, Nitesh & Sahoo, Bhabagrahi & Tripathi, Poonam & Behera, Priti & Srivastav, Sushil & Roy, Parth & Thakur, Praveen & Aggarwal, Shiv & Krishnamurthy, Y. (2018). Impact of LULC change on the runoff, base flow and evapotranspiration dynamics in eastern Indian river basins during 1985–2005 using variable infiltration capacity approach. Journal of Earth System Science. 127. 10.1007/s12040-018-0921-8.

Deshmukh, D.S.; Chaube, U.C.; Hailu, A.E.; Gudeta, D.A. and Kassa, M.T. 2013. Estimation and comparison of curve numbers based on dynamic land use land cover change, observed rainfall-runoff data and land slope. Journal of Hydrology. 492:89-101. https://doi.org/10.1016/j.hydrol.2013.04.001

Devia G. K., Ganasri B. P., and Dwarakish, G. S. 2015. A review on hydrological models. Aquatic Procedia, 4, 1001-1007.

Dhawale A. W. 2013. Runoff estimation for Darewadi watershed using RS and GIS. International Journal of Recent Technology and Engineering, 1(6), 46-50.

Dobriyal P., Badola R., Tuboi C., and Hussain S. A. 2017. A review of methods for monitoring streamflow for sustainable water resource management. Applied Water Science, 7(6), 2617-2628.

Easton Z.M., Walter M. T., Fuka D. R., White E.D and Steenhuis T.S. 2010. A simple concept for calibrating run off thresholds in quasi-distributed variable source area watershed models. J. Hydrological Processes. Vol. 25 (20): 3131- 3143.

Ely E(1994) A profile of volunteer monitoring. Volunteer Monitor 6(1):4

Emiroglu ME, Bilhan O, Kisi O (2011) Neural networks for estimation of discharge capacity of triangular labyrinth side weir located on a straight channel. Expert Syst Appl 38(1):867–874

Fernandes, A.J. and Rudolph, D.L. 2001. The influence of Cenozoic tectonics on the groundwater potential capacity of fractured zones: A case study in Sao Paulo, Brazil. Hydrogeology Journal. 9: 151-167.

Flener C, Wang Y, Laamanen L, Kasvi E, Vesakoski JM, Alho P (2015) Empirical modeling of spatial 3d flow characteristics using a remote-controlled ADCP system: monitoring a spring f lood. Water 7(1):217–247

Friederich H, Smart PL (1982) The classification of autogenic percolation waters in karst aquifers: a study in GB cave Mendip hills England. Proc Univ Bristol Spelaeol Soc 16(2):143-159

Gabale S. and Deshpande A. M. 2020. Geospatial technique for runoff estimation based on SCS-CN method in Sudha River basin of Indrayani River. International Journal of Multidisciplinary Research and Development, 7 :172-177

Gangarde P. A., Ayare B. L., Bhange H. N., Patil S.T. and Tharkar M. H.2023 Site suitability analysis of soil and water conservation structures in Kadivali watershed using remote sensing and GIS ; SP-12(10): 2145-2152

Garci-, J.M.; Lopez-Moreno, J.I.; Vicente-Serrano, S.M.; Lasanta-Martinez, T. and Begueria, S. 2011. Mediterranean water resources in a global change scenario. Earth Science Reviews. 105(3-4): 121-139. https://doi.org/10.1016/j.erascirev.2011.01.006

Gassman P. W., Reyes M., Green C. and Arnold J. G. 2007. The Soil and Water Assessment Tool: Historical Development, Applications and Future Research Directions. Transactions of ASABE, Vol. 50 (4): 1211-1250.

Gassman, P.W., Sadeghi, A.M. and Srinivasan, R. (2014), Applications of the SWAT Model Special Section: Overview and Insights. J. Environ. Qual., 43: 1-8. https://doi.org/10.2134/jeq2013.11.0466

Gassman, Philip W.; Reyes, Manuel R.; Green, Colleen H.; and Arnold, Jeffrey G., "The Soil and Water Assessment Tool: Historical Development, Applications, and Future Research Directions" (2007). Economics Publications. 28.

Gavit B.K., 2017 Rainfall Runoff modelling for upper and middle Godavari sub-basin using remote sensing and geographic information system. PhD thesis submitted to Maharana Pratap University of Agriculture and technology, Udaipur, Rajasthan

Gavit B.K., Purohit R.C., Bhange H.N., Ingle P.M. 2017. Hydrological modelling using SWAT. Research Journal of Recent Sciences.;6(11):10-15

Genjebo, M.G.; Kemal, A. and Nannawo, A. S. 2023. Assessment of surface water resource and allocation optimization for diverse demands in Ethiopia's upper Bilate watershed. Heliyon. 9: e20298. https://doi.org/10.1016/j.heliyon.2023.e20298

Gharde, K. D. 2015 Hydrological modelling runoff and sediment yield for Konkan region. Ph.D. thesis submitted to Maharana Pratap University of Agriculture and technology, Udaipur, Rajasthan

Gharde, K.D. and Kothari, M. 2016. Hydromorphometric analysis and prioritization of Savitri basin of Maharashtra, India using GIS. International Journal of Civil, Structural, Environmental and Infrastructure Engineering Research and Development. 6(2): 1-10.

Ghodsian M (2003) Supercritical flow over a rectangular side weir. Can J Civ Eng 30:596–600

Gordon, N.D.; McMahon, T.A. Finlayson, B.L.; Gippel, C.J. 2004. Stream hydrology: an introduction for ecologists. 2nd edition. Wiley, England.

Groundwater Technical Workgroup. 2010. Evaluation of models and tools for assessing groundwater availability and sustainability: Priorities for investment. Minnesota Department of Natural Resources, 500 Lafayette Road, St Paul, MN 55155.

Guo, X.; Fu, Q.; Hang, Y.; Lu, H.; Gao, F. and Si, J. 2020. Spatial variability of soil moisture in relation to land use types and topographic features on hillslopes in the black soil (Mollisols) area of Northern China. Sustainability. 12(9): 3552-3572. https://doi.org/10.3390/su12093552

Gurav, C. and Babar, Md. 2019. Hydro-geomorphological studies for groundwater potential of Mangyal Nala watershed of Landi river, Nanded district, Maharashtra. Journal of Geosciences Research: Challenges in groundwater and surface water in India. Vol. 2. 61-66.

Hardcastle, K.C. 1995. Photolineament factor: A new computer-aided method for remotely sensed fractured. Photogrammetric Engineering and Remote Sensing. 61(6): 739-747.

Harmel RD, Smith DR, King KW, Slade RM (2009) Estimating storm discharge and water quality data uncertainty: a software tool for monitoring and modelling applications. Environ Model Softw 24(7):832-842

Harpold AA, Mostaghimi S, Vlachos PP, Brannan K, Dillaha T (2006) Stream discharge measurement using a large-scale particle image velocimetry (LSPIV) prototype. Trans ASABE 49(6):1791–1805

Hatefi, A.A.H. and Ekhtesasi, M.R. 2016. Groundwater potentiality through Analytic Hierarchy Process (AHP) using remote sensing and GIS. JGeope. 6(1): 75-88.

Hauet A, Creutin JD, Belleudy P (2008) Sensitivity study of large-scale particle image velocimetry measurement of river discharge using numerical simulation. J Hydrol 349(1):178–190

Hengade N and Eldho T (2016) Assesemnet of LULC and climate change on the hydrology of Asthi Catchment, India using VIC Model J Eart Syst Sci 125 1623-1634

Herndon, K.; Muench, R.; Cherrington, E. and Griffin, R. 2020. As assessment of surface water detection methods for water resource management in the Nigerien Sahel. Sensor. 20(2): 431-444. https://doi.org/10.3390/s20020431

Herschy RW (2008) Streamflow measurement, 3rd edn. Taylor and Francis, USA

Hilgersom, K. P. and Luxemburg, W. M. J.: Technical Note: How image processing facilitates the rising bubble technique for discharge measurement, Hydro. Earth Syst. Sci., 16, 345–356, https://doi.org/10.5194/hess-16-345-2012, 2012.

Horton, R.E. 1945. Erosional development of streams and their drainage basins, hydro physical approach to quantitative morphology. Geological Society of America Bulletin. 56: 275-370.

Hudson JA (2004) The impact of sediment on open channel flow measurement in selected UK experimental basins. J Flow Measure Instrum 15(1):49–58

Hudson NW (1993) Field measurements of soil erosion. Food and agriculture organization of United Nations, Rome

Hussain, S.; Mubeen, M. and Karuppannan, S. 2022. Land use and land cover (LULC) change analysis using TM, ETM+ and OLI Landsat images in district of Okara, Punjab, Pakistan. Physical Chemistry of Earth. 126: 103117. https://doi.org/10.1016/j.pce.2022.103117

Ishak, M.G.; Sutapa, I.W.; Basong, A. and Dedi, A. 2020. Analysis of water availability in Omu watershed. MATEC web of conferences. 331. 04003. https://doi.org/10.1051/matecconf/202033104003

Jain S. K., Sharma G. S., and Verma S. G. 2010. Simulation of Runoff and Sediment Yield for a Himalayan Watershed Using SWAT model. J. Water Res. and Protection: 276-281.

Jedhe S.H. 2018. Assessment of water resources and planning in context of climatic variability for Konkan region [PhD thesis]. Dapoli: D.B.S.K.K.V.

Jethe A., Gaikwad S., Thakare L and Nikam S. 2022. Application of Surface Runoff Estimation Using NRCS- SCS Curve Number Method Using Remote Sensing And GIS: A Case Study of Tavarja Lake Catchment of Maharashtra. UGC CARE Listed (Group -I) Journal, 11: 488.

John P. H. 1978. Discharge measurement in lower order streams. Internationale Revue der gesamten Hydrobiology und Hydrography, 63(6), 731-755.

Juniati, A.T.; Sutjingsih, D.; Soeryantono, H. and Kusratmoko, E. 2018. Proposing water balance method for water availability estimation in Indonesian regional spatial planning. 4th

International Seminar on Sustainable Urban Development. IOP Conference Series: Earth and Environmental Science. 106: 012073. https://doi.org/10.1088/1755-1315/106/1/012073

Kaczmarek, Z., 1993. Water balance model for climate impact analysis. ACTA Geophysica Polonica, Vol. 41 (4): 1-16.

Kadam, A.K.; Kale, S.S.; Umrikar, B.N.; Sankhua, R.N. and Pawar, N.J. 2017. Identifying possible locations to construct soil-water conservation structures by using Hydro-geological and Geospatial analysis. Hydrospatial Analysis. 1(1): 18-27.

Kalbus E., Reinstorf F., and Schirmer M. Measuring mrthods for groundwater- surface water interactions: a review, Hydrol. Earth Syst. Sci., 10, 873-887, https://doi.org/10.5194/hess-10-873-2006, 2006.

Kale S. S., Ayare B. L., Bhange H. N., Patil S. T. and Bansode P. B. 2022. (b) Estimation of Runoff of Kudavale Micro Watershed Using SCS Curve Number Method and GIS Approach. International Journal of Novel Research and Development . 7: 296- 304.

Kousari M. R., Malekinezhad H., Ahani H., and Zarch M. A. 2010. Sensitivity analysis and impact quantification of the main factors affecting peak discharge in the SCS curve number method. An analysis of Iranian watersheds,Quat. Int. Vol. (226): 66–74.

Kumar, Rakesh & Sharma, K.D. & Jha, Ramakar. (2007). Availability and management of surface and ground water resources in India.

Lee, D.R. 2005. Agricultural sustainability and technology adoption: issues and policies for developing countries. Americal Journal of Agricultural Economics. 87(5): 1325-1334. https://doi.org/10.1111/j.1467-8276.2005.00826.x

Letvin, D.G.; Tucker, G.E.; Barnhart, K.R. and Harman, C.J. 2022. Groundwater affects the geomorphic and hydrologic properties of coevolved landscapes. Journal of Geophysical Research: Earth surface. 127. E2021JF006239. https://doi.org/10.1029/2021JF006239

Liang, X. and Xie,Z.H. 2003. Important factors in land-atmospheric interactions: surface runoff generations and interactions between surface and groundwater. Global Planet Change 38(1-2), pp.101-114

Lohar Tushar, 2018. Site suitability analysis for establishing soil and water conservation structures using Geoinformatics – a case study in Chinnar watershed, Tamil Nadu. Journal of Geoinformatics 12(2): 146-157

Mabee, S.B,; Hardcastle, K.C. and Wise, D.U. 1994. A method of collecting and analyzing lineaments for regional-scale fracture-bedrock aquifer studies. Ground Water. 32(6): 884-894.

Magesh, N.S.; Chandrasekar, N. and Soundranayagam, J.P. 2012. Delineation of grounwater potential zones in Theni district, Tamil Nadu, using remote sensing, GIS and MIF techniques. Geoscience Frontier. 3: 189-196. https://doi.org/10.1016/j.gsf.2011.10.007

Magowe, M. and Carr, J.R. 1999. Relationship between lineaments and groundwater occurrence in western Botswana. Ground Water. 37(2): 282-286.

Malunjekar S. 2018. Simulation of Runoff and Sediment Yield in Agricultural Watershed using SWAT and WEPP Models (Doctoral dissertation, Department of Soil and Water Conservation Engineering Dr. Annasaheb Shinde College of Agricultural Engineering and Technology, Mahatma Phule Krishi Vidyapeeth).

Martin EC(2006) Measuring water flow in surface irrigation ditcheds and gated pipe. Cooperative Extension Pub No AZ1329 Arizona Water series No 31, The University of Arizona

Mbajiorgu, Constantine. (2020). ASSESSMENT OF SURFACE WATER HYDROLOGY.

Mehendale, N. M. 2016. Hydrological streamflow modelling of Morna catchment using soil and water assessment tool (SWAT). M.Tech Thesis submitted to D.B.S.K.K.V., Dapoli.

Melkamu, T.; Bagyaraj, M.; Adimaw, M.; Ngusie, A. and Karuppannan, S. 2022. Detecting and mapping flood inundation areas in Fogera-Dera Floodplain, Ethiopia during an extreme wet season using Sentinel – 1 data. Physical Chemistry of the Earth. 127. 103189. https://doi.org/10.1016/j.pce.2022.103189

Mengistu, A.; Wayessa, Y.E.; van Rensburg, L.D. and Tesfuhuney, W.A. 2021. Analysis of the spatio-temporal variability of soil water dynamics in an arid catchment in South Africa. Geoderma Regional. 25. e00395. https://doi.org/10.1016/j.geodrs.2021.e00395

Mengistu, A.; Wayessa, Y.E.; van Rensburg, L.D. and Tesfuhuney, W.A. 2021. Analysis of the spatio-temporal variability of soil water dynamics in an arid catchment in South Africa. Geoderma Regional. 25. e00395. https://doi.org/10.1016/j.geodrs.2021.e00395

Merz, J and Doppmann, G. 2006. Measuring mountain stream discharge using the salt dilution method: A practical guide. ICIMOD publication.

Mistry A. K., and Joshi B. R. 2018. Rainfall Runoff Modelling of Shakkar River using SWAT Model. International Journal of Science Technology & Engineering, 4(10), 49-52.

Mondal, Arpita & Narasimhan, Balaji & Sekhar, Muddu & Mujumdar, P.. (2016). Hydrologic Modelling. Proceedings of the Indian National Science Academy. 82. 10.16943/ptinsa/2016/48487.

Moore, R.D. 2004. Introduction to salt dilution gauging for streamflow measurement. Part 2. Constant-rate inject. 8(1): 11-15.

Munoth, P., & Goyal, R. (2019). Impacts of land use land cover change on runoff and sediment yield of Upper Tapi River Sub-Basin, India. *International Journal of River Basin Management*, *18*(2), 177–189. https://doi.org/10.1080/15715124.2019.1613413

Munyaneza, O.; Mukubwa, A.; Maskey, S.; Uhlenbrrok, S. and Wenninger, J. 2014. Assessment of surface water resources availability using catchment modelling and the results of tracer studies in the mesoscale Migina catchment, Rwanda. Hydrology & Earth System Sciences. 18: 5289-5301. https://doi.org/10.5194/hess-18-5289-2014

Murugesan, B.; Thirunavukkarasu, R.; Senapathi, V. and Balasubramanian, G. 2012. Application of remote sensing and GIS analysis for groundwater potential zone in Kodaikanal Taluka, South India. Earth Science. 7(1): 65-75.

Mutz M, Kalbus E, Meinecke S (2007) Effect of in-stream wood on vertical water flux in low-energy sand bed flume experiments. Wat Resour Res 43:10

Nag, S.K. 1998. Morphometric analysis using remote sensing techniques in the Chaka subbasin, Purulia, West Bengal. Journal of Indian Society of Remote Sensing. 26: 69-76.

Najafi M.R., Moradkhani H., and Piechota T.C. 2012. Ensemble streamflow prediction: climate signal weighting methods vs climate forecast system reanalysis. J Hydrol 442:105–116

Nandhagopal, N.; Kumar, R.S.; Kannadasan, T. and Mawthoh, M.B. 2015. Influences from satellite images for locating Kimberlite: Mahabubnagar area, Telangana, South India. Elixir Earth Science. 84: 33547-33553.

Neelam Kumari; Ayare, B.L.; Bhange, H.N.; Ingle, P.M. and Kasture, M.C. 2023. Geospatial analysis of morphometric parameters in the Kal reiver basin, Western Konkan: Implications for hydrological characteristics. The Pharma Innovation Journal. SP-12(12): 2657-2667.

Neitsch S. L., Arnold J. G., Kiniry J. R., and Williams J. R. 2009. Soil & Water Assessment Tool - Theoretical Documentation Version 2009. Texas.

Neitsch, S. L., J. G. Arnold, J. R. Kiniry, R. Srinavasan, and J. R. Wiliams. 2009. Soil and Water Assessment Tool Theoretical Documentation Version 2009, Temple, Tex.: Grassland, Soil and Water Research Laboratory

Nguyen, D. L. and K. L. Nguyen. 2012 Assessing water discharge in be river basin, Vietnam using SWAT Model. *International Symposium on Geo-informatics for spatial Infrastructure Development in Earth and Allied Sciences:* 230-235

Nijssen,B., Lettenmaier, D.P., Liang Xu, Wetzel, S. W. and Wood, E. F., 1997. Streamflow simulation for continental – scale river basins. Journal of Geophysics Research

Oyebande L., 2001. Water problems in Africa-How can the sciences help? Special issue: Can Science and Society Avert the World Water Crisis in the 21st Century. J. Hydrological Sciences.Vol.46 (6): 947-961.

Pande, C.B.; Moharir, K.N.; Singh, S.K. and Varade, A.M. 2020. An integrated approach to delineate the groundwater potential zones in Devdari watershed area of Akola district, Maharashtra, Central India. Environment Development and Sustainability. 22:4867-4887. https://doi.org/10.1007/s10668-019-00409-1

Pandey, V. P., S. Dhaubanjanr, L. Bharati and B.R. Thapa. 2020 Spatio-temporal distribution of water availability in Karnali-Mohana basin, Western Nepal-Hydrological model development using multi-site calibration approach (Part-A). Journal of Hydrology: Regional studies. 29

Parikh, Mansi & Parekh, Falguni. (2019). Hydrological Modelling of Deo River Sub-Basin using SWAT Model and Performance Evaluation using SWAT-CUP. International Journal of Innovative Technology and Exploring Engineering. 8. 2890-2896. 10.35940/ijitee.K2224.1081219.

Patel D. P., and Srivastava P. K., 2013. Flood hazards mitigation analysis using remote sensing and GIS: Correspondence with the town planning scheme. J. Water Resource Management, Vol. 27: 2353-2368.

Pfeffer MJ, Wagenet LP (2007) Volunteer environmental monitoring knowledge creation and citizen-scientists interaction. In Pretty J, Ball A et al. The sage handbook of environment and society. Sage Publication, London

Prajapati, R.N.; Ibrahim, N.; Goyal, M.K.; Thapa, B.R.and Maharjan, K.R. 2023. Groundwater availability assessment for a data-scarce river basin in Nepal using SWAT hydrological model. Water supply. 24(1): 254-271. https://doi.org/10.2166/ws.2023.332

Prasad AK (2000) Particle image velocimetry. Curr Sci 79(1):51–60

Ranjan S., and Singh V. 2023. Effect of land use land cover changes on hydrological response of Punpun River basin. Environmental Monitoring and Assessment, 195(9), 1137.

Rankova, M. 2019. Surface water resources assessment methodologies application in case of Vit River. Internation Scientific Journal of Mechanization in Agriculture & Conserving of the Resources. 5: 171-173.

Rickard C, Day R, Purseglove J (2003) River weirs- good practice guide. R&D Publication, Bristol UK

Saaty, T.L. 2012. Decision making for leaders: The analytical hierarchy process for decisions in a complex world. Third revised edition. Pittsburgh: RWS Publications.

Sai, G.S.; Mohan, K.R.; and Shankar, K. 2024. Identification of vulnerable areas using geospatial technologies in the lower Manair River basin of Geomatisc, Nat. Hazards Risk. 15. https://doi.org/10.1080/19475705.2023.2296379

Samal D. R., and Gedam S. 2021. Assessing the impacts of land use and land cover change on water resources in the Upper Bhima River basin, India. Environmental Challenges, 5, 100251.

Samboko, H.T. & Abas, I. & Luxemburg, W.M.J. & Savenije, Hubert & Makurira, Hodson & Banda, Kawawa & Winsemius, Hessel. (2020). Evaluation and improvement of remote sensing-based methods for river flow management. Physics and Chemistry of the Earth, Parts A/B/C. 117. 102839. 10.1016/j.pce.2020.102839.

Saravanan, S.; Saranya, T.; Jennifer, J.J.; Singh, L.; Selviraj, A. and Abijith, D. 2020. Delineation of groundwater potential zone using analytical hierarchy process and GIS for Gundihalla watershed, Karnataka, India. Arab Journal of Geoscience Journal. 13: 695.

Shope C.L., Bartsch S., Kim K., Kim B., Tenhunen J., Peiffer S., Park J., Ok S.Y., Fleckenstein J., Koellner T. 2013. A weighted, multimethod approach for accurate basin-wide streamflow estimation in an ungauged watershed. J Hydrol 494:72–82

Siddi R , Sudarsana R, and Rajasekhar M. 2018. Estimation of rainfall runoff using SCS-CN method with RS and GIS techniques for Mandavi Basin in YSR Kadapa District of Andhra Pradesh, India. Hydro spatial Anal, 2(1) :1-15.

Sieber J., Yates D., Huber Lee A., and Purkey D. 2005. WEAP a demand, priority, and preference driven water planning model: Part1, model characteristics. Water International. Vol. 30 (4), 487–500.

Singh A., and Jha S. K. 2020. Identification of sensitive parameters in daily and monthly hydrological simulations in small to large catchments in Central India. Journal of Hydrology, 601, 126632.

Singh,R., Subramanian, K. and Refsgaard, J.C., 1999. Hydrological modelling of a small watershed using MIKE SHE for irrigation planning. Agricultural Water Management 41, 149-166

Smith, P.; House, J.I.; Bustamante, M.; Sobocka, J.; Harper, R.; Pan, G.; West, P.C.; Clark, J.M.; Adhya, T.; Rumpel, C.; Paustian, K.; Kuikman, P.; Cotrufo, M.F.; Elliott, J.A.; McDowell, R.; Griffiths, R.I.; Asakawa, S.; Bondeau, A.; Jain, A.K. Meersmans, J. and Pugh, T.A.M. 2016. Global change pressures on soils from land use and management. Global Change Biology. 22(3): 1008-1028. https://doi.org/10.1111/gcb.13068

Somura H., Hoffman D., and Arnold J. 2007. Application of the SWAT model to the Hii River basin, Shimane prefecture, Japan. Proceedings of 4th International SWAT Conference, Delft, 4-7 July 2007, UNESCO-IHE, Netherlands.101-110.

Srivastava P. K., Han D., Rico-Ramirez M. A., Al-Shrafany D., and Islam T. 2013. Data fusion techniques for improving soil moisture deficit using SMOS satellite and WRF-NOH land surface model. J. Water Resource Manag., 27: 5069–5087.

Srivastava P. K., Han D., Rico-Ramirez M. A., Bray M. and Islam T., 2013. Selection of classification techniques for land use/land cover change investigation. J. Advance Space Res., Vol. 50 (9):1250–1265. Doi: 10.1016/ j.asr.2012.06.032.

Stamhuis EJ (2006) Basics and principles of particle image velocimetry (PIV) for mapping biogenic and biologically relevant flows. Aquat Ecol 40(4):463–479

Sudhakar M , R. Sai Teja, B. Shanmukh, Ch. Mallika, M.Greeshmikaw, Bala Rama Krishna Murthy. 2019. Simulation of Runoff in Hydrological Modelling Using Swat in Case Study of Godavari Basin. International Journal of Computer Science and Mechatronics., Vol. 5(3): 22-33

Suresh R. Soil and water conservation engineering ISNB: 978-81-8014-186-7 (2020) A.K. Jain Standard Publishers Distributors, Delhi (27-32)

Talawar R., Seelam J. 2023. Estimation of River Discharge in Mandovi Basin, Goa. In: Timbadiya, P.V., Patel, P.L., Singh, V.P., Sharma, P.J. (eds) Hydrology and Hydrologic Modelling. HYDRO 2021. Lecture Notes in Civil Engineering, vol 312. Springer, Singapore. https://doi.org/10.1007/978-981-19-9147-9_11.

Tamsegen, Y.; Atlabachew, A. and Jothimani, M. 2023. Groundwater potential assessment in the Nile River catchment, Ethiopia, using geospatial and multi-criteria decision-making techniques. Heliyon. 9. https://doi.org/10.1016/j.heliyon.2023.e17616

Tauro F, Olivieri G, Petroselli A, Porfiri M, Grimaldi S (2016) Flow monitoring with a camera: a case study on a flood event in the Tiber River. Environ Monit Assess 188(2):1–11

Thapa, R.; Gupta, S.; Guin, S. and Kaur, H. 2017. Assessment of groundwater potential zones using multi-influencing factor (MIF) and GIS: a case study from Birbhum district, West Bengal. Applied Water Science. 7: 4117-4131.

Touseef, M.; Chen, L. and Yang, W. 2021. Assessment of surface water availability under climate change using coupled SWAT0WEAP in Hongshui River Basin, China. ISPRS International Journal of Geoinformation. 10(5): 298-316.

Tucker, G.E.; Catani, F.; Rinaldo, A. and Bras, R.L. 2001. Statistical analysis of drainage density from digital terrain data. Geomorphology. 36: 187-202.

USFWS (United States Fish and Wildlife Services)2006 Water measurement Mountain-Prairie region. Water Resources Divi sion,United State of America

USGS (United States Geological Survey) (2007) How streamflow is measured? The discharge measurement, US Department of the Interior, United State of America

Valentina Krysanova & Mike White (2015) Advances in water resources assessment with SWAT—an overview, Hydrological Sciences Journal, 60:5, 771-783, DOI: 10.1080/02626667.2015.1029482

Van Gent MRA, de Vries JVT, Coeveld EM, De Vroeg JH, Van de Graaff J (2008) Large-scale dune erosion tests to study the influence of wave periods. Coastal Eng 55(12):1041–1051

Vara Prasad 2012. Modelling of blue and green water for sustainable water resources management in watershed. P. G. Thesis. Acharya N. G. Ranga Agricultural University, Hyderabad, India.

Varade, A.M.; Khare, Y.D.; Yadav, P.; Doad, A.P.; Das, S.; Kanetkar, M. and Golekar, R.B. 2018. 'Lineaments' the potential groundwater zones in hard rock area: a case study of basaltic terrain of WGKKC-2 watershed from Kalmeshwar Tahsil of Nagpur district, Central India. Journal of Indian Society of Remote Sensing. 46: 539-549.

Vijay P., 2005. Watershed models. CRC Press is an imprint of Taylor & Francis Group.

Viswanathan, P. M.; Sabarathinam, C.; Karuppannan, S. and Gopalkrishnan, G. 2021. Determination of vulnerable regions of SARS-CoV-2 in Malaysia using meteorology and air quality data. Environment Development Sustainability. 24: 8856-8882. https://doi.org/10.1007/s10668-021-01719-z

Wagner P. D., Kumar S., and Schneider K. 2013. An assessment of land use change impacts on the water resources of the Mula and Mutha Rivers catchment upstream of Pune, India. Hydrology and Earth System Sciences, 17(6), 2233-2246.

Waikar, M.L. and Nilawar, A.P. 2014. Identification of groundwater potential zone using remote sensing and GIS technique. International Journal of Innovative Research Science & Engineering Technology. 3: 12163-12174.

Wang, C.; Zhang, G.; Zhu, P.; Chen, S. and Wan, Y. 2023. Spatial variation of soil functions affected by land use type and slope position in agricultural small watershed. Catena. 225: 107029. https://doi.org/10.1016/j.catena.2023.107029

Wang, S.; Li, J.; Russell, A.J. 2023. Methods for estimating surface water storage changes and their evaluations. Journal of Hydrometeorology. 24(3): 445-461. https://doi.org/10.1175/JHM-D-22-0098.s1

Ward, M.; Poleacovschi, C.; Perez, M. Using AHP and Spatial Analysis to Determine Water Surface Storage Suitability in Cambodia. Water 2021, 13, 367. https://doi.org/ 10.3390/w13030367

Weight WD, Sonderegger JL (2001) Manual of applied field hydrogeology. McGraw-Hill, New York

Wenming N., Yongping Y., Kepner W., Maliha S. N., Jackson M. and Erickson C. 2011. Assessing impacts of Land use and Land cover changes on hydrology. J. Hydrology. 407: 105-114.

Yan B., Fang N. F., Zhang P. C. and Shi Z. H. 2013. Impacts of land use change on watershed stream flow and sediment yield an assessment using hydrologic modelling and partial least squares regression. J. Hydrology. 484: 26–37.

Yang, D., Herath S., and Musiake, K., 2000 Comparison of different distributed hydrological models for characterisations of catchment spatial variability. Journal of Hydrological Procedia 14(3), 403-416

Yeh, H.F.; Cheng, Y.S.; Lin, H.I. and Lee, C.H. 2016. Mapping groundwater recharge potential zone using a GIS approach in Hualian River, Taiwan. Sustainable Environment Research. 26: 33-43.

Zha,o R-J., Zhang, Y.L., Fang,L.R. et al. 1980. The Xinanjiang model. Hydrological Forecasting Proceedings Oxford Symposium, IAHS, International Association of Hydrological Scieneces Press, Wallingford, UK (1980).pp.351-356

Zhang, Z.; Sheng, L.; Yang, J.; Chen, X.A.; Kong, L. and Wagan, B. 2015. Effects of land use and slope gradient on soil erosion in a red soil hilly watershed of southern China. Sustainability. 7:14309-14325. https://doi.org/10.3390/su7104309

Zhu, G.; Tang, Z.; Shangguan, Z.; Peng, C. and Deng, L. 2019. Factors affecting the spatial and temporal variations in soil erodibility of China. Journal of Geophysical Research: Earth Surface. 124: 737-749. https://doi.org/10.1029/2018JF004918

Ziadat, F.M. and Taimeh, A.Y. 2013. Effect of rainfall intensity, slope, land use and antecedent soil moisture on soil erosion in an arid environment. Land Degradation and Development. 24(6): 582-590. https://doi.org/10.1002/ldr.2239

APPENDICES

Appendix – I

Details of weather station

(A) Geographic details of weather station

District	Valley	Basin Name	Station	Latitude	Longitude
Palghar	21	Vaitarna	Andhari	19.7808	73.19944
			Chinchghar	19.7694	73.00278
			Khodala	19.7917	73.39583
			Khutal	19.7106	72.9675
			Payarchapada	19.8814	73.05833
			Savarkhand	19.6014	73.14944
			Suksale	19.7994	73.11778
			Suryamal	19.7544	73.3475
			Ogade	19.7206	73.26667
Thane		Ullas	Dhamni(Kjt)	18.9936	73.4922
			Kalamb	19.0925	73.3919
			Kondhane	18.8483	73.3756
			Naldhe	19.0319	73.4122
			Nandgaon(Kjt)	19.0972	73.4917
			Tadwadi	19.0711	73.4447
			Kaman	19.3844	72.91056
			Khapari	19.3244	73.59333
			Kochara	19.3511	73.57806
Raigad	22	Patalganga-Amba	Khandpoli	18.6292	73.2561
			Pali	18.5311	73.2014
			Payarwadi	18.55	73.2667
			Tuksai	18.6969	73.3
			Borgaon.	18.9228	73.2781
			Chowk(kjt)	18.8983	73.2469
			Hatond	18.6933	73.2569
			Kamarli	18.7244	73.1689
			Khanav	18.7431	73.2686
			Nadewadi	18.7217	73.2186

			Ransai	18.8958	73.0589
			Varsai	18.7769	73.1667
		Kundalika	Mahan	18.5361	73.03722
			Sudkoli	18.4186	73.02667
		Savitri	Ambiwali	18.0225	73.3917
			Bhave	18.0939	73.5339
			Birwadi	18.1056	73.5275
			Kangule	18.07	73.475
			Kotheri	18.0567	73.4333
			Raigad	18.2467	73.45
			Varandoli	18.1939	73.4011
			Waki (Kd)	18.1711	73.57
Ratanagiri	23	Vashisthi	Dabhol	17.5919	73.1786
			Govalkot	17.5489	73.4861
			Karambavane	17.5689	73.4192
			Kolthare	17.6528	73.1353
			Kudup	17.4061	73.5528
			Lavel	17.6494	73.4761
			Poynar	17.7722	73.3333
			Talsar	17.4167	73.5933
	24	Shastri	Asurde	17.3542	73.5283
			Devghar	17.0236	73.635
			Gulvane	17.3811	73.4236
			Hedvi	17.3564	73.2194
			Kondiware	17.3075	73.4822
			Kumbharkhani	17.3192	73.5833
			Kurdhunda	17.155	73.4964
			Lajul	17.1028	73.4181
			Malgund	17.16	73.2703
		Kajivi	Harcheri	16.9475	73.4406
			Kheravase	16.8819	73.6083
			Pastewadi	16.9758	73.7028
			Pawas	16.8706	73.3206

		Kodvali	Adivare	16.7156	73.36
			Karak	16.7186	73.7703
			Raipatan	16.7017	73.7131
			Solgaon	16.655	73.435
			Soliwade	16.6583	73.6725
			Yerdav	16.7447	73.7786
		Waghton	Kakewadi	16.6144	73.6667
			Kolamb	16.6597	73.8078
			Girye	16.5	73.3483
			Het	16.5908	73.7739
			Kharepatan	16.5786	73.6314
Sindhudurg		Devghar	Baparde	16.4464	73.0106
			Ghonsari	16.4214	73.7978
			Phondaghat	16.3764	73.7883
			Talere	16.4533	73.8214
			Ghansori(L)	16.3994	73.79
		Gad	Digawale	16.2381	73.8333
			Golvan	16.1411	73.56
			Kankawali	16.2786	73.7125
			Nardave	16.1989	73.8703
			Palsamb	16.2347	73.5475
			Tarandale	16.3028	73.7069
		Karli	Awalegaon	16.1231	73.7592
			Dukanwadi	16.0314	73.88
			Nerur	16.0536	73.9014
			Walawal	16.0053	73.6197
	25	Terekhol	Amboli	15.9611	74
			Banda	15.8172	73.8658
			Sarambala	15.8653	73.9108
			Sawantwadi	15.8894	73.8408
			Shirshingi	16.0075	73.9511

Appendix – II

Monthly Climatic Data

A. Monthly rainfall data across river basins of Konkan region

District	River basin	Average Monthly rainfall (mm)												Total rainfall (mm)
		June	July	Aug	Sep	Oct	Nov	Dec	Jan	Feb	Mar	Apr	May	
Palghar	Vaitarna	533.0	1134.9	817.8	418.9	92.8	9.2	16.7	11.2	6.7	3.2	1.5	9.2	3055.1
Thane	Ulhas	410.6	942.4	681.4	391.2	114.3	5.8	1.5	0.5	0.6	1.1	0.9	6.9	2557.2
Raigad	Patalganga-Amba	510.7	1048.3	801.0	386.0	123.0	1.0	0.1	0.0	0.0	0.0	0.2	2.8	2873.2
	Kundalika	669.5	1117.7	713.4	397.5	92.0	0.0	0.0	0.0	0.0	0.0	0.0	3.1	2993.3
	Savitri	753.6	1367.5	1047.6	470.2	138.2	0.7	0.2	0.0	0.0	0.0	0.2	1.6	3779.8
Ratnagiri	Vashisthi	778.7	1326.3	846.1	419.9	147.8	2.9	0.4	0.1	0.1	0.2	0.2	3.0	3525.7
	Shastri	795.3	1286.8	844.6	440.7	173.1	0.0	0.0	0.0	0.0	0.0	0.0	0.1	3540.7
	Kajivi	748.8	1217.0	777.2	425.8	157.3	0.0	0.0	0.0	0.0	0.0	0.0	0.0	3326.0
	Muchkundi	816.5	1275.1	893.7	494.8	207.2	3.0	1.6	0.1	0.0	0.6	0.9	7.3	3700.8
	Kodvali	809.8	1230.9	845.2	442.5	186.5	0.0	0.0	0.0	0.0	0.0	0.0	0.0	3514.9
	Waghton	777.4	1182.5	782.7	424.1	190.6	2.5	0.8	0.6	0.0	0.2	1.1	5.9	3368.2
Sindhudurg	Devghar	832.9	1279.1	844.4	452.0	217.8	15.1	11.6	0.0	1.7	1.6	0.6	13.3	3670.0
	Gad	809.1	1268.0	888.0	429.7	193.2	2.8	0.0	0.0	0.0	0.0	0.4	5.1	3596.4
	Karli	901.4	1329.0	918.9	429.3	217.7	0.0	0.0	0.0	0.0	0.0	2.7	49.0	3847.9
	Terekhol	1003.2	1563.1	1160.6	532.6	236.6	12.5	1.2	0.5	0.0	0.0	2.1	29.3	4541.5
Total		11150.5	18568.5	12862.6	6555.2	2488.2	55.5	34.0	13.0	9.1	7.0	10.7	136.5	51890.8

B. Average relative humidity monthly data across river basins of Konkan region

District	River basin	Average Monthly relative humidity (%)											
		June	July	Aug	Sep	Oct	Nov	Dec	Jan	Feb	Mar	Apr	May
Palghar	Vaitarna	78	90	91	88	75	58	44	38	38	39	50	59
Thane	Ulhas	78	89	91	89	78	68	55	46	39	34	41	56
Raigad	Patalganga-Amba	80	89	90	88	79	70	61	53	47	47	54	62
	Kundalika	81	89	90	88	79	71	62	55	49	49	56	63
	Savitri	82	90	91	89	80	72	62	54	47	44	49	61
Ratnagiri	Vashisthi	83	90	90	88	81	72	61	53	49	50	56	66
	Shastri	83	90	90	88	81	72	61	53	50	51	57	66
	Kajivi	84	90	91	89	82	72	59	50	49	51	56	66
	Muchkundi	84	91	91	89	82	72	59	50	48	50	55	65
	Kodvali	84	90	90	88	82	72	60	53	54	58	62	69
	Waghton	84	90	91	89	83	72	59	52	51	55	59	67
Sindhudurg	Devghar	84	92	92	90	83	73	58	49	47	50	55	64
	Gad	85	91	91	89	83	73	60	53	52	55	58	67
	Karli	85	91	91	89	83	73	61	55	54	57	60	68
	Terekhol	85	91	91	89	83	73	61	55	54	57	60	68
Average		83	90	91	89	81	71	59	51	49	50	55	64

C. Average maximum temperature monthly data across river basins of Konkan region

District	River basin	Average Monthly maximum temperature (°c)											
		June	July	Aug	Sep	Oct	Nov	Dec	Jan	Feb	Mar	Apr	May
Palghar	Vaitarna	33	29	28	29	32	33	33	33	35	38	40	39
Thane	Ulhas	31	28	27	28	30	30	30	31	34	37	39	38
Raigad	Patalganga-Amba	32	28	28	29	31	31	31	32	34	37	39	37
	Kundalika	31	28	28	29	31	31	31	32	34	37	38	37
	Savitri	30	27	27	27	29	29	29	30	33	36	38	36
Ratnagiri	Vashisthi	30	27	27	28	29	29	30	31	33	36	37	35
	Shastri	30	27	27	28	29	30	30	31	33	35	36	35
	Kajivi	30	27	27	28	29	30	31	32	34	37	38	35
	Muchkundi	30	27	27	28	29	30	31	32	35	37	38	36
	Kodvali	30	27	27	28	29	30	31	32	34	35	36	34
	Waghton	30	27	27	28	30	30	31	33	35	37	37	35
Sindhudurg	Devghar	30	27	27	28	30	31	32	34	36	39	39	37
	Gad	29	27	27	28	30	31	32	34	35	37	38	35
	Karli	29	27	27	28	30	31	32	33	35	36	37	35
	Terekhol	29	27	27	28	30	31	32	33	35	36	37	35
Average		30	27	27	28	30	30	31	32	34	37	38	36

D. Average minimum temperature monthly data across river basins of Konkan region

District	River basin	Average Monthly minimum temperature (°c)											
		June	July	Aug	Sep	Oct	Nov	Dec	Jan	Feb	Mar	Apr	May
Palghar	Vaitarna	26	25	24	23	21	19	17	16	18	21	23	25
Thane	Ulhas	24	24	23	22	20	17	15	15	17	20	22	24
Raigad	Patalganga-Amba	26	25	24	24	22	20	17	17	19	21	24	26
	Kundalika	26	25	24	24	22	20	18	17	19	21	24	26
	Savitri	24	23	23	22	21	18	16	15	17	20	22	24
Ratnagiri	Vashisthi	25	24	24	23	22	20	18	18	19	21	23	25
	Shastri	25	24	24	23	22	20	18	18	19	22	24	25
	Kajivi	25	24	23	23	22	19	18	18	19	21	23	25
	Muchkundi	24	24	23	23	21	19	17	17	19	21	23	25
	Kodvali	26	25	24	24	23	21	19	20	21	22	24	26
	Waghton	25	24	24	23	22	20	18	19	20	22	24	25
Sindhudurg	Devghar	24	24	23	22	21	19	17	17	18	21	23	25
	Gad	25	24	24	23	22	20	19	19	20	22	24	25
	Karli	25	25	24	24	23	21	19	19	20	22	24	26
	Terekhol	25	25	24	24	23	21	19	19	20	22	24	26
Total		18	25	24	24	23	22	20	18	19	21	24	25

E. Average wind speed monthly data across river basins of Konkan region

District	River basin	Average Monthly wind speed (m/s)											
		June	July	Aug	Sep	Oct	Nov	Dec	Jan	Feb	Mar	Apr	May
Palghar	Vaitarna	3.8	4.1	3.4	2.2	1.7	1.9	2.0	2.1	2.1	2.2	2.3	3.0
Thane	Ulhas	4.0	4.5	3.7	2.4	1.7	1.9	1.9	1.9	2.1	2.2	2.4	3.2
Raigad	Patalganga-Amba	3.7	4.2	3.5	2.4	1.8	2.1	2.1	2.1	2.2	2.3	2.3	2.7
	Kundalika	3.7	4.2	3.6	2.4	1.9	2.1	2.2	2.1	2.2	2.3	2.3	2.7
	Savitri	4.1	4.8	4.1	2.6	2.0	2.1	2.2	2.1	2.2	2.3	2.5	3.1
Ratnagiri	Vashisthi	4.2	4.9	4.2	2.9	2.2	2.4	2.6	2.5	2.6	2.6	2.7	3.2
	Shastri	4.4	5.0	4.4	3.0	2.3	2.5	2.7	2.6	2.7	2.7	2.9	3.3
	Kajivi	4.2	4.8	4.2	2.8	2.1	2.4	2.5	2.4	2.5	2.6	2.8	3.3
	Muchkundi	4.1	4.8	4.1	2.7	2.1	2.3	2.5	2.3	2.4	2.5	2.7	3.2
	Kodvali	4.4	5.0	4.4	3.1	2.3	2.6	2.8	2.7	2.9	2.8	3.0	3.3
	Waghton	4.4	5.0	4.4	3.0	2.3	2.5	2.7	2.6	2.7	2.7	2.9	3.3
Sindhudurg	Devghar	5.2	6.0	5.2	3.6	2.8	3.3	3.5	3.1	3.1	3.1	3.2	3.9
	Gad	5.1	5.8	5.1	3.5	2.7	3.1	3.2	3.1	3.1	3.1	3.2	3.7
	Karli	4.0	4.6	4.0	2.8	2.1	2.3	2.4	2.3	2.5	2.5	2.5	2.9
	Terekhol	4.0	4.6	4.0	2.8	2.1	2.3	2.4	2.3	2.5	2.5	2.5	2.9
Average		4.2	4.8	4.1	2.8	2.1	2.4	2.5	2.4	2.5	2.6	2.7	3.2

Appendix III

Details of Hydrometeorological station and average monthly observed streamflow data across river basins of Konkan region

A) Details of hydrometeorological station of basins

District	River basin	Station name	Latitude	Longitude
Palghar	Vaitarna	Saivan	19.4833	72.98333
Thane	Ulhas	Kalamb	19.0925	73.3919
Raigad	Patalganga-Amba	Pali	18.5311	73.20566
	Kundalika	Mahan	18.5491	73.00076
	Savitri	Kangule	18.07	73.475
Ratnagiri	Vashisthi	Chatav	17.7664	73.54056
	Shastri	Kumbharkhani	17.3222	73.58123
	Kajivi	Pastewadi	16.9758	73.70381
	Muchkundi	Pawarwadi	16.8151	73.63002
	Kodvali	Karak	16.7186	73.7703
	Waghton	Kakewadi	16.6144	73.6667
Sindhudurg	Devghar	Ghansori(L)	16.4007	73.78327
	Gad	Shivadev	16.2598	73.80196
	Karli	Dukanwadi	16.0314	73.88
	Terekhol	Sarambala	15.8649	73.90738

B) Average monthly observed streamflow data across river basins of Konkan region

District	River basin	Station name	Average Monthly streamflow (cumec)			
			July	Aug	Sep	Oct
Palghar	Vaitarna	Saivan	131.86	126.24	74.12	30.55
Thane	Ulhas	Kalamb	35.37	40.22	28.11	11.53
Raigad	Patalganga-Amba	Pali	94.05	90.76	36.41	23.91
	Kundalika	Mahan	14.43	12.03	13.18	13.19
	Savitri	Kangule	140.38	105.58	33.19	18.10
Ratnagiri	Vashisthi	Chatav	11.50	8.01	3.33	1.94
	Shastri	Kumbharkhani	19.08	16.35	5.96	2.88
	Kajivi	Pastewadi	11.07	13.49	8.52	10.62
	Muchkundi	Pawarwadi	32.61	31.18	20.54	10.62
	Kodvali	Karak	65.59	62.93	31.06	17.91
	Waghton	Kakewadi	4.06	3.25	2.05	1.53
Sindhudurg	Devghar	Ghansori(L)	22.19	19.22	8.87	5.47
	Gad	Shivadev	168.55	120.42	60.27	7.98
	Karli	Dukanwadi	53.35	48.00	26.67	12.49
	Terekhol	Sarambala	24.05	22.65	9.32	6.55

Appendix IV

Details of calibration parameters

1) Vaitarna River

Sr. No	Parameter Name	Min_Value	Max_Value	Fitted_Value
1	r_CH2.mgt	-0.2	0.2	0.12
2	v_ALPHA_BF.gw	0.0	1.0	0.75
3	v_GE_DELAY.gw	30.0	450.0	215.48
4	v_GWQMN.gw	0.0	2.0	0.42

2) Ullas River

Sr. No	Parameter Name	Min_Value	Max_Value	Fitted_Value
1	r_CH2.mgt	-0.2	0.2	0.13
2	v_ALPHA_BF.gw	0.0	1.0	0.15
3	v_GE_DELAY.gw	30.0	450.0	111.75
4	v_GWQMN.gw	0.0	2.0	0.15

3) Patalganga-Amba

Sr. No	Parameter Name	Min_Value	Max_Value	Fitted_Value
1	r_CH2.mgt	-0.2	0.2	0.12
2	v_ALPHA_BF.gw	0.0	1.0	0.88
3	v_GE_DELAY.gw	30.0	450.0	443.69
4	v_GWQMN.gw	0.0	2.0	0.99

4) Kundalika River

Sr. No	Parameter Name	Min_Value	Max_Value	Fitted_Value
1	r_CH2.mgt	-0.2	0.2	0.17
2	v_ALPHA_BF.gw	0.0	1.0	0.27
3	v_GE_DELAY.gw	30.0	450.0	218.99
4	v_GWQMN.gw	0.0	2.0	0.34

5) Savitri River

Sr. No	Parameter Name	Min_Value	Max_Value	Fitted_Value
1	r_CH2.mgt	-0.2	0.2	0.17
2	v_ALPHA_BF.gw	0.0	1.0	0.971
3	v_GE_DELAY.gw	30.0	450.0	263.94
4	v_GWQMN.gw	0.0	2.0	0.16

6) Vashisthi River

Sr. No	Parameter Name	Min_Value	Max_Value	Fitted_Value
1	r_CH2.mgt	-0.2	0.2	0.18
2	v_ALPHA_BF.gw	0.0	1.0	0.17
3	v_GE_DELAY.gw	30.0	450.0	157.91
4	v_GWQMN.gw	0.0	2.0	0.3

7) Shastri River

Sr. No	Parameter Name	Min_Value	Max_Value	Fitted_Value
1	r_CH2.mgt	-0.2	0.2	0.023
2	v_ALPHA_BF.gw	0.0	1.0	0.19
3	v_GE_DELAY.gw	30.0	450.0	135.45
4	v_GWQMN.gw	0.0	2.0	1.27

8) Kajivi River

Sr. No	Parameter Name	Min_Value	Max_Value	Fitted_Value
1	r_CH2.mgt	-0.2	0.2	0.18
2	v_ALPHA_BF.gw	0.0	1.0	0.09
3	v_GE_DELAY.gw	30.0	450.0	348.77
4	v_GWQMN.gw	0.0	2.0	0.71

9) Muchkundi River

Sr. No	Parameter Name	Min_Value	Max_Value	Fitted_Value
1	r_CH2.mgt	-0.2	0.2	0.18
2	v_ALPHA_BF.gw	0.0	1.0	0.07
3	v_GE_DELAY.gw	30.0	450.0	326.09
4	v_GWQMN.gw	0.0	2.0	1.89

10) Kodvali river

Sr. No	Parameter Name	Min_Value	Max_Value	Fitted_Value
1	r_CH2.mgt	-0.2	0.2	0.18
2	v_ALPHA_BF.gw	0.0	1.0	0.55
3	v_GE_DELAY.gw	30.0	450.0	219.0
4	v_GWQMN.gw	0.0	2.0	0.7

11) Waghton River

Sr. No	Parameter Name	Min_Value	Max_Value	Fitted_Value
1	r_CH2.mgt	-0.2	0.2	0.18
2	v_ALPHA_BF.gw	0.0	1.0	0.92
3	v_GE_DELAY.gw	30.0	450.0	158.00
4	v_GWQMN.gw	0.0	2.0	1.25

12) Devghar River

Sr. No	Parameter Name	Min_Value	Max_Value	Fitted_Value
1	r_CH2.mgt	-0.2	0.2	0.11
2	v_ALPHA_BF.gw	0.0	1.0	0.45
3	v_GE_DELAY.gw	30.0	450.0	210.0
4	v_GWQMN.gw	0.0	2.0	0.8

13) Gad River

Sr. No	Parameter Name	Min_Value	Max_Value	Fitted_Value
1	r_CH2.mgt	-0.2	0.2	0.19
2	v_ALPHA_BF.gw	0.0	1.0	0.76
3	v_GE_DELAY.gw	30.0	450.0	132.00
4	v_GWQMN.gw	0.0	2.0	1.90

14) Karli River

Sr. No	Parameter Name	Min_Value	Max_Value	Fitted_Value
1	r_CH2.mgt	-0.2	0.2	0.16
2	v_ALPHA_BF.gw	0.0	1.0	0.45
3	v_GE_DELAY.gw	30.0	450.0	131.26
4	v_GWQMN.gw	0.0	2.0	1.61

15) Terekhol River

Sr. No	Parameter Name	Min_Value	Max_Value	Fitted_Value
1	r_CH2.mgt	-0.2	0.2	0.14
2	v_ALPHA_BF.gw	0.0	1.0	0.88
3	v_GE_DELAY.gw	30.0	450.0	298.0
4	v_GWQMN.gw	0.0	2.0	0.48

THESIS ABSTRACT

This study assesses surface water resource availability in the Konkan region, Maharashtra, by employing various methods and models to analyse hydrological patterns, water surplus, and deficit conditions. Water is central to sustainable development, supporting socioeconomic growth, agriculture, ecosystems, and human survival. With increasing water demand due to population growth, urbanization, and agricultural and industrial expansion, effective water management is crucial. The Konkan region relies heavily on monsoon precipitation, with surface runoff generated from this rainfall serving as the primary source for agriculture and development. However, significant shifts in precipitation patterns have been observed, including an increase in rainfall intensity but a decrease in duration, leading to both flooding and water scarcity during the summer. This variability in climatic parameters affects annual and intra-annual water resource availability, making basin-scale assessment critical for sustainable water management. The Konkan region, located along the Arabian Sea coastline, is a distinct physiographic entity with a rugged terrain, consisting of hills, plateaus, and plains, and is separated from upland Maharashtra by the Sahyadri Mountains. The region covers a total geographical area of 3.08 million hectares, about 10% of Maharashtra's total area. Agro-climatically, the Konkan region is characterized by high rainfall (2500-3500 mm) and varying soil types, with medium black soils in the north and lateritic soils with high infiltration in the south. The region is catogrised into five valley i.e Valley 21 to 25 comprising of 15 river basins. The primary objectives of this study were: (1) to evaluate different methods used to assess surface water availability; (2) to analyze the impact of soil, land use, and slope on the temporal and spatial variability of water resources; and (3) to estimate total surface water availability and identify water surplus and deficit conditions. Various methodologies were employed, including direct measurement techniques, velocity-area methods, rainfall-runoff models, and hydrological simulations using the SWAT model.

Direct measurement methods such as the timed-volume and dilution gauging techniques were effective for small streams but limited in scale and duration. Velocity-area methods like the float and current meter techniques provided reliable streamflow estimates in turbulent conditions, although they required specialized equipment. Rainfall-runoff models, such as Cook's Method and the Curve Number (CN) Method, were crucial for estimating runoff in watersheds. Cook's Method, while simple, lacked accuracy when applied outside its region of origin, while the CN Method, widely used due to its integration with Geographic Information Systems (GIS), showed declining performance in larger watersheds. The impact of slope, soil, and land use on water availability was analyzed using various thematic factors, including slope, soil texture, geomorphology, lineament density, rainfall, drainage density, land use land cover (LULC), and runoff depth. The Analytical Hierarchy Process (AHP) model was employed to rank and assign weights to these factors, helping to identify water retention suitability zones. In 2017, the analysis revealed that 11.45% of the area was highly suitable for water retention, 30.32% moderately suitable, 36.65% less suitable, and 21.57% not suitable. By 2019, increased barren land and decreased forest cover resulted in highly

suitable areas increasing to 12.63%, moderately suitable areas to 31.98%, while less suitable areas decreased to 35.71% and not suitable areas to 19.68%. Urbanization, particularly in Thane district, further reduced groundwater recharge, emphasizing the need for targeted water conservation strategies.

Surface water availability in the region was assessed using the ArcSWAT model, which was calibrated and validated using the SWAT-CUP SUFI2 algorithm. Historical data, including rainfall, temperature, relative humidity, and wind speed, were collected from 93 meteorological stations, and river basins were evaluated for water resource availability from 1991 to 2019. The study revealed significant temporal variability in river flow, with the highest flow occurring during the monsoon months of June to September, peaking in July. Evapotranspiration, inversely related to precipitation, peaked during April and May, coinciding with low rainfall, resulting in water deficits from January to May. Conversely, from June to October, evapotranspiration decreased while precipitation peaked, leading to water surplus. A district-wise analysis showed that Sindhudurg recorded the highest annual water surplus (2838 mm), followed by Ratnagiri (2413 mm) and Palghar (1321 mm). The study emphasized the importance of identifying surplus zones and developing strategies to store water for use during the lean season. Conservation structures were suggested, particularly in high runoff zones and flat storage areas, to balance seasonal water availability. The SWAT model demonstrated high accuracy in predicting streamflow and surface water availability, indicating its reliability for future water resource management and planning.

In conclusion, this study highlights the critical role of surface water assessments and hydrological modelling in understanding the spatiotemporal variability of water resources. The findings underscore the need for strategic water conservation efforts, particularly in light of changing land use patterns and increasing water demand in the Konkan region. By integrating advanced modelling techniques with GIS data, the study provides valuable insights for sustainable water management and regional development planning.

Keywords: *Hydrological modelling, Konkan, SWAT, Surface water*

THESIS ABSTRACT

a)	Title of the thesis	:	ASSESSMENT OF SURFACE WATER RESOURCE AVAILABILITY IN RIVER BASINS OF KONKAN REGION
b)	Full name of student	:	Miss. Salvi Akanksha Dipak
c)	Name and address of Major Advisor	:	Dr. R. T. Thokal Chief Scientist, AICRP, IWM and Associate Dean, ATE, DBSKKV, Dapoli
d)	Degree to be awarded	:	M. Tech. (Irrigation and Drainage Engineering)
e)	Year of award of a degree	:	2024
f)	Major subject	:	Irrigation and Drainage Engineering
g)	Total number of pages in the thesis	:	162
h)	Number of words in the abstract	:	811
i)	Signature of student	:	Salvi
j)	Signature, Name and address of forwarding authority	:	Professor and Head Deptt. of Irrigation & Drainage Engg. College of Agril. & Technology Dapoli-415712, Dist-Ratnagiri(M.S)

E-ISSN: 2618-0618
P-ISSN: 2618-060X

www.agronomyjournals.com
2024; 7(12): 113-120
Received: 28-10-2024
Accepted: 02-12-2024

Akanksha D Salvi
PG Scholar, Department of Irrigation and Drainage Engineering, CAET, Dr. BSKKV, Dapoli, Maharashtra, India

RT Thokal
Professor and Head, Department of Irrigation and Drainage Engineering, CAET, Dr. BSKKV, Dapoli, Maharashtra, India

PM Ingle
Professor, Department of Irrigation and Drainage Engineering, CAET, Dr. BSKKV, Dapoli, Maharashtra, India

ST Patil
Associate Professor, Department of Irrigation and Drainage Engineering, CAET, Dr. BSKKV, Dapoli, Maharashtra, India

SS More
Junior Soil Scientist, Regional fruit Research Station, Vengurla, Maharashtra, India

Aniket A Kale
PG Scholar, Department of Irrigation and Drainage Engineering, CAET, Dr. BSKKV, Dapoli, Maharashtra, India

Corresponding Author:
Akanksha D Salvi
PG Scholar, Department of Irrigation and Drainage Engineering, CAET, Dr. BSKKV, Dapoli, Maharashtra, India

Surface water assessment methods and tools for water resource management

Akanksha D Salvi, RT Thokal, PM Ingle, ST Patil, SS More, Aniket A Kale

DOI: https://doi.org/10.33545/2618060X.2024.v7.i12b.2101

Abstract
Assessing surface water availability is important for resources planning and management. Surface water resources are vital for sustainable water management amid growing global water demand driven by population growth, urbanization, and agricultural and industrial expansion. Various methods are used to measure and analyse surface water availability, each with specific strengths and limitations. Direct measurement methods, such as timed-volume and dilution gauging, are accurate for small streams but limited in scale. Velocity-area techniques, including float and current meter methods, provide reliable stream flow estimates but require specialized equipment. Formed constriction methods, such as weirs and flumes, are effective but environmentally disruptive. Rainfall-runoff models like Cook's Method, the Rational Method, and the Curve Number (CN) Method are widely used, though their accuracy varies based on watershed size and characteristics. Hydrological models, including SWAT, HEC-HMS, and MIKE SHE, simulate water movement across watersheds, with SWAT being particularly effective for long-term assessment of both surface and groundwater dynamics, especially in agricultural regions.

Keywords: Assessment methods, surface water, hydrological model

1. Introduction
Water is at the core of sustainable development and is critical for socioeconomic development and the necessity for life, agriculture, healthy ecosystems, and human survival. Water is one of the important natural resources essential for every civilization's survival and livelihood, including food production, access to clean drinking water, sanitation, and hygiene. Adequate water in both quantity and quality underpins health and basic quality of life. It influences the course of a wide variety of ecosystem services. Water availability is the critical link for major development challenges including food security, rapid urbanization, sustainable rural development, disaster risk management, and adaptation to climate change. The planning, development, operation, and maintenance of all the water resources for the security of the population, in response to the growing need for drinking water, industrial production, agricultural products, and electricity, a general improvement of living conditions is of utmost importance. Global water demand has surged by 600% in the last century, currently increasing at the rate of about 1% annually. By 2050, demand is projected to rise by 20-30%, reaching 5,500-6,000 km³ per year. Population growth, especially in Africa and Asia, and urbanization drive this trend. Agricultural water use, presently 70% of the total available water, expected to increase by 60% by 2025 due to increasing food demand. With manufacturing demand quadrupling, industrial water use, now 20% of the total, will significantly increase, especially in Asia. Energy sector water use will rise by 85% by 2050. Domestic water use, currently 10% of total demand, will grow notably, particularly in Asia [1].
In India, approximately 60-70% of the total irrigation water demand is met by groundwater, making it the largest consumer of this resource in the world [2]. As per the latest assessment (2022), the Annual Extractable Ground Water Resource is 398 BCM. The Annual Ground Water Extraction for all uses is 239.16 BCM, out which 208.49 BCM (87%) has been utilized for agriculture activities. However, the over-reliance on groundwater for irrigation has led to a rapid depletion of aquifers. Studies indicate that groundwater levels in major agricultural regions have been declining at an alarming rate of 0.2 to 1 meter per year, with regions like Punjab and Haryana experiencing even higher rates of depletion.

Study conducted in Konkan region shows that region is already facing moderate to poor groundwater potential in nearly 71% of its area. If unregulated extraction continues, aquifers may collapse or become irreversibly depleted, leading to long-term water scarcity [3, 4].

The consequence is a vicious cycle: as groundwater levels drop, farmers are compelled to drill deeper wells, leading to higher energy consumption and increased production costs. Moreover, excessive withdrawal disrupts the natural hydrological balance, leading to land subsidence, reduction in streamflow, and loss of wetlands, which in turn affects biodiversity and ecosystem services [5]. The quality of groundwater is also deteriorating due to contamination from agrochemicals, such as fertilizers and pesticides, which leach into aquifers. High levels of nitrates, heavy metals, and salinity have been reported in many regions, rendering the water unfit for drinking and even irrigation purposes in some cases [6, 62]. Additionally, industrial and domestic effluents further compound the pollution problem, particularly in peri-urban areas where wastewater management is inadequate. Given the critical importance of groundwater, its sustainable management is essential. Restricting groundwater withdrawal is necessary to prevent irreversible damage to aquifers and to ensure long-term water security. Effective policies such as regulated extraction, improved irrigation efficiency through drip and sprinkler systems, and conjunctive use of surface and groundwater can help mitigate the over-extraction issue. Supply-side measures encompass the construction of groundwater recharge structures and improved accessibility to surface irrigation [7]. Ultimately, balancing groundwater withdrawal with natural recharge rates and addressing pollution challenges is crucial for achieving sustainable agricultural productivity and safeguarding water resources for future generations.

Assessing surface water availability is important for resources planning and management. This also can be used to study climate change impact, natural hazards trends as well as different land use and land cover water retention capacity. It also provides information about status and trend in water quality. This also can be used as a tool to understand the contribution of water to economic development and human well-being. Advances in scientific knowledge, along with improvements in measurement and modelling techniques, have emphasized the importance of investigating effective conservation and management strategies for these critical resources [8]. Main objective of this paper is to study various methods used for assessing surface water resource availability and their suitability across different agroecological regions.

2. Different methods of surface water assessment

Streamflow monitoring methods are tailored to different stream types. Stream channels can be classified based on eight major variables width, depth, velocity, discharge, slope, roughness of bed and bank materials, sediment load and sediment size. Various methods exist for quantifying and monitoring surface water flow, categorized as follows [9-11]: (a) direct measurement methods, (b) velocity-area methods, (c) formed constriction or constricted flow methods, (d) Rainfall-Runoff method, and (e) non-contact measurement methods. These methods can be further classed as shown in Table 1.

Table 1: Different methods of surface water assessment

A) Direct measurement methods	B) Velocity-area methods	C) Formed Construction or constricted flow method	D) Rainfall-Runoff method	E) Non-contact measurement method
Timed volume method	Float Method	Weir Method	Rational Method	Particle image velocimetry method
	Dilution Gauging method	Flume Method	Cooks Method	Hydrological Modelling
	Current meter method		Curve Number method	
	Trajectory method		Unit Hydrograph Method	
	Electromagnetic Method		Infiltration Method	
	Acoustic Doppler current profiler method (ADCP)		Empirical Formulae	
	Salt-Velocity Method			

Based on Volume of water to be measured, the degree of accuracy desired, type of installation i.e. permanent or temporary, financial investment required, and availability of data method can be selected for further study.

2.1 Direct measurement method

In this method, known as time-volume method, the flow rate is determined by measuring the time it takes to fill a container of known volume. This technique is particularly useful for streams where the entire flow converges into a single descent. To ensure accuracy and reliability, a large container should be used, and the flow rate should be measured at least five times, with more than three replications across different stream width and depth [12, 13]. The flow rate is then calculated as the ratio of the average stream cross-sectional area to the average time taken to fill the container.

It operates on the time-volume principle and known for being accurate, cost and time-efficient, and environmentally friendly. Additionally, it requires minimal resources and technical expertise [14, 15]. However, this method is best suited for small, narrow streams with uniform cross-sectional area [16, 17].

2.2 Velocity-Area method

Velocity-area methods are based on the principle of fluid flow continuity and are used for instantaneous streamflow measurements and establishing the stage-discharge relationship [18] Discharge and stage measurements are crucial in areas where water management is a priority. This method involves determining the cross-sectional area of the stream flow and the mean velocity, multiplying these values to calculate the stream flow.

The float method is simple, non-polluting, and requires minimal resources, but it is often inaccurate due to vertical turbulence causing differences in surface velocities of flow. It works best in small, straight streams with uniform flow but is unreliable for larger water bodies [19, 20]. The dilution gauging method is effective in turbulent conditions where conventional methods struggle. However, errors may arise due to incomplete mixing or tracer loss, and obtaining permission for tracer use can be challenging due to pollution concerns [21, 22].

The current meter method offers accuracy and efficiency, especially in hilly terrains, but its high cost limits its use to short-term applications [23]. The trajectory method is useful for discharge measurements in diverted flows or small open channels but requires trained personnel and complex calculations [24]. Electromagnetic methods work well in streams up to 70 m wide, though they require specialized training [25]. The ADCP method is fast and accurate for large streams, though expensive and requiring skilled operators. It can be adapted for smaller rivers using tethered boats or catamarans [26, 27].

2.3 Formed construction or constricted flow method

The weir method involves constructing a physical barrier or check-dam in a stream's cross-section to measure discharge. A weir can be made from materials like plywood, wooden boards, or reinforced concrete, and can be either permanent or portable. The water flows over the weir's notch, which may be rectangular, trapezoidal, or triangular. Rectangular and 90° V-notch weirs are most used.

Discharge through the weir is estimated using predefined tables [28] or a weir equation that accounts for flow rate, water head height, and crest width [29, 30]. The weir method is accurate but requires careful installation, skilled operation, and specific conditions, such as a significant water surface drop between the upstream and downstream sides. This method also necessitates the construction of a pool or stilling basin upstream of the weir to slow down water velocity, which can be time-consuming and disruptive to local habitats [31]. The major limitations of the weir method include siltation, which can affect accuracy, and its inability to handle wide flow ranges without using compound weirs. Moreover, it may not easily integrate with other water infrastructure, and a pre-measured flow rate is required before installation [32].

Flumes are artificial open-channel structures that narrow the stream cross-section and alter its slope, increasing the water velocity to calculate discharge. Unlike weirs, flumes do not cause water impoundment, which can reduce flow disruption. Discharge is determined by measuring water height using a stilling well [33], and flow is calculated using standardized tables [34, 35]. There are different types of flumes, each designed for specific uses. For example, HL, H, and HS flumes are used for intermittent runoff, while venturi flumes measure irrigation water, and San Dimas flumes are suited for debris-laden streams [36]. Flumes, when manufactured and installed correctly, offer accurate flow measurements without requiring calibration, but their accuracy can be influenced by water approach velocity and siltation [35]. Flumes are more limited than weirs in terms of the flow range they can measure and are generally suitable for smaller streams. Additionally, the construction and installation of flumes are more challenging compared to weirs, especially in areas with debris or high sediment loads.

Ultrasonic gauging measures water velocity by transmitting sound waves across the stream and recording the time differences between sound pulses. This method is particularly useful in rivers up to 300 meters wide, where constructing a physical structure would be impractical or too costly. It is ideal in conditions where backwater effects, such as tides or dams, influence water flow. However, the ultrasonic method can be affected by factors like an unstable cross-section, fluctuating weed growth, suspended solids, and changes in water temperature or salinity, all of which can alter signal velocity and flow measurements. Calibration is often performed using the current-meter method. The choice of flow measurement method depends on stream characteristics and operational requirements. While weirs and flumes offer precise flow measurement for smaller streams, they require careful installation and can be limited by site conditions. The ultrasonic method, though less intrusive, may face accuracy challenges in certain environments.

2.4 Rainfall-Runoff method

This category includes methods such as Rational Method, Cook's Method, Curve Number Method, Unit Hydrograph, and various empirical formulae, including Runoff Coefficient Method, Inglis Method, Khosla's method. Rational method is suitable for small watershed area, where it is easier to account for variations in hydrological responses. This method is usually used to calculate peak runoff rate from small watershed. It involves formula for computing design runoff

$Q_{Peak} = 1/360 \times (CIA)$

Where, Q_{Peak} is peak runoff rate, m^3/s; C = runoff coefficient; I is rainfall intensity, mm/h, for duration equal to time of concentration and given recurrence interval; and A is watershed area, ha However, it has limitations, as it assumes constant rainfall intensity over the entire watershed during the storm, which is not common. It also neglects losses due to declining storage and infiltration. Additionally, the runoff coefficient used in this method does not account for seasonal variations or changes in rainfall characteristics. One of the primary drawbacks of the Rational Method is that it typically provides only a single point on the runoff hydrograph.

Cook's Method is an empirical approach to estimating peak runoff rates based on the characteristics of a watershed. The method evaluates four key factors: relief, infiltration rate, vegetation cover, and surface storage, assigning numerical values to each characteristic based on their similarity to other watersheds with known conditions. The sum of these values ($\sum W$) is used to calculate an initial, uncorrelated runoff value from a runoff curve. This method is relatively simple and accessible to practitioners with limited hydrological expertise. It relies on numerical values derived from watersheds with similar conditions. As an empirical method, it is based on observations rather than theoretical principles, which can limit its accuracy if local conditions differ significantly from those used to develop the method.

The Curve Number method computes the direct runoff or excess, Strom wise. This method is based on potential retention capacity of watershed, which is determined based on antecedent moisture condition and physical characteristics of watershed. This method assumes that the ratio of direct runoff to rainfall depth minus initial losses (interception, infiltration, depression storage etc) is equal to ratio of actual retention of rainfall to retention capacity. It is widely accepted due to its simplicity and minimal input requirements. It has been successfully applied in various hydrological studies and engineering projects. Based on extensive empirical data and field observations, this method is reliable for a range of agricultural conditions, soil types, land uses and moisture levels. It also integrates with Geographic Information System (GIS) for spatial analysis and large-scale hydrological modelling however, the method is sensitive to the choice of curve number, leading to potential variability in runoff estimates. Additionally, it assumes uniform rainfall distribution across the catchment, which is often unrealistic. The method may not be suitable for large or highly urbanized watersheds where hydrological processes are more complex.

The Unit Hydrograph (UH) is a fundamental concept in hydrology used to describe the temporal distribution of runoff generated by a unit volume of effective rainfall (typically 1 cm)

distributed uniformly over a watershed area. It helps in predicting the runoff hydrograph resulting from any given rainfall event. In this method portion of the total rainfall that contributes to runoff after accounting for losses like infiltration and evaporation is calculated. Then a hydrograph that represents runoff from a unit depth of effective rainfall distributed evenly over the watershed for a specific duration is created. Runoff hydrograph is derived from applying unit hydrograph to the actual effective rainfall using convolution [47]. This method is suitable for small to medium-sized watersheds (more than 25 km^2) and assumes uniform rainfall distribution and homogenous watershed characteristics. It is particularly useful in areas where rapid runoff response is important for flood forecasting and management. However, the assumption of uniform distribution makes it less applicable for large or heterogenous watersheds. This method is not recommended for large, urbanized watersheds with significant spatial variability in rainfall and land use, or where detailed physical modelling is required.

2.5 Non-contact measurement methods

These methods are based on the principle of radar system and may be used to make continuous, near-real-time flow measurements during high and medium flows.

Particle Image Velocimetry (PIV) is a widely used non-contact technique for measuring fluid flow velocity by tracking the movement of small tracer particles within the fluid. These particles, typically light and small enough to accurately follow the local fluid velocity, are illuminated by a laser light sheet, which scatters light that is captured by a high-resolution CCD camera [37, 38]. In most applications, tracer particles are added to the fluid to ensure that they closely follow the flow dynamics [39]. The fluid is illuminated twice, with a short time interval between two superimposed laser pulses. This creates two consecutive exposures of the fluid flow, captured by the CCD sensor [40]. The time interval between the laser pulses, combined with the camera calibration data (including image magnification and projection of the local velocity vector), defines small interrogation areas within the recorded images. For each interrogation area, the particle displacement is computed as the distance between the particle positions in the two consecutive images. The velocity of the fluid is then calculated by dividing the particle displacement by the time interval between the laser pulses [41]. PIV provides detailed, high-resolution flow velocity data over a two-dimensional plane at a specific moment in time, making it a valuable tool for flow analysis [42]. However, the method requires specialized equipment and training and is generally best suited for flat terrains [44]. Despite its precision, PIV does not involve direct measurement, necessitating result validation through other methods [45].

Traditional method for assessing natural resources is often cumbersome, time-consuming and not cost-effective. Geographic Information System have emerged as a proven technology for site-specific assessment and planning of water and land resources. GIS is now integrated with various hydrological models to assess and simulate land and water resources in areas of interest.

Hydrological modelling is a vital tool in hydrology used to estimate the movement, distribution, and quality of water within a watershed. By applying mathematical models and incorporating remote sensing data, hydrologists can replicate the hydrological cycle and predict water flow and storage across various environmental components. A model is simplified representation of real-world system, and the best model is one that closely approximates reality while minimizing the number of parameters and complexity. Models are primarily used for predicting system behaviour and gaining insights into different hydrological processes. The selection of a hydrological model depends on the purpose of study, data availability and the model's capability and suitability for both small and larger catchment hydrologic applications. Hydrological models vary in terms of input parameters and the extent of physical principles they incorporate. Models can be classified based on model input, parameters and the degree to which they incorporate physical principles. They can be classified as lumped and distributed models based on the whether parameters are a function of space and time, and into deterministic and stochastic models depending on how uncertainty is handled with specific details provided in Table 2.

Table 2: Distinguishing characteristics of different models [46]

Parameters	Empirical Model	Conceptual Model	Physically based model
Type	Data based or black box model	Parametric or grey box model	Mechanistic or white box model
Based On	Mathematical equations, derived values from available time series	Model of reservoirs and on physical basis include semi-empirical equations	Spatial distribution based, evaluation of parameters describing physical characteristics
Consideration	Little consideration of features and process system	Parameter derived from field data and calibration	Require data about initial state of model and morphology of catchment
Features	High predictive power, low explanatory depth	Simple and can be easily implemented in computer code	Complex model, requires human expertise and computation capability
Limitations	Cannot be generated to other catchments	Require large hydrological and meteorological data	Suffer from scale related problems
Examples	ANN, Unit hydrograph	TOPMODEL, HBV model	SHE or MIKE SHE models, SWAT
Other	Valid within the boundary of given domain	Calibration is involved, curve fitting makes difficult physical interpretation	Valid for wide range of situations

2.5.1 Variable Infiltration Capacity Model (VIC Model)

VIC Model is a semi distributed, macro-scale, grid-based hydrology model that incorporates both energy and water balance equations. The primary inputs for the model include precipitation, daily minimum and maximum temperatures, and wind speed. The model allows for multiple land cover types within each model grid cell. Key hydrological processes such as infiltration, runoff, and base flow are modelled using various empirical relationships. Surface runoff is generated through two mechanisms: infiltration-excess runoff (Hortonian flow) and saturation excess runoff (Dunne flow). The VIC model simulates saturation-excess runoff by accounting for soil heterogeneity and precipitation patterns [48]. It incorporates the representation of sub-grid variability of precipitation with representation of spatial variability of infiltration to simulate energy and water budget.

VIC model is coupled with simple grid-based network which shows it perform well in moist area [49]. VIC model represents sub-grid variability in soil moisture storage capacity as a spatial

probability distribution which is related to surface runoff [50]. VIC Model applied this model for irrigation planning in small watershed and found that it can be efficiently used for management of water for agricultural purposes [51]. VIC model applied on Ashti catchment to assesses the impact of LULC change and rainfall trend on hydrological model [52].

Various hydrological models are available that integrate GIS interface, including HEC-HMS, VIC, MIKE SHE, WEAP and SWAT. Specifications of these models are given in Table 3.

Table 3: Hydrologic models with their specifications [46]

Model	HEC-HMS	Swat	Mike	Vic
Advantage	Focus on runoff, channel routing and water control structures	Focus on water quantity, quality and representation of groundwater	Simulates complete land phase of hydrologic cycle	Sub grid variability, Macroscale model, large scale effect
Limitations	Suitable only for events and not for long-term hydrological simulations	Snow process representation requires improvement	Simplified representation of forest cover	Large grid size, does not consider urban class in LULC
Runoff	Empirical	Empirical	Physical	Physical
Baseflow/ Groundwater	Empirical	Empirical	Physical	Physical
Watershed Scale	Small to Large	Small to Large	Small to Large	Medium to Large
Climate Regime	Rain or snow	Rain or snow	Rain or snow	Rain or snow/Mixed
Output	FH, AY, PF, LF, SW, ET, WB, SM, IF, OF, SF, GF, RO	FH, AY, PF, LF, SW, ET, WB, SM, IF, OF, SF, GF, RO, SE, NF, WQ	FH, AY, PF, LF, SW, ET, WB, SM, IF, OF, SF, GF, RO, WQ	FH, AY, PF, LF, SW, ET, WB, SM, IF, OF, SF, GF, RO

FH = Full hydrograph, AY = Annual Yield, PF = Peak Flow, LF = Low flow, SW = Snow water equivalent, ET = Evapotranspiration, WB = Water balance, SM = Soil moisture, IF = Infiltration, WT = Water Table, OF = Overland flow, SF= Shallow subsurface flow, GF = Groundwater flow, RO = Basin total runoff, SE = Sediment soil erosion, NF = Nutrient Fluxes, WQ = Water quality

2.5.2 MIKE SHE model (System Hydrologique European)

The model developed in 1990, is physically based and thus requires extensive physical parameters. It simulates various processes of the hydrological cycle, including precipitation, evapotranspiration, interception, river flow, saturated ground water flow, unsaturated ground water flow. The model is capable of simulating surface and groundwater movement, their interactions, and transport of sediment, nutrient and pesticides within the model area. It is also useful for addressing various water quality issues and can be applied to large watersheds. The model includes pre-processing and post-processing modules and offers various options for displaying results.

Yang *et al* (2000) compared three models and suggested that MIKE SHE model can be used in smaller catchments [53]. MIKE SHE requires extensive model data and physical parameter which may not be available all the time and make it difficult to set up model. It has extensive graphical capabilities for pre and post processing.

2.5.3 HEC-HMS (HEC-Hydrological Modelling System)

The HEC Hydrological Modelling System (HMS) is a conceptually lumped and straightforward model that requires a few parameters, most of which can be derived from land cover data. It is sensitive to land cover changes and provides a convenient platform for simulating rainfall-runoff processes, as well as impacts assessing the impacts of land use and land cover changes. The model mainly focusses on runoff, channel routing and water control structures. HEC-HMS consists of three components: the basin model, the meteorological model and control specifications. These components offer various options for simulating different hydrological processes at lumped scales.

2.5.4 Water Evaluation and Planning (WEAP)

The Water Evaluation and Planning (WEAP) system, along with integrated hydrology models, has a long history of development and application in the water planning, effectively addressing the complex dynamics of water system. WEAP can be applied at local scales as well as in more complex river basin systems. It operates on the fundamental principle of water balance accounting. The model's hydrologic processes can be utilized as both forecasting tool and a policy analysis tool.

2.5.5 Soil and Water Assessment Tool (SWAT)

SWAT is complex physically is a complex, physically based model designed to simulate and forecast water and sediment circulation, as well as agricultural production and chemical transport in ungauged basins. It is highly efficient for performing long-term simulations. The model divides the entire catchment into sub-catchments, which are further broken down into Hydrologic Response Units (HRUs) based on land use, vegetation and soil characteristics. The model utilizes daily inputs of rainfall, maximum and minimum air temperatures, solar radiation, relative humidity and wind speed to describe water and sediment circulation, vegetation growth and nutrients dynamics. Snowfall rates can be determined based on precipitation levels and mean daily air temperatures. For estimating evapotranspiration, SWAT employs methods such as Penman Monteith, Priestly-Taylor and Hargreaves. Accurate forecasting of water, nutrient and sediment circulation requires simulating the hydrologic cycle, which integrates overall water circulation in the catchment area, and SWAT uses the following water balance equation for this purpose.

$$SW_t = SW_0 + \sum_{i=0}^{t}(R_v - Q_s - W_{seepage} - ET - Q_{gw})$$

Where, SW_t is humidity of soil; SW_0 is base humidity; R_v is rainfall volume in mm water; Qs is surface runoff; $W_{seepage}$ is seepage of water from soil to underlying layers; ET is evapotranspiration; Q_w is groundwater runoff and t is time in days.

Soil Water Assessment Tool (SWAT) model, developed by the USDA Agricultural Research Service in collaboration with Texas Agricultural University, is widely regarded as a reliable tool for basin-scale studies [55]. This GIS-based interface is universally adopted for various works such as water and land resource planning, water quality analysis, crop planning, and water budgeting, provided proper calibration and validation are conducted [57]. The Arc SWAT model has been applied across diverse regions, watershed scales, climatic zones, environmental conditions and management systems globally, showcasing its capacity for quantitative evaluating hydrological regimes and water resources [56].

SWAT offers comprehensive capabilities for assessing and modelling surface water, groundwater dynamics, soil water, snow processes, irrigation systems, impoundment and water management strategies. It also evaluates water quality by analysing nonpoint-source pollution, sediment transport and losses. Furthermore, SWAT is effective in assessing the impact of best management practices (BMPs) in agriculture, urban settings and land use changes. It can evaluate the effects of global and regional climate change and human activities such as land-use expansion, deforestation, and unsustainable water use on hydrological balance components.

The model estimates daily overland flow for each Hydrologic Response Unit (HRU) by resolving water budget components, including precipitation, runoff, evapotranspiration, percolation, and groundwater flow. SWAT conceptualizes landscapes as large fields (HRUs) with uniform soil and vegetation sloping towards streams, though real-world flow paths are often more complex. HRUs, which represent unique combination of land use, soil type and slope, dictate hydrologic responses. SWAT partitions daily rainfall into infiltration and runoff using a modified curve-number method and calculates evapotranspiration based on soil moisture and climate. It also accounts for runoff interception by ponds and wetlands within subbasins.

Compared to other land surface models, the following are the distinguishing hydrologic features of SWAT model:

- SWAT divides watersheds into sub-basins, which are further subdivided into hydrologic response units (HRUs) based on land use, soil type, and slope. This approach allows for a detailed spatial representation of the watershed characteristics [57].
- SWAT can integrate various climate change scenarios and LULC changes to evaluate their impacts on hydrology and water resources, making it a valuable tool for assessing the effect of both climate change and LULC changes in related studies [58].
- SWAT integrates surface water and groundwater interactions, enabling a comprehensive assessment of water movement, storage and dynamics within the watershed. This can be used for gauged as well as ungauged river basin.
- SWAT has capability to model urban hydrology, accounting for the effects of impervious surfaces, stormwater runoff, and the implementation of urban best management practices [59].
- It provides a user-friendly interface and extensive documentation, making it accessible to a broad range of users, including researchers to practitioners [60].

3. Conclusion

Effective assessment of surface water resources is critical for sustainable water management, particularly considering increasing global water demand due to population growth, urbanization, and agricultural and industrial expansion. Various methodologies are employed to measure and analyse surface water availability, each with specific applications, advantages, and limitations. Direct measurement methods, such as the timed-volume and dilution gauging techniques, offer accurate, cost-effective solutions for small streams but are limited in scale and duration. Velocity-area methods, including float and current meter techniques, are widely used for streamflow estimation and provide reliable results in turbulent conditions, though they require specialized equipment. Formed constriction methods, such as weirs and flumes, accurately measure discharge in small to medium-sized streams but can disrupt ecosystems and are sensitive to site-specific factors.

Rainfall-runoff models, including Cook's Method, the Rational Method, and the Curve Number (CN) Method, are essential for runoff estimation in watersheds. Cook's Method is a simple empirical approach, though it lacks accuracy when applied outside its region of origin. The Rational Method, suitable for small watersheds, is limited by its assumption of constant rainfall intensity. The CN Method is widely used due to its simplicity and integration with Geographic Information Systems (GIS), though its performance declines in larger watersheds. The Unit Hydrograph (UH) method effectively predicts runoff hydrographs for rainfall events, making it valuable for flood forecasting in small to medium-sized watersheds. Hydrological models, such as SWAT, HEC-HMS, and MIKE SHE, simulate water movement and storage across watersheds, integrating GIS data for enhanced analysis. SWAT is particularly effective for long-term simulation of both surface and groundwater dynamics and is widely used to assess watershed responses to land-use and climate changes, especially in agricultural regions.

4. Disclaimer (Artificial Intelligence)

Author(s) hereby declare that generative AI technologies such as Large Language Models, etc. have been used during the writing or editing of manuscripts. This explanation will include the name, version, model, and source of the generative AI technology and as well as all input prompts provided to the generative AI technology.

5. Reference

1. Boretti A, Rosa L. Reassessing the projections of the World Water Development Report. NPJ Clean Water. 2019;2:15. https://doi.org/10.1038/s41545-019-0039-9
2. Pandey V, Singh K, Ahmad N, Srivastava S. Challenges and issues of groundwater management in India. Curr Sci. 2022;123:856-864. https://doi.org/10.18520/cs/v123/i7/856-864
3. Gavit SB, Bhange HN, Ayare BL, Patil ST, Kolhe PR. Identification of groundwater potential zones in Wakawali watershed using remote sensing and geographic information system (GIS). Int J Environ Climate Change. 2024;14(8):333-346. Available: https://doi.org/10.9734/ijecc/2024/v14i8435
4. Kale AA, Thokal RT, Ingle PM, Bhange HN, Meshram NA, Salvi AD, *et al*. Assessment of groundwater potential zones in the Konkan region using geospatial techniques. Int J Environ Climate Change. 2024;14(10):285-305. https://doi.org/10.9734/ijecc/2024/v14i104487.
5. Konikow LF, Kendy E. Groundwater depletion: A global problem. Hydrogeol J. 2005;13(1):317-320.
6. Rao NS, *et al*. Groundwater quality and pollution in India. Environ Monit Assess. 2020;192(3):115.
7. Foster SSD. Groundwater: the processes and global significance of aquifer degradation. Phil Trans R Soc Lond B. 2003;358:1957-1972. http://doi.org/10.1098/rstb.2003.1380
8. Kalbus E, Reinstorf F, Schirmer M. Measuring methods for groundwater-surface water interactions: A review. Hydrol Earth Syst Sci. 2006;10:873-887. https://doi.org/10.5194/hess-10-873-2006
9. John PH. Discharge measurement in lower order streams. Int Rev Gesamte Hydrobiol Hydrogr. 1978;63(6):731-755.
10. Martin EC. Measuring water flow in surface irrigation

ditches and gated pipe. Cooperative Extension Pub No AZ1329, Arizona Water Series No 31, The University of Arizona, 2006.
11. Herschy RW. Streamflow measurement. 3rd ed. Taylor and Francis, 2008.
12. Ely E. A profile of volunteer monitoring. Volunteer Monitor. 1994;6(1):4.
13. Pfeffer MJ, Wagenet LP. Volunteer environmental monitoring knowledge creation and citizen-scientists interaction. In: Pretty J, Ball A, *et al*. The Sage Handbook of Environment and Society. Sage Publications, 2007.
14. Friederich H, Smart PL. The classification of autogenic percolation waters in karst aquifers: A study in GB cave Mendip hills England. Proc Univ Bristol Spelaeol Soc. 1982;16(2):143-159.
15. Najafi MR, Moradkhani H, Piechota TC. Ensemble streamflow prediction: climate signal weighting methods vs climate forecast system reanalysis. J Hydrol. 2012;442:105-116.
16. Weight WD, Sonderegger JL. Manual of applied field hydrogeology. McGraw-Hill, 2001.
17. Shope CL, Bartsch S, Kim K, Kim B, Tenhunen J, Peiffer S, *et al*. A weighted, multimethod approach for accurate basin-wide streamflow estimation in an ungauged watershed. J Hydrol. 2013;494:72-82.
18. Harmel RD, Smith DR, King KW, Slade RM. Estimating storm discharge and water quality data uncertainty: a software tool for monitoring and modelling applications. Environ Model Software. 2009;24(7):832-842.
19. Hilgersom KP, Luxemburg WMJ. Technical Note: How image processing facilitates the rising bubble technique for discharge measurement. Hydrol Earth Syst Sci. 2012;16:345-356. https://doi.org/10.5194/hess-16-345-2012
20. Hudson NW. Field measurements of soil erosion. Food and Agriculture Organization of the United Nations; Rome, 1993.
21. Gordon ND, McMahon TA, Finlayson BL, Gippel CJ. Stream hydrology: an introduction for ecologists. 2nd Ed. Wiley, 2004.
22. Moore RD. Introduction to salt dilution gauging for streamflow measurement-part 2. Constant-rate Inject. 2004;8(1):11-15.
23. United States Geological Survey (USGS). How streamflow is measured? The discharge measurement. US Department of the Interior, 2007.
24. Boman B, Shukla S. Water measurement for agricultural irrigation and drainage systems. Agricultural and Biological Engineering Department, Florida Cooperative Extension Service, University of Florida, 2009.
25. Gent VMRA, Vries DJVT, Coeveld EM, Vroeg DJH, Graaff VDJ. Large-scale dune erosion tests to study the influence of wave periods. Coastal Eng. 2008;55(12):1041-1051.
26. Flener C, Wang Y, Laamanen L, Kasvi E, Vesakoski JM, Alho P. Empirical modeling of spatial 3D flow characteristics using a remote-controlled ADCP system: monitoring a spring flood. Water. 2015;7(1):217-247.
27. Herschy RW. Streamflow measurement. 3rd ed. Taylor and Francis, 2008.
28. British Columbia. Water supply factsheet. Ministry of Agricultural and Lands; Abbotsford, British Columbia, 2006.
29. Ghodsian M. Supercritical flow over a rectangular side weir. Can J Civ Eng. 2003;30:596-600.
30. Emiroglu ME, Bilhan O, Kisi O. Neural networks for estimation of discharge capacity of triangular labyrinth side weir located on a straight channel. Expert Syst Appl. 2011;38(1):867-874.
31. Rickard C, Day R, Purseglove J. River weirs-good practice guide. R&D Publication; Bristol, UK; 2003.
32. Martin EC. Measuring water flow in surface irrigation ditches and gated pipe. Cooperative Extension Pub No AZ1329, Arizona Water Series No 31, The University of Arizona, 2006.
33. Mutz M, Kalbus E, Meinecke S. Effect of in-stream wood on vertical water flux in low-energy sand bed flume experiments. Water Resour Res. 2007;43:10.
34. Bos MG. Discharge measurement structures. Publication 20. International Institute for Land Reclamation and Improvement (ILRI); Wageningen, 1976.
35. Hudson JA. The impact of sediment on open channel flow measurement in selected UK experimental basins. J Flow Measure Instrum. 2004;15(1):49-58.
36. United States Fish and Wildlife Services (USFWS). Water measurement Mountain-Prairie region. Water Resources Division; United States of America, 2006.
37. Prasad AK. Particle image velocimetry. Curr Sci. 2000;79(1):51-60.
38. Tauro F, Olivieri G, Petroselli A, Porfiri M, Grimaldi S. Flow monitoring with a camera: a case study on a flood event in the Tiber River. Environ Monit Assess. 2016;188(2):1-11.
39. Brossard C, Monnier JC, Barricau P, Vandernoot FX, Le Sant Y, Champagnat F, Le Besnerais G. Principles and applications of particle image velocimetry. Aerosp Lab J. 2009;1:1-11.
40. Bosbach J, Kühn M, Wagner C. Large scale particle image velocimetry with helium filled soap bubbles. Exp Fluids. 2009;46(3):539-547.
41. Harpold AA, Mostaghimi S, Vlachos PP, Brannan K, Dillaha T. Stream discharge measurement using a large-scale particle image velocimetry (LSPIV) prototype. Trans ASABE. 2006;49(6):1791-1805.
42. Stamhuis EJ. Basics and principles of particle image velocimetry (PIV) for mapping biogenic and biologically relevant flows. Aquat Ecol. 2006;40(4):463-479.
43. Adrian RJ, Westerweel J. Particle image velocimetry. Vol. 30. Cambridge University Press; Cambridge; 2011.
44. Hauet A, Creutin JD, Belleudy P. Sensitivity study of large-scale particle image velocimetry measurement of river discharge using numerical simulation. J Hydrol. 2008;349(1):178-190.
45. Devia GK, Ganasri BP, Dwarakish GS. A review on hydrological models. Aquatic Procedia. 2015;4:1001-1007.
46. Beckers J, Smerdon B, Wilson M. Review of hydrologic models for forest management and climate change applications in British Columbia and Alberta. Forum for Research and Extension in Natural Resources Society (FORREX) Series 25; Kamloops, British Columbia, Canada, 2009.
47. Suresh R. Soil and water conservation engineering. 1st Ed. A.K. Jain Standard Publishers Distributors; Delhi, ISBN: 978-81-8014-186-7, 2020, p. 27-32.
48. Liang X, Xie ZH. Important factors in land-atmospheric interactions: surface runoff generations and interactions between surface and groundwater. Global Planet Change. 2003;38(1-2):101-114.
49. Nijssen B, Lettenmaier DP, Xu L, Wetzel SW, Wood EF.

Streamflow simulation for continental-scale river basins. J Geophys Res. 1997;102(D16):19599-19617.
50. Zhao RJ, Zhang YL, Fang LR, *et al*. The Xinanjiang model. In: Hydrological Forecasting Proceedings, Oxford Symposium, IAHS, International Association of Hydrological Sciences Press; Wallingford, UK, 1980, p. 351-356.
51. Singh R, Subramanian K, Refsgaard JC. Hydrological modelling of a small watershed using MIKE SHE for irrigation planning. Agric Water Manag. 1999;41:149-166.
52. Hengade N, Eldho T. Assessment of LULC and climate change on the hydrology of Asthi Catchment, India using VIC Model. J Earth Syst Sci. 2016;125:1623-1634.
53. Yang D, Herath S, Musiake K. Comparison of different distributed hydrological models for characterizations of catchment spatial variability. J Hydrol Procedia. 2000;14(3):403-416.
54. Arnold JG, Moriasi DN, Gassman PW, Abbaspour KC, White MJ, Srinivasan R, *et al*. SWAT: Model use, calibration, and validation. Trans ASABE. 2012;55(4):1491-1508.
55. Gassman PW, Sadeghi AM, Srinivasan R. Applications of the SWAT Model Special Section: Overview and insights. J Environ Qual. 2014;43:1-8.
https://doi.org/10.2134/jeq2013.11.0466
56. Krysanova V, White M. Advances in water resources assessment with SWAT: An overview. Hydrol Sci J. 2015;60(5):771-783.
DOI: 10.1080/02626667.2015.1029482
57. Arnold JG, Srinivasan RSM, Williams JR. Large-area hydrologic modelling and assessment: Part I. Model development. J Am Water Resour Assoc. 1998;34(1):73-89.
58. Gassman PW, Reyes MR, Green CH, Arnold JG. The Soil and Water Assessment Tool: Historical development, applications, and future research directions. Economics Publications, 2007, 28.
59. Bosch DD, Arnold JG, Martin V, Allen PM. Simulation of a low-gradient coastal plain watershed using the SWAT landscape model. Trans ASABE. 2010;53(5):1445-1456.
60. Neitsch SL, Arnold JG, Kiniry JR, Srinivasan R, Williams JR. Soil and Water Assessment Tool Theoretical Documentation Version 2009. Temple, Tex.: Grassland, Soil and Water Research Laboratory, 2009.
61. Central Ground Water Board (CGWB). National Compilation on dynamic ground water resources of India; 2023. Available: www.cgwb.gov.in
62. Ingle P. Appraisal of ground water quality to estimate its appropriateness for use. 2018;21-24.
63. Badgujar GB, Sawant ST, Mahale DM. Groundwater study of Priyadarshini Watershed in Ratnagiri District, Maharashtra, India.

Dr. Balasaheb Sawant Konkan Krishi Vidyaapeeth,

Certificate of Plagiarism Check for Thesis

Author Name	Akanksha Dipak Salvi
Course of Study	M.Tech. (Agricultural Engineering)
Name of Guide	Dr. Rajesh T. Thokal
Department	Irrigation and Drainage Engineering.
Acceptable Maximum Limit	20 %
Submitted By	rhutujanpalte@gmail.com
Paper Title	Assessment of Surface Water Resource Availability in Riverbasins of Konkan Region
Similarity	19%
Paper ID	2396961
Total Pages	37
Submission Date	2024-10-09 15:55:07

Signature of Student

Signature of Guide

Head of the Department

Professor and Head
Deptt. of Irrigation & Drainage Engg.
College of Agril. & Technology
Dapoli-415712, Dist-Ratnagiri(M.S)

* This report has been generated by DrillBit Anti-Plagiarism Software

VITA

1. Name of Student	:	Miss. Akanksha Dipak Salvi
2. Father's Name	:	Mr. Dipak Laxman Salvi
3. Date of Birth	:	10/03/2000
4. Name of the College	:	College of Agricultural Engineering & Technology, Dapoli
5. Residential address	:	401, Landmark, Near SBI Bank, Rohidas Nagar, Mahad 4 Raigad 402301
6. Email ID	:	akankshasalvi1610@gmail.com

7. Academic Qualification:

Sr. No.	Name of Degree Awarded	Year in which obtained	Division/Class	Name of Awarding University	Subject
1.	B. Tech (Agril. Engg.)	2021	First class	Dr. Balasaheb Sawant Konkan Krushi Vidyapeeth, Dapoli	Agriculture Engineering

8. Academic Trainings Completed:

Sr. No.	Name of Institute	Period	Subject
In B. Tech.			
1.	NRFMTT, Hisar, Haryana	May, 2019 (One Month)	Farm Machinery and Tractor
2.	NAHEP, PDKV, Akola	Jun, 2020 (Four Month)	Renewable Energy
In M. Tech.			
1.	NAHEP, JNKVV, Jabalpur (M.P).	Sept, 2023 (One Month)	Remote Sensing and GIS

9. Abstract Published:

10. Research Paper Published:

Salvi A. D., Thokal R. T., Ingle P. M., Patil S. T., More S.S. and Kale A. A. 2024. Surface water assessment methods and tools for water resource management,. International Journal of Agronomy, 7(12), 113–120.

Place: Dapoli

Signature of Student

Date: 30 DEC 2024